

For one thing, physics is a much different field today. In Einstein's day, there were a few thousand physicists worldwide, and the theoreticians who could intellectually spar with Einstein probably would fit into a streetcar with seats to spare.

Education is different, too. One crucial aspect of Einstein's training that is overlooked,, is the years of philosophy he read as a teenager -- Kant, Schopenhauer and Spinoza, among others. It taught him how to think independently and abstractly about space and time....

In April 1911 Einstein was appointed as a full **professor of theoretical physics** at the German part of Prague's Charles University. By that time, he had already won acclaim as the author of his special theory of relativity and a number of successful studies in thermodynamics and molecular physics and in particular in quantum theory and statistical physics.

Albert Einstein left the city of Prague after his sixteen-month long stay in July 1912 when he accepted the chair of theoretical physics at the Polytechnical Institute of Zurich. Direct evidence suggests that Einstein was happy during his professorship in Prague.

Electric discharges – Paschen law



Professor Dr. Yuri P. Raizer

This edition is based on the original second Russian edition: *Fizika gazovogo razryadu*
© Nauka, Moscow 1987, 1992

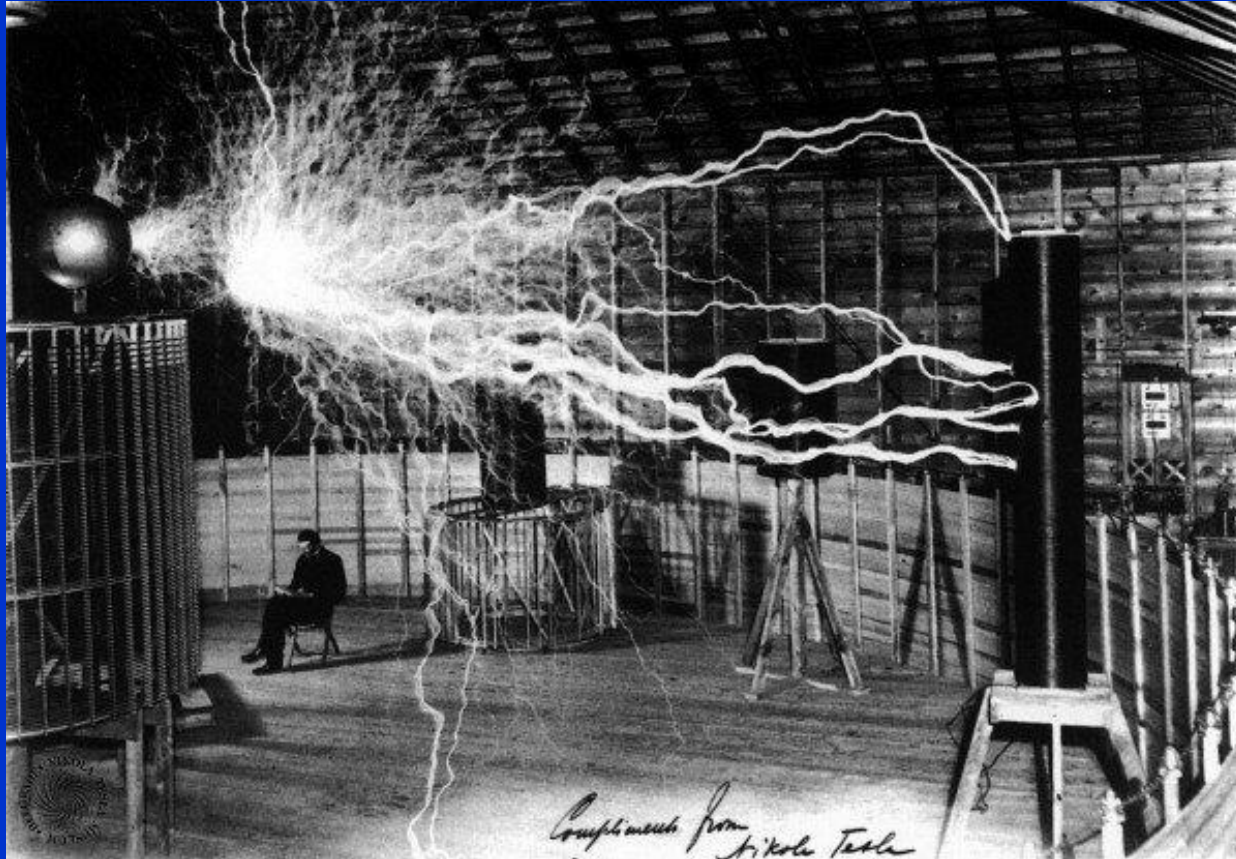
1st Edition 1991
Corrected 2nd Printing 1997

ISBN 3-540-19462-2 Springer-Verlag Berlin Heidelberg New York

Úvod do fyziky plazmatu
ČSAV, Academia Praha 1984
Francis F. Chen

Viktor Martišovič
ZÁKLADY FYZIKY PLAZMY
Bratislava 2004
Učebný text pre 3. ročník magisterského štúdia
FAKULTA MATEMATIKY, FYZIKY A INFORMATIKY
UNIVERZITA KOMENSKÉHO

The voltage of Nicola Tesla's man-made lightning can be calculated from altitude and gap



Natural lightning is now considered an electric spark, not an arc.





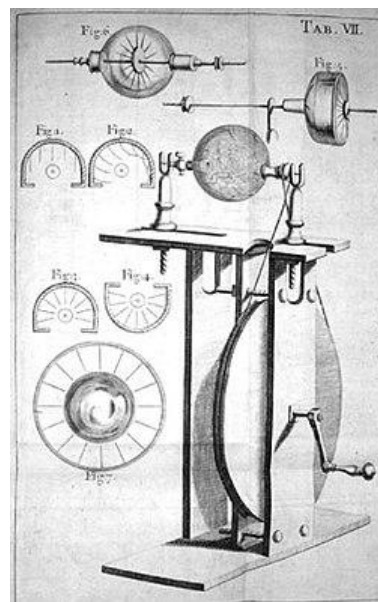
Historical overview

- › 1675: Phenomenon of glowing vacant space in a Barometer while moving it, discovered by Jean-Felix Picard
- › 1705: First Demonstration of gas discharge lamp by Francis Hauksbee
- › 1857: Development of Geissler Tubes (low-pressure gas discharge tubes) by Heinrich Geissler
- › 1898: Discovery of Neon by William Ramsay and Morris W. Travers
- › 1910: Commercialization of Geissler Tubes as neon lighting, used in neon signs



Jean Picard (1620-1682)
Astronom
Zodpovědný za první
přesné měření poloměru
Země

Jean Picard si všiml, že prázdný prostor v jeho rtuťovém barometru zářil, jak se rtuť chvěla, když nesl barometr. Francis Hauksbee poprvé předvedl plynovou výbojku v roce 1705. Ukázal, že evakuovaná nebo částečně evakuovaná skleněná koule, do které umístil malé množství rtuti, nabíjená statickou elektřinou, může produkovat světlo dostatečně jasné, aby se dalo číst.

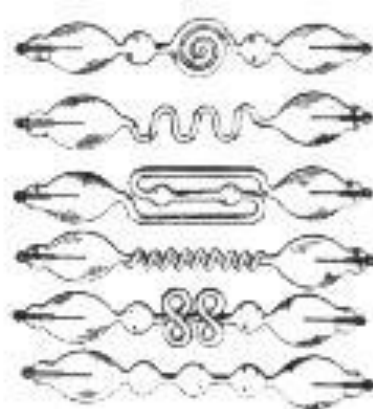


Generator built by Francis Hauksbee. From
Physico-Mechanical Experiments, 2nd Ed.,
London 1719

Geisslerovy trubice



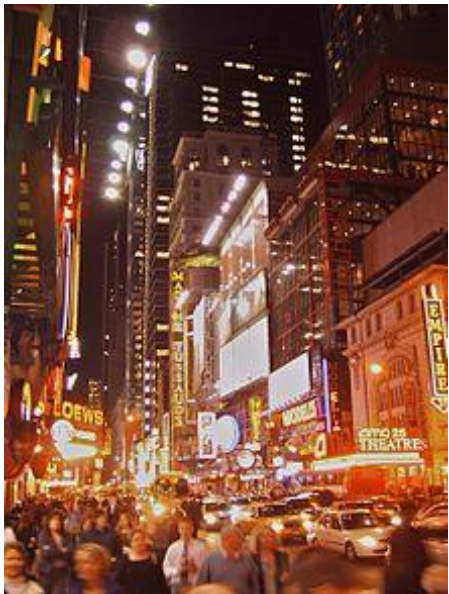
Heinrich Geissler (1814-1879)



Dvě elektrody v trubici s plynem (neon, argon, krypron, xenon, vodík, CO₂) o nízkém tlaku, doutnavý výboj



Neonové výbojky



Komerčně produkoval Georges Claude od roku 1910

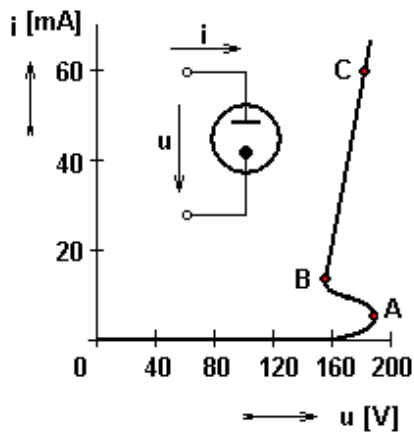
0.4 – 3 kPa, doutnavý výboj (hlavně pozitivní sloupec)

Oranžová barva (neon)

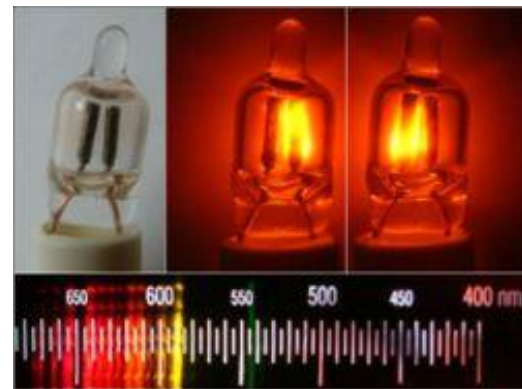
Další barvy s využitím jiných plynů (vodík – červená, helium – žlutá, CO₂ – bílá, rtuť – modrá) a luminoforů



Neon glow lamp (doutnavka)



Tlak řádově stovky Pa
Dvě elektrody blízko
sebe, doutnavý výboj



Vypínače, indikátory,
ochrana proti přepětí,
stabilizátory napětí atd.



Zkoušečka

Types of gas light sources

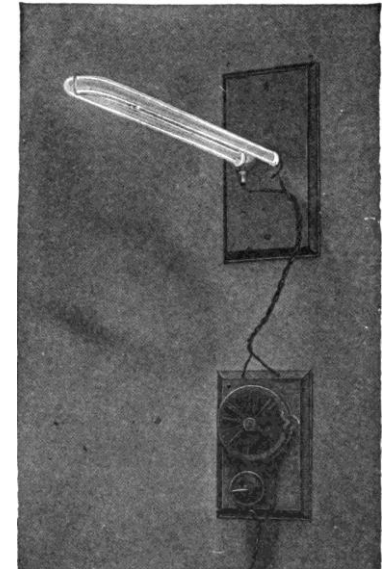
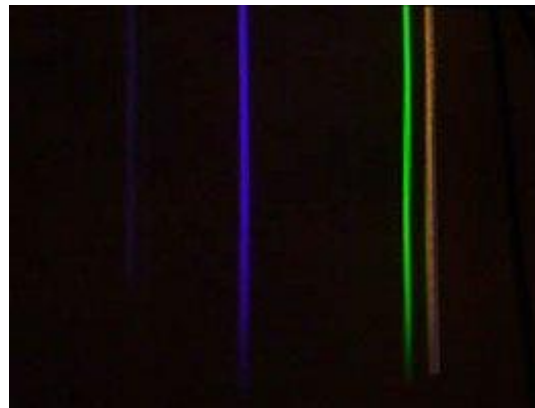
Overview

Overview:

- Low pressure gas discharge lamps
- High pressure gas discharge lamps
- Excimer lamp

Rtuťová výbojka (za atmosférického tlaku)

| Wavelength (nm) | Name (see photoresist) | Color |
|-----------------|--|-------------------|
| 184.45 | | ultraviolet (UVC) |
| 253.7 | | ultraviolet (UVC) |
| 365.4 | I-line | ultraviolet (UVA) |
| 404.7 | H-line | violet |
| 435.8 | G-line | blue |
| 546.1 | | green |
| 578.2 | | yellow-orange |
| 650 | | red |



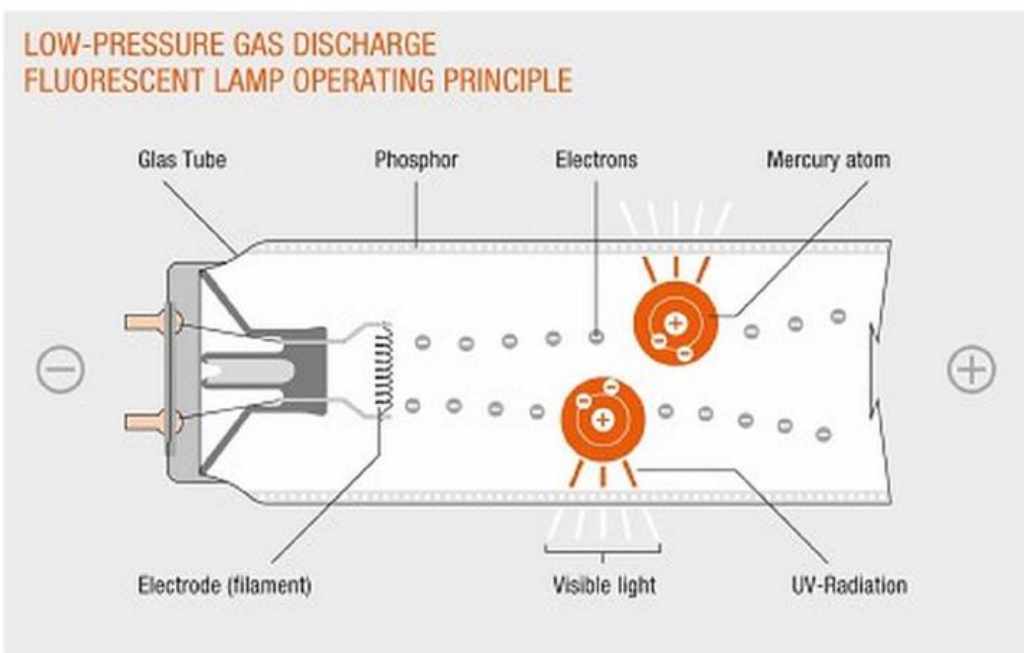
Výbojem v argonu se začne vypařovat rtuť a tlak vzroste na 2 – 18 atmosfér -> výboj v parách rtuti, tato nástupní fáze trvá několik minut během nichž lampa svítí čím dál tím více. Luminofor kolem výbojky se používá, aby bylo záření příjemnější pro oči).

Přítomnost silného ultrafialového záření se využívala k desinfekci.

Dnes se většinou k osvětlení nepoužívají (příliš mnoho rtuti)

Types of gas light sources

Low pressure gas discharge lamp



Sketch of a low pressure mercury vapour gas discharge fluorescent lamp.

Obloukový výboj v parách rtuti



Komerční vývoj zářivek byl inicializován výzkumy Arthur Comptona (Nobel prize 1927) ve třicátých letech.

A **fluorescent lamp**, also called fluorescent tube, is a low pressure mercury vapor gas-discharge lamp that works on the principle of fluorescence to emit visible light.

When an electric current is passed through the fluorescent tube, it excites the mercury vapor which produces UV rays that then causes a phosphor coating on the inside of the lamp to glow.

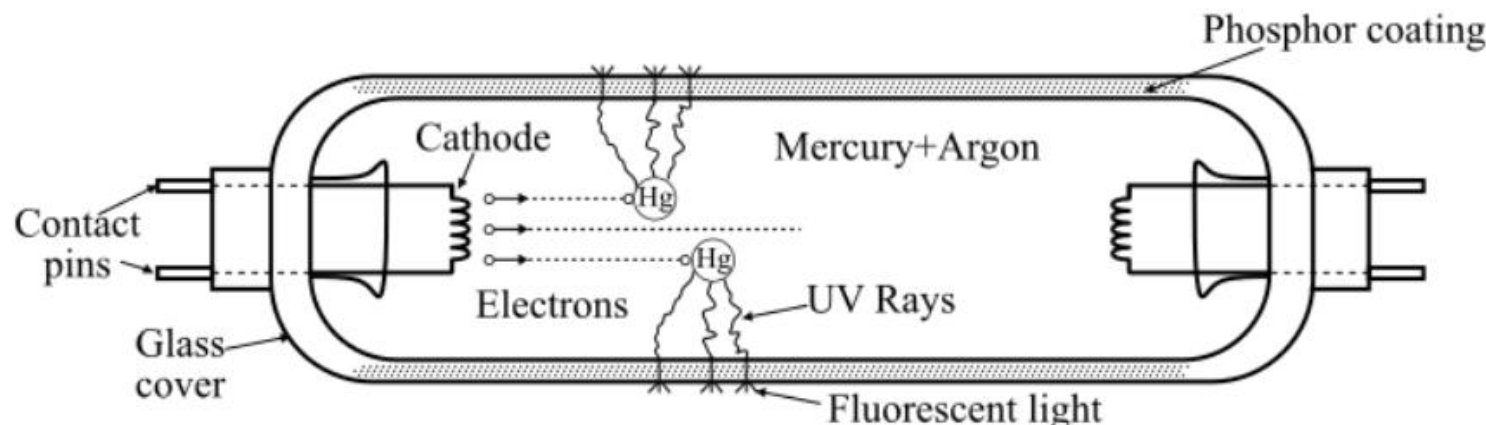


Figure-1 Fluorescent Lamp

The fluorescent lamp is a low pressure mercury vapor lamp. Thus, due to low pressure, the lamp is made in the form of a long tube whose inside walls are coated with some phosphor. The tube is filled with a small amount of mercury vapor and a small amount of argon gas.

At both ends of the tube, the electrodes are attached. The electrodes are of spiral form, made of tungsten and coated with an electron emitting material. A choke is also connected in series with the tube filament that provides a voltage impulse for starting the fluorescent lamp and once the lamp is started, it acts as a ballast. The lamp filament is connected to a starter switch which is a small cathode glow lamp with bimetallic strip at the electrodes.

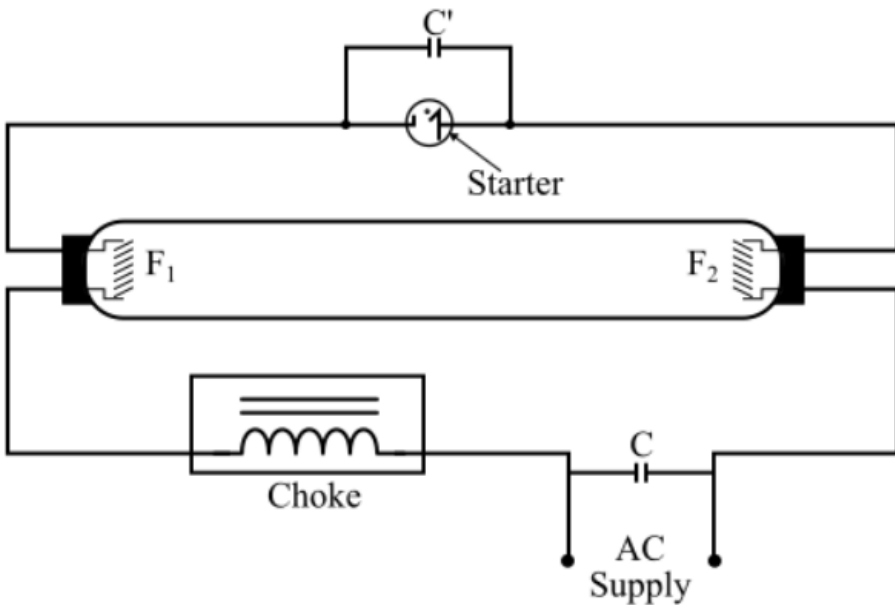
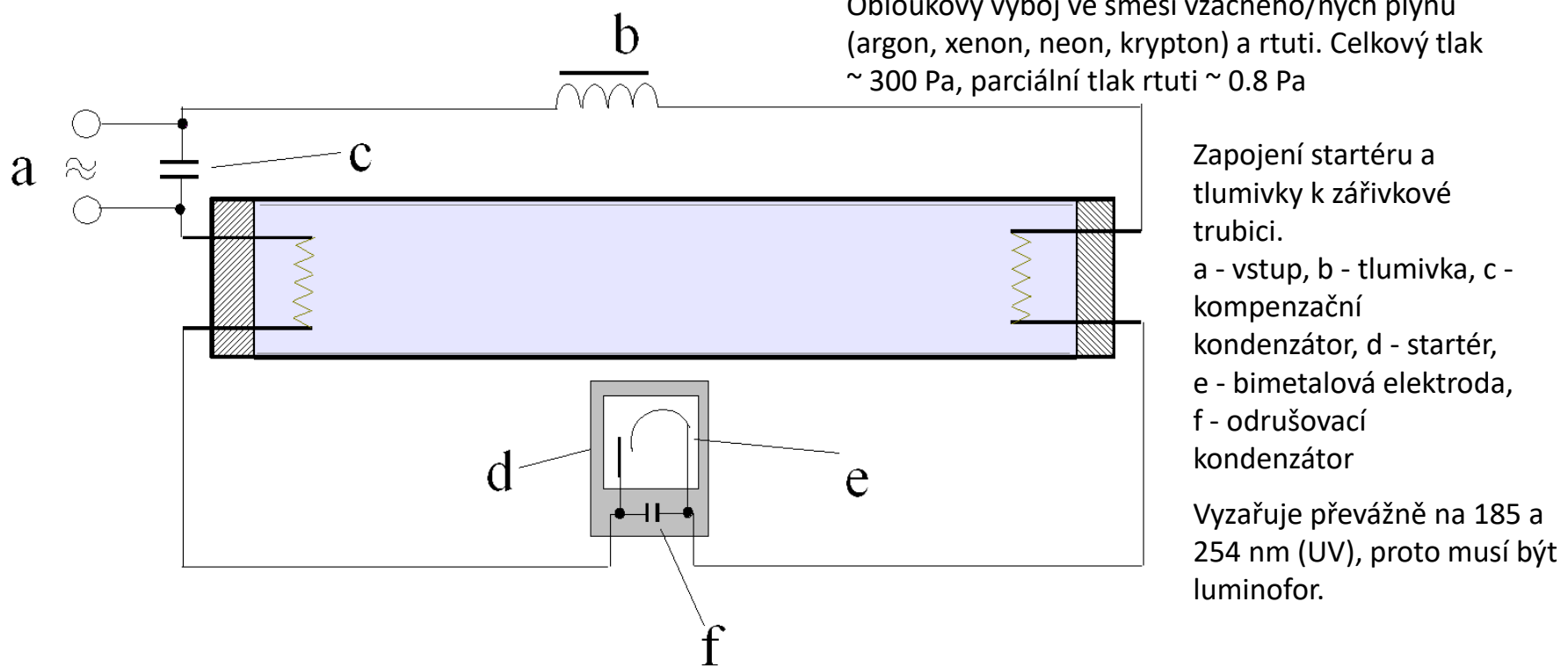


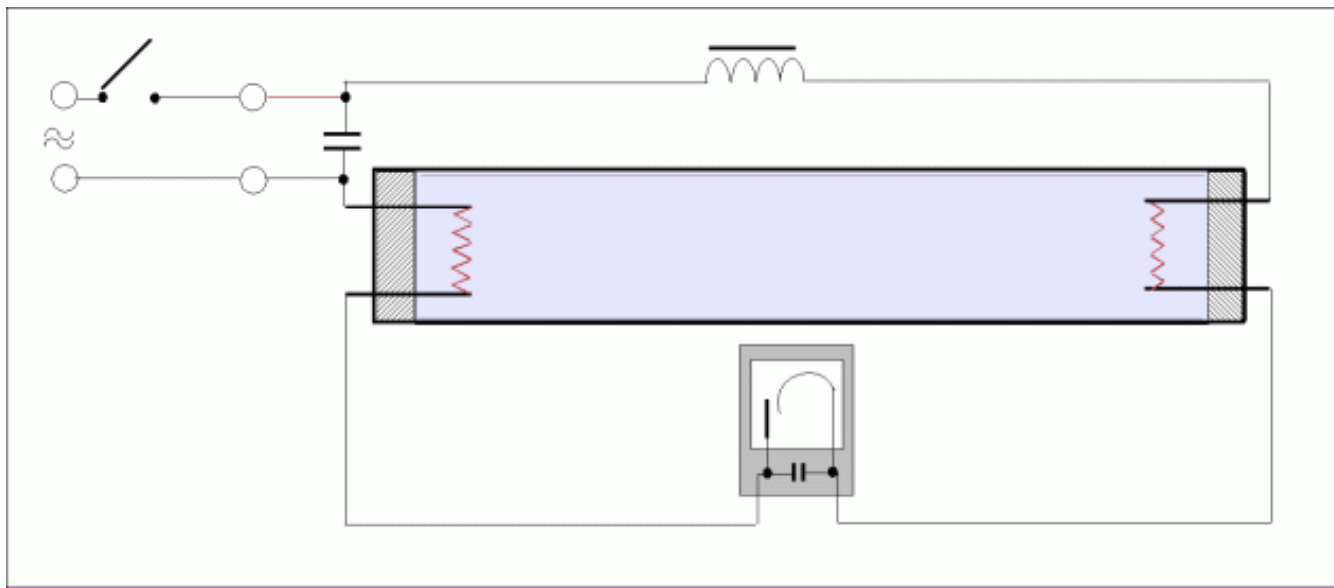
Figure 2 - Circuit for Fluorescent Lamp

When the circuit is energized, nearly full supply voltage appears across the starter terminals due to low resistance of the filaments and a negligible current flows through the choke. The starter switch is filled with argon gas. This argon gas ionized and a glow appears inside the starter switch, which heats up the bimetallic strip carrying a moving contact. In a while, the bimetallic strip bends and short circuits the starter terminals. This results in a high current to flow through the filaments F₁ and F₂ and the choke circuit. The filaments are coated with oxides of barium and strontium, resulting in thermionic emission which can ionize the argon gas inside the tube.

Zářivky (Low pressure fluorescent lamp)



Zářivky (Low pressure fluorescent lamp)



Types of gas light sources

Low pressure gas discharge lamp

Phosphor composition:

› „Old“ Halophosphate-type Phosphor:

- › Mainly emits yellow and blue light
- › Weak emission of red and green light
- › Appears white to the eye
- › Has incomplete Spectrum => CRI ~ 60

CRI – color rendering index (100 sun
black body radiation)

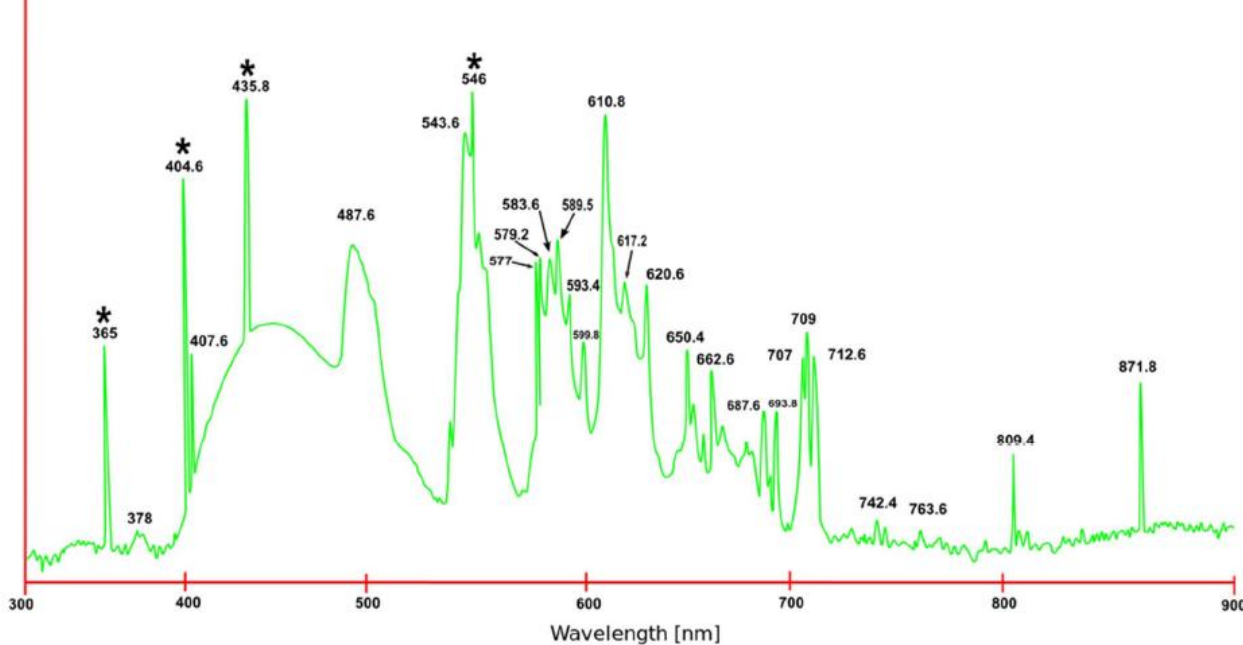
› „New“ Triphosphor mixture (since 1990s):

- › Based on Eu and Tb
- › More evenly distributed VIS spectrum
- › CRI typically 82-100

Types of gas light sources

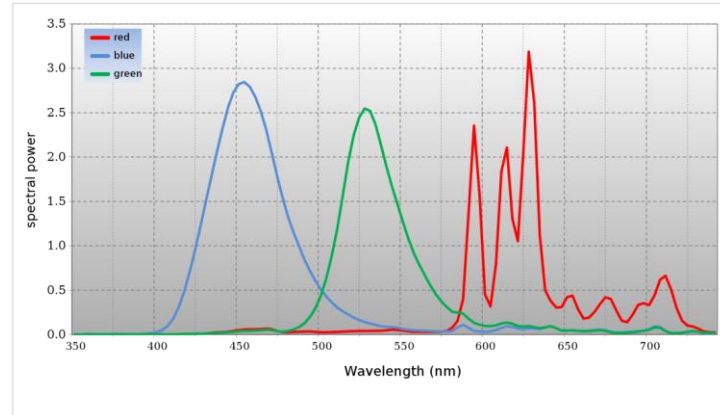
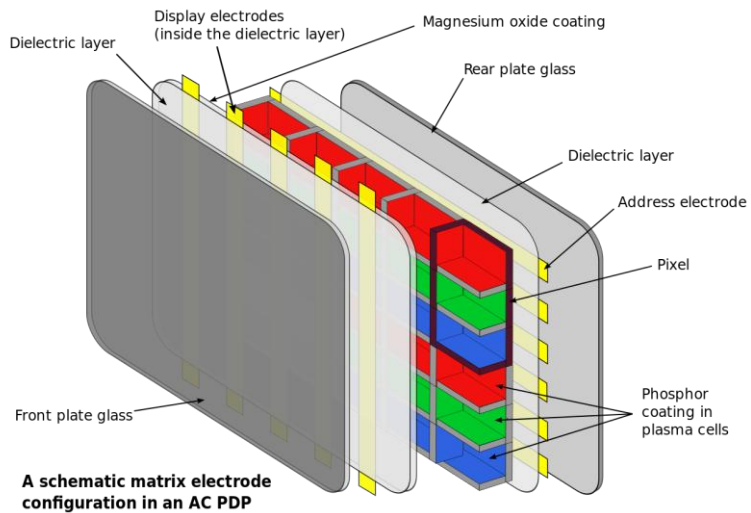
Low pressure gas discharge lamp

* Mercury lines



Spectrum from a 48" Philips F32T8 natural sunshine fluorescent light

Plazmové zobrazovače



Spektralni charakteristiky typicky používaných luminoforů

Plazmové zobrazovače



Lepší kontrast než LCD, velmi dobrá reprodukce barev

Velmi široký úhel, ze kterého je možné se na televizi dívat

Vysoká obnovovací frekvence a odezva

Relativně velká spotřeba elektřiny

„Vypalování obrazu“ – přehřátí luminoforu

Dnes už komerčně nahrazeny LCD a OLED

Větší hmotnost než LCD obrazovky

Plasma displays were first used in PLATO computer terminals. This PLATO V model illustrates the display's monochromatic orange glow seen in 1981

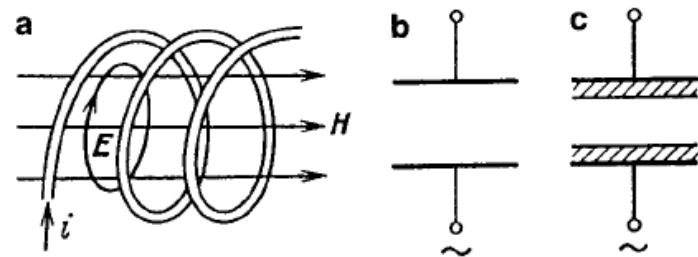


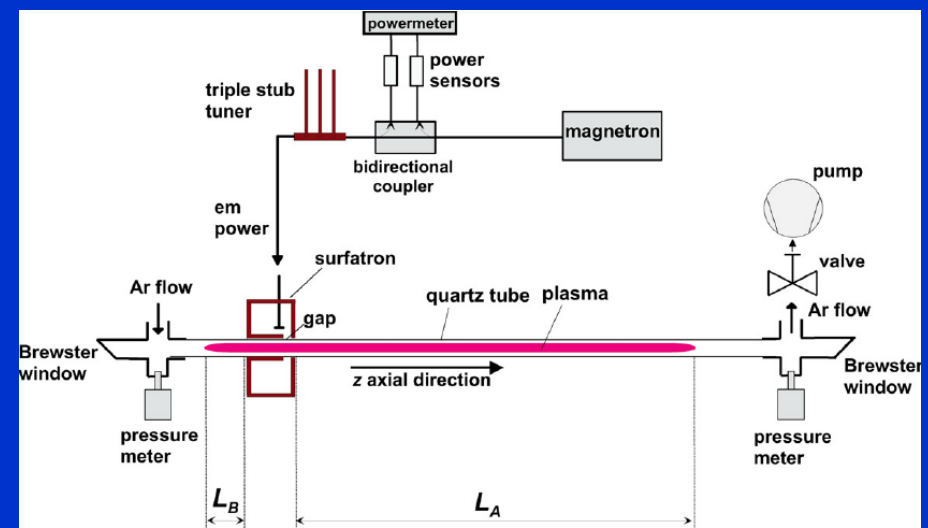
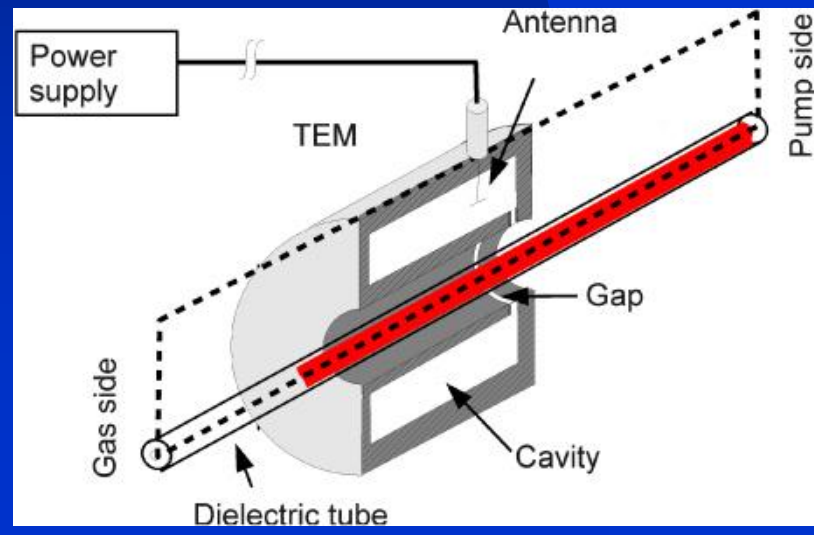
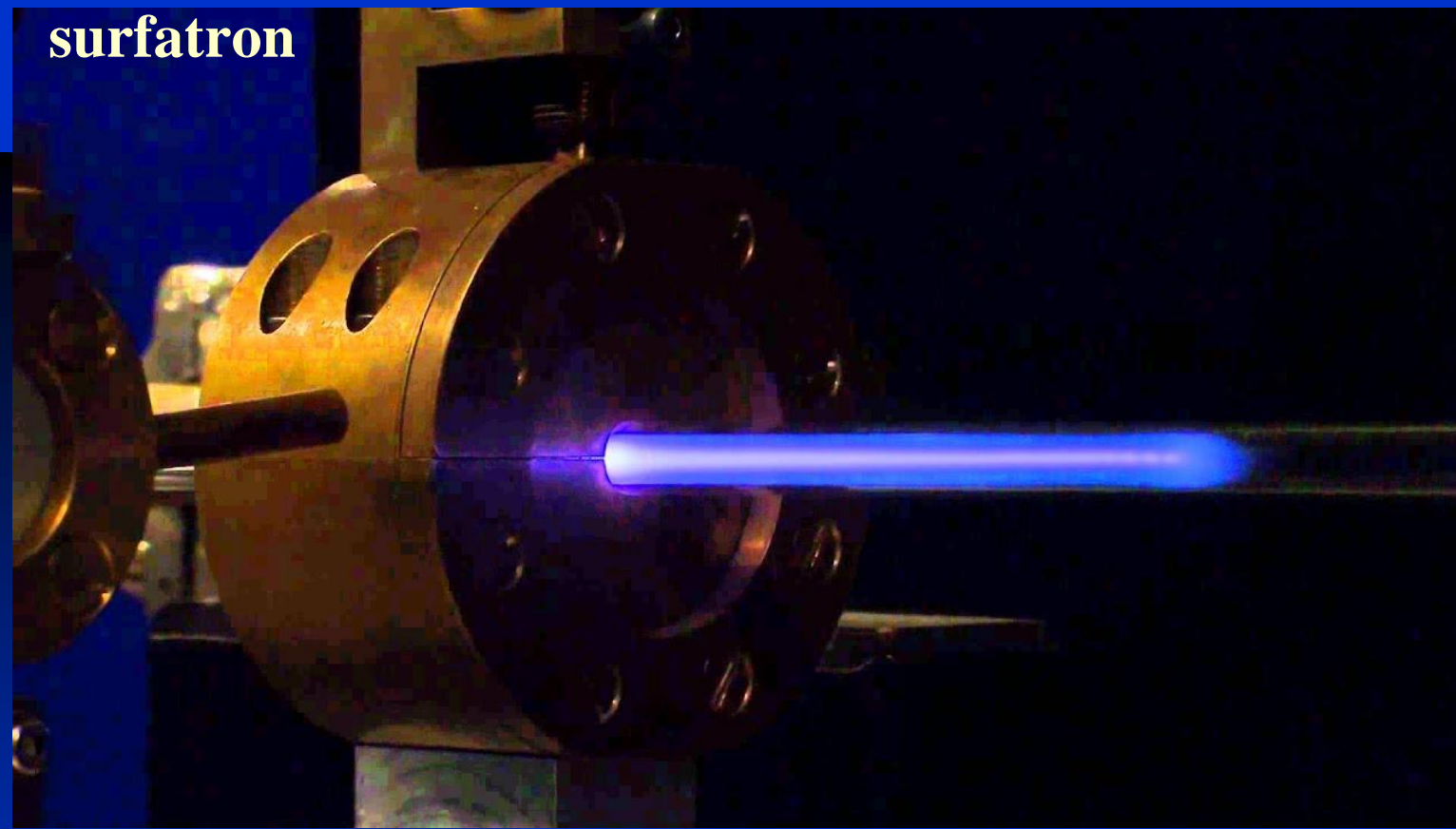
Fig. 7.18. Excitation of rf discharges: (a) inductively coupled through a solenoid coil; (b) voltage applied to electrodes in contact with plasma; (c) electrodes insulated from plasma (electrodeless, capacitively coupled rf discharge)

Raizer, Y.P. (1991) Gas Discharge Physics. Springer-Verlag, New York.

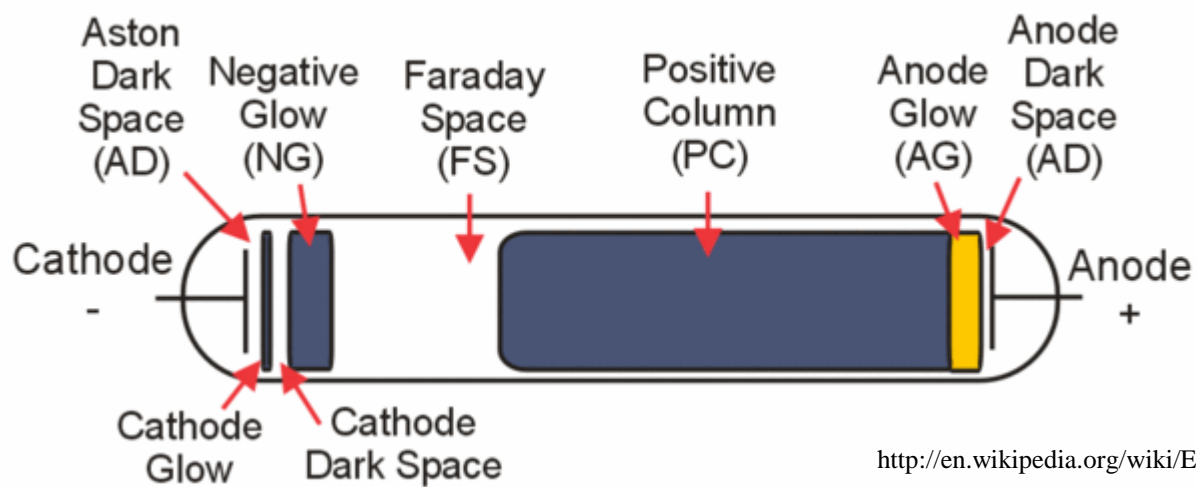
A typical – and most frequent – approach to implementing this principle is as follows (Fig. 7.18). A high-frequency current is passed through a solenoid “coil” (in fact, the coil may consist of only one or several turns). The oscillating magnetic field of this current within the coil is directed along its axis and induces a vortex electric field, whose lines of force are closed circles concentric with the turns of the coil. This electric field can ignite and sustain a discharge, its currents also being closed and flowing along the closed circular lines of force of the electric field. In actual experiments, a dielectric tube filled with a gas to be studied is inserted into the coil so that breakdown occurs under certain conditions and the discharge can be sustained after breakdown. Pulsed discharges can be produced if a sufficiently strong current pulse is fed into the coil. This type of discharge is known as the inductively coupled, or *H*-type, rf discharge, with the latter *H* pointing to the decisive role of the magnetic field. Inductively coupled discharges are apparently *electrodeless*.

In the methods belonging to the second group, the high-frequency (or any other waveform) voltage is applied to the electrodes. In the simplest (and the most widespread) geometry, two parallel plane electrodes are employed. The electrodes may be *bare* and be in direct contact with the discharge plasma, or they may be *insulated* by a dielectric (Fig. 7.18b,c). A system of two electrodes behaves with respect to a variable voltage as a capacitor, so that in contrast to induction discharges, those in this category are known as *capacitively coupled*, or *E*-type, rf discharges (ccrf). The letter *E* symbolizes the decisive role of the electric field. A capacitively coupled discharge can be ignited in a tube via a pair of ring electrodes fixed on the outside surface at the ends of the tube, creating the longitudinal field. As a result, the discharge can be observed through the end faces.⁵

surfatron



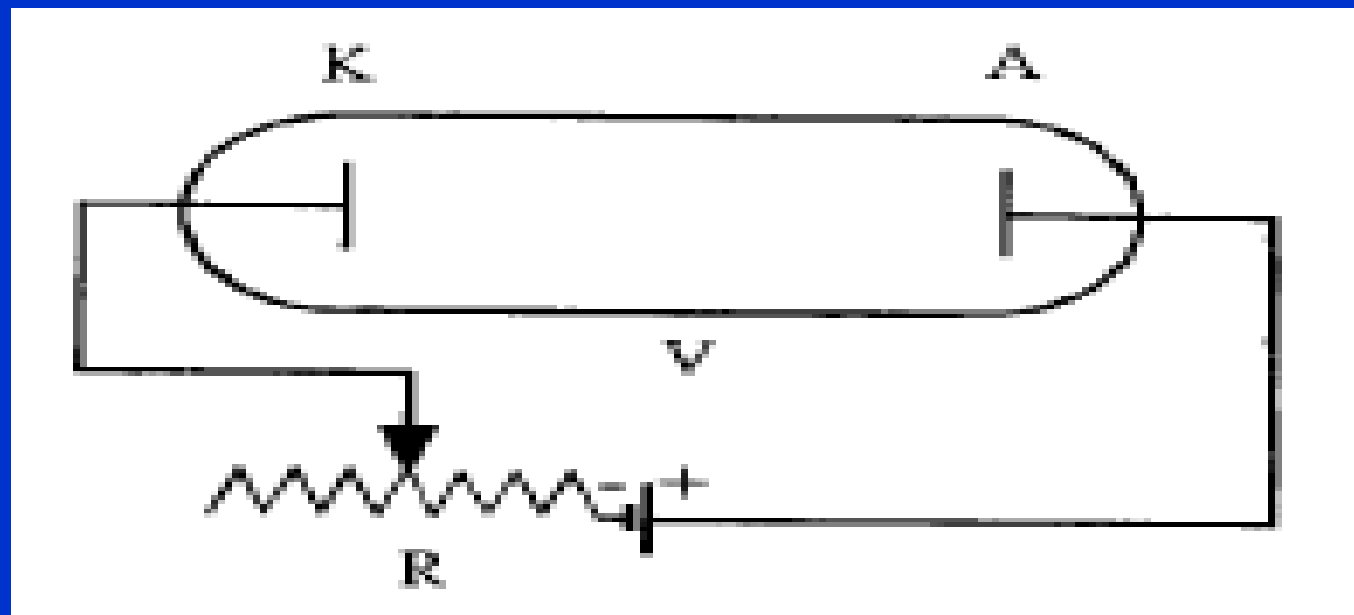
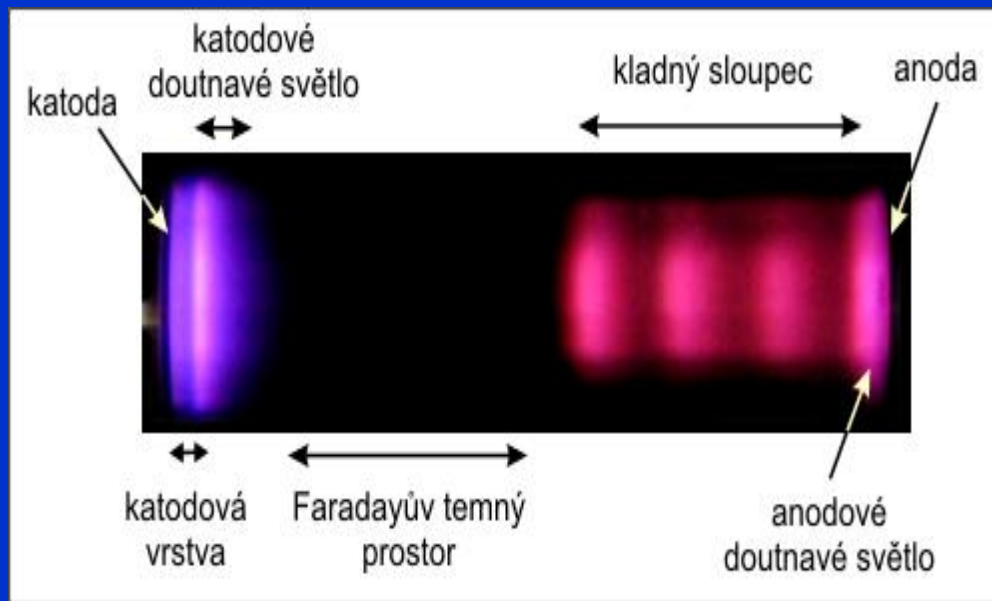
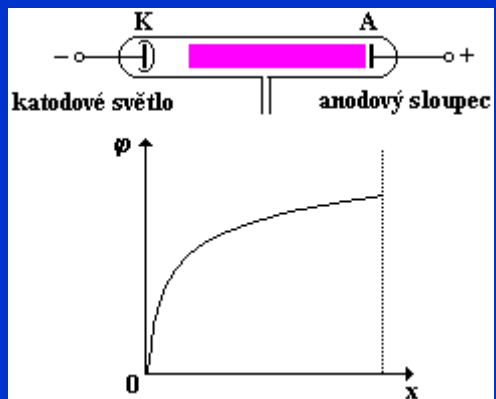
Glow discharges



http://en.wikipedia.org/wiki/Electric_glow_discharge

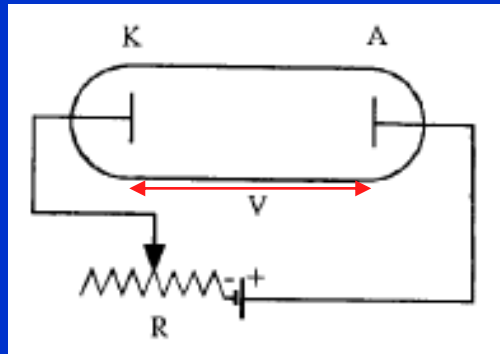
<http://www.exo.net/~pauld/origins/glowdischarge.html>

Glow discharges



Electric discharges V-A characteristic

Direct current (DC) glow discharge



$$V = V_0 - RI$$

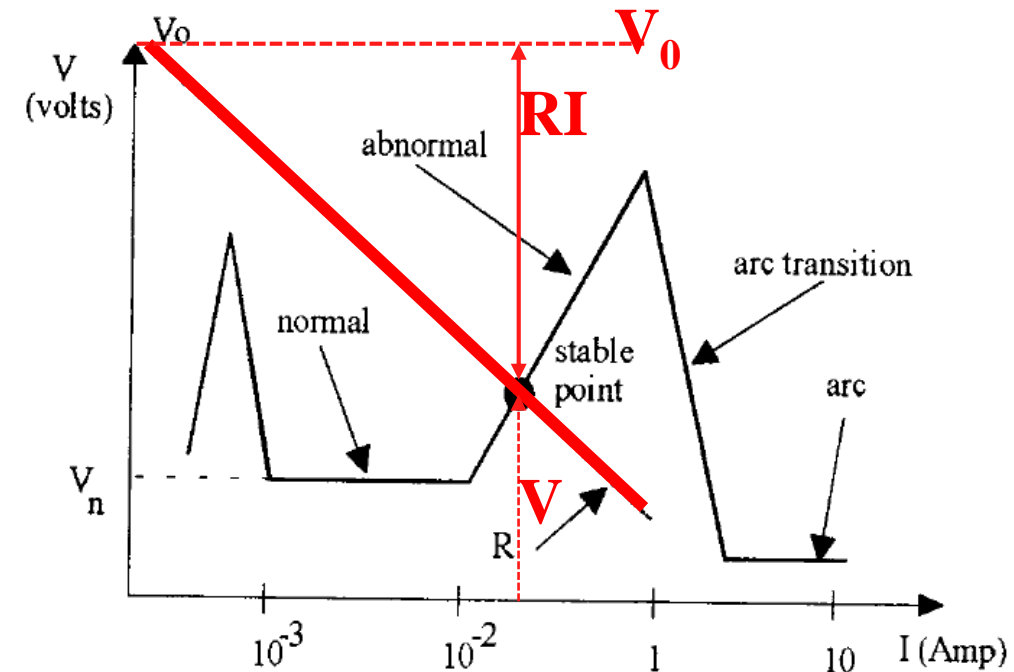


Fig. I-3

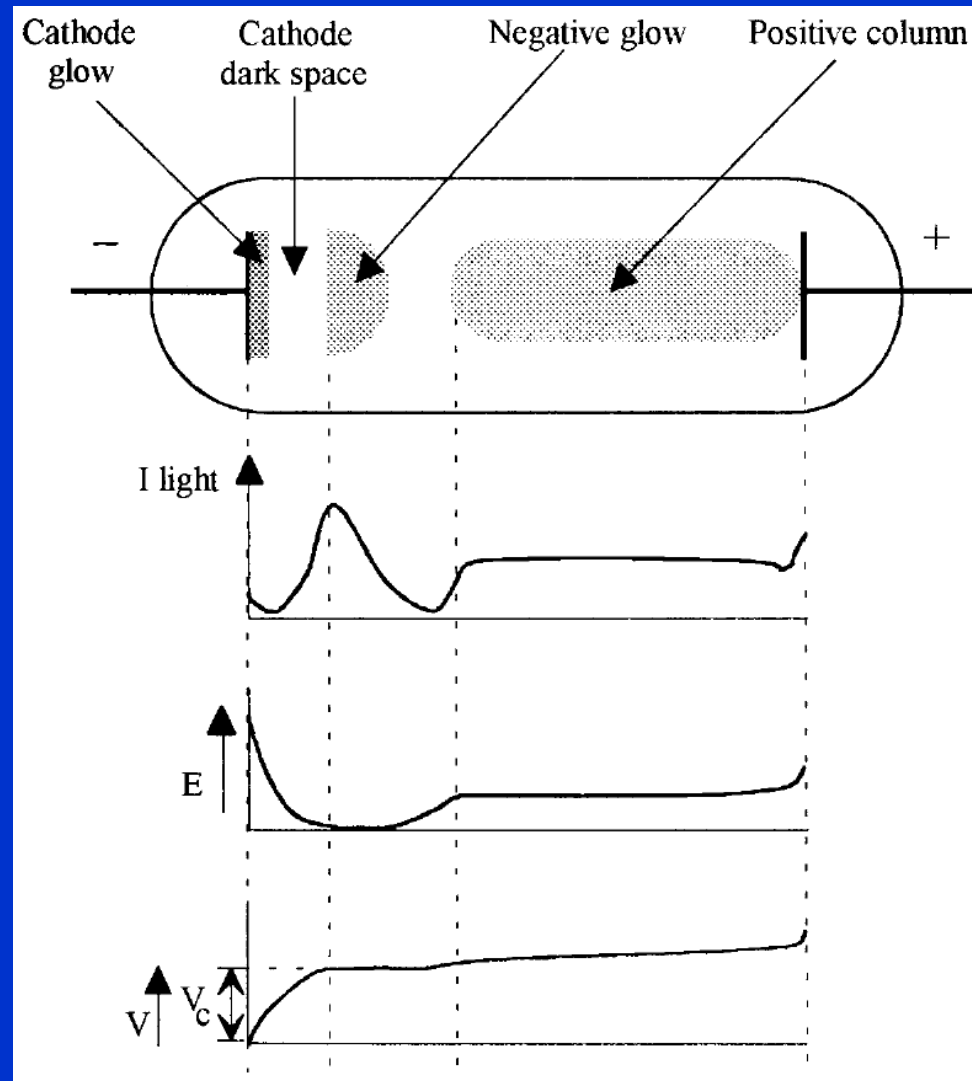
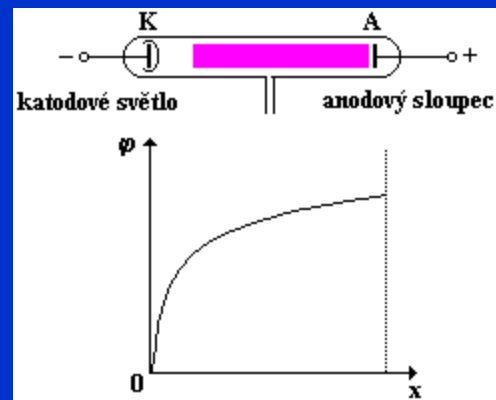
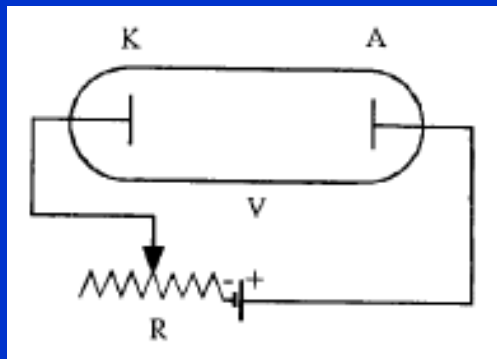
Glow discharge setup (a)

$V = f(I)$ Characteristic in glow discharge. Stable working point (b).

Doporučená literatura:

Reactive plasmas
Andre Ricard

Glow discharges

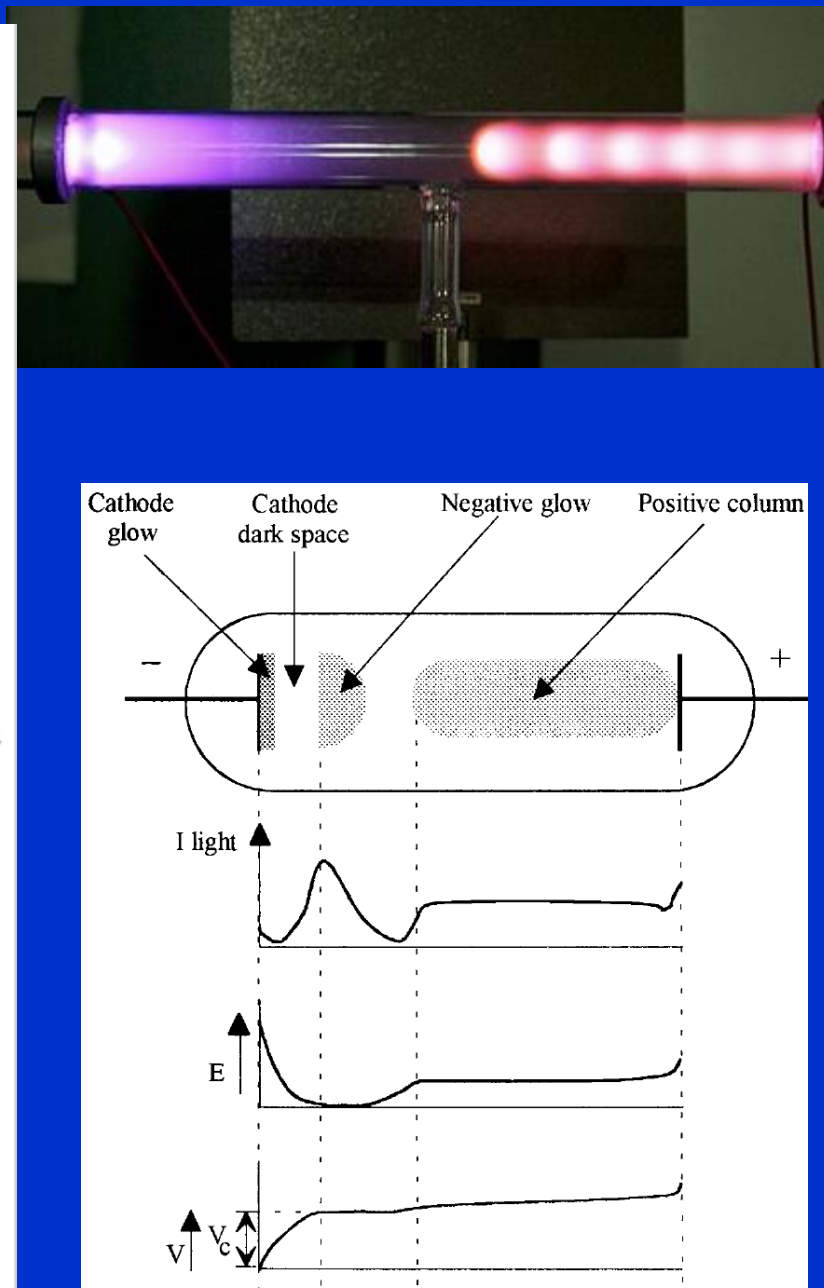
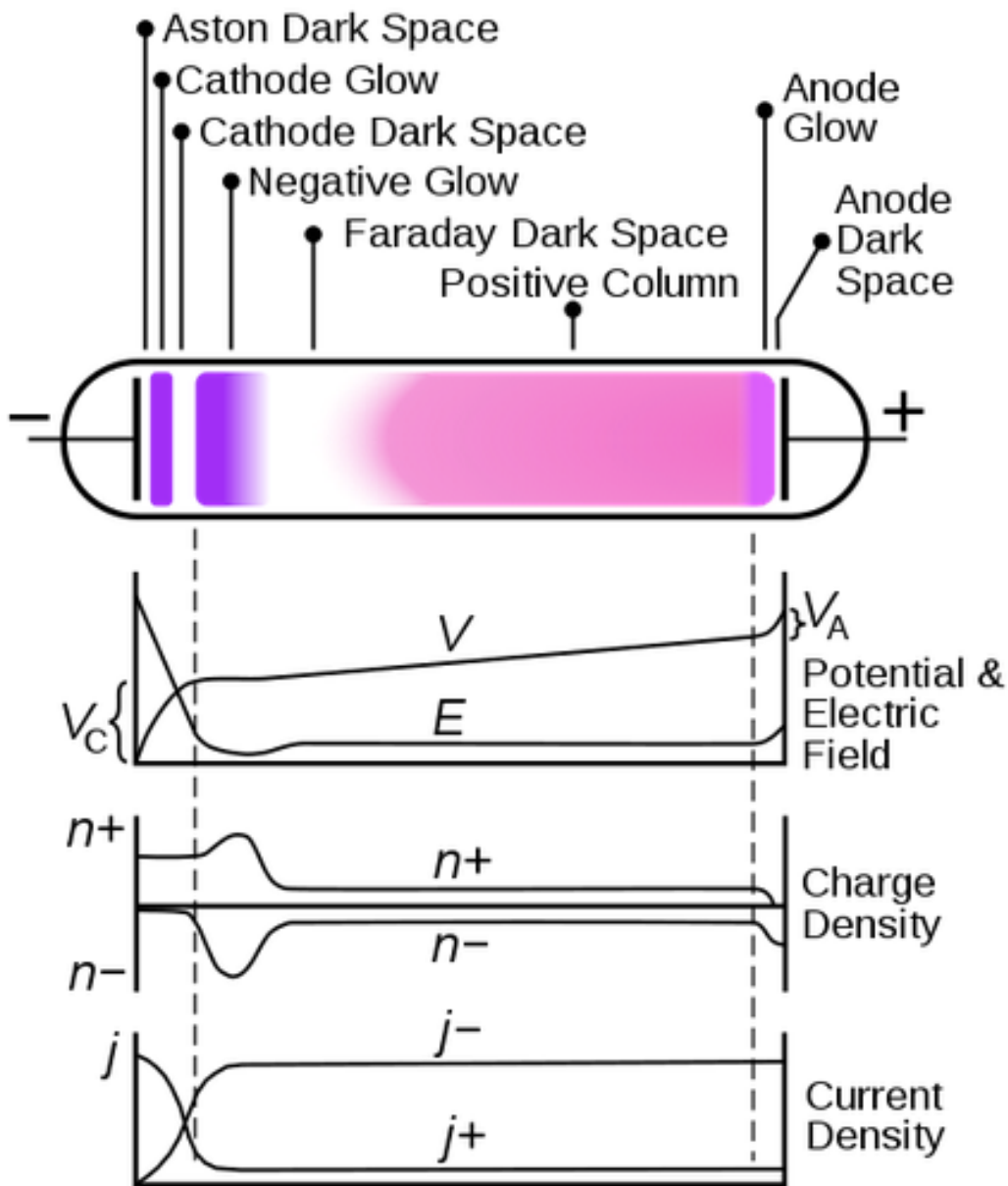


Several parts of a glow discharge.

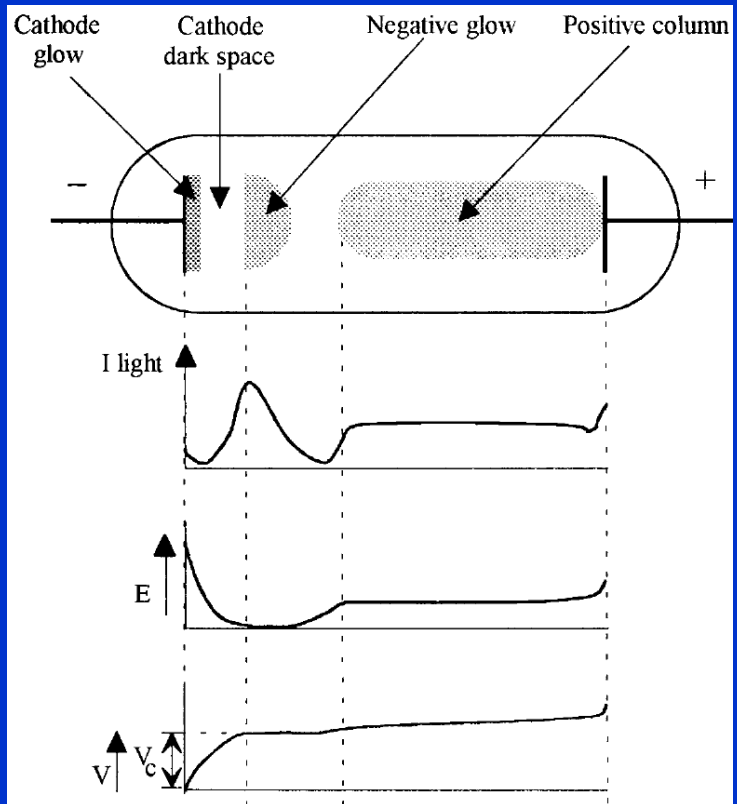
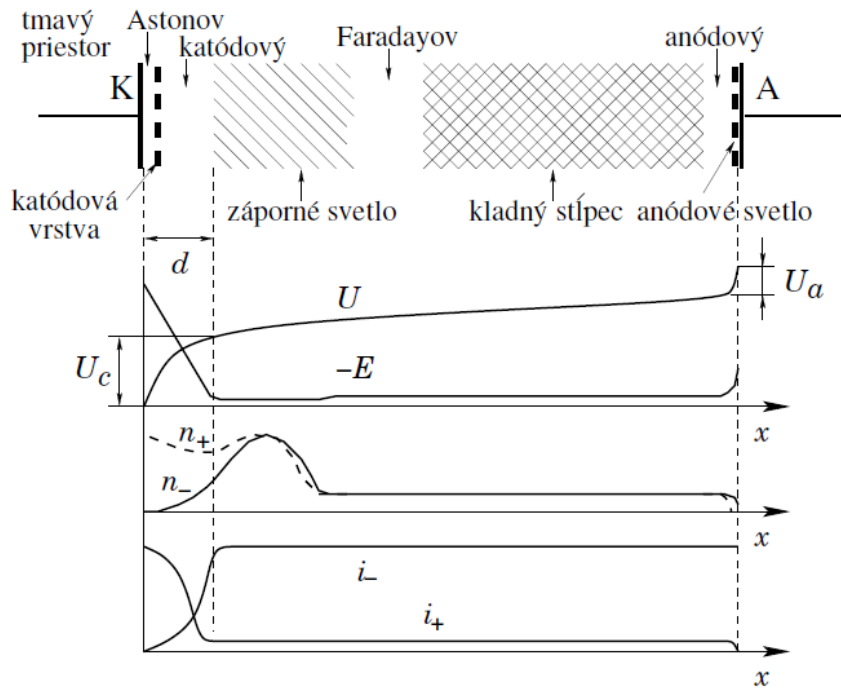
????

Luminous intensity (I_{light}), electric field (E) and voltage (V).

V_c cathode potential. ????



A glow discharge illustrating the different regions comprising it and a diagram giving their names.



Obr. 5.9: Štruktúra tlečieho výboja a priebehy pozdĺžneho poľa E , potenciálu U , koncentrácie nabitých častíc n_+ a n_- a hustoty prúdu kladných iónov i_+ a i_-

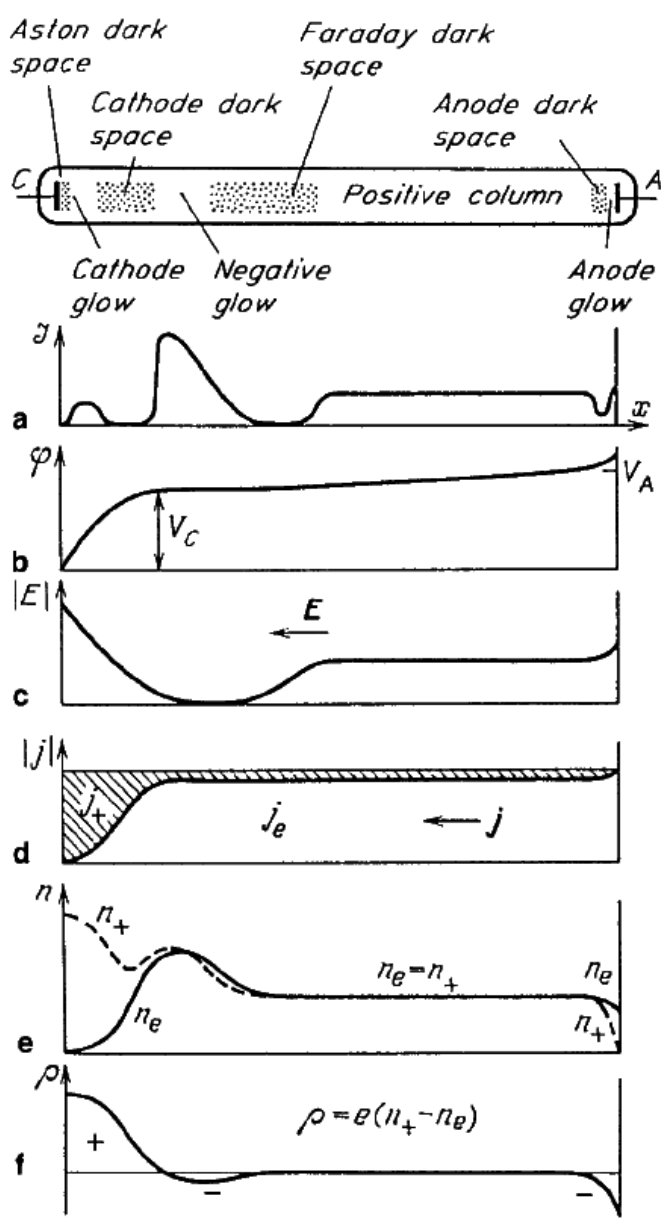
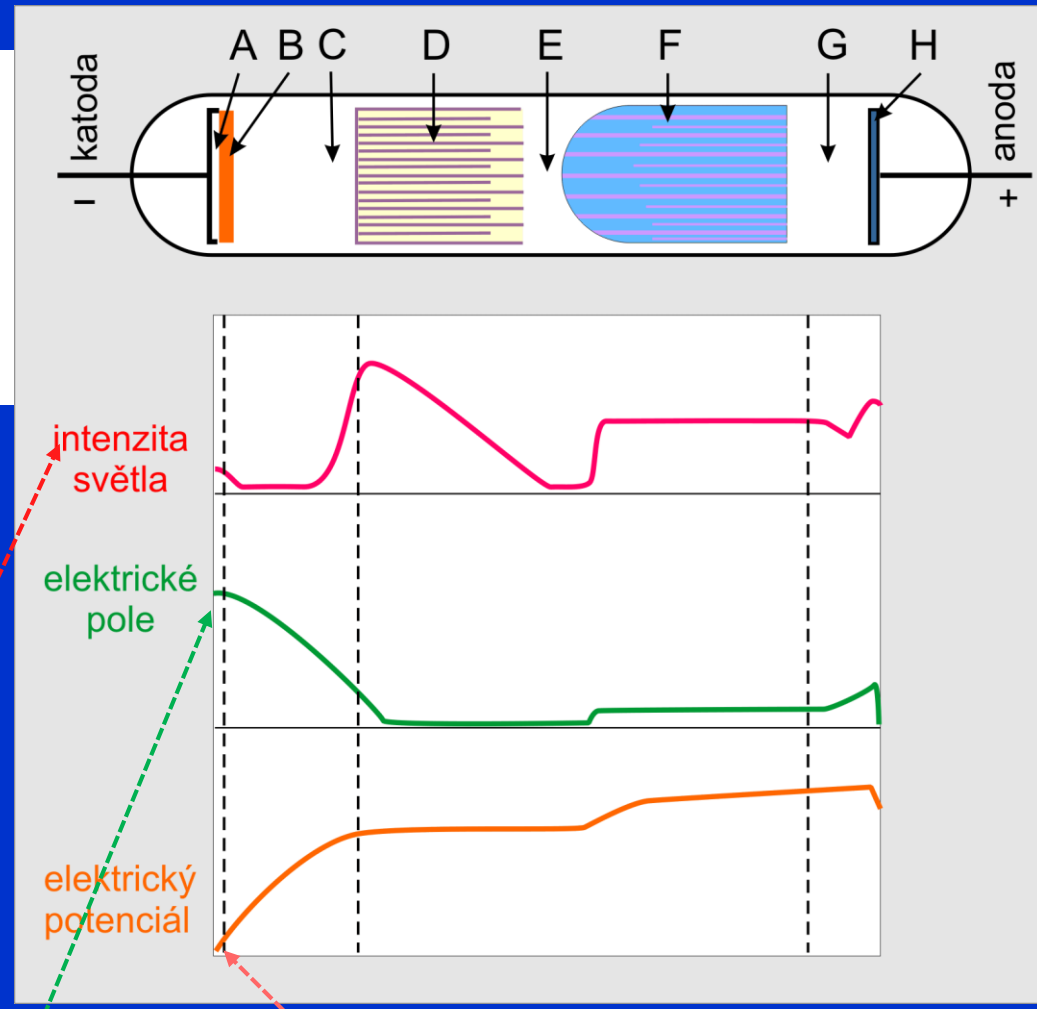
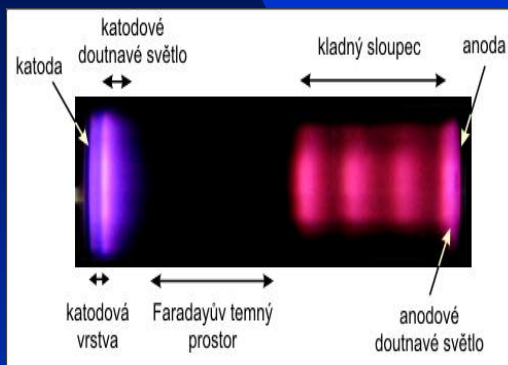
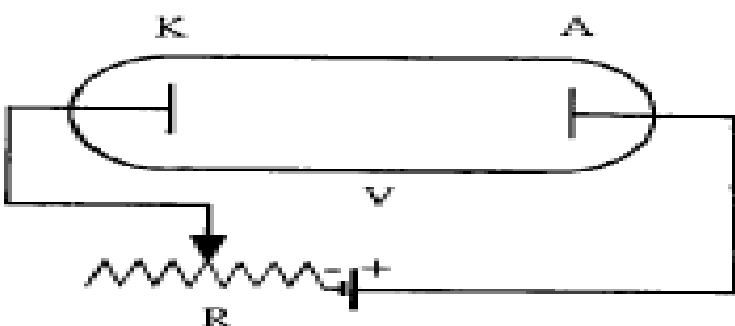


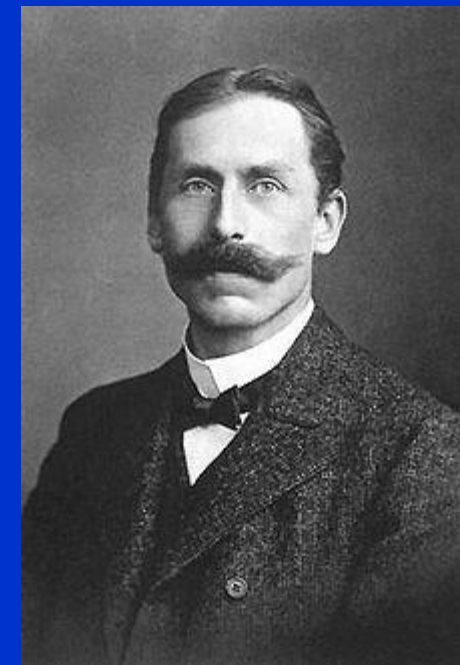
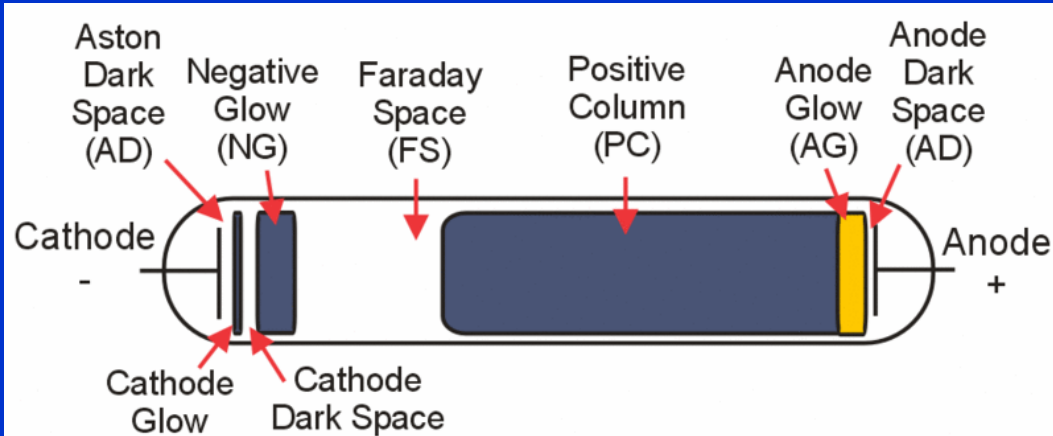
Fig. 8.2. Glow discharge in a tube and the distribution of: (a) glow intensity, (b) potential φ , (c) longitudinal field E , (d) electronic and ionic current densities j_e and j_+ , (e) charge densities n_e and n_+ , and (f) space charge $\rho = e(n_+ - n_e)$

Glow discharges

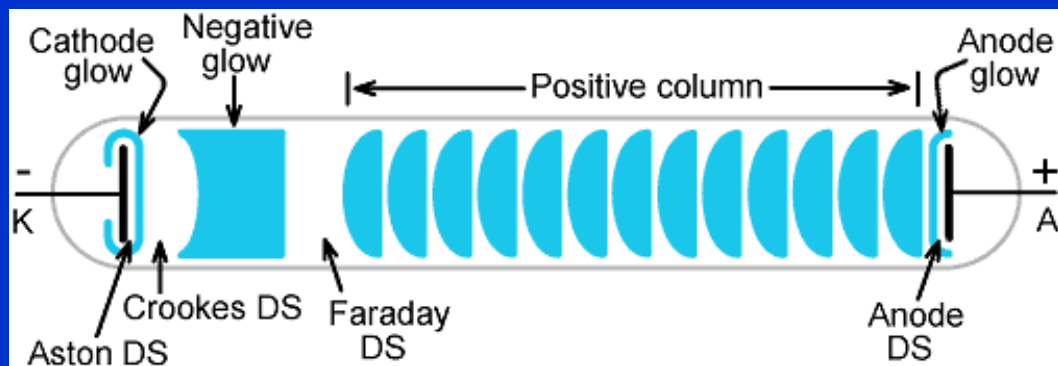


Several parts of a glow discharge.
Luminous intensity (I light), electric field (E) and voltage (V).
 V_c cathode potential. ????

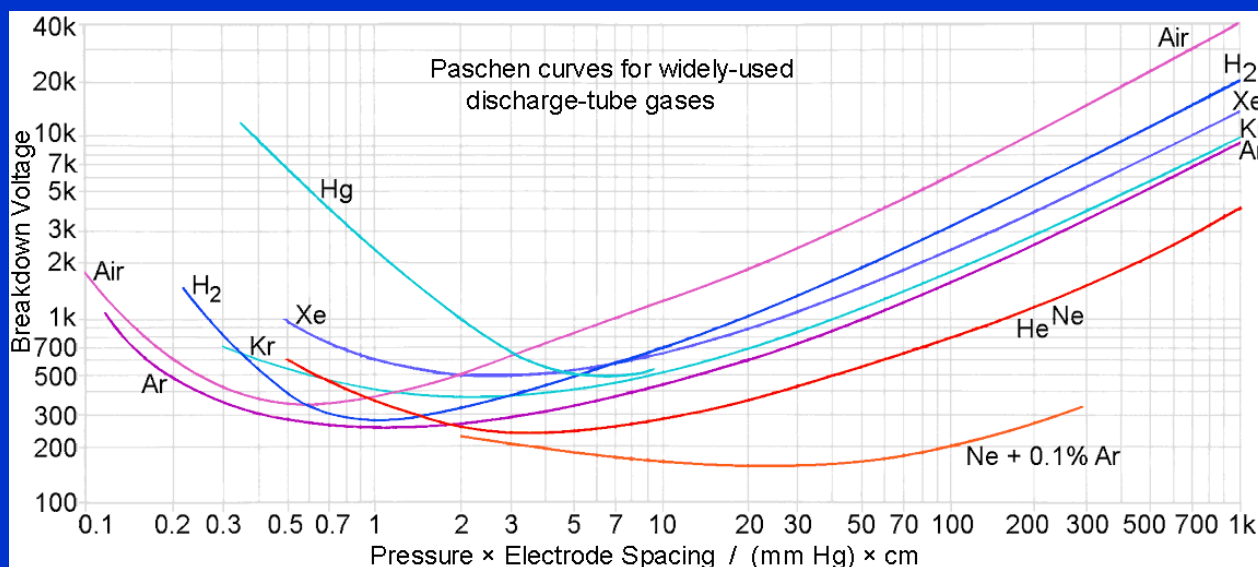
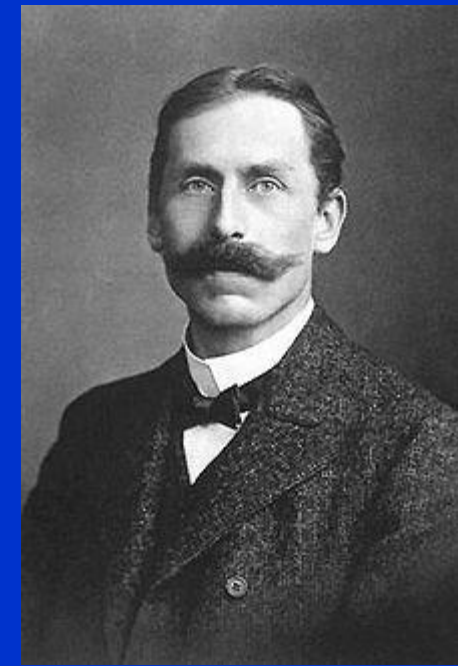
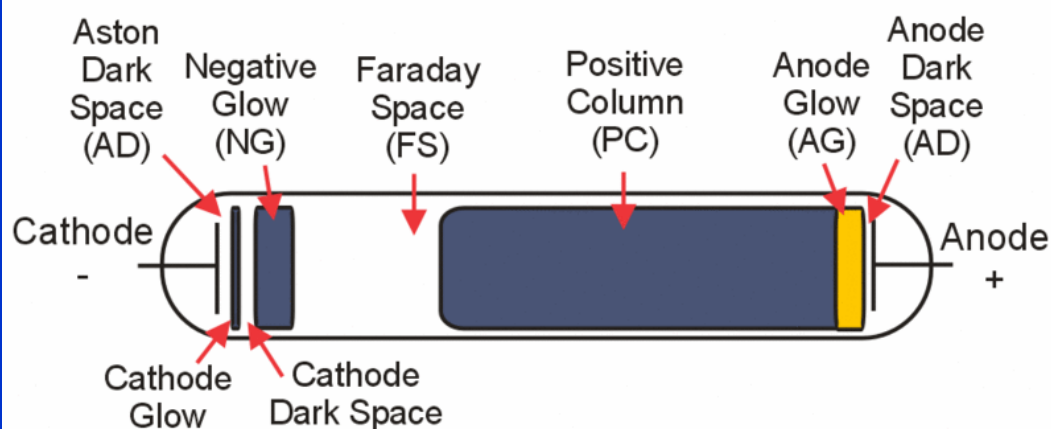
Louis Carl Heinrich Friedrich Paschen (22 January 1865 - 25 February 1947)



He is also known for the [Paschen series](#), a series of hydrogen spectral lines in the infrared region that he first observed in 1908. He established the now widely used [Paschen curve](#) in his article "*Über die zum Funkenübergang in Luft, Wasserstoff und Kohlensäure bei verschiedenen Drücken erforderliche Potentialdifferenz*".^[1]



Louis Carl Heinrich Friedrich Paschen (22 January 1865 - 25 February 1947)

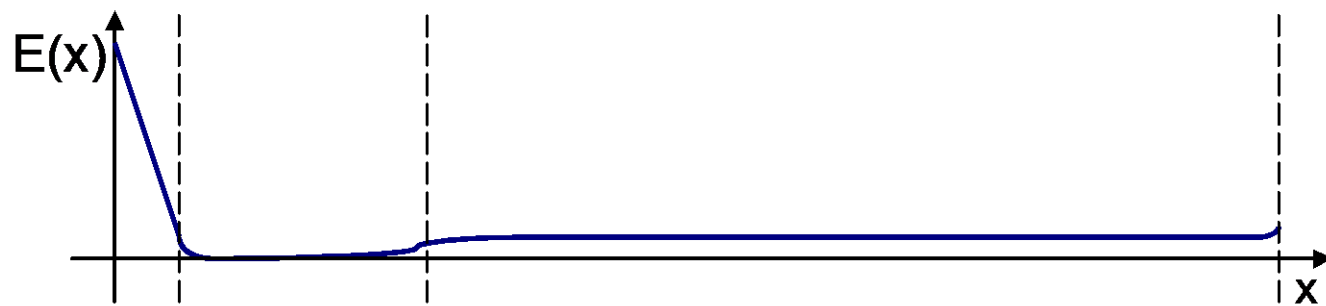
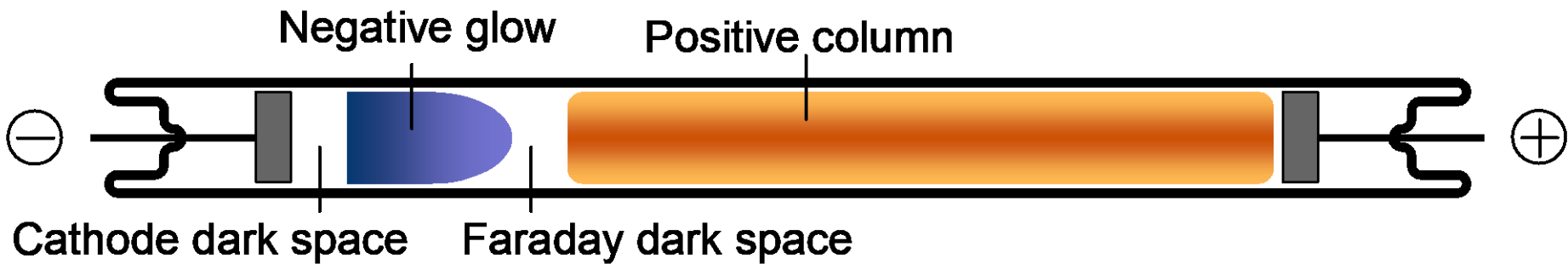


He is also known for the [Paschen series](#), a series of hydrogen spectral lines in the infrared region that he first observed in 1908. He established the now widely used [Paschen curve](#) in his article "*Über die zum Funkenübergang in Luft, Wasserstoff und Kohlensäure bei verschiedenen Drücken erforderliche Potentialdifferenz*".^[1]

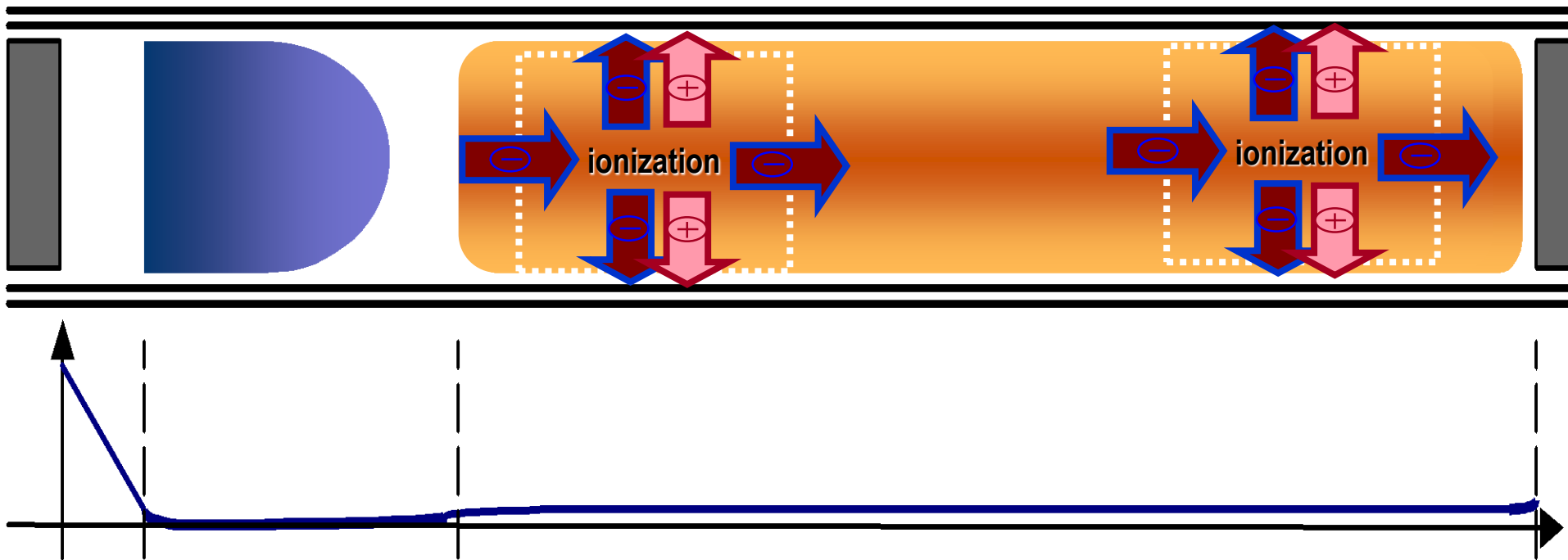
Paschen's law is an equation that gives the [breakdown voltage](#), that is, the [voltage](#) necessary to start a discharge or [electric arc](#), between two electrodes in a gas [as a function of pressure and gap length](#).^{[2][3]} It is named after [Friedrich Paschen](#) who discovered it empirically in 1889.

Glow discharges

$$p \approx 0.1 - 10 \text{ mbar} ; U \approx 150 - 2000 \text{ V}$$



A simple glow discharge theory I. – the positive column

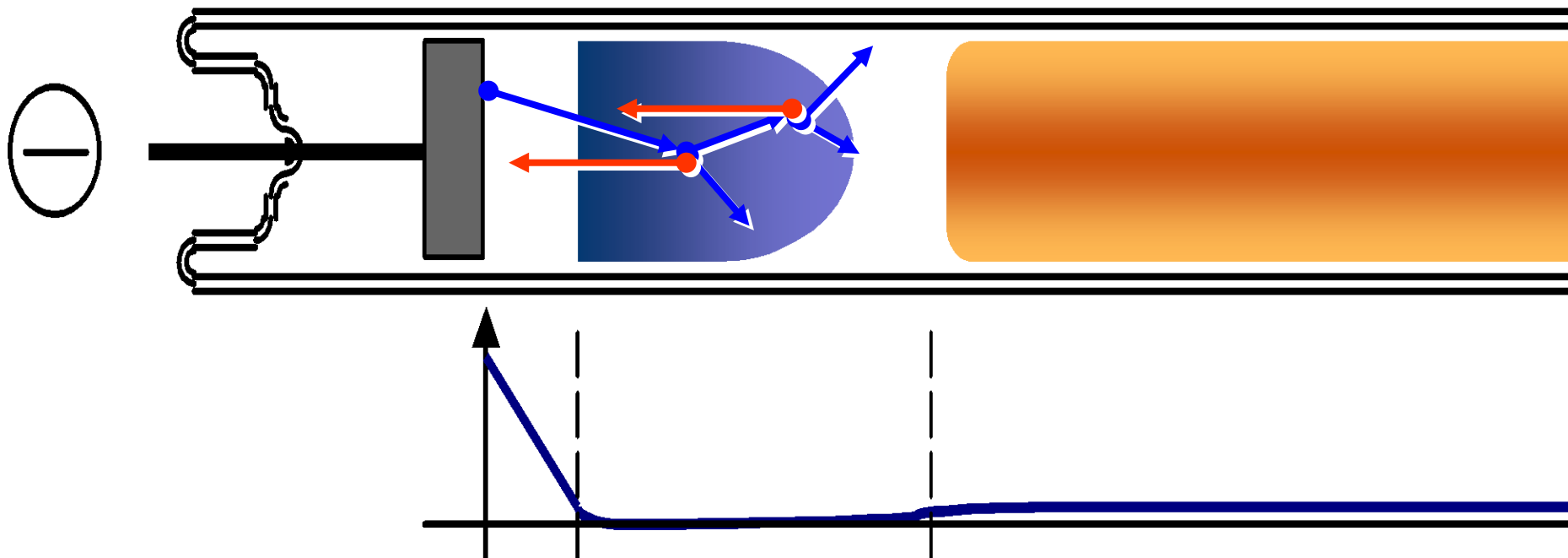


Electron emission from the cathode:

- ~~field (auto) emission~~
- ~~thermal emission~~
- due to bombarding ions

secondary electron emission coef. $\gamma \approx 0.1$

A simple glow discharge theory II. – the negative glow



Self sustained discharge: the number of ions created in an avalanche can produce one new electron on the cathode

Gas lasers

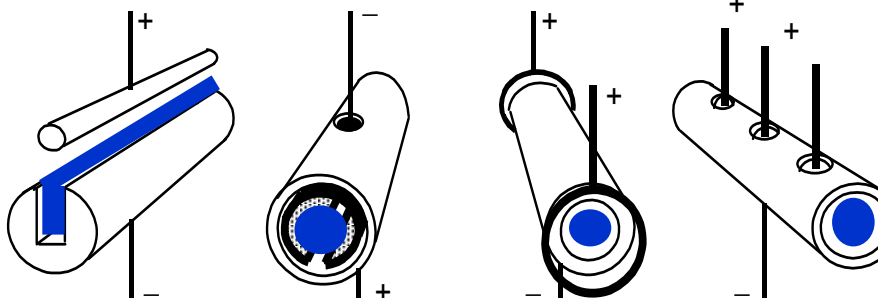


1. Negative glow lasers –
hollow cathode lasers

2. Positive column lasers



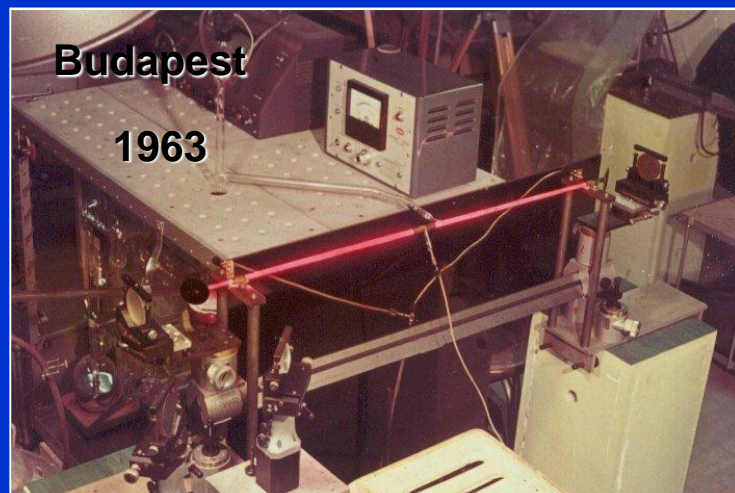
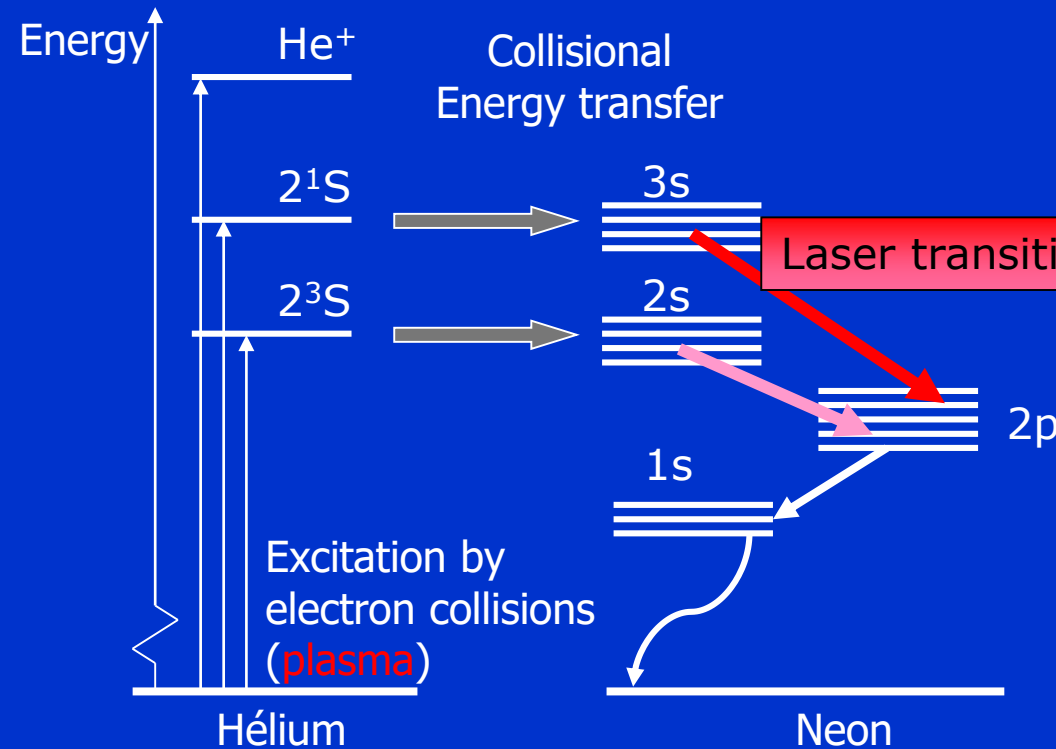
He-Ne laser



Silver ion laser

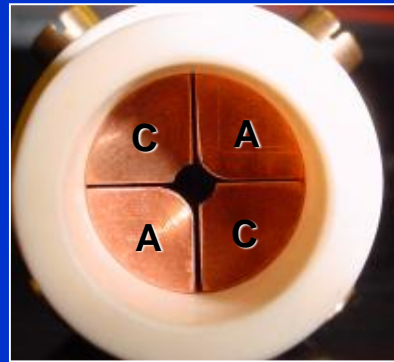
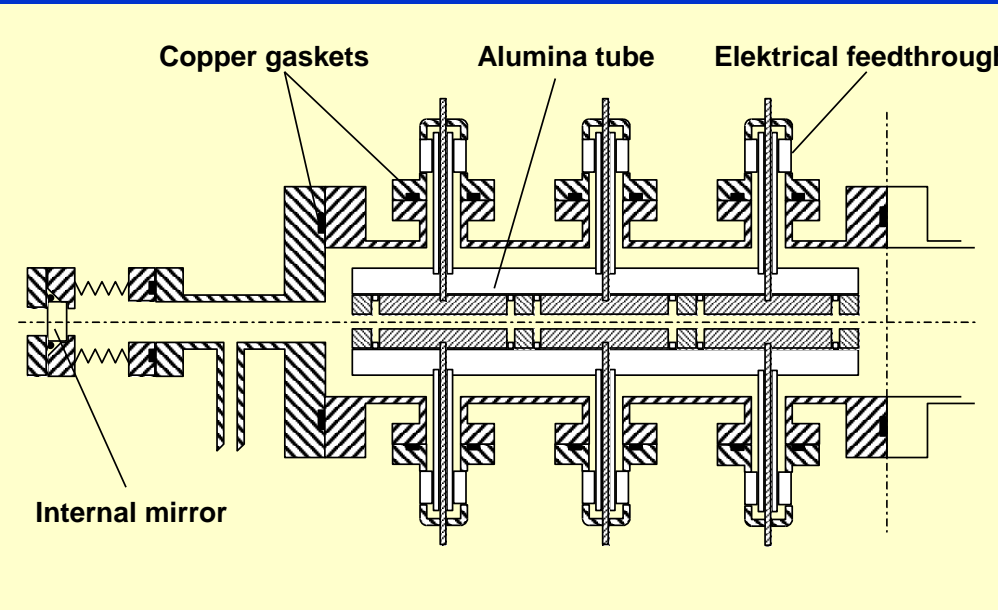
The He-Ne laser

how to make
population inversion ?



Iranian American physicist and inventor. He was the first to propose the concept of the gas laser in 1959 at the Bell Telephone Laboratories. **1960 Iran**

Segmented hollow-cathode silver ion laser



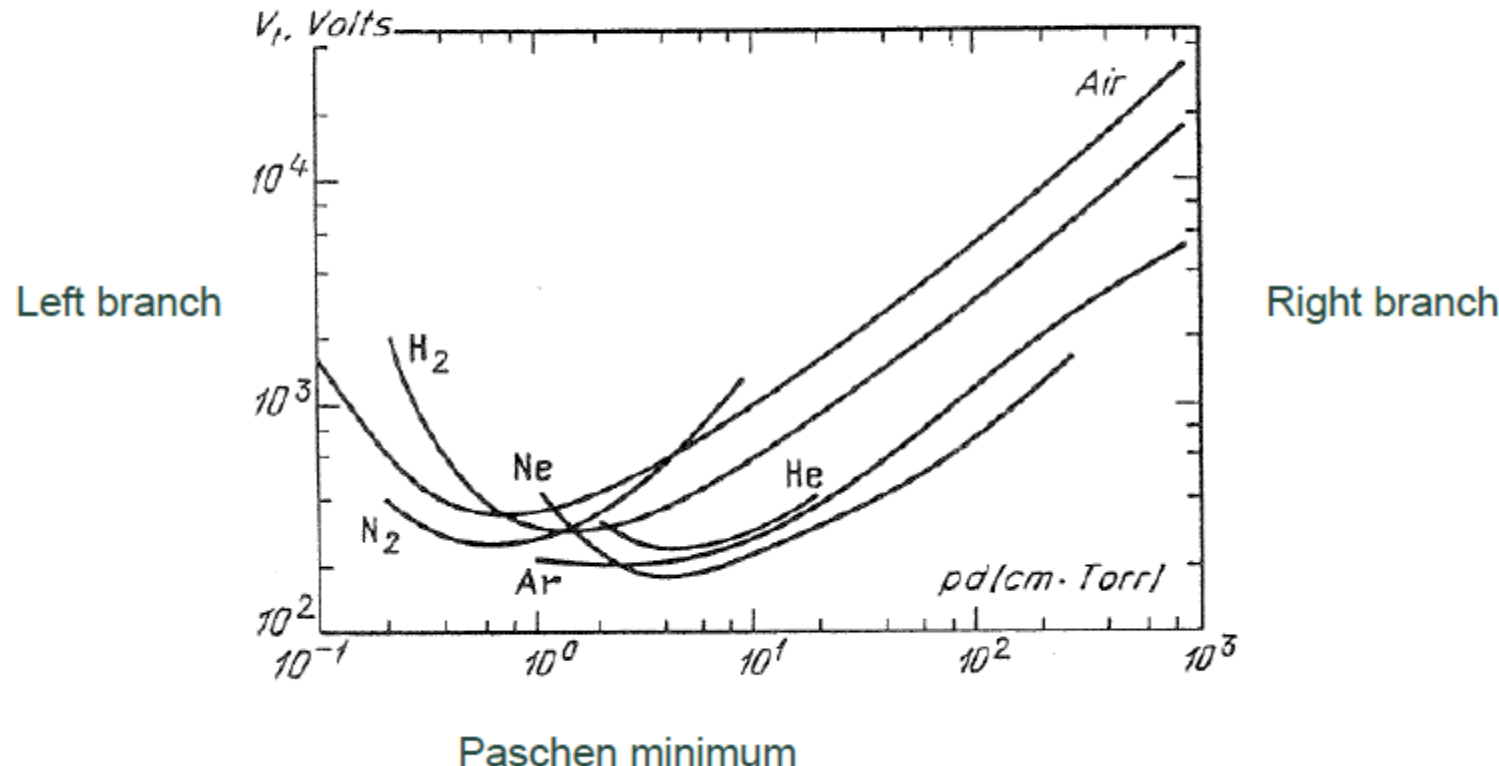
+ 20 μm silver



Paschen's curves

Gas breakdown: Paschen's curves for breakdown voltages in various gases

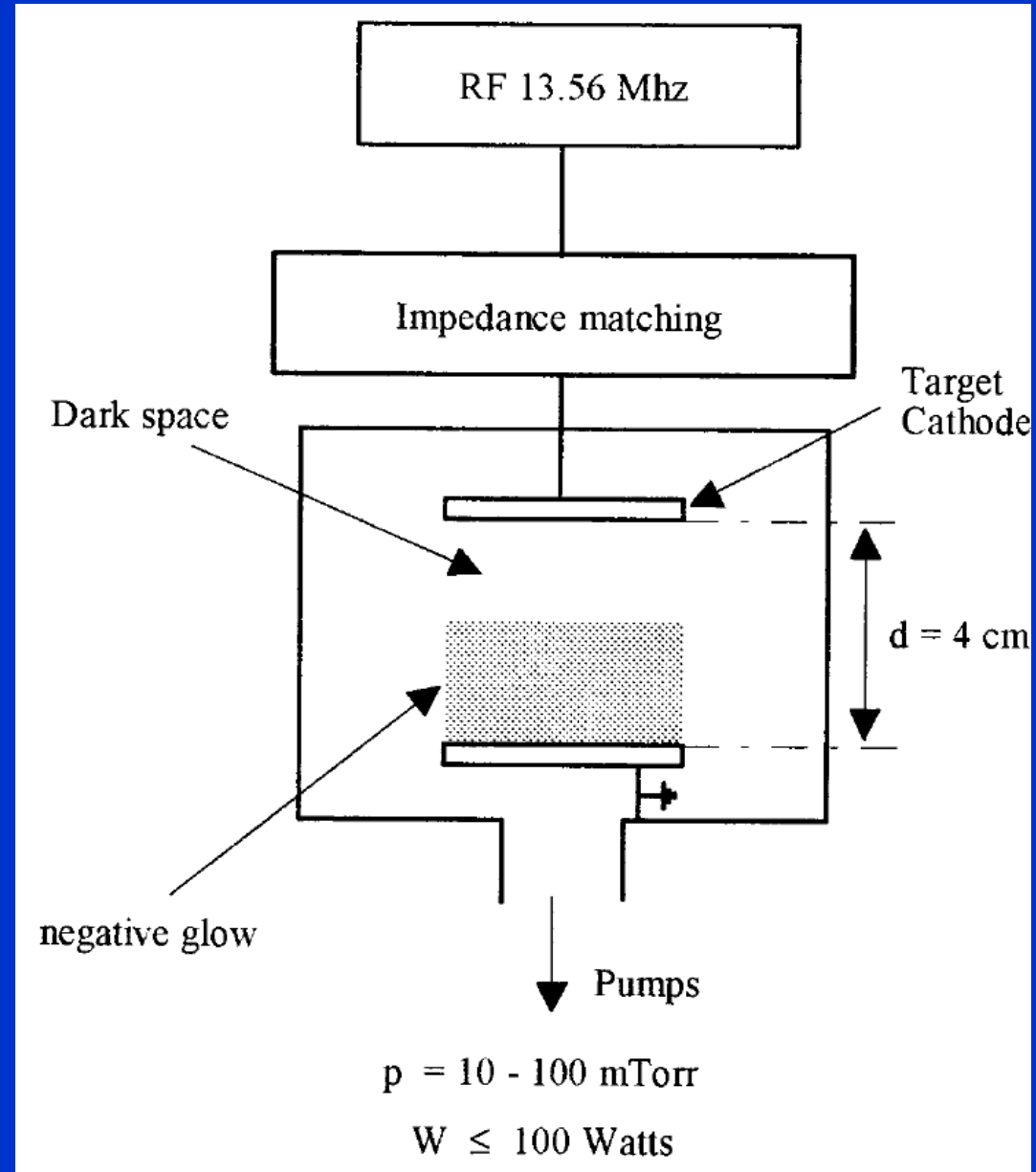
- Friedrich Paschen discovered empirically in 1889.



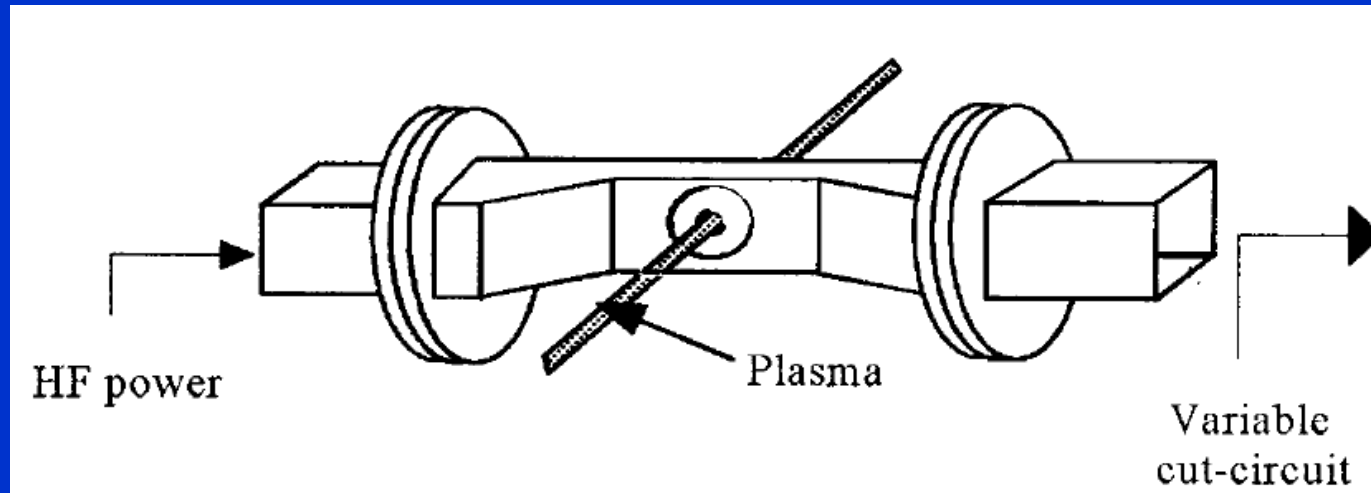
F. Paschen, Wied. Ann. 37, 69 (1889)]

RF diode discharge

For technological applications –
surface treatments



Microwave discharge



Microwave discharge → surfaguige discharge

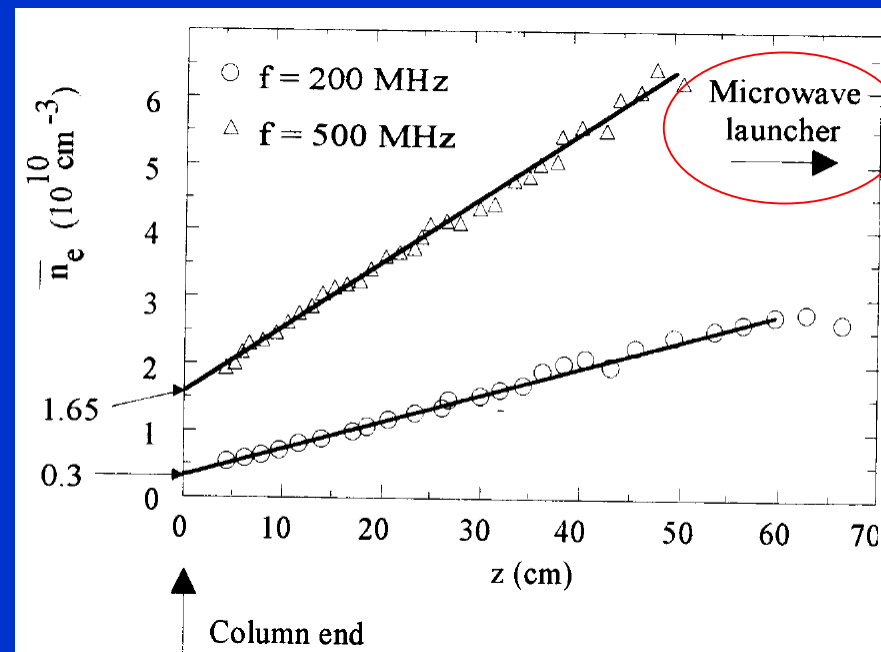
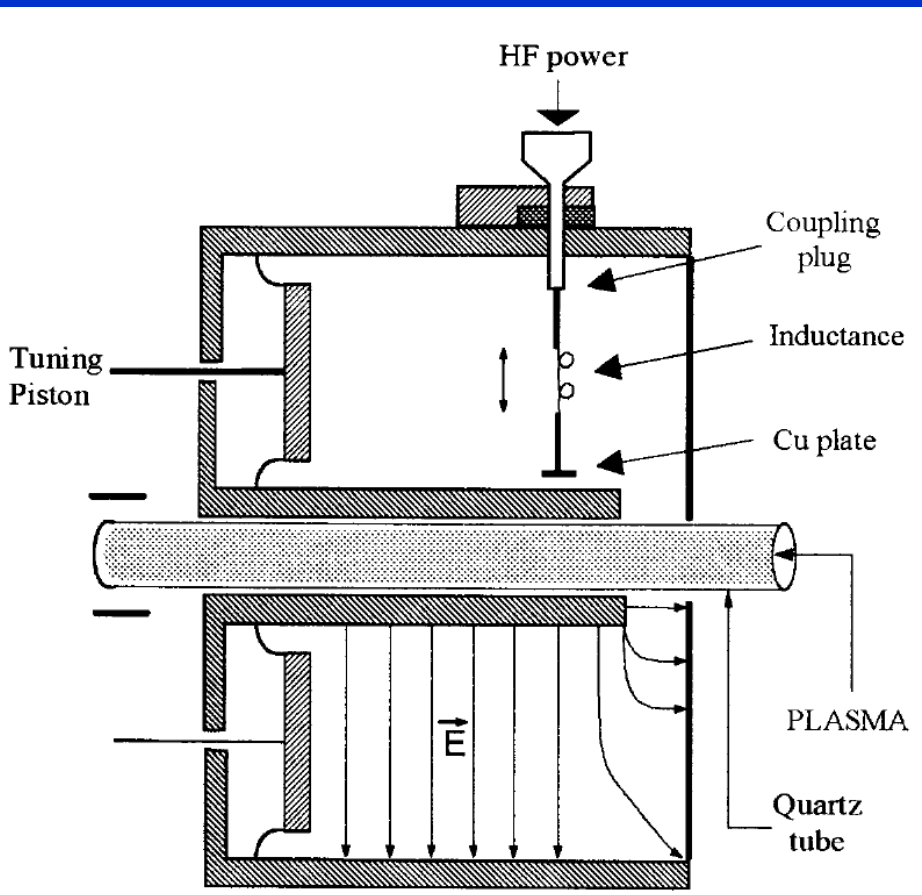
Vlnovodwaveguide

Surfatron discharge

A special characteristic of surface waves is to propagate along the discharge tube wall and to penetrate inside the tube to create the plasma. The radial distribution of electric field is given by the following equation (note 2 p. 11) :

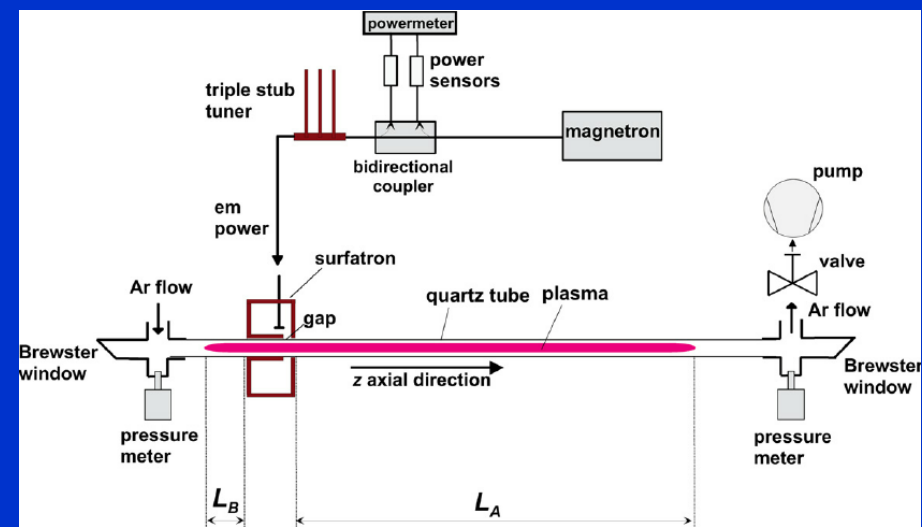
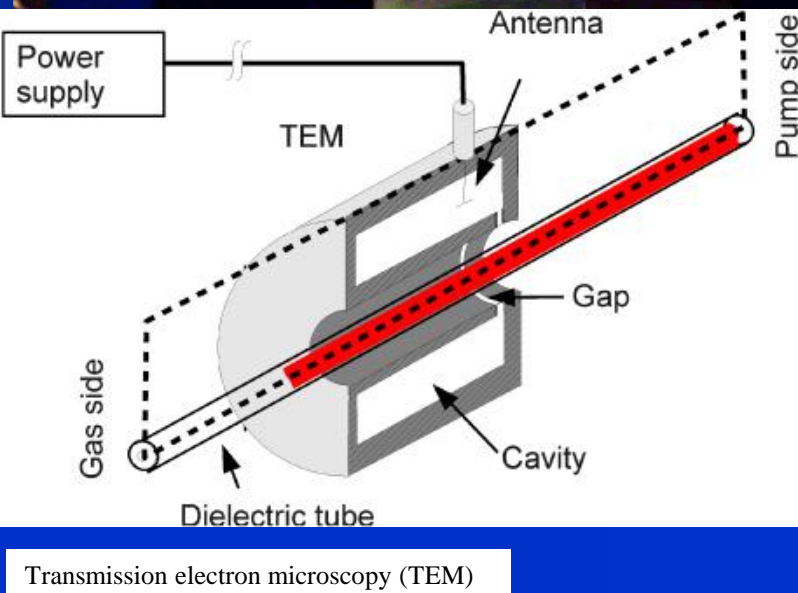
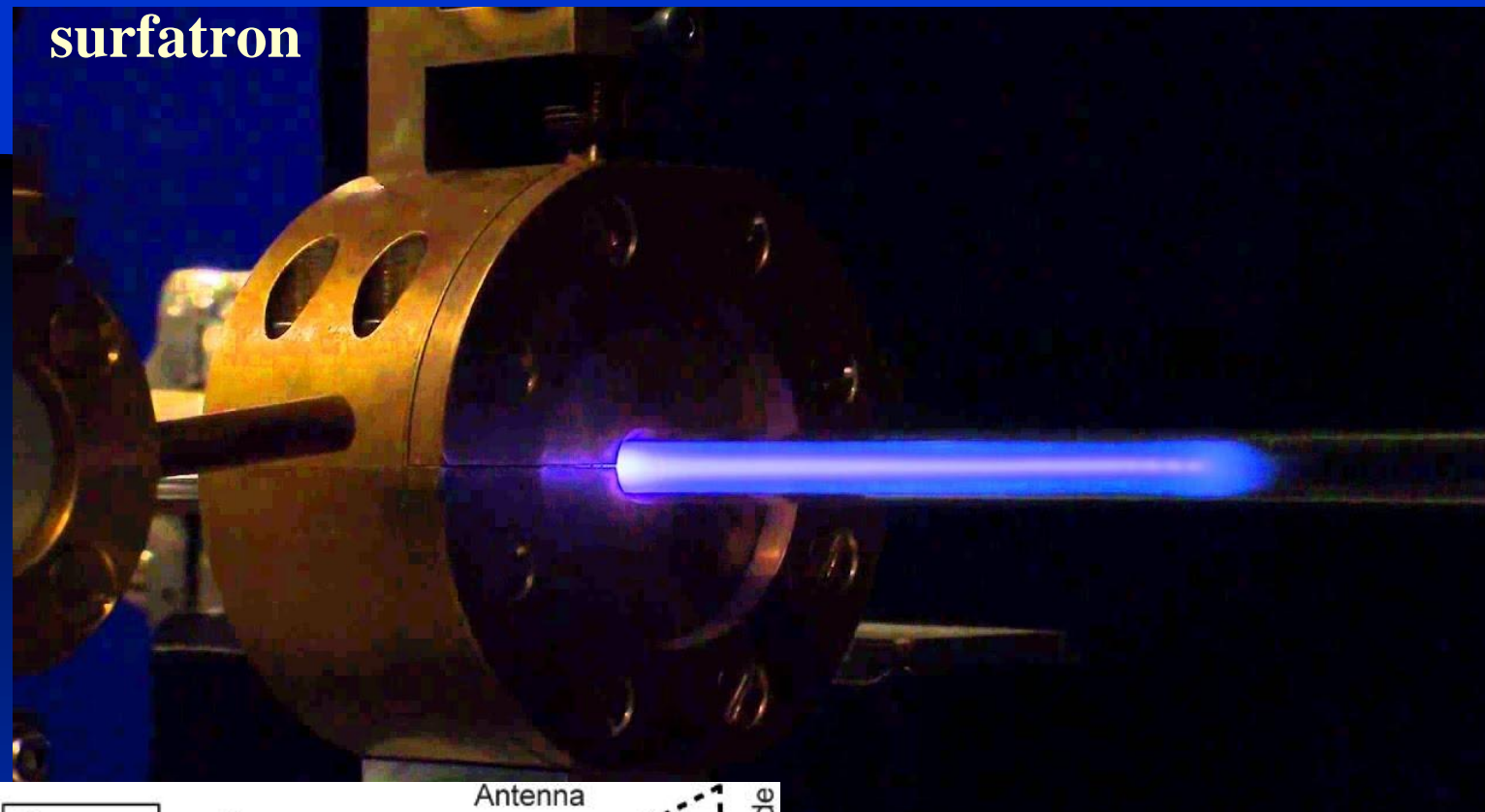
$$E(r) = A I_0 (B n_e^{1/2} r) \quad (1-34)$$

where A and B are constant values and I_0 is the modified Bessel function.



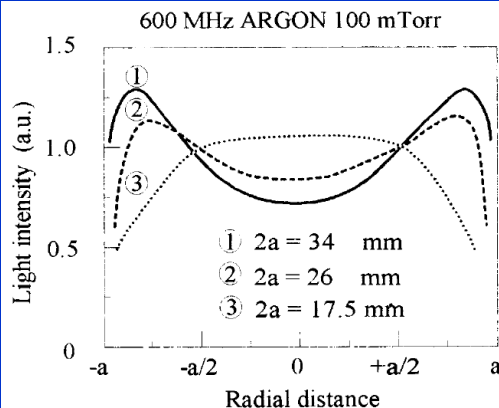
Axial distribution of electron density, measured in microwave plasma columns (Ar, 0.1 Torr, $R = 1.3 \text{ cm}$) at 200 and 500 MHz.

surfatron

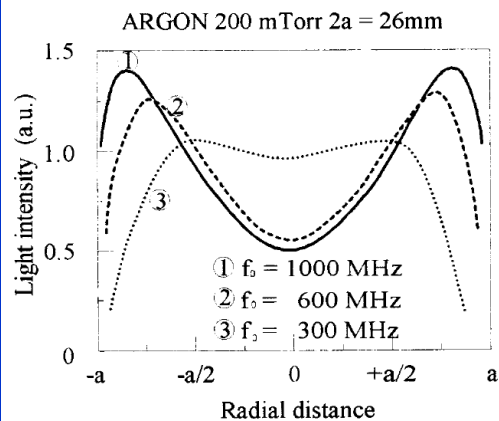


Surfatron

Thus, the $E(r)$ value is maximum for $r = R$ and it is minimum for $r = 0$. The local maximum of electric field at the tube wall is more pronounced as the electron density and the tube radius increase. This effect has been observed by analyzing the plasma light⁽⁹⁾



(a)



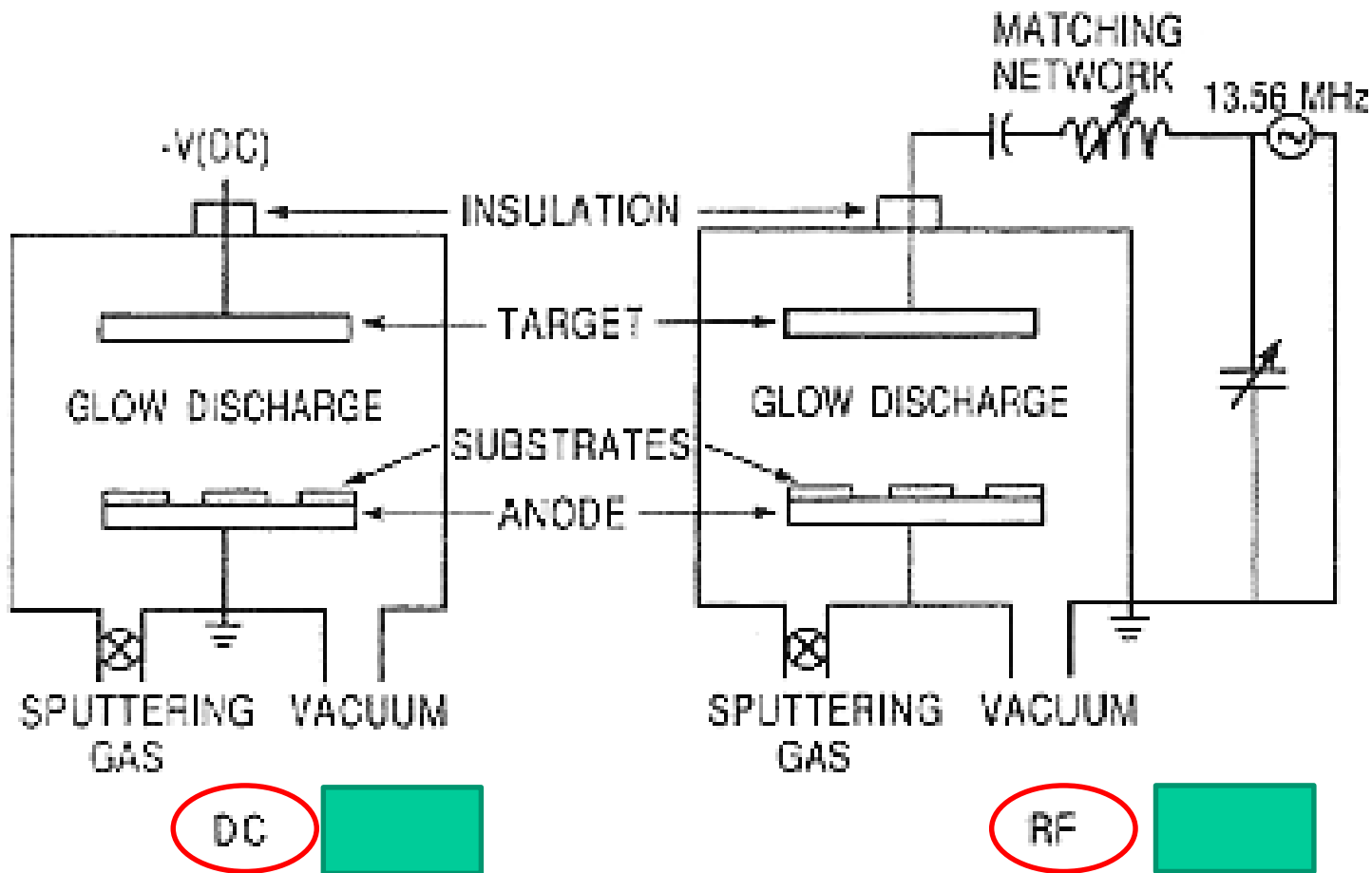
(b)

Radial distribution of the Ar I 549.6 nm line intensity in microwave discharge.

(a) 600 MHz, 0.1 Torr and several values of diameter ($2a$)

(b) diameter $2a = 26 \text{ mm}$ and several values of microwave frequencies.

Two Sputtering Systems



Several kilovolts are applied and gas pressures usually range from a few to a hundreds millitorr.

Types of plasmas (electron density)

- Stars (density $n < 10^7 \text{ cm}^{-3}$)
- Solar winds (density $n < 10^7 \text{ cm}^{-3}$)
- Coronas (density $n < 10^7 \text{ cm}^{-3}$)
- Ionosphere (density $n < 10^7 \text{ cm}^{-3}$)
- Glow discharge (density $n = 10^8 \sim 10^{14} \text{ cm}^{-3}$)
- Arcs (density $n = 10^8 \sim 10^{14} \text{ cm}^{-3}$)
- High-pressure arc (density $n \sim 10^{20} \text{ cm}^{-3}$)
- Shock tubes (density $n \sim 10^{20} \text{ cm}^{-3}$)
- Fusion reactors (density $n \sim 10^{20} \text{ cm}^{-3}$)



The Townsend (symbol Td) is a physical unit of the reduced electric field (ratio E/N), Where E is electric field and N is concentration of neutral particles.

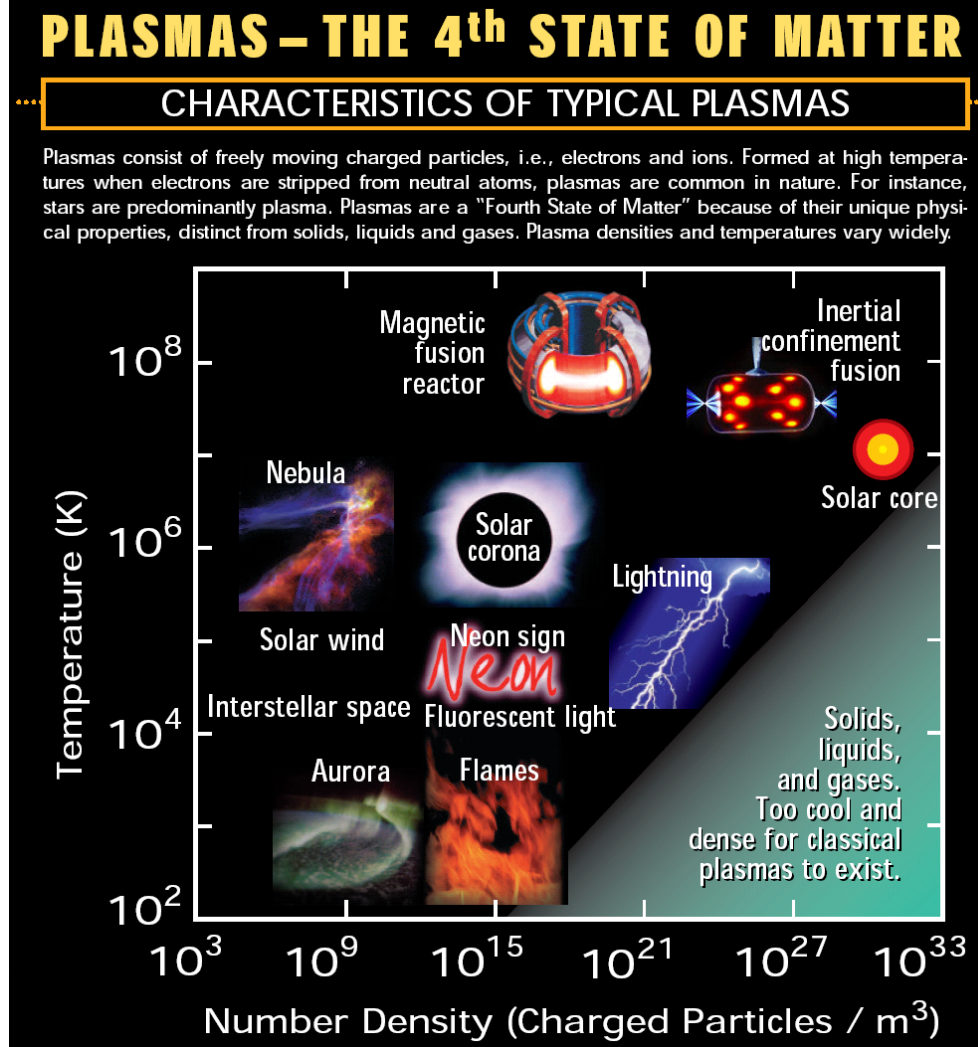
$$1 \text{ Townsend} = 1 \text{ Td} = 10^{-17} \text{ Vcm}^2 = 10^{-21} \text{ Vm}^2.$$

$$1 \text{ V/cm Torr} = 3,034 \text{ Td}; \quad \text{resp.} \quad 1 \text{ Td} = 0,3296 \text{ V/cm Torr}.$$

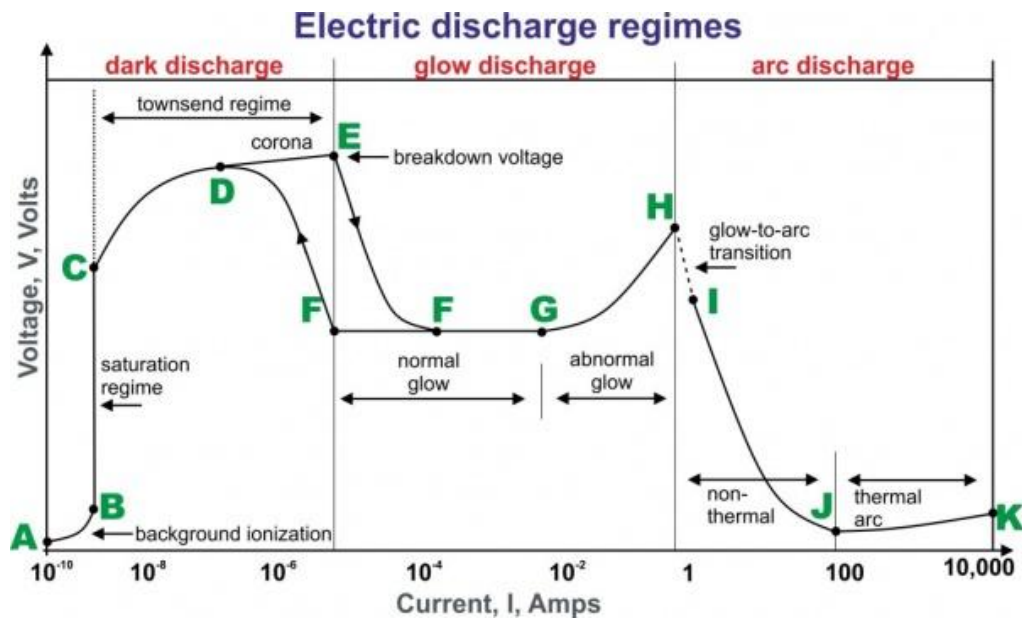
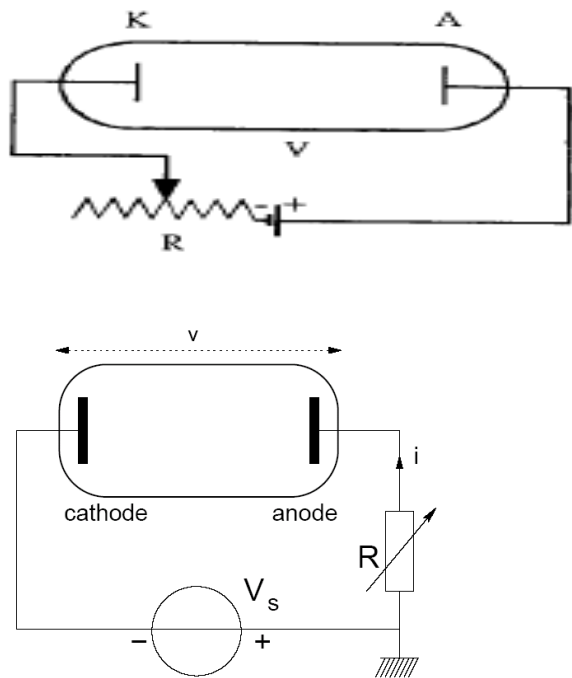
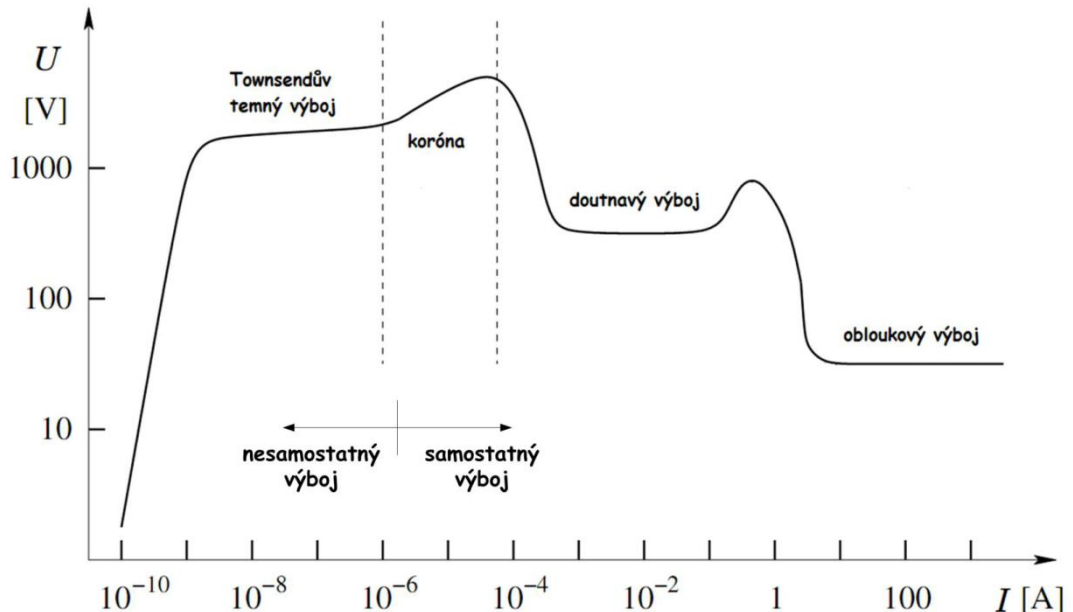


Types of plasmas (electron density)

- Stars (density $n < 10^7 \text{ cm}^{-3}$)
- Solar winds (density $n < 10^7 \text{ cm}^{-3}$)
- Coronas (density $n < 10^7 \text{ cm}^{-3}$)
- Ionosphere (density $n < 10^7 \text{ cm}^{-3}$)
- Glow discharge (density $n = 10^8 \sim 10^{14} \text{ cm}^{-3}$)
- Arcs (density $n = 10^8 \sim 10^{14} \text{ cm}^{-3}$)
- High-pressure arc (density $n \sim 10^{20} \text{ cm}^{-3}$)
- Shock tubes (density $n \sim 10^{20} \text{ cm}^{-3}$)
- Fusion reactors (density $n \sim 10^{20} \text{ cm}^{-3}$)



Principal Glow Discharge Mechanism by Biased Parallelplate



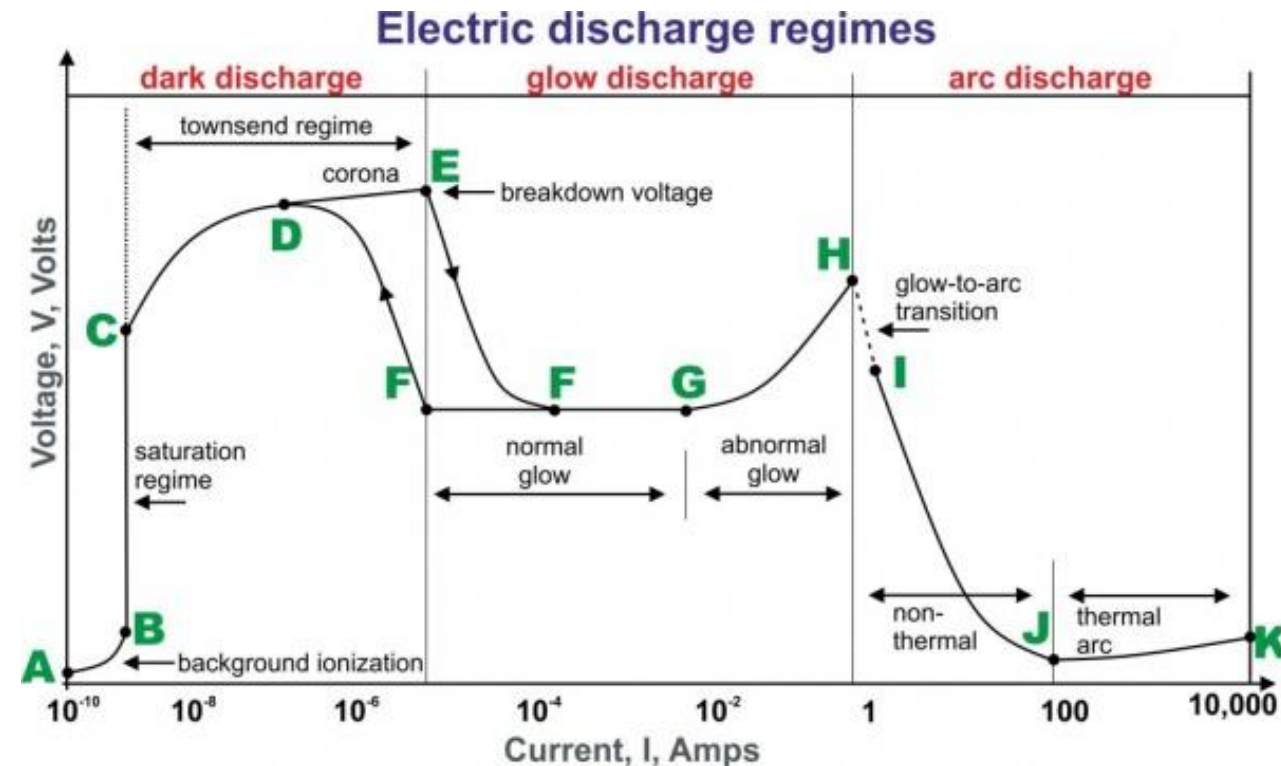
The regime between A and E on the voltage-current characteristic is termed a dark discharge because, except for corona discharges and the breakdown itself, the discharge remains invisible to the eye.

A – B During the background ionization stage of the process the electric field applied along the axis of the discharge tube sweeps out the ions and electrons created by ionization from background radiation. Background radiation from cosmic rays, radioactive minerals, or other sources, produces a constant and measurable degree of ionization in air at atmospheric pressure. The ions and electrons migrate to the electrodes in the applied electric field producing a weak electric current. Increasing voltage sweeps out an increasing fraction of these ions and electrons

B – C If the voltage between the electrodes is increased far enough, eventually all the available electrons and ions are swept away, and the current saturates. In the saturation region, the current remain constant while the voltage is increased. This current depends linearly on the radiation source strength, a regime useful in some radiation counters.

C – E If the voltage across the low pressure discharge tube is increased beyond point C, the current will rise exponentially. The electric field is now high enough so the electrons initially present in the gas can acquire enough energy before reaching the anode to ionize a neutral atom. As the electric field becomes even stronger, the secondary electron may also ionize another neutral atom leading to an avalanche of electron and ion production. The region of exponentially increasing current is called the Townsend discharge.

D – E Corona discharges occur in Townsend dark discharges in regions of high electric field near sharp points, edges, or wires in gases prior to electrical breakdown. If the coronal currents are high enough, corona discharges can be technically “glow discharges”, visible to the eye. For low currents, the entire corona is dark, as appropriate for the dark discharges. Related phenomena include the silent electrical discharge, an inaudible form of filamentary discharge, and the brush discharge, a luminous discharge in a non-uniform electric field where many corona discharges are active at the same time and form streamers through the gas.



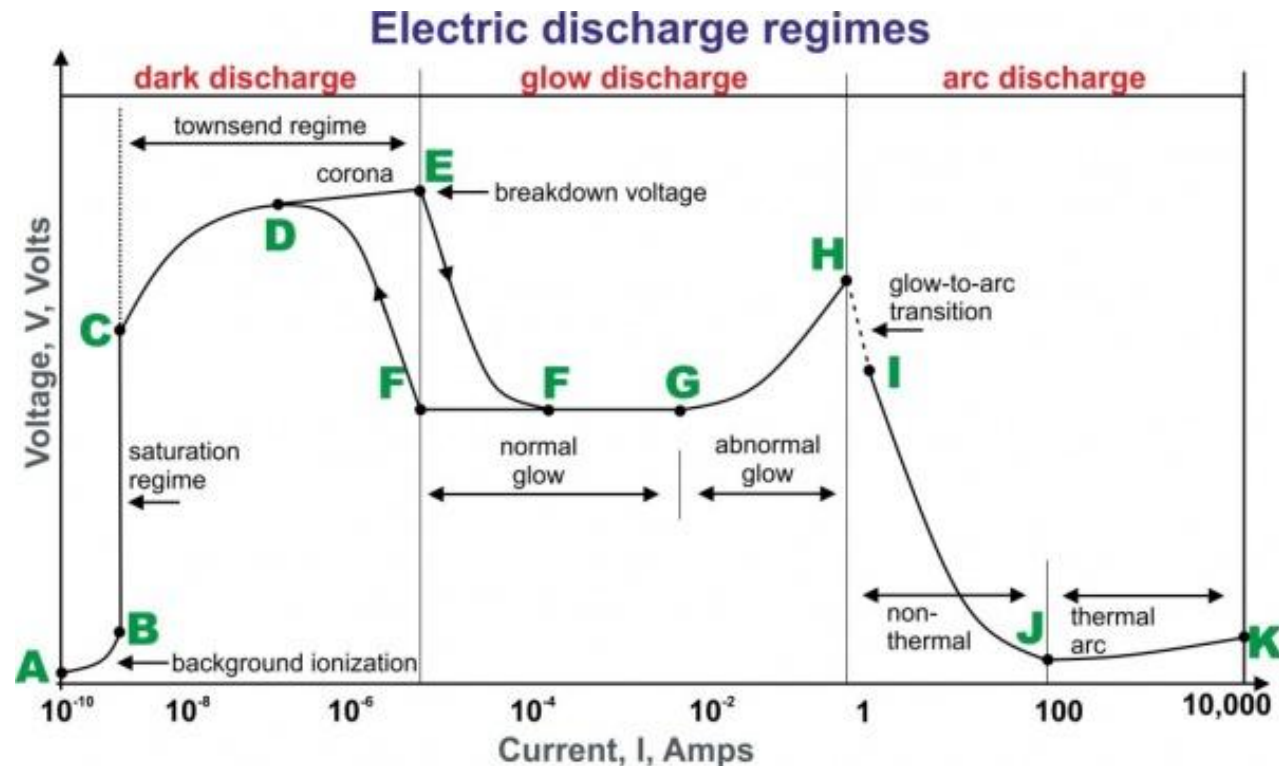
E Electrical breakdown occurs in Townsend regime with the addition of secondary electrons emitted from the cathode due to ion or photon impact. At the breakdown, or sparking potential V_B , the current might increase by a factor of 10^4 to 10^8 , and is usually limited only by the internal resistance of the power supply connected between the plates. If the internal resistance of the power supply is very high, the discharge tube cannot draw enough current to break down the gas, and the tube will remain in the corona regime with small corona points or brush discharges being evident on the electrodes. If the internal resistance of the power supply is relatively low, then the gas will break down at the voltage V_B , and move into the normal glow discharge regime. The breakdown voltage for a particular gas and electrode material depends on the product of the pressure and the distance between the electrodes, pd , as expressed in Paschen's law (1889).

Glow Discharge (normal glow mode)

The glow discharge regime owes its name to the fact that the plasma is luminous. The gas glows because the electron energy and number density are high enough to generate visible light by excitation collisions. The applications of glow discharge include fluorescent lights, dc parallel plate plasma reactors, "magnetron" discharges used for depositing thin films, and electro bombardment plasma sources.

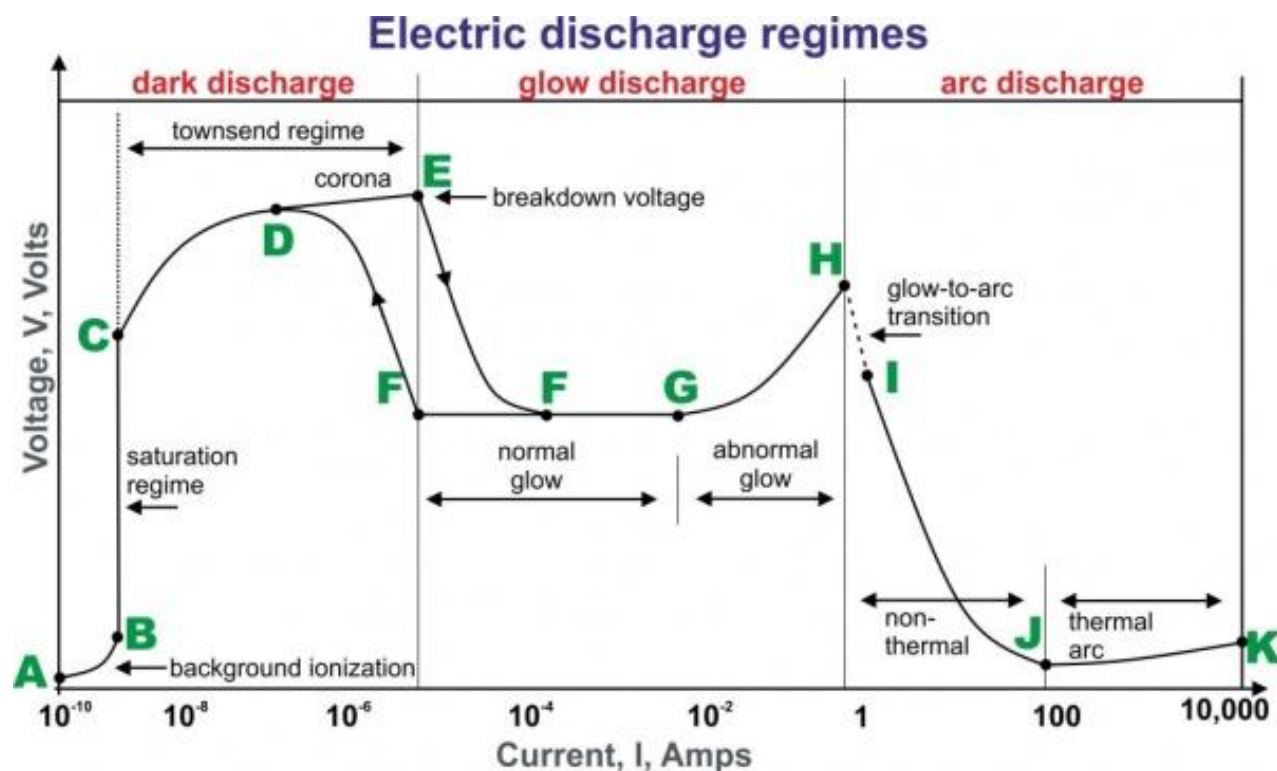
F – G After a discontinuous transition from E to F, the gas enters the normal glow region, in which the voltage is almost independent of the current over several orders of magnitude in the discharge current. The electrode current density is independent of the total current in this regime. This means that the plasma is in contact with only a small part of the cathode surface at low currents. As the current is increased from F to G, the fraction of the cathode occupied by the plasma increases, until plasma covers the entire cathode surface at point G.

G – H In the abnormal glow regime above point G, the voltage increases significantly with the increasing total current in order to force the cathode current density above its natural value and provide the desired current. Starting at point G and moving to the left, a form of hysteresis is observed in the voltage-current characteristic. The discharge maintains itself at considerably lower currents and current densities than at point F and only then makes a transition back to Townsend regime.



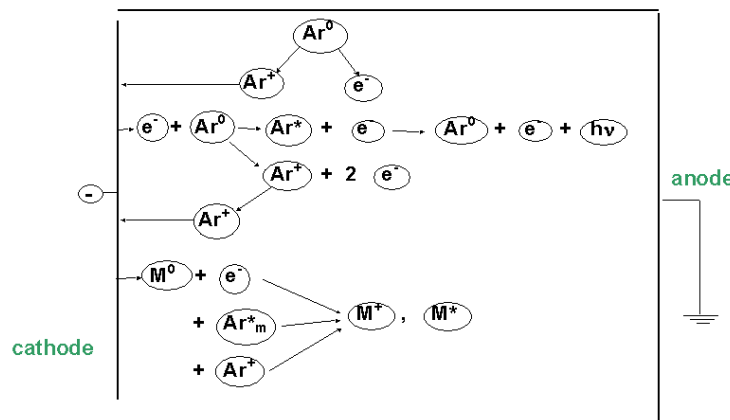
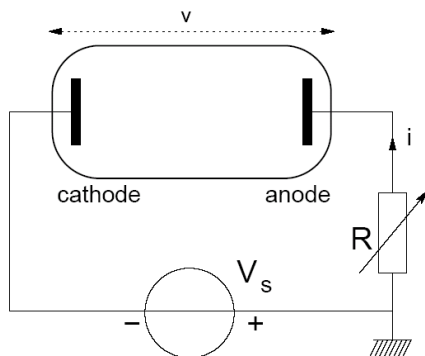
Arc Discharges (arc mode)

H – K At point H, the electrodes become sufficiently hot that the cathode emits electrons thermionically. If the DC power supply has a sufficiently low internal resistance, the discharge will undergo a glow-to-arc transition, H-I. The arc regime, from I through K is one where the discharge voltage decreases as the current increases, until large currents are achieved at point J, and after that the voltage increases slowly as the current increases.



Principal Glow Discharge Mechanism by Biased Parallelplate

1. A stray electron near the cathode carrying an initial current i_0 is accelerated toward the anode by the applied electric field (E).
2. After gaining sufficient energy the electron collides with a neutral gas atom (A) converting it into a positively charged ion (A^+), i.e., $e^- + A \rightarrow 2e^- + A^+$.
3. Two electrons are generated and are accelerated and bombard two additional neutral gas atoms, generating more ions and electrons, and so on.
4. Meanwhile, the electric field drives ions in the opposite direction.
5. Ions collide with the cathode, ejecting, among other particles, *secondary electrons*.
6. Secondary electrons also undergo charge multiplication. (step 2)
7. The effect snowballs until a sufficiently large avalanche current ultimately causes the gas to breakdown.



Electrical Breakdown in Gases

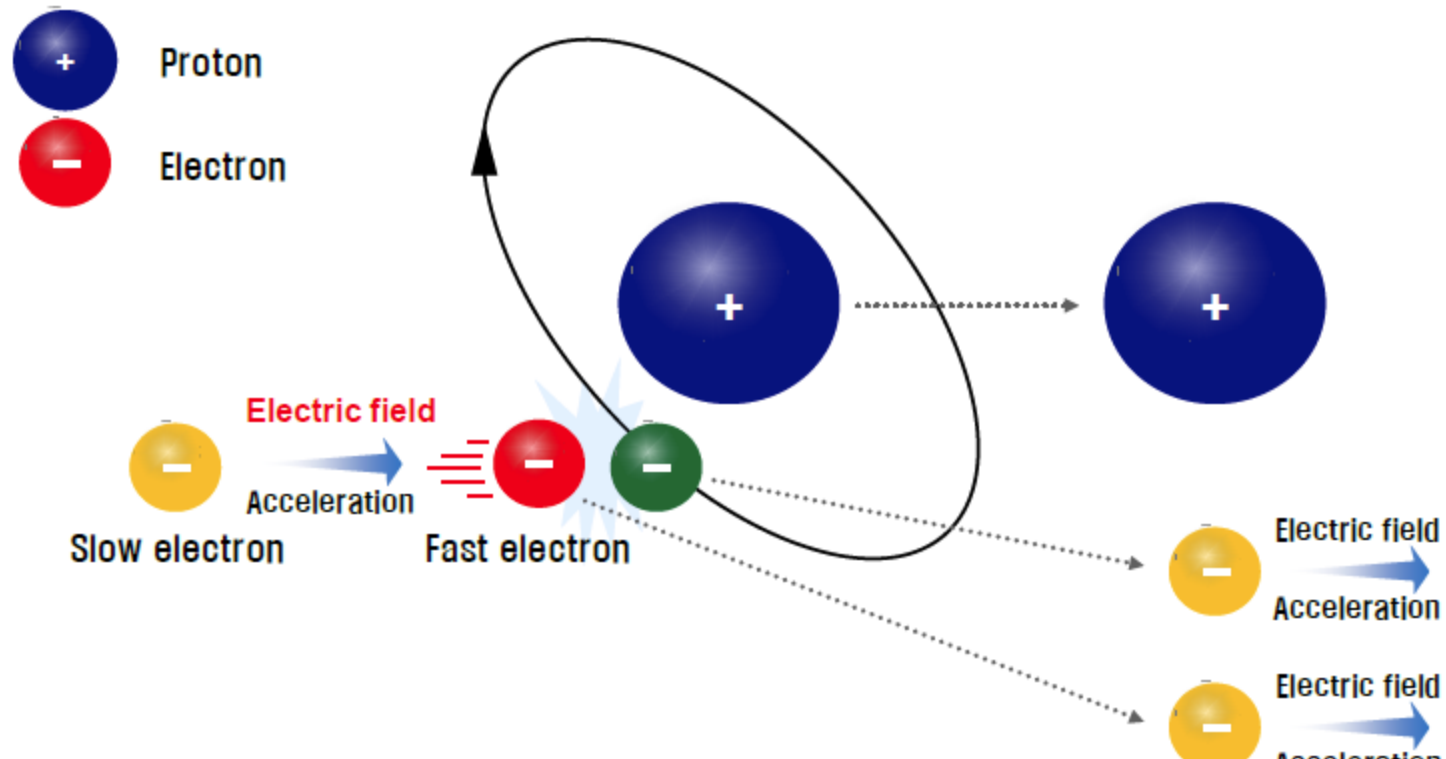
Fall, 2018

Kyoung-Jae Chung

Department of Nuclear Engineering

Seoul National University

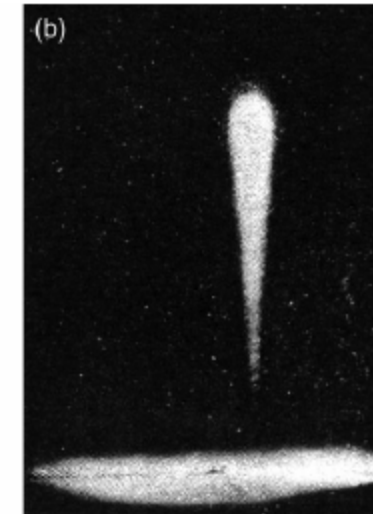
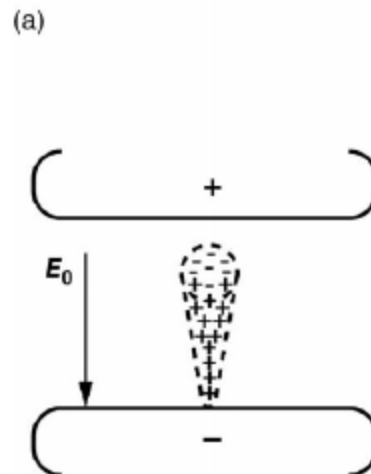
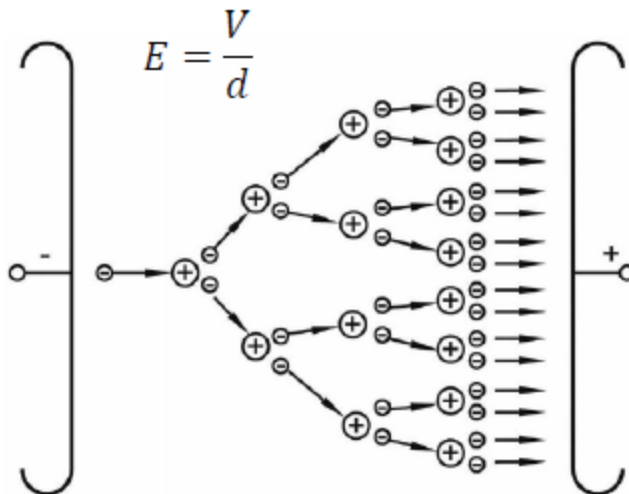
Generation of charged particles: electron impact ionization



Ionization energy of hydrogen: 13.6 eV

Electron avalanche

Townsend mechanism: electron avalanche



- Townsend ionization coefficient (α) : electron multiplication
- : production of electrons per unit length along the electric field
(ionization event per unit length)

$$\frac{dn_e}{dx} = \alpha n_e$$

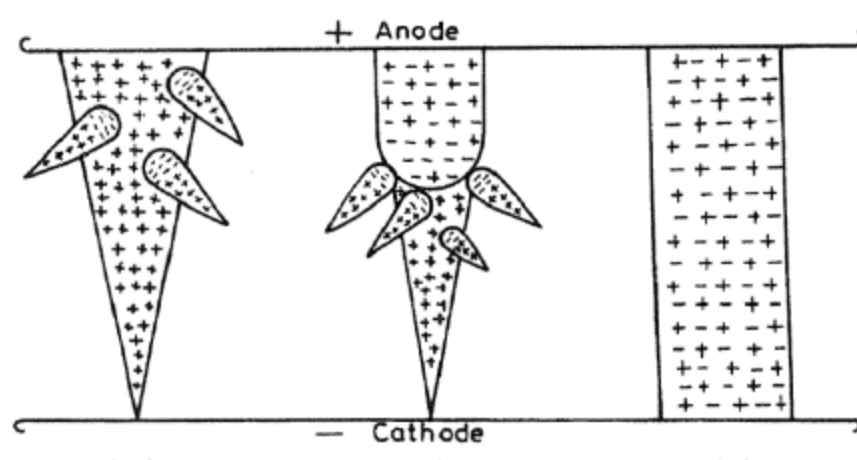
$$n_e = n_{e0} \exp(\alpha x)$$

$$M = \frac{n_e}{n_{e0}} = e^{\alpha x}$$

Streamer mechanism

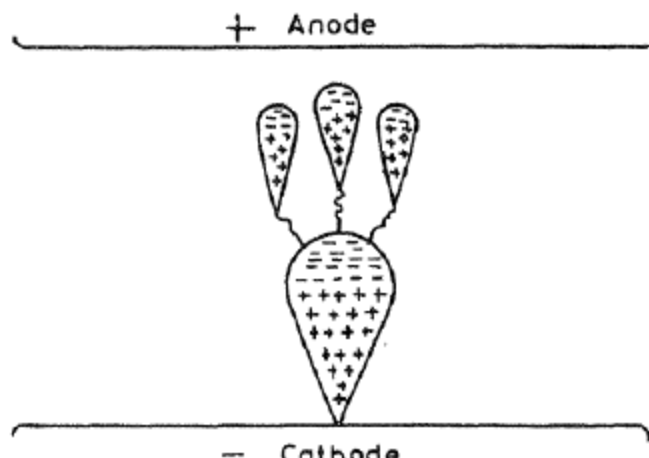
- The streamer concept was proposed by Loeb and Meek for the positive streamer and, independently by Raether for the negative streamer.
- Basic idea is that at a certain stage in the development of a single avalanche, **photoionization** of the gas in the inter-electrode space becomes the most important mechanism in determining the breakdown of the gap.

Meek & Loeb



Cathode-directed streamer

Raether

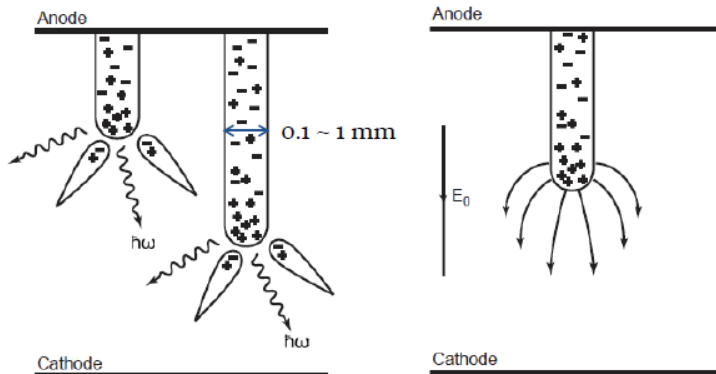


Anode-directed streamer

Calculation of avalanche...

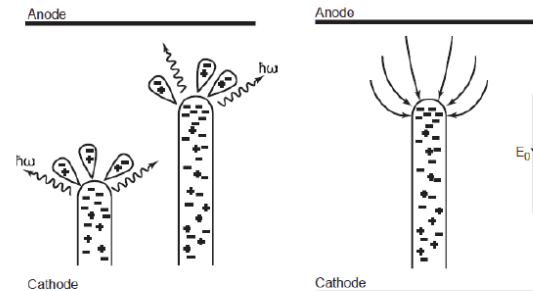
Positive streamer (cathode-directed streamer)

- If the gap is short, the transformation occurs only when the avalanche reaches the anode. Such a streamer that grows from anode to cathode and called the cathode-directed or positive streamer.



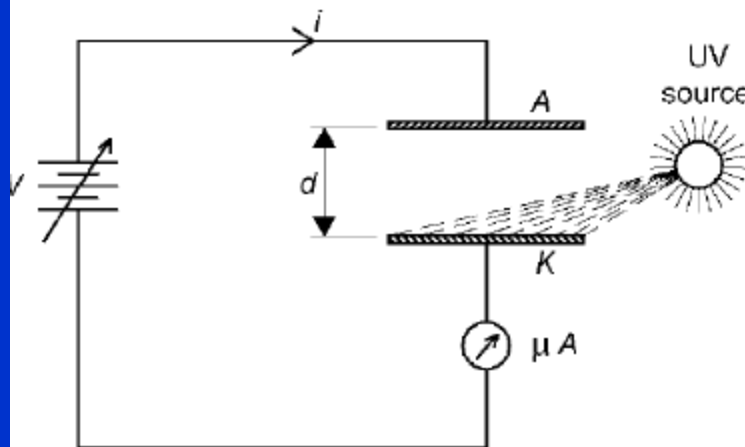
Negative streamer (anode-directed streamer)

- If the gap and overvoltage are large, the avalanche-to-streamer transformation can take place far from the anode, and the anode-directed or negative streamer grows toward both electrodes.



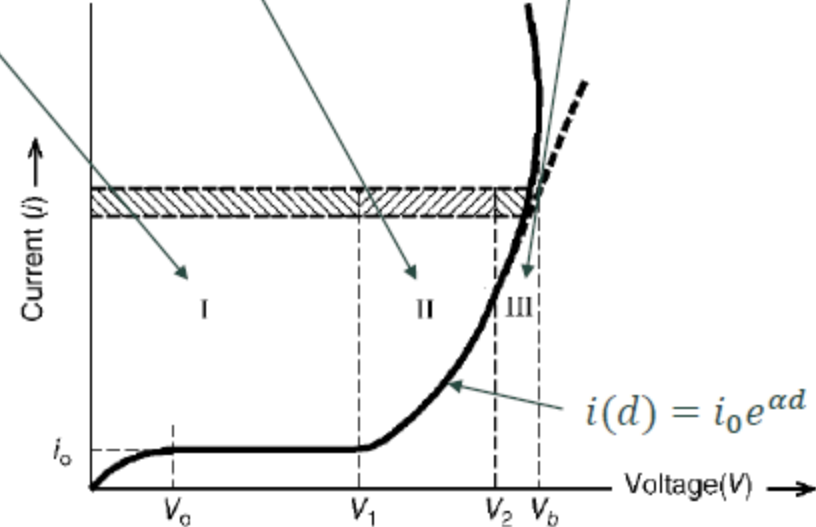
Townsend's avalanche process is not self-sustaining

Ionization-free region (recombination region + saturation region)



Townsend first ionization region

Townsend second ionization region



- Townsend's avalanche process cannot be sustained without external sources for generating seed electrons.

$j \sim f(d)$

E/N

$j \sim f(d, E/N)$

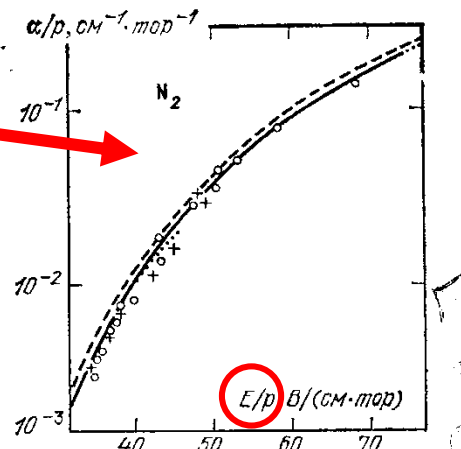
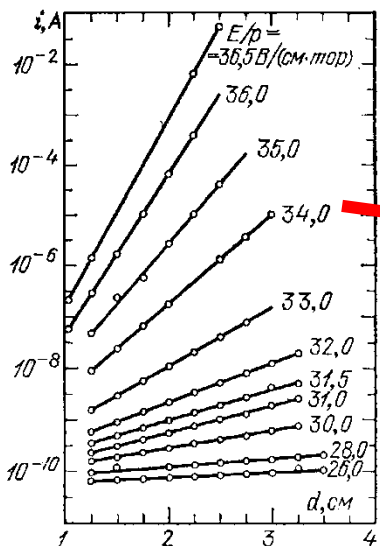
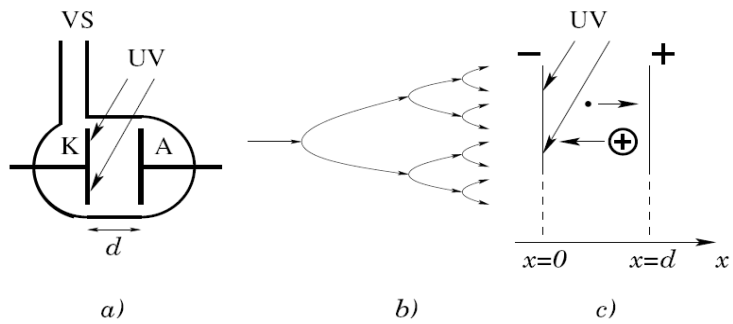


Рис. 5.3. Экспериментальный график, демонстрирующий постоянство α и экспоненциальный характер нарастания тока в разрядном промежутке; ионизационные коэффициенты определяются наклонами прямых [6]

Рис. 5.4. Ионизационный коэффициент Таунсенда α в N_2 по разным измерениям



Obr. 5.2: Zapaľovanie výboja: a) výbojka na meranie zapaľovacieho napätia: K - katóda, A - anóda, UV - ultrafialové žiarenie zabezpečujúce emisiu primárnych elektrónov, VS - napojenie na vákuový systém; b) elektrónová lavína; c) označenie polohy elektrod

$$\frac{dj_-}{dx} = \alpha n_- = \frac{\alpha}{V_-} n_- V_- = \delta j_-$$

$$j \sim j_0 \exp(\alpha x)$$

$$E/N \dots 1 \text{ Townsend} = 1 \text{ Td} = 10^{-17} \text{ Vcm}^2 = 10^{-21} \text{ Vm}^2$$

$$E/p \text{ at } 293 \text{ K (cca } 20 \text{ C)} \dots 1 \text{ V/cmTorr} = 3.034 \text{ Td, resp.} \quad 1 \text{ Td} = 0,3296 \text{ V/cmTorr}$$

Electric discharges

Electron Impact Ionization in a Constant Field

Ionization in case of Maxwell distribution

Ionization Frequency

$n(\varepsilon)$ is the electron energy distribution

$$(dn_e/dt)_i = \nu_i n_e = k_i N n_e$$

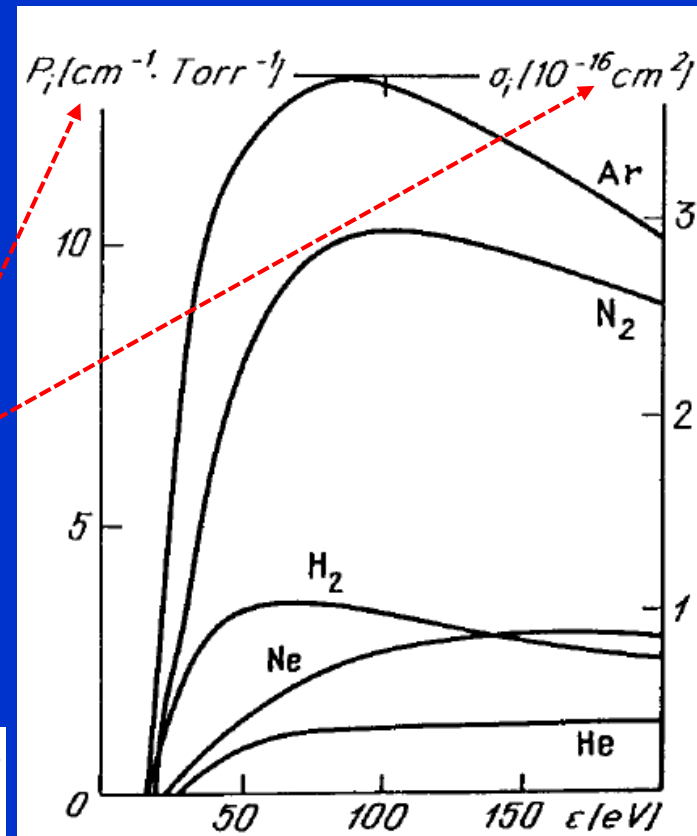
$$\nu_i = N \int n(\varepsilon) v \sigma_i(\varepsilon) d\varepsilon / \int n(\varepsilon) d\varepsilon = N \langle v \sigma_i \rangle \equiv N k_i$$

$$n(\varepsilon) \propto \exp(-\varepsilon/kT_e)$$

$$\sigma_i(\varepsilon) = C_i(\varepsilon - I)$$

$$\nu_i = N \bar{v} C_i (I + 2kT_e) \exp(-I/kT_e), \quad \bar{v} = (8kT_e/\pi m)^{1/2}$$

Fig. 4.1. Cross sections and probabilities of electron impact ionization. From [4.1]



For example, in argon, $C_i = 2 \cdot 10^{-17} \text{ cm}^2/\text{eV}$. If $T_e = 1 \text{ eV}$, then $\bar{v} = 6.7 \cdot 10^7 \text{ cm/s}$ and $k_i = \langle v \sigma_i \rangle = 3 \cdot 10^{-16} \text{ cm}^3/\text{s}$. If $p = 50 \text{ Torr}$ and $T = 300 \text{ K}$, then $N = 1.7 \cdot 10^{18} \text{ cm}^{-3}$. This gives $\nu_i = 510 \text{ s}^{-1}$. At these T_e and N , the equilibrium degree of ionization is $(n_e)_{\text{eq}}/N = 0.021$. The values of C_i for several other gases (in $10^{-17} \text{ cm}^2/\text{eV}$) are

$$\text{He} - 0.13, \text{Ne} - 0.16, \text{Hg} - 7.9, \text{N}_2 - 0.85, \text{O}_2 - 0.68, \text{H}_2 - 0.59.$$

Breakdown cannot be simply explained by ionization

Ionization frequency and ionization coefficient

For example, in argon, $C_i = 2 \cdot 10^{-17} \text{ cm}^2/\text{eV}$. If $T_e = 1 \text{ eV}$, then $\bar{v} = 6.7 \cdot 10^7 \text{ cm/s}$ and $k_i = \langle v\sigma_i \rangle = 3 \cdot 10^{-16} \text{ cm}^3/\text{s}$. If $p = 50 \text{ Torr}$ and $T = 300 \text{ K}$, then $N = 1.7 \cdot 10^{18} \text{ cm}^{-3}$. This gives $\nu_i = 510 \text{ s}^{-1}$. At these T_e and N , the equilibrium degree of ionization is $(n_e)_{\text{eq}}/N = 0.021$. The values of C_i for several other gases (in $10^{-17} \text{ cm}^2/\text{eV}$) are

$$\text{He} - 0.13, \text{ Ne} - 0.16, \text{ Hg} - 7.9, \text{ N}_2 - 0.85, \text{ O}_2 - 0.68, \text{ H}_2 - 0.59.$$

N will be double within 1.4ms \rightarrow if $n_0=1$ \rightarrow at $T=1\text{eV}$ equilibrium will be reached within 75ms
Experiments are giving time many times shorter

It is more convenient, therefore, to characterize the rate of ionization not by frequency $\nu_i \text{ s}^{-1}$, but by the ionization coefficient $\alpha \text{ cm}^{-1}$, that is, the number of ionization events performed by an electron in a 1cm path along the field.

$$\alpha = \nu_i / v_d, \quad \nu_i = \alpha v_d$$

Note that the primary and complete characteristic of the rate of ionization is the frequency ν_i , not α . The distribution function gives us this frequency, as well as the drift velocity. The ionization coefficient α is a derived quantity, found from (4.3). Actually, α is not very meaningful in fast-oscillating fields. However, dc measurements give us α , not ν_i .

Breakdown cannot be simply explained by ionization

medzi elektródami (obr. 5.2 c). Povrch katódy K sa nachádza v mieste $x = 0$ a povrch anódy A v mieste $x = d$. Elektróny sa pohybujú smerom k anóde a vytvorené kladné ióny ku katóde, kde zanikajú. Podobne ako v odseku 4.3.1, môžeme napísť rovnicu kontinuity pre elektróny v jednorozmernej geometrii a v ustálenom stave

$$\frac{dj_-}{dx} = \alpha n_- = \frac{\alpha}{V_-} n_- V_- = \delta j_- , \quad (5.2)$$

kde V_- je driftová rýchlosť elektrónov v elektrickom poli (v homogénnom poli je konštantná) a $\delta = \alpha/V_-$ je **prvý Townsendov koeficient**. Analogická rovnica platí aj pre kladné ióny

$$\frac{dj_+}{dx} = \alpha n_- = \delta j_- . \quad (5.3)$$

Prvý Townsendov koeficient δ má rozmer m^{-1} a označuje počet ionizácií, ktoré vykoná jeden elektrón v smere elektrického poľa na jednotkovej dráhe (na rozdiel od ionizačnej frekvencie α udávajúcej počet ionizácií za jednotku času). Ak rovnice odčítame, dostaneme

$$\frac{d(j_+ - j_-)}{dx} = 0 \Rightarrow j_+ - j_- = K = \text{konšt.}$$

Potom hustota elektrického prúdu medzi elektródami $i = e(j_+ - j_-) = eK$ je taktiež konštantná, napriek tomu, že hustoty toku elektrónov a iónov sa menia s polohou x . V homogénnom poli je Townsendov koeficient δ konštantný a preto môžeme rovnice kontinuity ľahko integrovať

$$j_- = C \exp(\delta x) ; \quad j_+ = C \exp(\delta x) + i/e ,$$

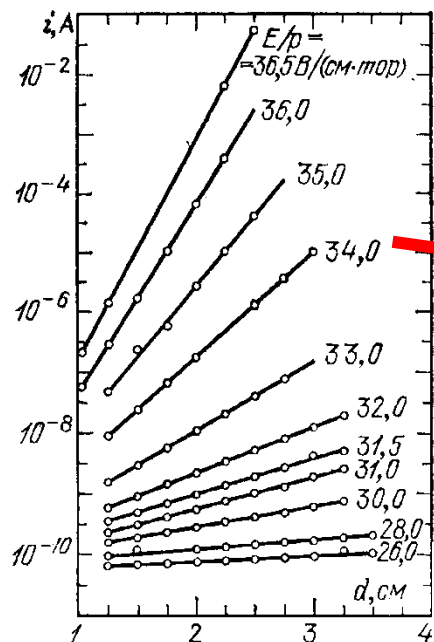
kde C je integračná konštanta. Hodnota tejto integračnej konštanty sa dá určiť z hustoty toku elektrónov na katóde: $C = j_-(0)$. Potom

$$j_- = j_-(0) \exp(\delta x) ; \quad j_+ = j_-(0) \exp(\delta x) + i/e . \quad (5.4)$$

Problém určenia hustoty toku $j_-(0)$ spočíva v tom, že okrem primárnych elektrónov emitovaných z katódy ultrafialovým žiareniom (ich hustotu toku označíme j_0), elektróny emitujú aj dopadajúce kladné ióny. Tento typ emisie sa nazýva **potenciálová emisia**.

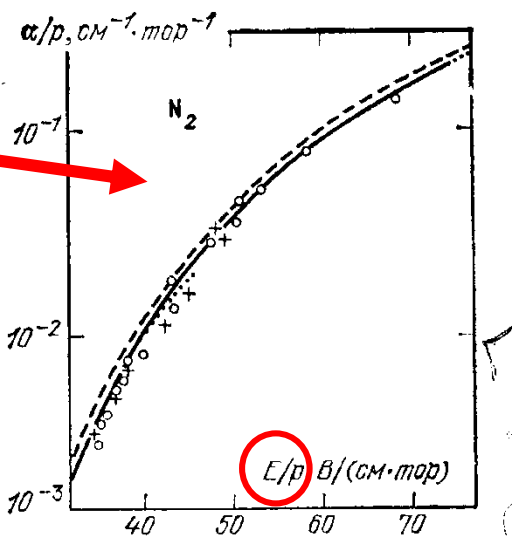
Experimental data

i



d

α/p



Р и с. 5.3. Экспериментальный график, демонстрирующий постоянство α и экспоненциальный характер нарастания тока в разрядном промежутке; ионизационные коэффициенты определяются наклонами прямых [6]

Р и с. 5.4. Ионизационный коэффициент Таунсенда α в N_2 по разным измерениям

$$\frac{dj_-}{dx} = \alpha n_- = \frac{\alpha}{V_-} n_- V_- = \delta j_-$$

i : charge current

α : Townsend ionization coefficient

γ_e : Townsend secondary-electron emission coefficient

d : Distance between electrodes

Measurements of α and similarity laws



$$dN/dx = \alpha N, \quad N(x) = N_0 \exp(\alpha x)$$

The electron current at the anode is $i = eN_0 \exp(\alpha d)$

α/p

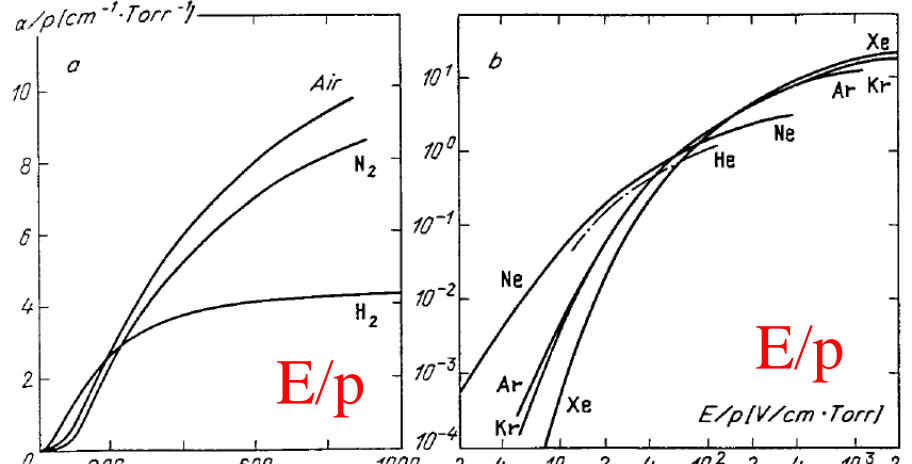


Fig. 4.3. Ionization coefficients for a wide range of E/p values (a) in molecular gases, (b) in inert gases. From [4.3]

dU/dt is not considered

E/p

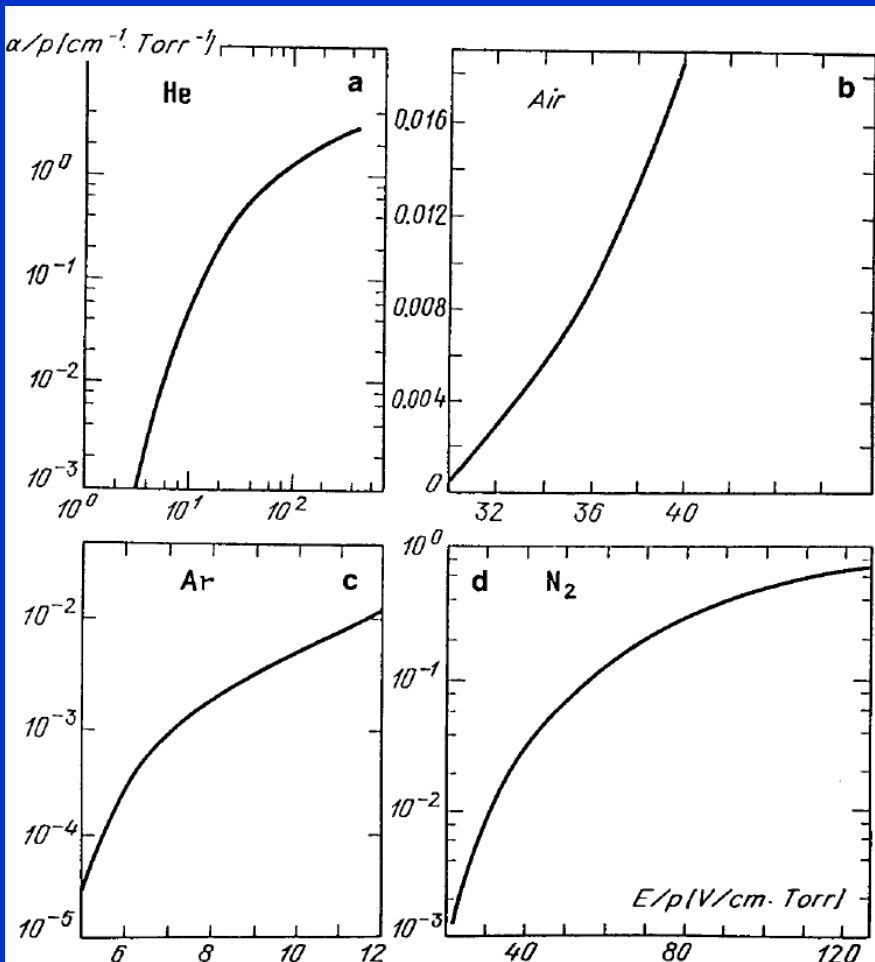


Fig. 4.2. Ionization coefficient in a) He, b) air, c) Ar, d) N₂. From [4.2]

Data for Paschen law

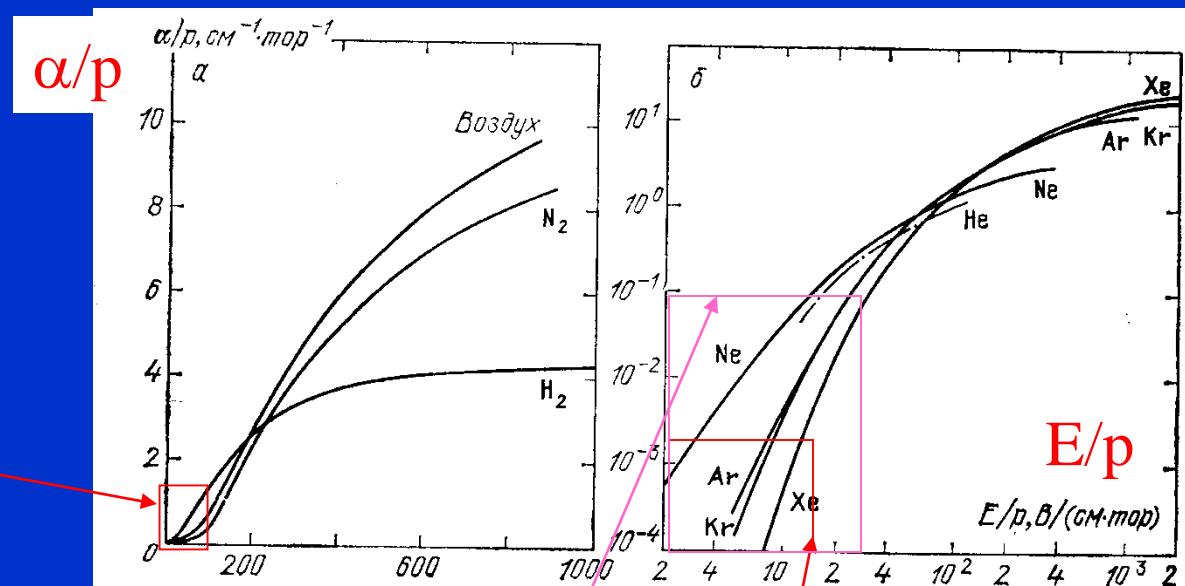
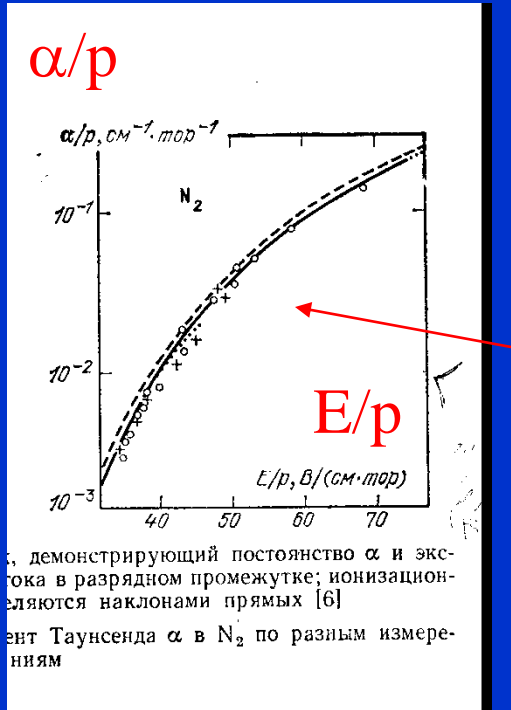


Рис. 5.6. Ионизационный коэффициент в широком диапазоне E/p : а — в H_2 , N_2 и в воздухе, б — в инертных газах [6]

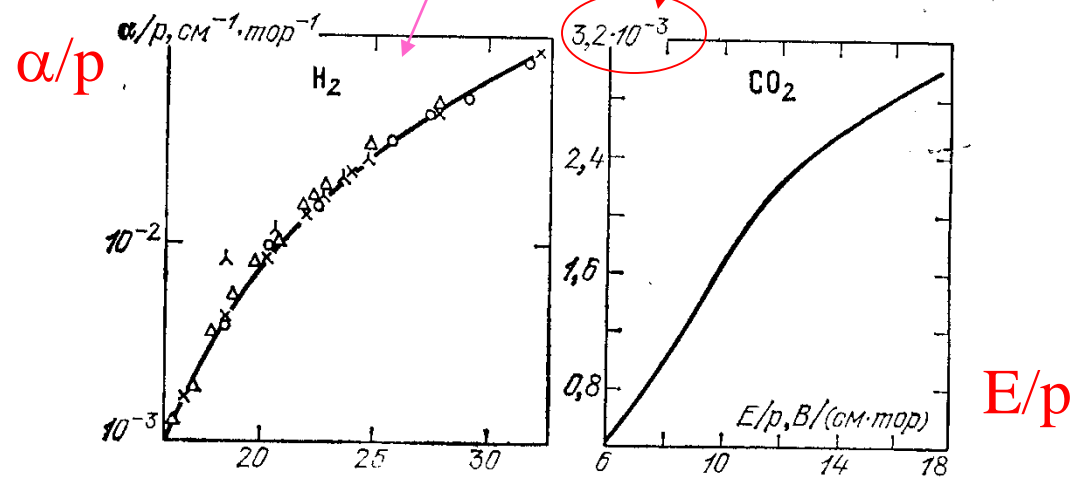


Рис. 5.7. Ионизационный коэффициент в H_2 [26] и CO_2 [6]

Electric discharges

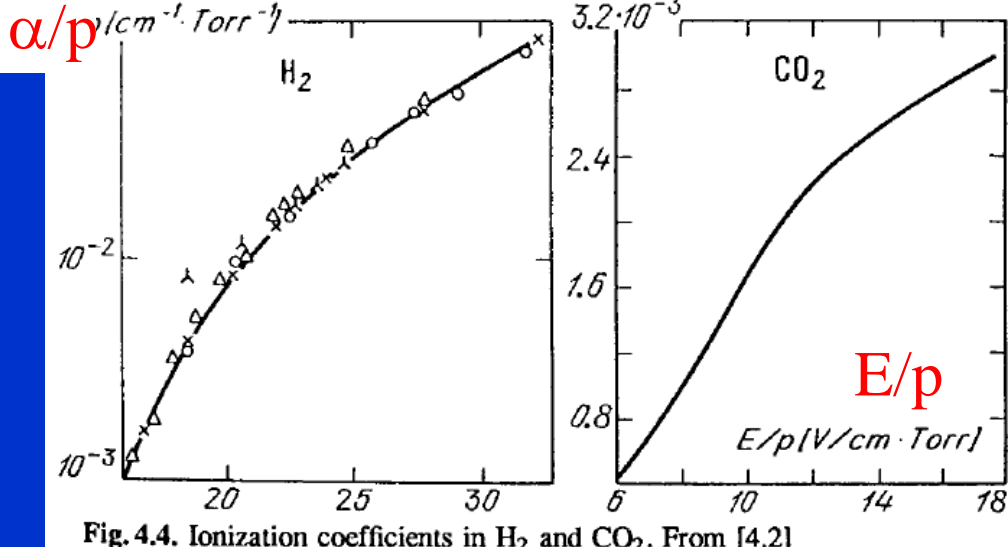
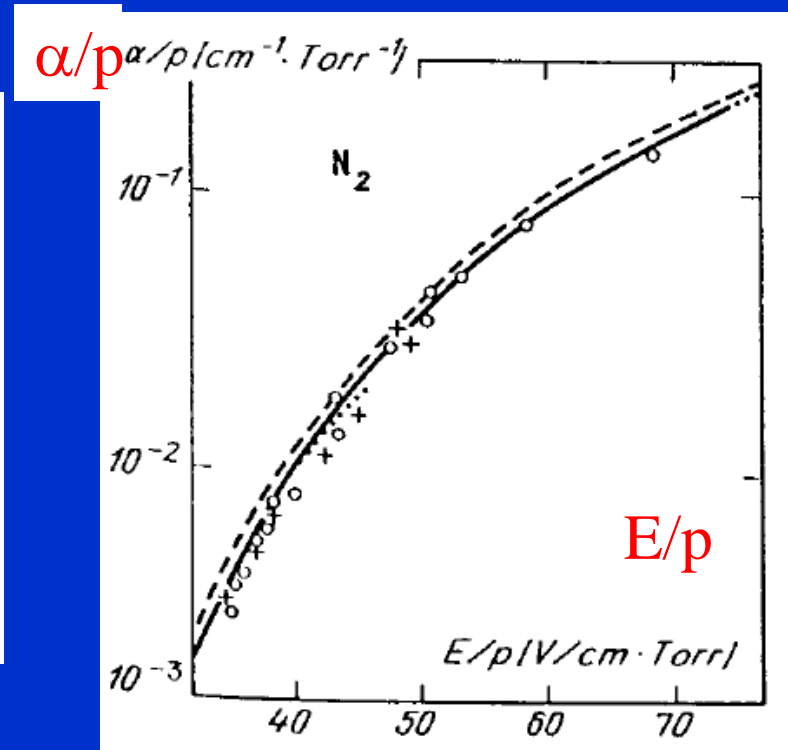


Fig. 4.4. Ionization coefficients in H_2 and CO_2 . From [4.2]



Interpolation formula

$$dN/dx = \alpha N, \quad N(x) = N_0 \exp(\alpha x)$$

See next slide

4.1.5 Interpolation Formula for α

The theoretical and numerical analysis of discharges widely uses a conventional empirical formula suggested by Townsend:

$$\alpha = Ap \exp(-Bp/E). \quad (4.5)$$

The constants A and B are determined by approximating the experimental curves (Table 4.1). In a number of cases the relation (4.5) can be attributed a certain physical meaning. Assume, for example, that an electron undergoes only ionizing collisions. (This assumption may be realistic at high E/p and moderate energies.) The energy picked up by an electron along a free path length x is slightly greater than the ionization potential I . The probability that it will move the distance $x = I/eE$ without collisions and then be involved in an ionizing collision in a distance dx is $\alpha dx = dx l^{-1} \exp(-I/eEl)$, where $l = l_1/p$ is the mean-free-path length. This gives us (4.5) with $A = l_1^{-1}$, $B = I/el_1$. If $\sigma = 5 \cdot 10^{-16} \text{ cm}^2$, then $l_1 = 0.06 \text{ cm} \cdot \text{Torr}$; if $I = 15 \text{ eV}$, then $A = 17$, $B = 250$, which is quite close to tabulated values.

The fraction of electrons in a Maxwellian spectrum that are capable of ionizing an atom is proportional to $\exp(-I/kT_e)$. If $T_e \propto E/p$ (see Sect. 2.3.5), we again arrive at a dependence of ν_i and α on E of type (4.5), but now the constant B has a different meaning. It will be shown in Sect. 7.4.7 that an approximate solution of the kinetic equation that takes into account the large role of inelastic losses of electron energy on excitation also leads to a relation of type (4.5), but again with a changed meaning of B . For inert gases, the formula

$$\alpha = Cp \exp[-D(p/E)^{1/2}] \quad (4.6)$$

See next slide

Electric discharges

$$dN/dx = \alpha N, \quad N(x) = N_0 \exp(\alpha x)$$

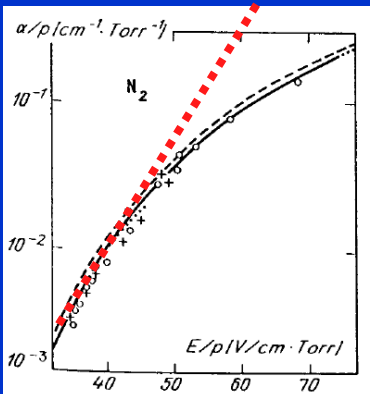


| Table 4.1. Constants in the formulas for the ionization coefficient, and regions of applicability [4.4,5] | | | | | |
|---|----------------------------------|---------------|---------------|----------------------------------|------------------------|
| Gas | A | B | E/p | C | D |
| | $\text{cm}^{-1}\text{Torr}^{-1}$ | V/(cm · Torr) | V/(cm · Torr) | $\text{cm}^{-1}\text{Torr}^{-1}$ | V/(cm · Torr) $^{1/2}$ |
| He | 3 | 34 | 20-150 | 4.4 | 14 |
| Ne | 4 | 100 | 100-400 | 8.2 | 17 |
| Ar | 12 | 180 | 100-600 | 29.2 | 26.6 |
| Kr | 17 | 240 | 100-1000 | 35.7 | 28.2 |
| Xe | 26 | 350 | 200-800 | 65.3 | 36.1 |
| Hg | 20 | 370 | 150-600 | | |
| H ₂ | 5 | 130 | 150-600 | | |
| N ₂ | 12 | 342 | 100-600 | | |
| N ₂ | 8.8 | 275 | 27-200 | | |
| Air | 15 | 365 | 100-800 | | |
| CO ₂ | 20 | 466 | 500-1000 | | |
| H ₂ O | 13 | 290 | 150-1000 | | |

See next slide

4.1.5 Interpolation Formula for α

The theoretical and numerical analysis of discharges widely uses a conventional empirical formula suggested by Townsend:

$$\alpha = Ap \exp(-Bp/E). \quad (4.5)$$

The constants A and B are determined by approximating the experimental curves (Table 4.1). In a number of cases the relation (4.5) can be attributed a certain physical meaning. Assume, for example, that an electron undergoes only ionizing collisions. (This assumption may be realistic at high E/p and moderate energies.) The energy picked up by an electron along a free path length x is slightly greater than the ionization potential I . The probability that it will move the distance $x = I/eE$ without collisions and then be involved in an ionizing collision in a distance dx is $\alpha dx = dx l^{-1} \exp(-I/eEl)$, where $l = l_1/p$ is the mean-free-path length. This gives us (4.5) with $A = l_1^{-1}$, $B = I/el_1$. If $\sigma = 5 \cdot 10^{-16} \text{ cm}^2$, then $l_1 = 0.06 \text{ cm} \cdot \text{Torr}$; if $I = 15 \text{ eV}$, then $A = 17$, $B = 250$, which is quite close to tabulated values.

The fraction of electrons in a Maxwellian spectrum that are capable of ionizing an atom is proportional to $\exp(-I/kT_e)$. If $T_e \propto E/p$ (see Sect. 2.3.5), we again arrive at a dependence of ν_i and α on E of type (4.5), but now the constant B has a different meaning. It will be shown in Sect. 7.4.7 that an approximate solution of the kinetic equation that takes into account the large role of inelastic losses of electron energy on excitation also leads to a relation of type (4.5), but again with a changed meaning of B . For inert gases, the formula

$$\alpha = C p \exp[-D(p/E)^{1/2}] \quad (4.6)$$

Electric discharges semi-empirical approach

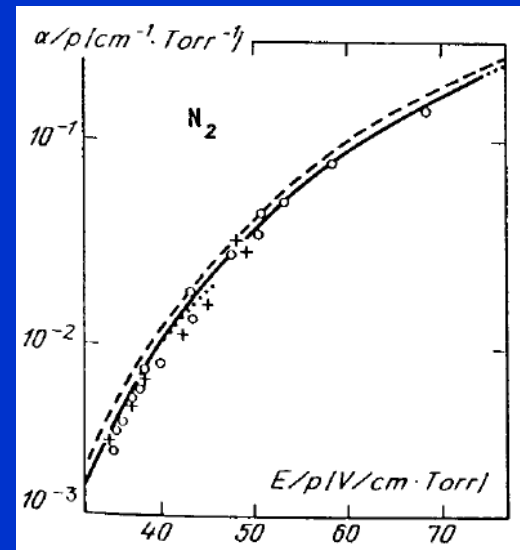
The theoretical and numerical analysis of discharges widely uses a conventional empirical formula suggested by Townsend:

$$\alpha = Ap \exp(-Bp/E)$$

$$\alpha = Cp \exp[-D(p/E)^{1/2}]$$

Table 4.1. Constants in the formulas for the ionization coefficient, and regions of applicability [4.4, 5]

| Gas | A | B | E/p | C | D | E/p < |
|------------------|----------------------------------|---------------|---------------|----------------------------------|--|---------------|
| | $\text{cm}^{-1}\text{Torr}^{-1}$ | V/(cm · Torr) | V/(cm · Torr) | $\text{cm}^{-1}\text{Torr}^{-1}$ | $\text{V}/(\text{cm} \cdot \text{Torr})^{1/2}$ | V/(cm · Torr) |
| He | 3 | 34 | 20–150 | 4.4 | 14 | 100 |
| Ne | 4 | 100 | 100–400 | 8.2 | 17 | 250 |
| Ar | 12 | 180 | 100–600 | 29.2 | 26.6 | 700 |
| Kr | 17 | 240 | 100–1000 | 35.7 | 28.2 | 900 |
| Xe | 26 | 350 | 200–800 | 65.3 | 36.1 | 1200 |
| Hg | 20 | 370 | 150–600 | | | |
| H ₂ | 5 | 130 | 150–600 | | | |
| N ₂ | 12 | 342 | 100–600 | | | |
| N ₂ | 8.8 | 275 | 27–200 | | | |
| Air | 15 | 365 | 100–800 | | | |
| CO ₂ | 20 | 466 | 500–1000 | | | |
| H ₂ O | 13 | 290 | 150–1000 | | | |



empirical formula for air at relatively high E/p (see also Table 12.1)

$$\alpha/p = 1.17 \cdot 10^{-4}(E/p - 32.2)^2 \text{ cm}^{-1} \text{ Torr}^{-1},$$

$$E/p \approx 44 - 176 \text{ V}/(\text{cm} \cdot \text{Torr}).$$

Electric discharges other processes involved in breakdown of a discharge

4.1.7 Stepwise Ionization

The atoms of a weakly ionized gas are mostly ionized from the ground state. Many excited atoms and molecules may be formed if the gas is highly ionized, and stepwise ionization may be predominant. Atoms are first excited by electron impact and then ionized by subsequent collisions. Long-lived metastable excited particles play an important role in this process (Table 4.2): their ionization cross sections are rather high (Fig. 4.6).

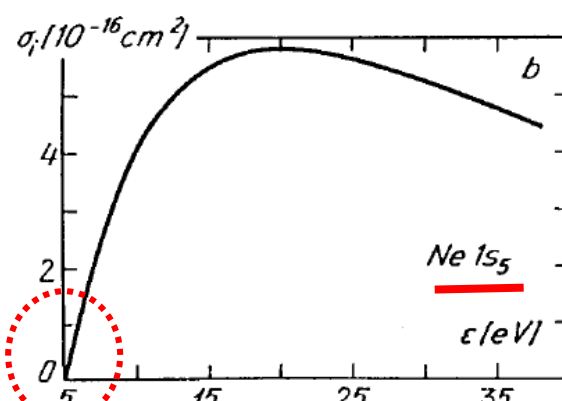
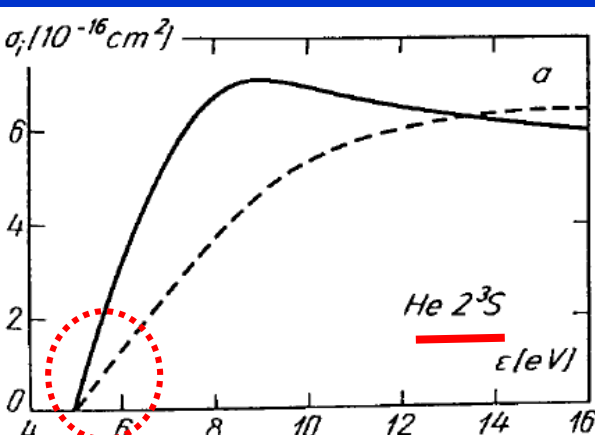
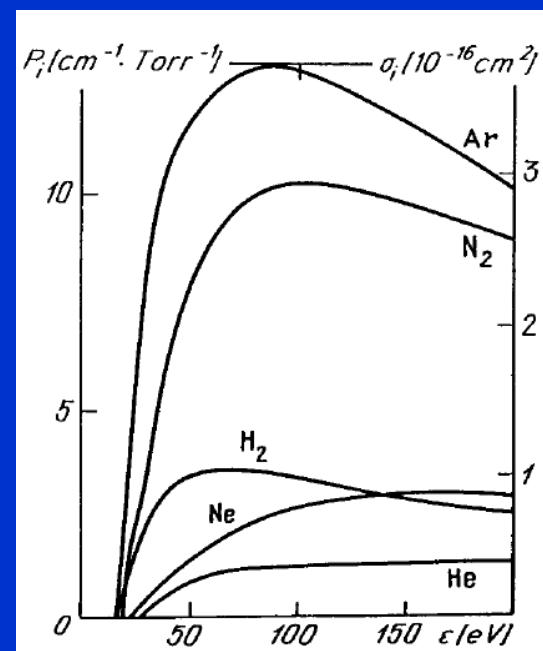


Fig. 4.6. Cross sections of ionization of excited metastables by electron impact: (a) $\text{He } 2^3\text{S}$; experimental data [4.6] – solid curve; theory [4.7] – dashed curve; (b) $\text{Ne } 1s_5$ – theory. From [4.7]



Comparable values
lower threshold energies → higher probability at given T_e

4.1.7 Stepwise Ionization

The atoms of a weakly ionized gas are mostly ionized from the ground state. Many excited atoms and molecules may be formed if the gas is highly ionized, and stepwise ionization may be predominant. Atoms are first excited by electron impact and then ionized by subsequent collisions. Long-lived metastable excited particles play an important role in this process (Table 4.2); their ionization cross sections are rather high (Fig. 4.6).

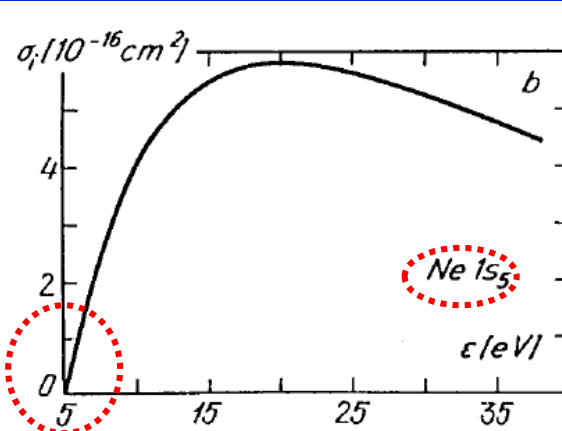
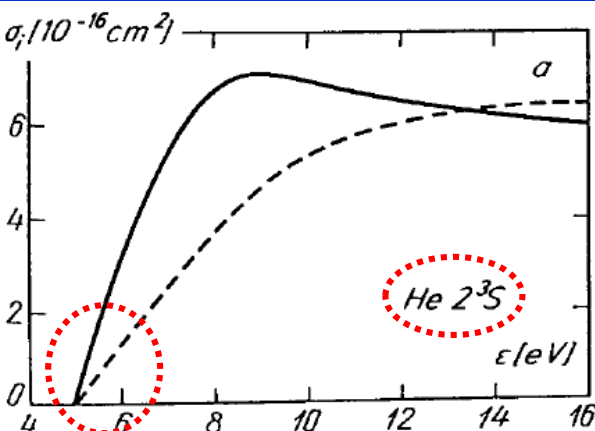


Fig. 4.6. Cross sections of ionization of excited metastables by electron impact: (a) $\text{He } 2^3\text{S}$; experimental data [4.6] – solid curve; theory [4.7] – dashed curve; (b) $\text{Ne } 1s_5$ – theory. From [4.7]

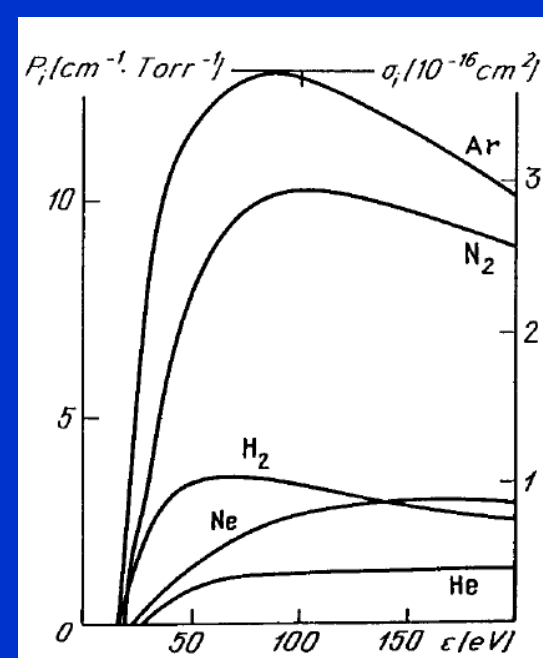


Fig. 4.1. Cross sections and probabilities of electron impact ionization. From [4.1]

Comparable values

lower threshold energies → higher probability at given T_e

photoionization

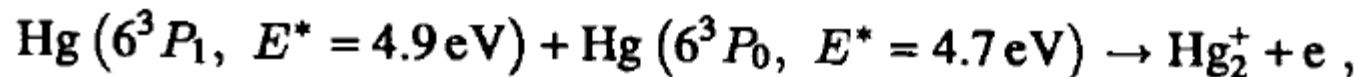
Table 4.3. Cross sections of photoionization of atoms and molecules from the ground state close to the threshold

| Gas | $\hbar\omega = I, \text{ eV}$ | $\lambda, \text{\AA}$ | $\sigma_\nu, 10^{-18} \text{ cm}^2$ |
|----------------|-------------------------------|-----------------------|-------------------------------------|
| H | 13.6 | 912 | 6.3 |
| He | 24.6 | 504 | 7.4 |
| Ne | 21.6 | 575 | 4.0 |
| Ar | 15.8 | 787 | 35 |
| Na | 5.14 | 2412 | 0.12 |
| K | 4.34 | 2860 | 0.012 |
| Cs | 3.89 | 3185 | 0.22 |
| N | 14.6 | 852 | 9 |
| O | 13.6 | 910 | 2.6 |
| O ₂ | 12.2 | 1020 | ~ 1 |
| N ₂ | 15.58 | 798 | 26 |
| H ₂ | 15.4 | 805 | 7 |

Hornbeck Molnar ionization

4.2.3 Associative Ionization

This process of type $A + A^* \rightarrow A_2^+ + e$, discovered by Hornbeck and Molnar in 1951, is sometimes important in inert gases. The separation of an electron is facilitated by the release of a small binding energy of order 1 eV in the association of an ion and an atom into a molecular ion. A reaction in helium involves atoms excited to states with the principal quantum number $n = 3$; their electron binding energies are from 1.52 to 1.62 eV. The binding energy of He_2^+ is somewhat higher, 2.23 eV, so that the electron can be ejected. At $T = 400\text{ K}$, the reaction cross sections are $2 \cdot 10^{-16} - 2 \cdot 10^{-15}\text{ cm}^2$. The *associative ionization* in mercury vapor involves two excited atoms,



the first atom being in a resonance and the second, in a metastable state. The total energy is 9.6 eV, less than that required to ionize an Hg atom ($I_{\text{Hg}} = 10.4\text{ eV}$); together with the binding energy of an Hg_2^+ molecular ion, however (0.15 eV), it is sufficient to ionize the molecule ($I_{\text{Hg}_2} = 9.7\text{ eV}$).

Penning ionization

4.2.2 Ionization by Excited Atoms

Even the high kinetic energy of slow heavy particles is not effective in ionization processes. Ionization requires the velocities of atoms and molecules to be comparable to the electron velocity in atoms, 10^8 cm/s , which corresponds to energies of 10 to 100 keV, not realizable in discharge conditions. On the other hand, the atomic excitation energy E^* is easily spent on liberating an electron from another atom, provided, of course, that it exceeds the ionization potential I . Resonance-excited atoms are especially effective in this respect. Thus the ionization cross sections of Ar, Kr, Xe, N₂, and O₂ in impacts by He($2^1 P$) atoms with $E^* = 21.2 \text{ eV}$ is $\sigma \approx 2 \cdot 10^{-14} \text{ cm}^2$, which is much greater than the gas-kinetic value [4.8]. Cross sections for ionization by metastable atoms, also with $E^* > I$ (*Penning effect*), are smaller but metastable atoms are much more numerous than short-lived resonance-excited atoms. Cross sections for ionization of Ar, Xe, N₂, CO₂ by metastable He($2^3 S$) atoms with $E^* = 19.8 \text{ eV}$ reach 10^{-15} cm^2 , and that of Hg is exceptionally large: $1.4 \cdot 10^{-14} \text{ cm}^2$ [4.8].

Processes going again ionization

4.3.1 Decay of Plasma

In the absence of an electric field, the charge densities $n_e = n_+$ in a plasma without electronegative components decay with time according to the law

$$\left(\frac{dn_e}{dt} \right)_r = -\beta n_e n_+, \quad n_e = \frac{n_e^0}{1 + \beta n_e^0 t} \xrightarrow[t \rightarrow \infty]{} \frac{1}{\beta t}. \quad (4.8)$$

For example, if the electron-ion recombination coefficient $\beta = 10^{-7} \text{ cm}^3/\text{s}$ and the initial plasma density $n_e^0 = 10^{10} \text{ cm}^{-3}$, then the characteristic decay time $\tau_r = (\beta n_e^0)^{-1} = 10^{-3} \text{ s}$. The recombination coefficient can be determined experimentally, by measuring $n_e(t)$ and plotting n_e^{-1} as a function of t . The slope of the straight line gives β .

?

4.3.2 Dissociative Recombination

4.3.3 Radiative Recombination

Cross sections of the process $A^+ + e \rightarrow A + h\nu$ are very small: $\sigma_c \sim 10^{-21} \text{ cm}^2$. The recombination coefficient is correspondingly small [4.9]

$$\beta_{rr} = \langle v \sigma_c \rangle \approx 2.7 \cdot 10^{-13} \{T_e[\text{eV}]\}^{-3/4} \text{ cm}^3/\text{s} \sim 10^{-12} \text{ cm}^3/\text{s}. \quad (4.9)$$

Electric discharges

4.3.4 Radiative Recombination in Three-Body Collisions

This process follows the scheme $A^+ + e + e \rightarrow A + e$; it is the main process in high-density low-temperature equilibrium plasma where $T \approx T_e \sim 10^4$ and the concentration of molecular ions is too low for dissociative recombination to be significant. In three-body collisions, electrons are captured by ions to form very high by excited atoms with a binding energy of order kT . An excited atom is then gradually deactivated by subsequent electron impacts, it “cascades” down the level staircase, and finally falls to the ground state from the lower excited state by radiative transition. This completes the process of recombination; its coefficient is [4.9]

$$\begin{aligned}\beta_{\text{ctr}} &= 8.75 \cdot 10^{-27} \{T[\text{eV}]\}^{-9/2} n_e \\ &= 5.2 \cdot 10^{-23} \{T[\text{kK}]\}^{-9/2} n_e \text{ cm}^3/\text{s}.\end{aligned}\quad (4.10)$$

According to (4.9, 10), β_{ctr} exceeds the radiative recombination coefficient if

$$n_e > 3.1 \cdot 10^{13} \{T[\text{eV}]\}^{3.75} = 3.2 \cdot 10^9 \{T[\text{kK}]\}^{3.75} \text{ cm}^{-3}. \quad (4.11)$$

The recombination rate constant of triple collisions involving an atom as a third particle, β/N , is less than β_{ctr}/n_e of (4.10) by a factor of $10^7 - 10^8$. This process is not typical for discharge conditions and can manifest itself only at very weak ionization and high pressures.

Electric discharges – Electron attachment

4.4 Formation and Decay of Negative Ions

4.4.1 Attachment

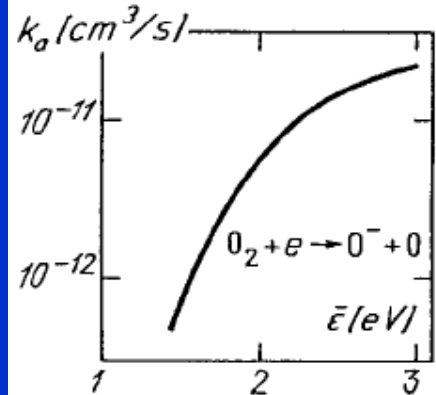
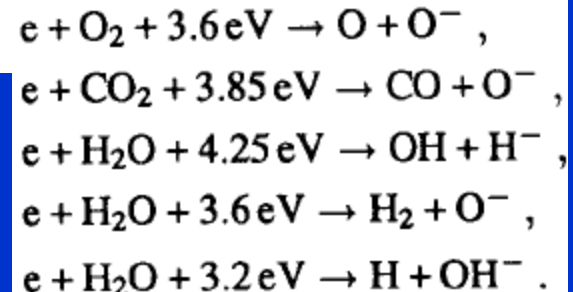


Fig. 4.11. Dissociative attachment rate constant of O_2 as a function of mean electron energy. From [4.12]

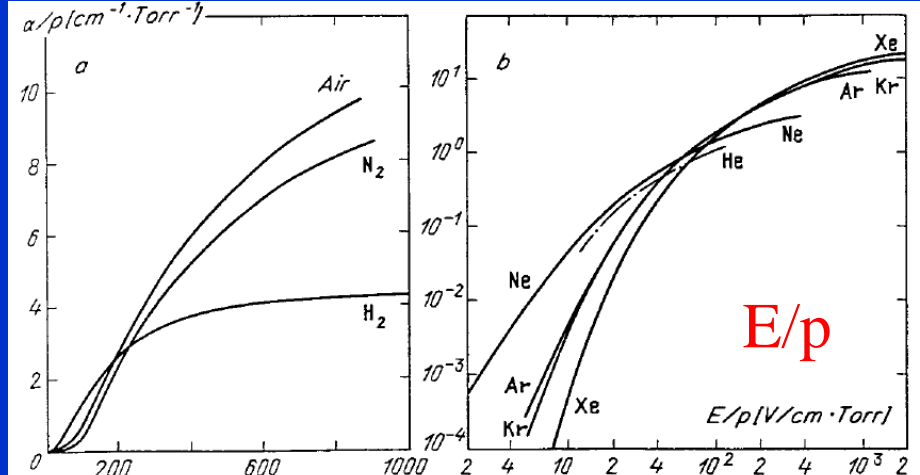


Fig. 4.3. Ionization coefficients for a wide range of E/p values (a) in molecular gases, (b) in inert gases. From [4.3]

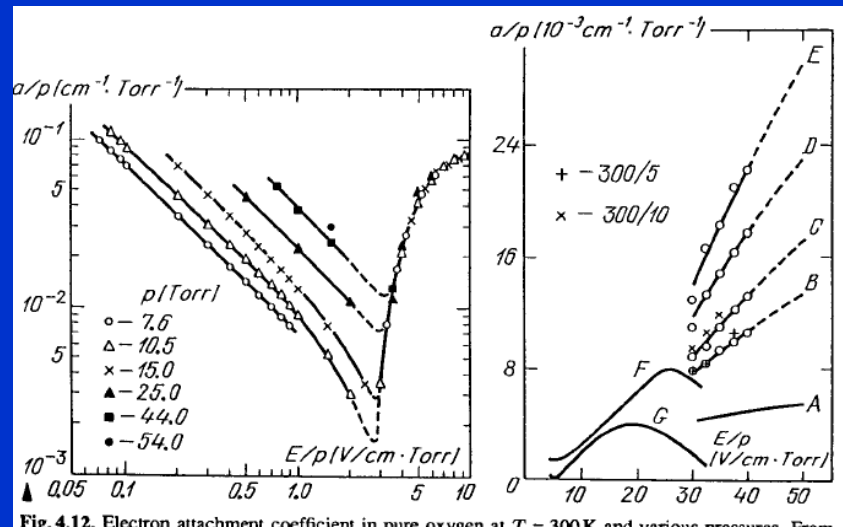


Fig. 4.12. Electron attachment coefficient in pure oxygen at $T = 300 \text{ K}$ and various pressures. From [4.12]

Fig. 4.13. Electron attachment coefficient in moist air, for various air humidity values: A: dry air; B: total pressure 150 Torr, water vapor pressure 2.5 Torr (150/2.5); C (150/5); D (150/9); E (150/15); F and G – air with negligible amount of water vapor. From [4.13, 14]

The multiplication of electrons in an avalanche is determined by the effective coefficient $\alpha_{\text{eff}} = \alpha - a$. If $\alpha < a$ (this happens at E/p less than a certain value for a given gas, see Sect. 7.2.5), multiplication becomes impossible.

E/p

Ionization contra electron attachment

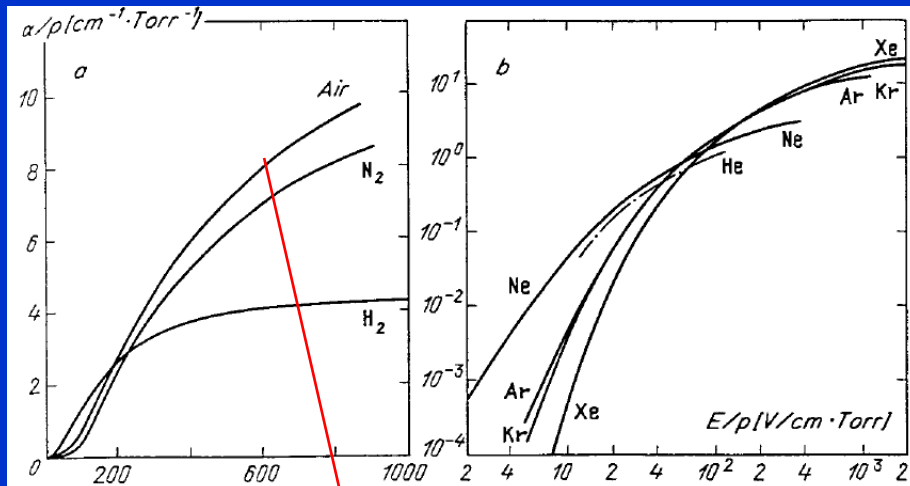


Fig. 4.3. Ionization coefficients for a wide range of E/p values (a) in molecular gases, (b) in inert gases. From [4.3]

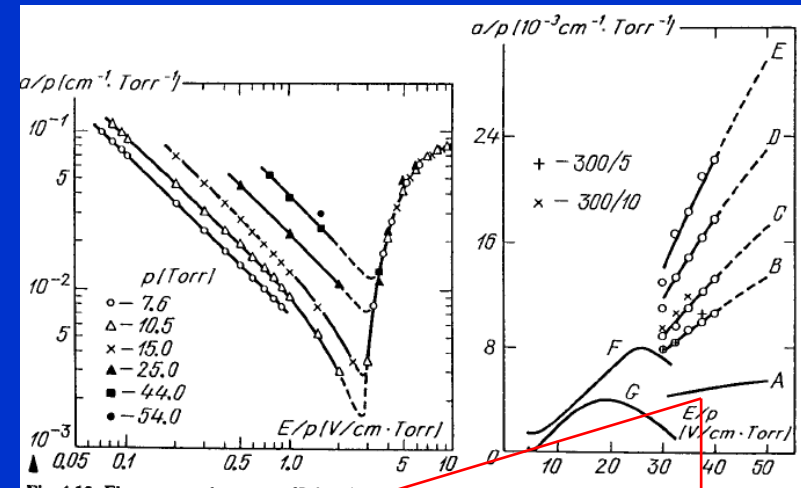
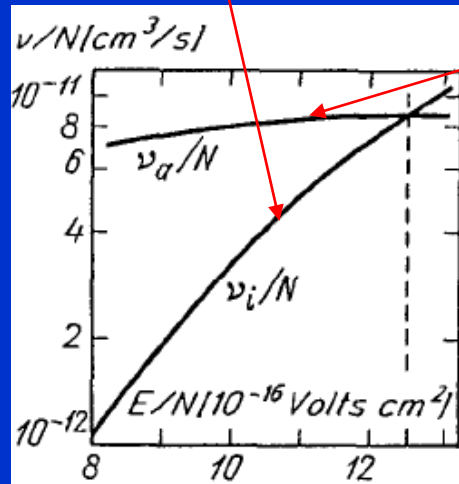


Fig. 4.12. Electron attachment coefficient in pure oxygen at $T = 300 \text{ K}$ and various pressures. From [4.12]

Fig. 4.13. Electron attachment coefficient in moist air, for various air humidity values: A: dry air; B: total pressure 150 Torr, water vapor pressure 2.5 Torr (150/2.5); C (150/5); D (150/9); E (150/15); F and G – air with negligible amount of water vapor. From [4.13, 14]



$$dN_e/dx = (\alpha - a)N_e, \quad N_e \propto \exp(\alpha - a)x;$$

Breakdown condition

Fig. 7.5. Ionization and attachment frequencies in air, calculated using the solution of the kinetic equation. Intersection at $E/p = 41 \text{ V/cm} \cdot \text{Torr}$

Electric discharges - cathode

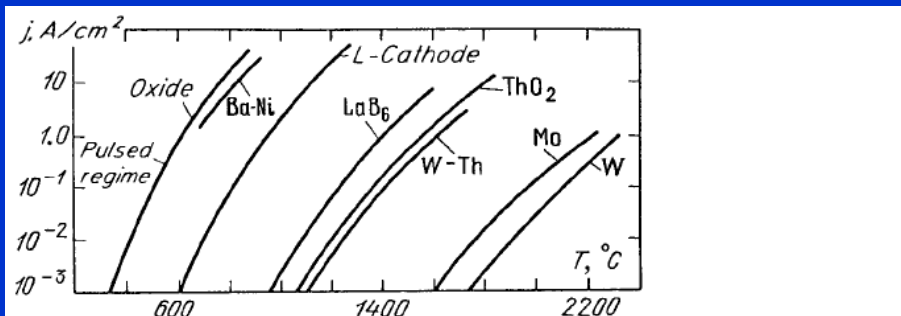


Fig. 4.14. Current density of thermionic emission as a function of cathode temperature for a number of materials. From [4.16]

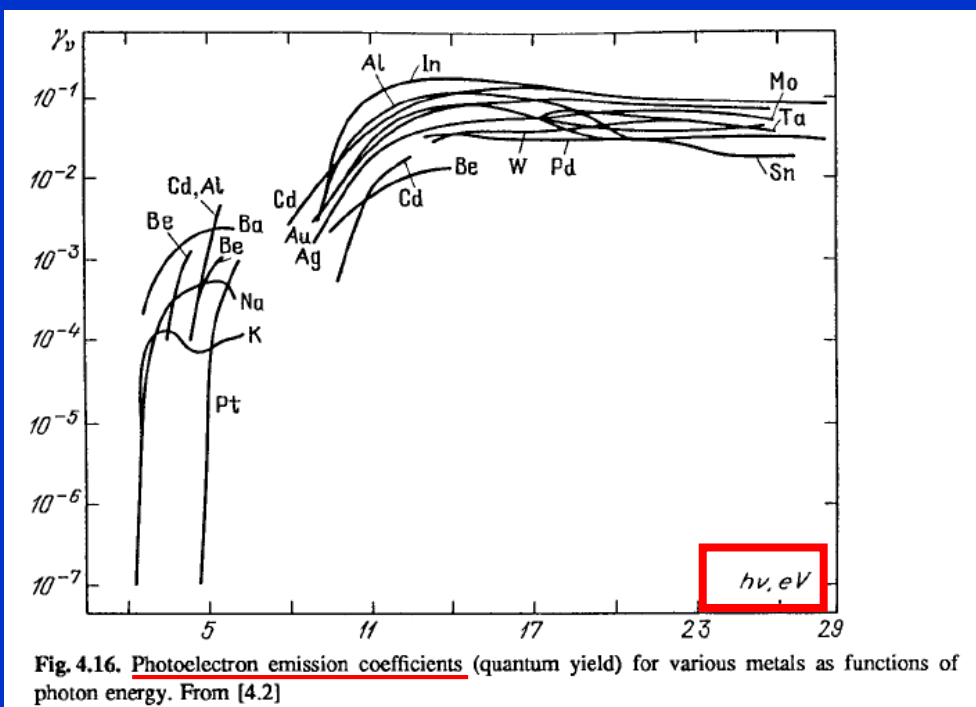


Fig. 4.16. Photoelectron emission coefficients (quantum yield) for various metals as functions of photon energy. From [4.2]

Paschen law – data gama

$$i = \frac{i_0 \exp(\delta d)}{1 - \gamma \exp(\delta d) - 1}, \quad (5.5)$$

V důsledku emise opouští povrch katody elektrony s hustotou toku γj_{\perp}

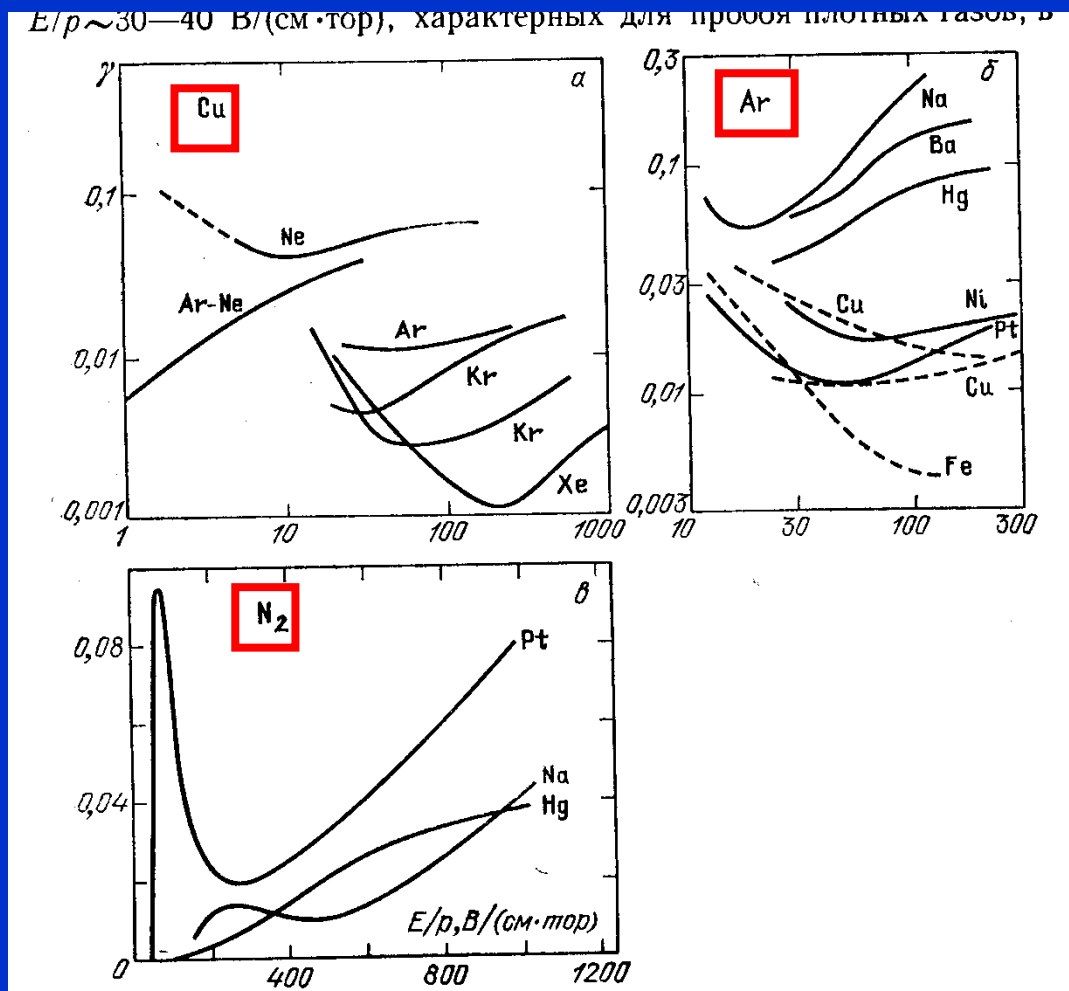
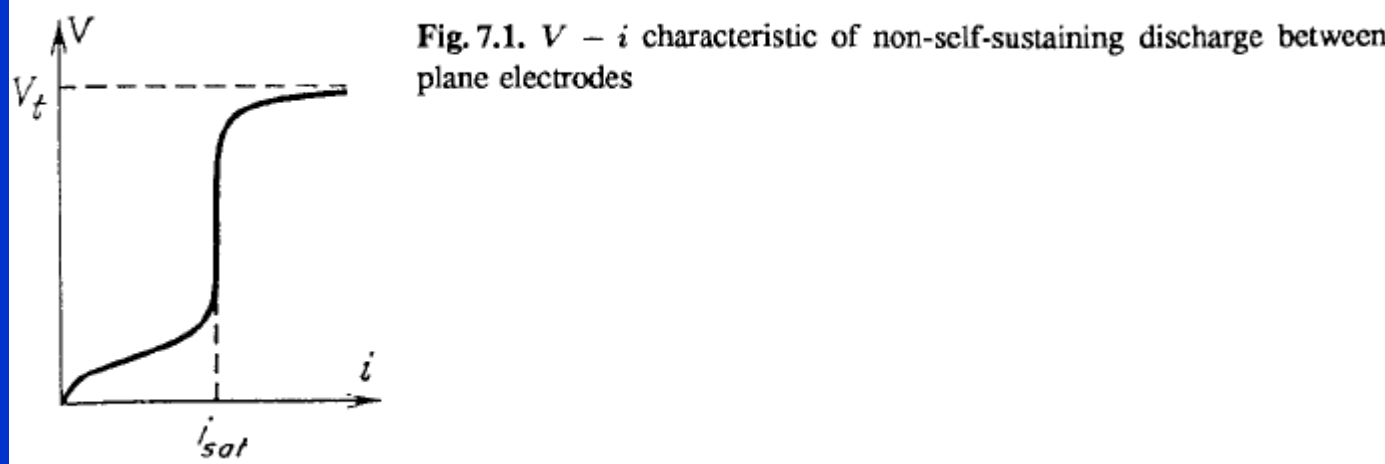


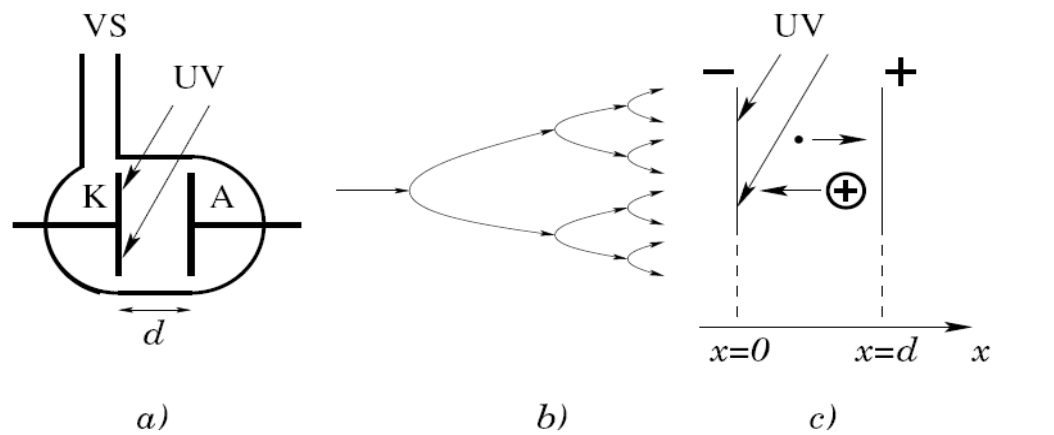
Рис. 6.13. Коеффициент ионно-электронной эмиссии, определенный из разрядного эксперимента (п. 4.1): *a* — медный катод в инертных газах; *б* — различные металлы в Ar; *в* — различные металлы в N₂ [6]

Electric discharges

7.2 Breakdown and Triggering of Self-Sustained Discharge in a Constant Homogeneous Field at Moderately Large Product of Pressure and Discharge Gap Width

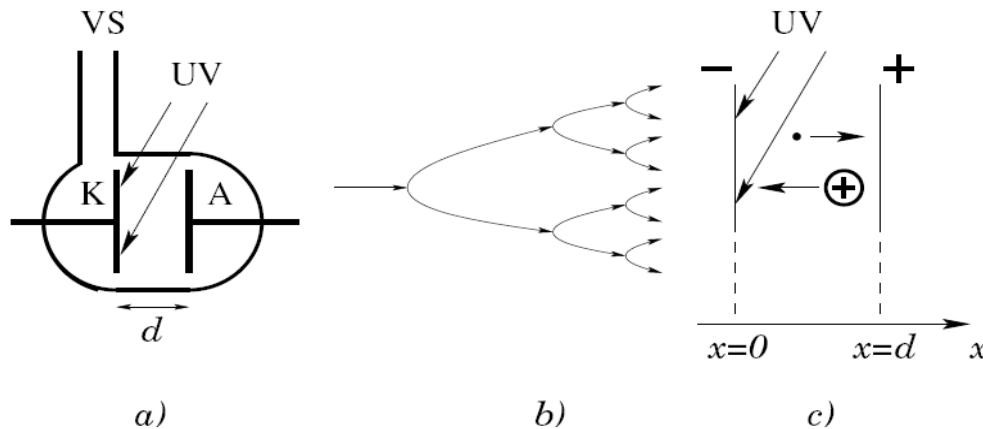


Electric discharges Townsend avalanche theory



Obr. 5.2: Zapaľovanie výboja: a) výbojka na meranie zapaľovacieho napäťia: K - katóda, A - anóda, UV - ultrafialové žiarenie zabezpečujúce emisiu primárnych elektrónov, VS - napojenie na vákuový systém; b) elektrónová lavína; c) označenie polohy elektród

Electric discharges Townsend avalanche theory



Obr. 5.2: Zapaľovanie výboja: a) výbojka na meranie zapaľovacieho napäťa: K - katóda, A - anóda, UV - ultrafialové žiarenie zabezpečujúce emisiu primárnych elektrónov, VS - napojenie na vákuový systém; b) elektrónová lavína; c) označenie polohy elektród

medzi elektródami (obr. 5.2 c). Povrch katódy K sa nachádza v mieste $x = 0$ a povrch anódy A v mieste $x = d$. Elektróny sa pohybujú smerom k anóde a vytvorené kladné ióny ku katóde, kde zanikajú. Podobne ako v odseku 4.3.1, môžeme napísť rovnicu kontinuity pre elektróny v jednorozmernej geometrii a v ustálenom stave

$$\frac{dj_-}{dx} = \alpha n_- = \frac{\alpha}{V_-} n_- V_- = \delta j_-, \quad (5.2)$$

kde V_- je driftová rýchlosť elektrónov v elektrickom poli (v homogénnom poli je konštantná) a $\delta = \alpha/V_-$ je **prvý Townsendov koeficient**. Analogická rovnica platí aj pre kladné ióny

$$\frac{dj_+}{dx} = \alpha n_+ = \delta j_-. \quad (5.3)$$

$$\frac{dj_-}{dx} = \alpha n_- = \frac{\alpha}{V_-} n_- V_- = \delta j_-$$

Prvý Townsendov koeficient δ má rozmer m^{-1} a označuje počet ionizácií, ktoré vykoná jeden elektrón v smere elektrického poľa na jednotkovej dráhe (na rozdiel od ionizačnej frekvencie α udávajúcej počet ionizácií za jednotku času). Ak rovnice odčítame, dostaneme

$$\frac{d(j_+ - j_-)}{dx} = 0 \quad \Rightarrow \quad j_+ - j_- = K = \text{konšt.}$$

Potom hustota elektrického prúdu medzi elektródami $i = e(j_+ - j_-) = eK$ je taktiež konštantná, napriek tomu, že hustoty toku elektrónov a iónov sa menia s polohou x .

V homogénnom poli je Townsendov koeficient δ konštantný a preto môžeme rovnice kontinuity ľahko integrovať

$$j_- = C \exp(\delta x); \quad j_+ = C \exp(\delta x) + i/e,$$

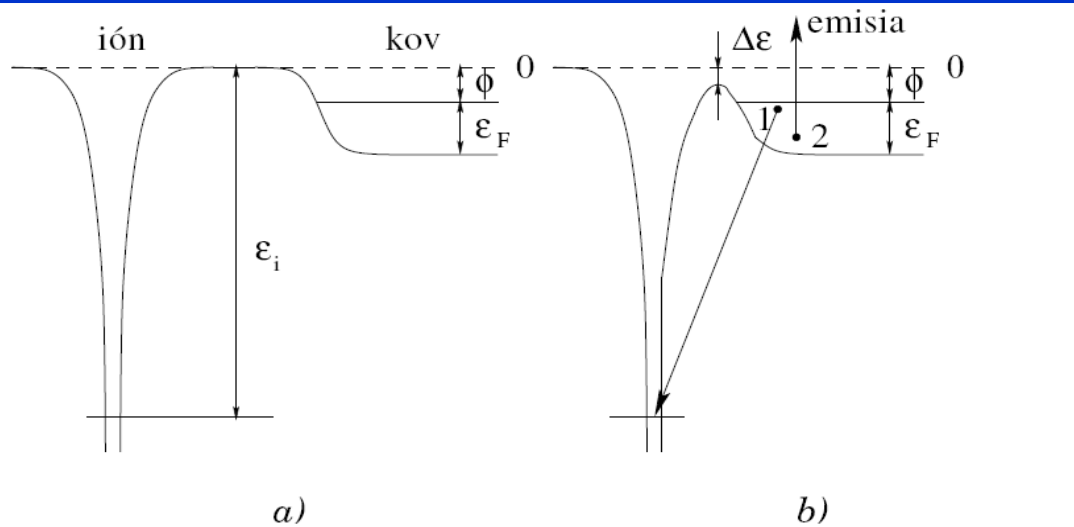
kde C je integračná konštanta. Hodnota tejto integračnej konštanty sa dá určiť z hustoty toku elektrónov na katóde: $C = j_-(0)$. Potom

$$j_- = j_-(0) \exp(\delta x); \quad j_+ = j_-(0) \exp(\delta x) + i/e. \quad (5.4)$$

Problém určenia hustoty toku $j_-(0)$ spočíva v tom, že okrem primárnych elektrónov emitovaných z katódy ultrafialovým žiarením (ich hustotu toku označíme j_0), elektróny emitujú aj dopadajúce kladné ióny. Tento typ emisie sa nazýva **potenciálková emisia**.

Electric discharges

Potenciálová emisia



Obr. 5.3: Emisia elektrónu pri dopade kladného iónu na povrch kovu: a) ión je ďaleko od povrchu: ϵ_i - ionizačná energia atómu, Φ - výstupná práca kovu a ϵ_F - Fermiho energia; b) kladný ión pri dopade na povrch kovu: 1 - elektrón prechádza na neobsadenú hladinu v ióne, 2 - emitovaný elektrón preberá prebytočnú energiu **Augerova emisia**

plynu. Ak však vypneme ultrafialové žiarenie, hustota primárnych elektrónov i_0 klesne na nulu a potom tiež $i = 0$. Lavínová ionizácia sa teda samostatne neudrží. Preto tento typ výboja nazývame **nesamostatný výboj** alebo tiež **Townsendov výboj**. Townsendov výboj je teda predprierazovým štádiom. Pri dostatočne silných poliach sa začne lovej emisie opúšťajú povrch elektróny s hustotou toku γj_+ . Koeficient γ reprezentuje výtažok elektrónov pri emisii, ktorý sa často (nelogicky) nazýva koeficient sekundárnej emisie. V teórii zapalovania výboja sa zvykne nazývať **druhý Townsendov koeficient** (v staršej literatúre aj tretí Townsendov koeficient). Obvykle nadobúda hodnoty $0,1 - 10^{-3}$ (pre ióny veľkých organických molekúl až 10^{-10}).

Breakdown condition: Paschen's law

When the electric field in the electrode space **E is sufficiently high to create the multiplication** of the electrons and ions, **the avalanche appears**. If this multiplication creates a sufficient number of electrons and ions, it will lead to the electrical breakdown. However, if the processes of free charge species losses are emphasized, the avalanche multiplication can cease. Due to the **statistical nature** of both creation and loss of free species, breakdown may not occur even if applied voltage U_w is higher than the breakdown voltage U_b .

The breakdown condition for the gases at low pressures can be obtained using Townsend's theory, including the fact that influence of the space charge can be neglected in the early stage of the breakdown. Space charge is needed for the determination of the regime that will be established after the breakdown.

$$N_a = N_0 \frac{\exp(\alpha d)}{1 - \gamma [\exp(\alpha d) - 1]},$$

The breakdown condition

$$\gamma [\exp(\alpha d) - 1] = 1 \quad \Rightarrow \quad \alpha d = \ln \left(1 + \frac{1}{\gamma} \right)$$

$$\alpha = A p \exp \left(-\frac{B p}{E} \right)$$

It also means that the current can be sustained if the external source of radiation is absent ($N_0 = 0$), i.e. it is self-sustaining discharge. In other words, equation (5) represents a condition for breakdown initiation.

$$A p d \exp \left(-\frac{B p}{E} \right) = \ln \left(1 + \frac{1}{\gamma} \right) \quad \Rightarrow \quad U_b = \frac{B p d}{\ln(A p d) - \ln[\ln(1 + 1/\gamma)]}$$

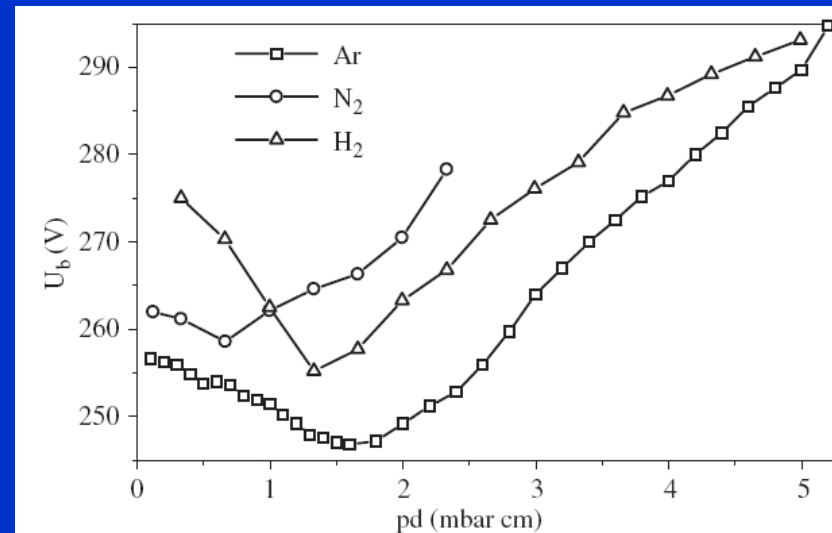


Figure 1. Breakdown voltage U_b in three gases as a function of pd values (Paschen curves).

Electric discharges

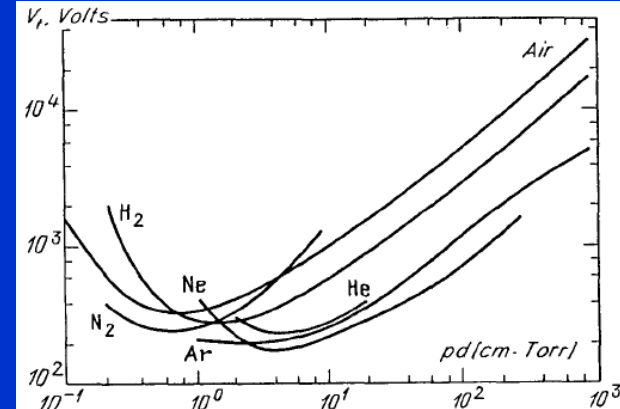
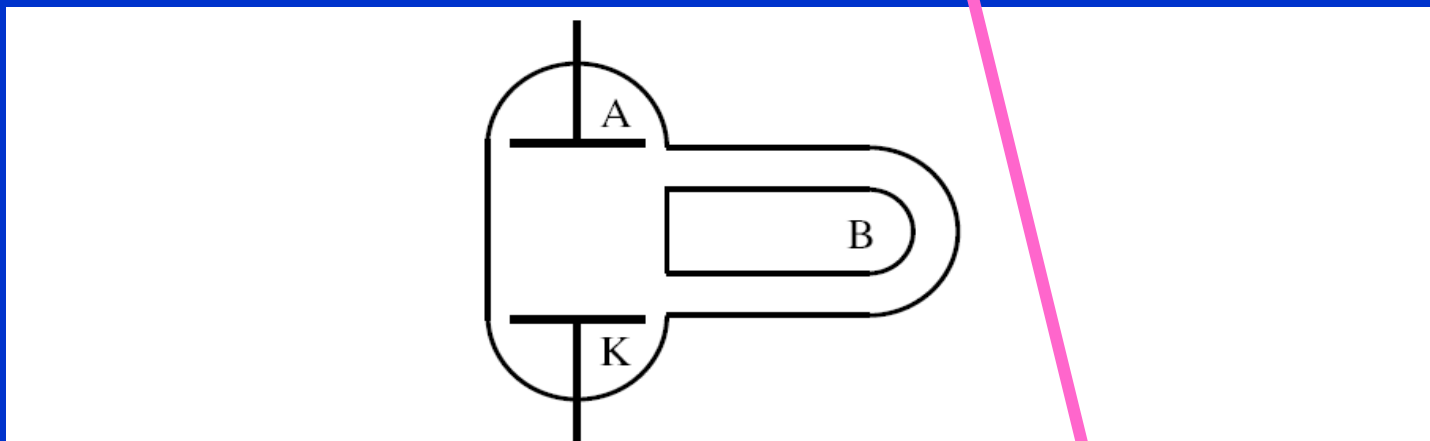


Fig. 7.2. Breakdown potentials in various gases over a wide range of ρd values (Paschen curves) on the basis of data given in [7.1, 2]



Obr. 5.6: Výbojka s bočnou dráhou B na demonštráciu nestability nízkotlakovej vetvy Paschenovej krvky

Calculation of avalanche...

Calculation of avalanche...

Calculation of avalanche...

Electric discharges

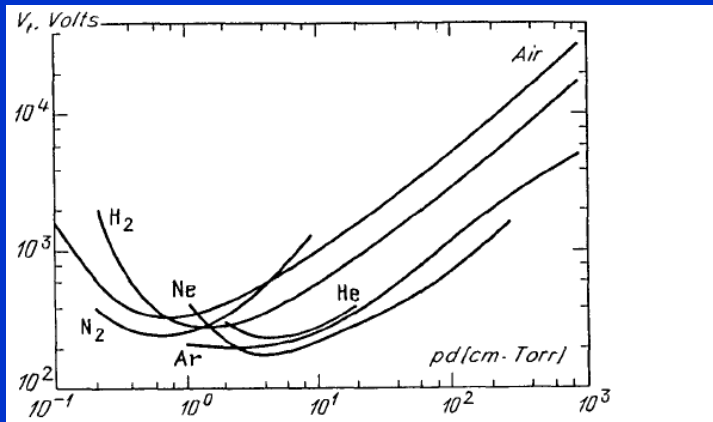


Fig. 7.2. Breakdown potentials in various gases over a wide range of pd values (Paschen curves) on the basis of data given in [7.1, 2]

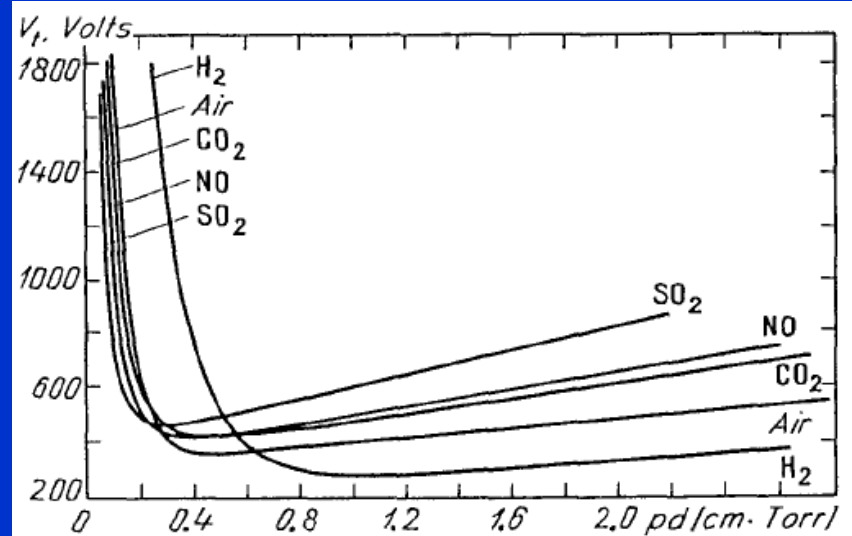


Fig. 7.3. Paschen curves on an enlarged scale [7.3]

$$U_b = \frac{Bpd}{\ln(Apd) - \ln[\ln(1 + 1/\gamma)]}$$

$$(pd)_{\min} = \frac{\bar{e}}{A} \ln \left(\frac{1}{\gamma} + 1 \right), \quad \left(\frac{E}{p} \right)_{\min} = B, \quad V_{\min} = \frac{\bar{e}B}{A} \ln \left(\frac{1}{\gamma} + 1 \right)$$

Paschen law curves

Ar

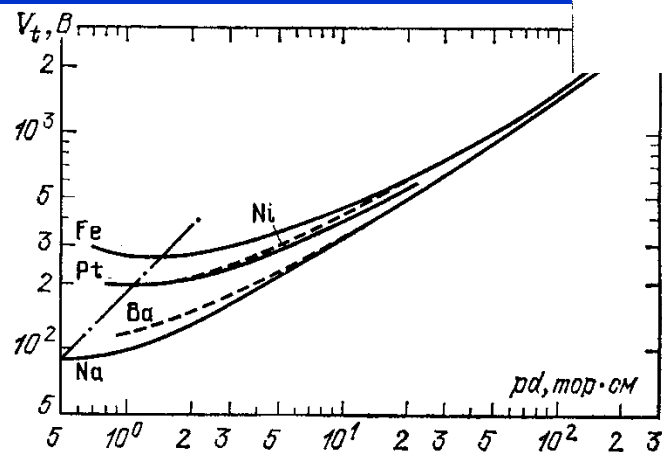


Рис. 13.3. Влияние материала катода на напряжение пробоя аргона. Штрих-пунктирная прямая соединяет точки минимума. Ее наклон 45° соответствует независимости $(E/p)_{\min}$ от материала катода [6]

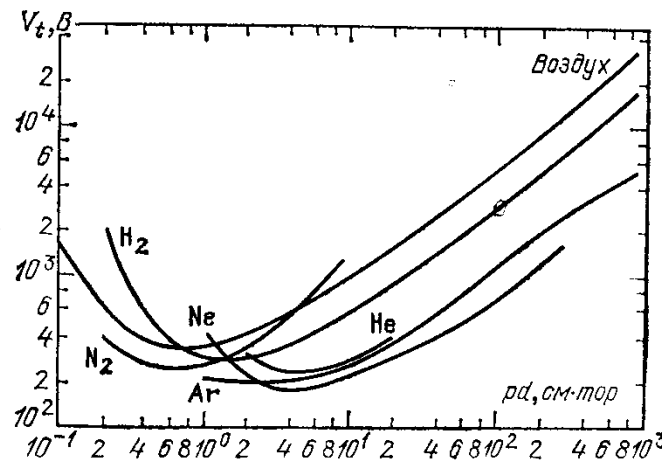


Рис. 13.2. Потенциал зажигания в различных газах в широком диапазоне pd (кривые Пащена)

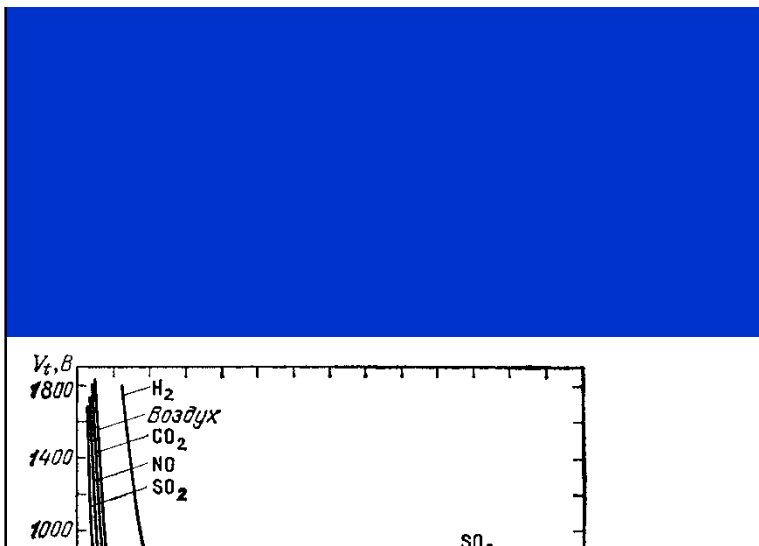


Рис. 13.4. Кривые Пащена в укрупненном масштабе [6]

Electric discharges

Breakdown Fields in Moderately Large Gaps in Air and Other Electronegative Gases at Atmospheric Pressure. Limiting Values of pd for the Townsend Breakdown Mechanism

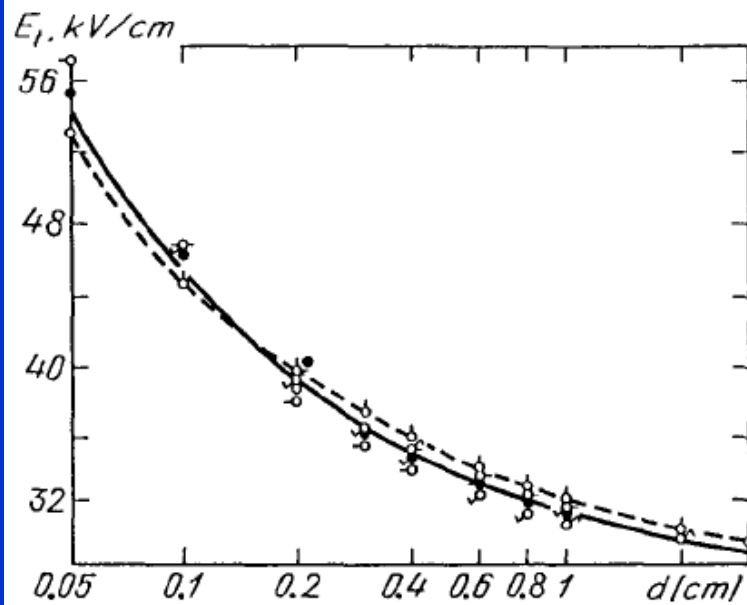
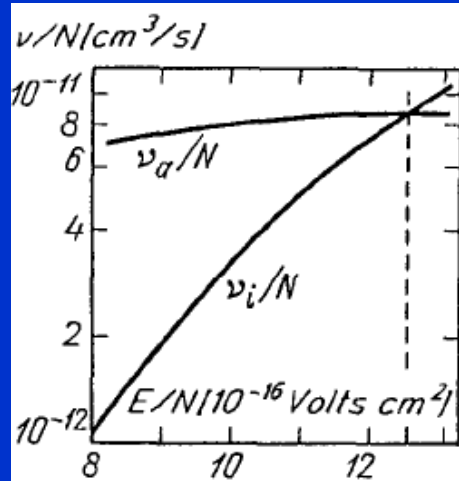


Fig. 7.4. Breakdown fields in a plane gap of length d in air at $p = 1$ atm.
From [7.1]



$$dN_e/dx = (\alpha - a)N_e, \quad N_e \propto \exp(\alpha - a)x;$$

Fig. 7.5. Ionization and attachment frequencies in air, calculated using the solution of the kinetic equation. Intersection at $E/p = 41$ V/cm-Torr

Electric discharges

Table 7.1. Approximate values of breakdown threshold at high pressure

| Gas | Constant field, gap width less than several cm, $p \sim 1$ atm | Microwaves, $p \sim 100\text{--}300$ Torr |
|-----------------------------------|--|---|
| | E/p kV/(cm·atm) | E/p V/(cm·Torr) |
| H ₂ | 10 | 13 |
| Ne | 1.4 | 1.9 |
| Ar | 2.7 | 3.6 |
| H ₂ | 20 | 26 |
| N ₂ | 35 | 46 |
| O ₂ | 30 | 40 |
| Air | 32 | 42 |
| Cl ₂ | 76 | 100 |
| CCl ₂ F ₂ * | 76 | 100 |
| CSF ₈ | 150 | 200 |
| CCl ₄ | 180 | 230 |
| SF ₆ | 89 | 117 |

* Freon

Breakdown

Таблица 13.1. Ориентировочные пороги пробоя газов при высоких давлениях

| Газ | Постоянное поле, недлинные промежутки, $p \sim 1$ атм | | СВЧ, $p \sim 100$ —300 тор |
|------------------------------------|---|----------------------|----------------------------|
| | E_t/p , кВ/(см·атм) | E_t/p , В/(см·тор) | |
| He | 10 | 13 | 3 |
| Ne | 1,4 | 1,9 | 3—5 |
| Ar | 2,7 | 3,6 | 5—10 |
| H ₂ | 20 | 26 | 10—15 |
| N ₂ | 35 | 46 | ~25 |
| O ₂ | 30 | 40 | 35 |
| Воздух | 32 | 42 | ~30 |
| Cl ₂ | 76 | 100 | |
| CCl ₂ F ₂ *) | 76 | 100 | |
| CSF ₈ | 150 | 200 | |
| CCl ₄ | 180 | 230 | |
| SF ₆ **) | 89 | 117 | |

*) Фреон
**) Элегаз

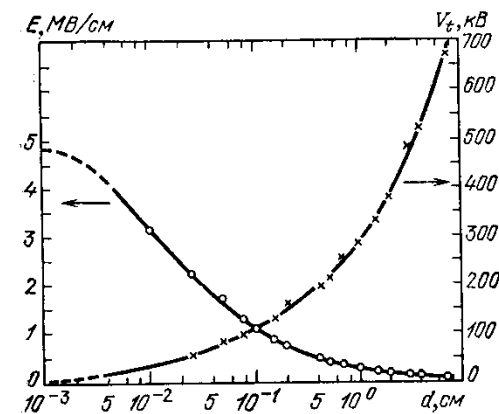


Рис. 13.7. Напряжение и поле пробоя вакуумного промежутка между шаром диаметром 2,5 см и диском диаметром 5 см из стали в зависимости от длины промежутка [3]

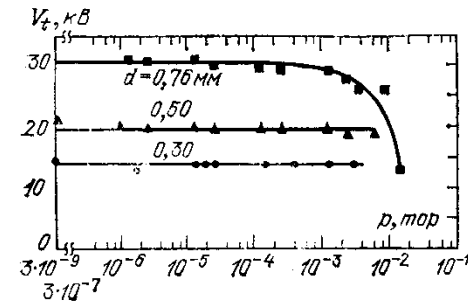


Рис. 13.8. Напряжения пробоя коротких промежутков d между стальными электродами в зависимости от давления заполняющего их водорода. Независимость от p свидетельствует о вакуумном характере пробоя. Загиб вниз верхней кривой соответствует переходу к левой ветви кривой Пашена [15.3]

Electric discharges

Breakdown in Microwave Fields and Interpretation of Experimental Data Using the Elementary Theory

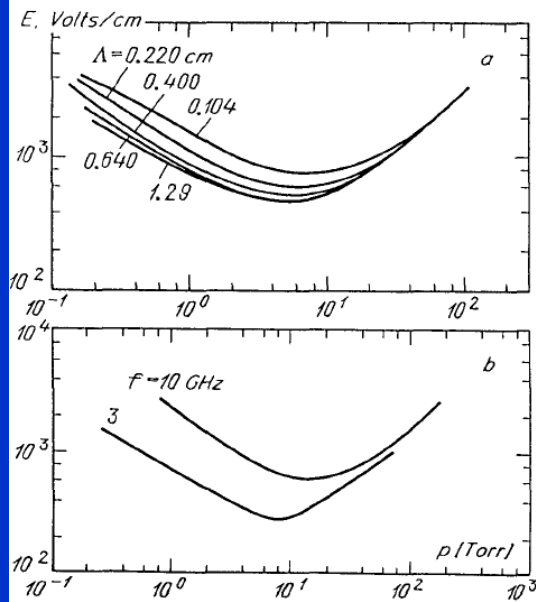


Fig. 7.8. Measured thresholds of microwave breakdown [7.6] (a) air, $f = 9.4$ GHz, diffusion length Λ is indicated for each curve; (b) He gas (He with an admixture of Hg vapor), $\Lambda \approx 0.6$ cm

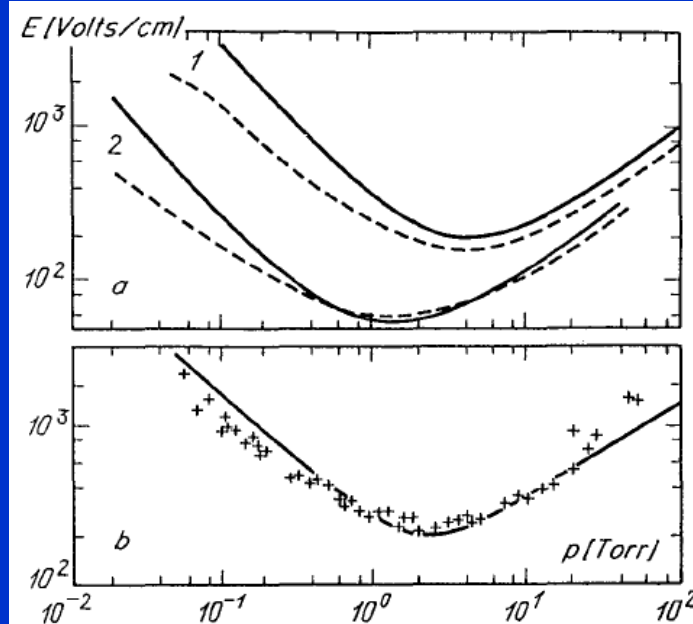


Fig. 7.10. Thresholds of microwave breakdown: (a) Ar, (1) $f = 2.8$ GHz, $\Lambda = 0.15$ cm; (2) $f = 0.99$ GHz, $\Lambda = 0.63$ cm; (b) Xe, $f = 2.8$ GHz, $\Lambda = 0.10$ cm. Solid curves, results of calculations [7.7]; dashed curves and crosses give experimental data [7.5]

for the total number of electrons, N_e , in the discharge volume:

$$\frac{dN_e}{dt} = (\nu_i - \nu_a - \nu_d)N_e , \quad \nu_d = D/\Lambda^2 , \quad (7.7)$$

where ν_d is the frequency of diffusion losses of electrons. This equation describes the ionization kinetics of the gas.

Influence of diffusion length

RF discharges

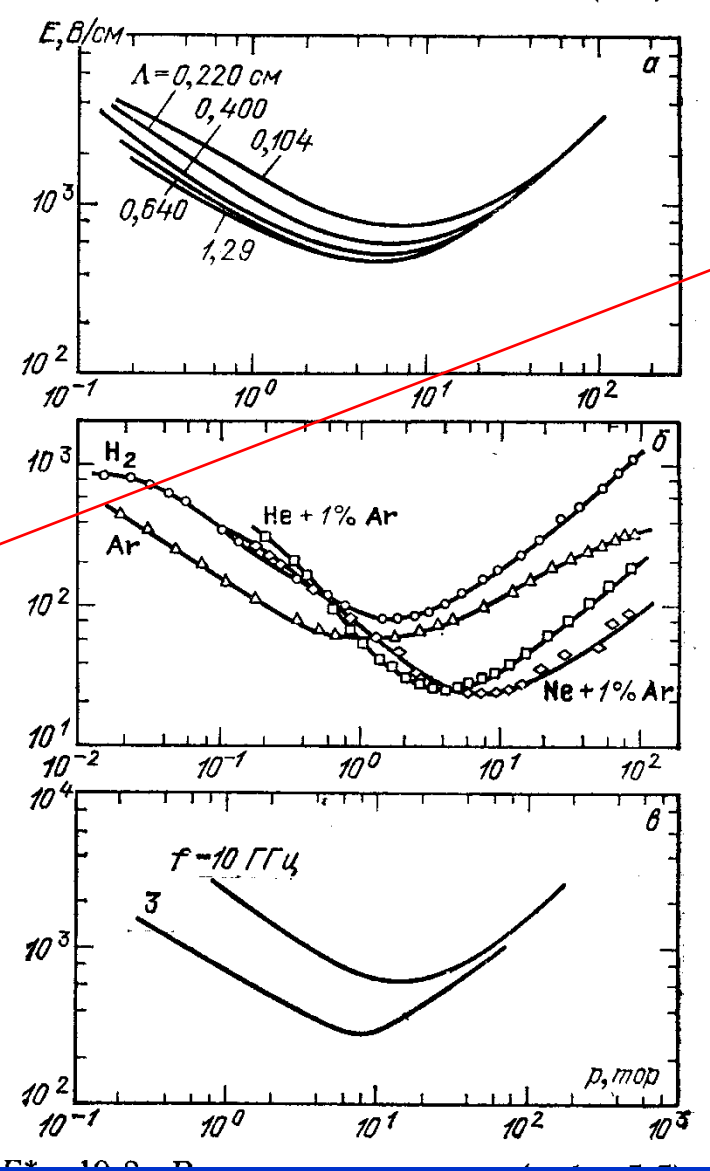


Рис. 13.10. Измеренные пороги СВЧ пробоя: *α* — воздух, частота $f=9,4 \text{ ГГц}$, около кривых указаны диффузионные длины Λ , *β* — несколько газов, $f=0,99 \text{ ГГц}$, $\Lambda=0,63 \text{ см}$; *γ* — Нег-газ (гелий с добавкой паров ртути), $\Lambda=0,6 \text{ см}$ [24]

Influence of diffusion length

Electric discharges

Influence of diffusion length

7.3.2 Ionization Kinetics Equation

When oscillation displacements are small, electron densities obey an equation of type (2.44):

$$\partial n_e / \partial t = D_{\nabla}^2 n_e + (\nu_i - \nu_a) n_e , \quad D \equiv D_e \quad (7.6)$$

(electrons diffuse freely in breakdown). If the condition $\omega \gg \nu_m \delta$ (Sect. 5.5.2) holds (it is satisfied for microwave frequencies), the electron energy distribution is quasisteady and the ionization and attachment frequencies, ν_i and ν_a , are determined by the root-mean-square field E . The dependencies $\nu_i(E)$, $\nu_a(E)$ are much stronger than $D_e(E)$, so that $D_e(E) \approx \text{const}$. For simplification, assume that the field is spatially homogeneous, and hence, ν_i and ν_a are independent of coordinates. Averaging (7.6) over the volume, we obtain, in accord with the results of Sect. 4.5, an equation for the mean density, or (which is equivalent) for the total number of electrons, N_e , in the discharge volume:

$$dN_e / dt = (\nu_i - \nu_a - \nu_d) N_e , \quad \underline{\nu_d = D / A^2} , \quad (7.7)$$

where ν_d is the frequency of diffusion losses of electrons. This equation describes the ionization kinetics of the gas.

Electric discharges

7.3.3 Steady-State Background Criterion

Assume that the external field is switched on in a time small in comparison with the characteristic time of multiplication and remains constant during the avalanche buildup. This constraint covers not only stationary, but also pulsed fields with not too short pulses and sufficiently small rise time. Under this assumption, $\nu_i(t), \nu_a(t) = \text{const}$ after the moment $t = 0$ at which the field is switched on, and (7.7) has an exponential solution typical of an avalanche process:

$$N_e = N_{e0} \exp [(\nu_i - \nu_a - \nu_d)] = N_{e0} \exp (t/\Theta), \quad (7.8)$$

where Θ is the *avalanche time constant*, and N_{e0} is the number of seed electrons that start the avalanche.¹ Breakdown is impeded in experiments with short pulses, since the probability of an electron appearing in the region of the field at the necessary moment is quite low and the avalanche has to be initiated by injecting a small number of electrons. For this purpose, a weak radioactive source is used.

According to (7.8), an avalanche develops if $\nu_i - \nu_a - \nu_d > 0$; this condition is met if the field exceeds a threshold E_t determined by the *steady-state breakdown criterion*:

$$\nu_i(E_t) = \nu_d + \nu_a(E_t). \quad (7.9)$$

As an example, consider breakdown in helium, for $p = 1 \text{ Torr}$, $\lambda = 3 \text{ cm}$, diffusion length $A = 1 \text{ cm}$, $D = 2 \cdot 10^6 \text{ cm}^2/\text{s}$, time of diffusion to the walls $\nu_d^{-1} \approx 5 \cdot 10^{-7} \text{ s}$, diffusion frequency $\nu_d \approx 2 \cdot 10^6 \text{ s}^{-1}$, and no attachment. The avalanche develops if $\nu_i > \nu_d \approx 2 \cdot 10^6 \text{ s}^{-1}$. We will show a little later that the ionization frequency $\nu_i \propto E^2$ under the most favorable conditions for multiplication (zero electron energy losses). If losses, especially inelastic, are nonzero, the ν_i vs. E curve is much steeper. Hence, if the field increases by 10 % in comparison with E_t , then $\Theta^{-1} = \nu_i - \nu_d \geq 0.2\nu_d \approx 4 \cdot 10^5 \text{ s}^{-1}$. The number of electrons is doubled every $\Theta / \ln 2 \leq 1.7 \mu\text{s}$, which is a very high rate. In many cases, it is sufficient for a reliable realization of breakdown. As a result, stationary criterion (7.9) determines with good accuracy [like criterion (7.1)] the breakdown threshold of gases for “not too short” pulses.

Electric discharges

7.5 Optical Breakdown

The discovery of the *optical breakdown* effect, in 1963 [7.8], became possible only after the development of *Q*-switched lasers that produce light pulses of tremendous power, called “giant pulses”. When the light of such a (ruby) laser was passed through a focusing lens, a spark flashed in the air, in the focal region, as in the electrical breakdown of a discharge gap. The discovery was a complete surprise for physicists and produced a sensation at the time, though the element of surprise has worn off by now. Gas breakdown at optical frequencies requires a tremendous field strength, 10^6 – 10^7 V/cm, in the light wave; this was unthinkable before the advent of the laser. Furthermore, the necessary light intensity, about 10^5 MW/cm², could only be reached by focusing the light of not just an ordinary laser, but one operating in the giant pulse regime. The new effect caused unparalleled interest among physicists. In a short time, it was experimentally and theoretically investigated to such a degree [7.7], that by now we know at least as much about it as about its closest analogue, the microwave field breakdown.

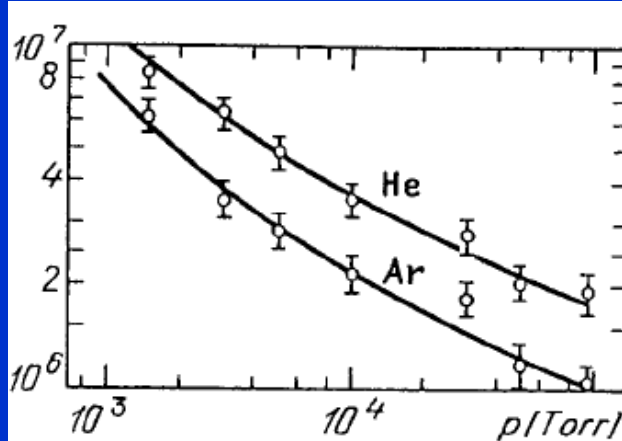


Fig. 7.11. Measured threshold fields for the breakdown of Ar and He by ruby laser radiation; pulse length 30 ns, diameter of focal spot $2 \cdot 10^{-2}$ cm [7.9]

Electric discharges

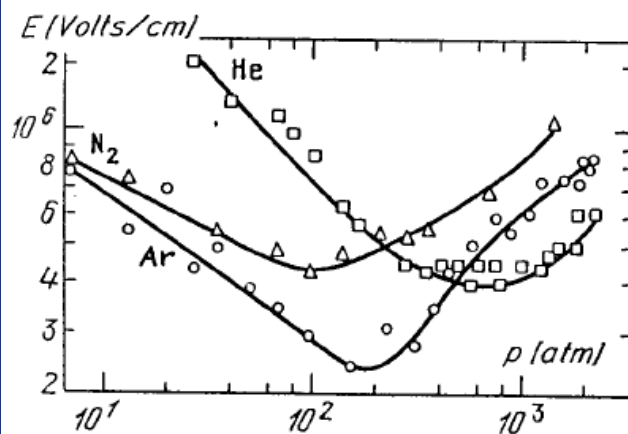


Fig. 7.12. Breakdown thresholds in Ar, He, N₂ for ruby laser radiation over a wide pressure range [7.10]. Pulse length 50 ns, focal spot diameter 10⁻² cm

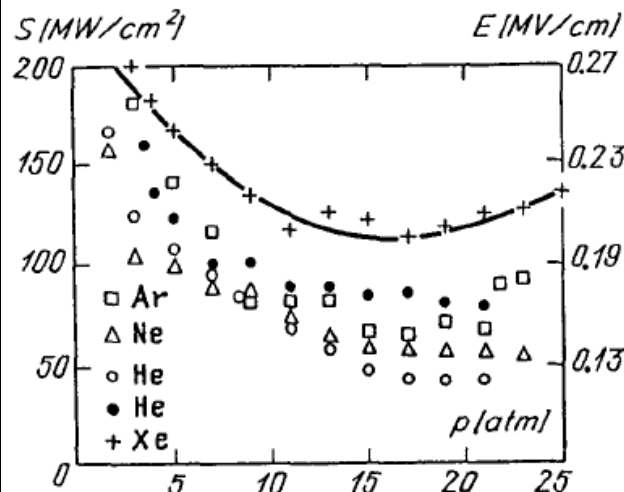


Fig. 7.13. Breakdown thresholds of inert gases in the radiation of a CO₂ laser [7.7]. The black dots represent data for helium of a higher purity

7.5.3 Breakdown Thresholds of Atmospheric Air

These data are very important. Quite a few physical experiments employ high-intensity laser beams. Electrical breakdown of air on the beam path to the target is an obstacle for light propagation because of absorption in the plasma. For example, in such experiments with high-power beams as target irradiation for fusion experiments one has to send the beam to the target through vacuum. The threshold intensity for the giant pulse of a ruby laser and an ordinary focal spot diameter of 10⁻² cm is $S_t \approx 10^{11} \text{ W/cm}^2$, and the field is $E_t \approx 6 \cdot 10^6 \text{ V/cm}$.

The breakdown threshold of nonfiltered air by focused CO₂ laser radiation is roughly $2 \cdot 10^9 \text{ W/cm}^2$, and that of dust-free air is not lower than 10^{10} W/cm^2 . The tiniest dust particles floating in the air greatly facilitate the breakdown by CO₂ laser radiation, while their effect is negligible for the neodymium and, in particular, ruby lasers. This difference appears because the short-wave radiation of solidstate lasers “supplies itself” with the seed electrons required for starting an avalanche. The long-wave radiation of CO₂ lasers cannot do this in a pure gas.

Electric discharges

7.7 Breakdown in RF and Low-Frequency Ranges

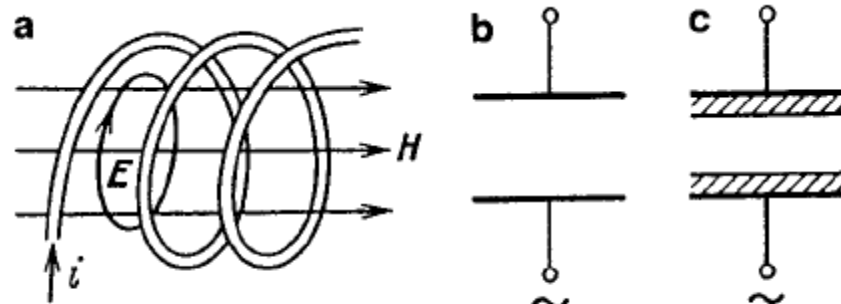


Fig. 7.18. Excitation of rf discharges: (a) inductively coupled through a solenoid coil; (b) voltage applied to electrodes in contact with plasma; (c) electrodes insulated from plasma (electrodeless, capacitively coupled rf discharge)

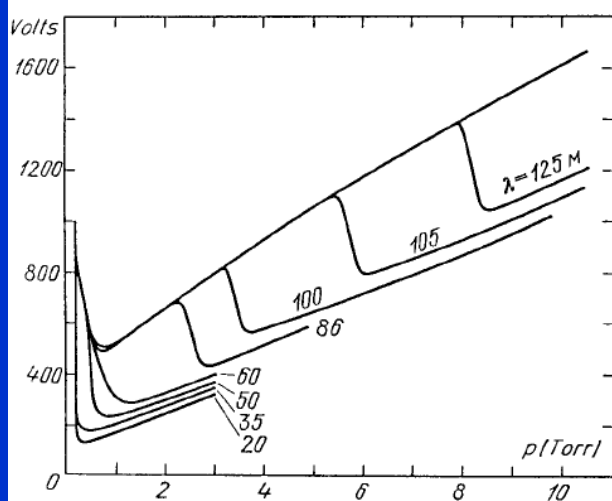


Fig. 7.20. Ignition potentials of ccrf discharge for various oscillation wavelengths [7.15]

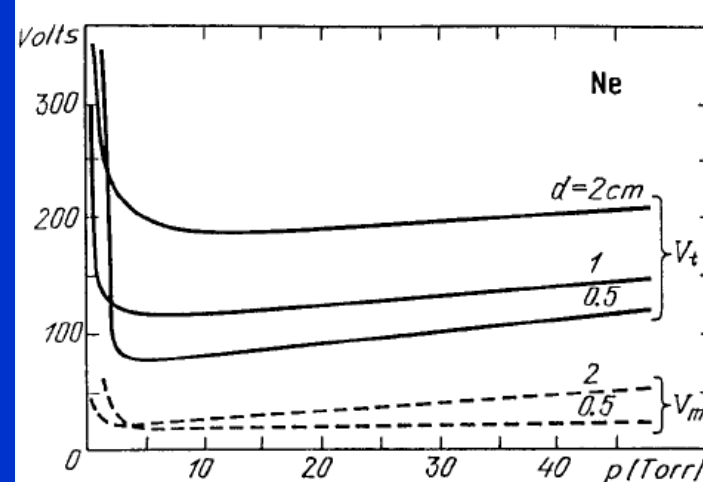


Fig. 7.19. Ignition potential of capacitively coupled rf discharge in neon (V_t), $f = 158$ MHz; d is the distance between the planar electrodes (which are covered by glass). Dashed curves show the burning voltage of a steady discharge, V_m [7.15]

Calculation of avalanche...

Electrical discharge regime

● Dark discharge

- A – B During the background ionization stage of the process the electric field applied along the axis of the discharge tube sweeps out the ions and electrons created by ionization from background radiation. Background radiation from cosmic rays, radioactive minerals, or other sources, produces a constant and measurable degree of ionization in air at atmospheric pressure. The ions and electrons migrate to the electrodes in the applied electric field producing a weak electric current. Increasing voltage sweeps out an increasing fraction of these ions and electrons.
- B – C If the voltage between the electrodes is increased far enough, eventually all the available electrons and ions are swept away, and the current saturates. In the saturation region, the current remains constant while the voltage is increased. This current depends linearly on the radiation source strength, a regime useful in some radiation counters.
- C – D If the voltage across the low pressure discharge tube is increased beyond point C, the current will rise exponentially. The electric field is now high enough so the electrons initially present in the gas can acquire enough energy before reaching the anode to ionize a neutral atom. As the electric field becomes even stronger, the secondary electron may also ionize another neutral atom leading to an avalanche of electron and ion production. The region of exponentially increasing current is called the Townsend discharge.
- D – E Corona discharges occur in Townsend dark discharges in regions of high electric field near sharp points, edges, or wires in gases prior to electrical breakdown. If the coronal currents are high enough, corona discharges can be technically "glow discharges", visible to the eye. For low currents, the entire corona is dark, as appropriate for the dark discharges. Related phenomena include the silent electrical discharge, an inaudible form of filamentary discharge, and the brush discharge, a luminous discharge in a non-uniform electric field where many corona discharges are active at the same time and form streamers through the gas.

● Breakdown

- E Electrical breakdown occurs in Townsend regime with the addition of secondary electrons emitted from the cathode due to ion or photon impact. At the breakdown, or sparking potential V_B , the current might increase by a factor of 10^4 to 10^8 , and is usually limited only by the internal resistance of the power supply connected between the plates. If the internal resistance of the power supply is very high, the discharge tube cannot draw enough current to break down the gas, and the tube will remain in the corona regime with small corona points or brush discharges being evident on the electrodes. If the internal resistance of the power supply is relatively low, then the gas will break down at the voltage V_B , and move into the normal glow discharge regime. The breakdown voltage for a particular gas and electrode material depends on the product of the pressure and the distance between the electrodes, pd , as expressed in Paschen's law (1889).

● Glow discharge

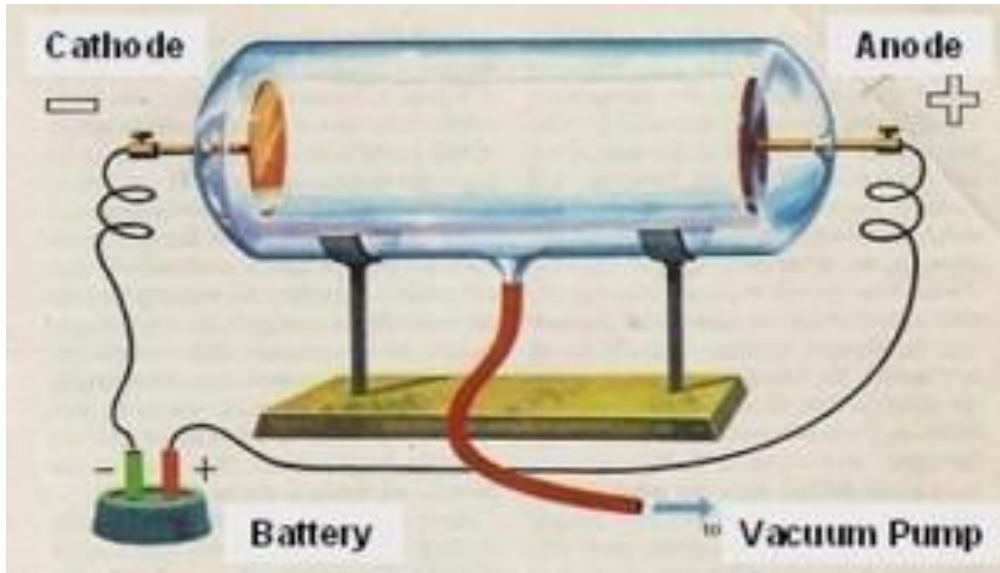
- F – G After a discontinuous transition from E to F, the gas enters the normal glow region, in which the voltage is almost independent of the current over several orders of magnitude in the discharge current. The electrode current density is independent of the total current in this regime. This means that the plasma is in contact with only a small part of the cathode surface at low currents. As the current is increased from F to G, the fraction of the cathode occupied by the plasma increases, until plasma covers the entire cathode surface at point G.
- G – H In the abnormal glow regime above point G, the voltage increases significantly with the increasing total current in order to force the cathode current density above its natural value and provide the desired current. Starting at point G and moving to the left, a form of hysteresis is observed in the voltage-current characteristic. The discharge maintains itself at considerably lower currents and current densities than at point F and only then makes a transition back to Townsend regime.

● Arc discharge

- H – K At point H, the electrodes become sufficiently hot that the cathode emits electrons thermionically. If the DC power supply has a sufficiently low internal resistance, the discharge will undergo a glow-to-arc transition, H-I. The arc regime, from I through K is one where the discharge voltage decreases as the current increases, until large currents are achieved at point J, and after that the voltage increases slowly as the current increases.

Regions in the DC Glow Discharge Tube

Resistance is missing !!!!!

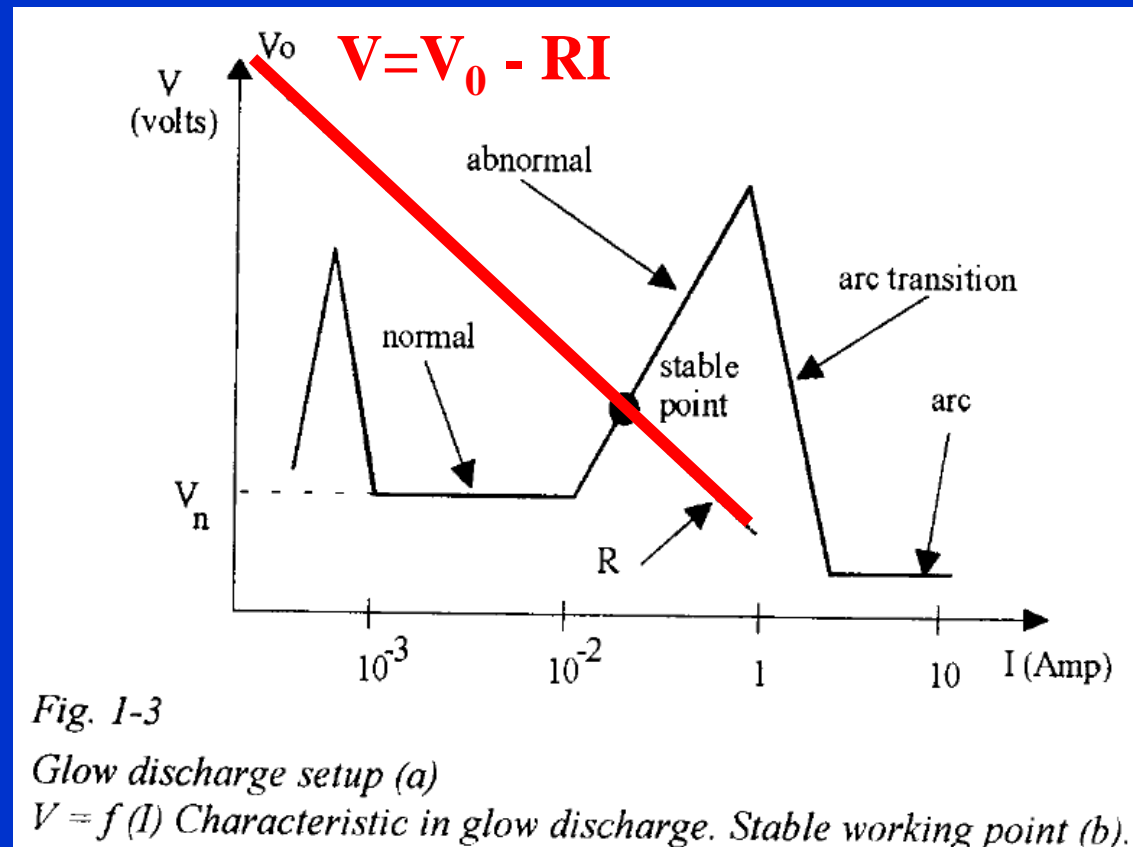
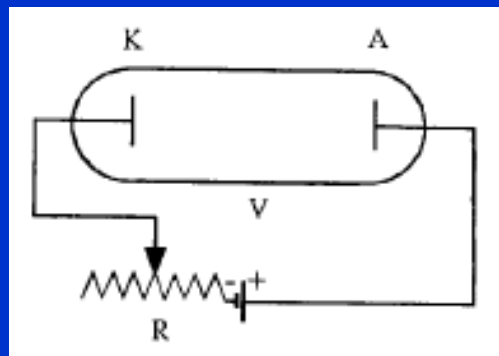


A glass tube, about *16 inches long* and *1 1/2 inches in diameter*, is hermetically sealed at both ends. Two metal probes are fused into the tube at each end. The physicist applies a potential of a few thousand volts across both probes. With the aid of a vacuum pump he sucks the *air* out of the tube, thus lowering the pressure inside the glass tube.

Electric discharges V-A characteristic

ZFP PGS 2006 lecture 4

Direct current (DC) glow discharge

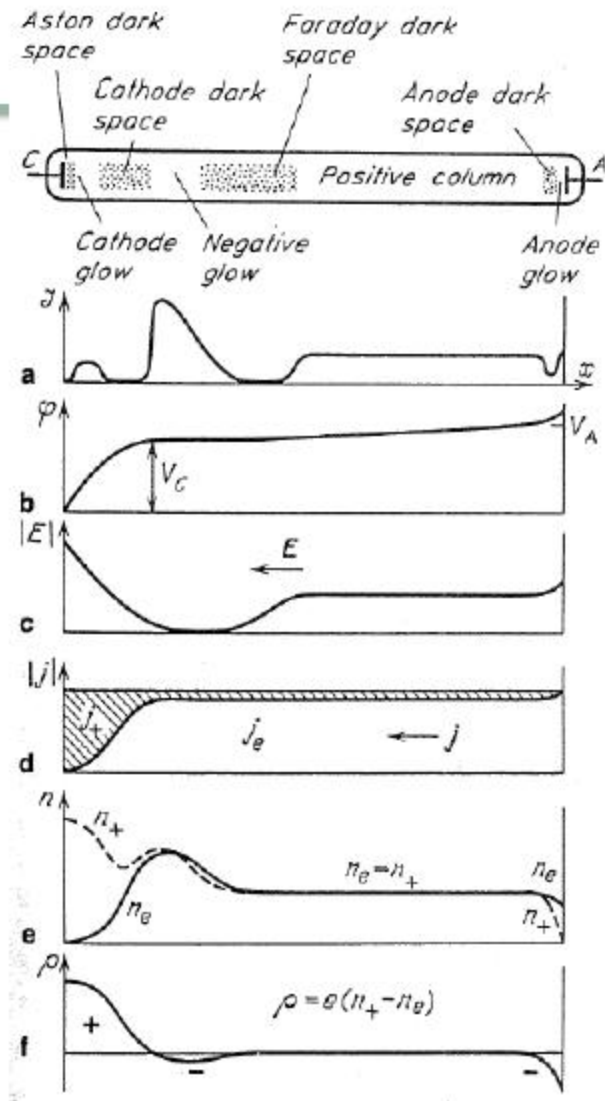
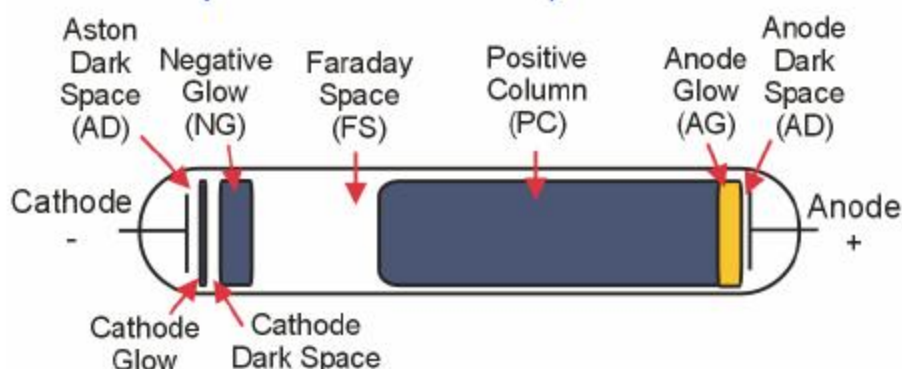
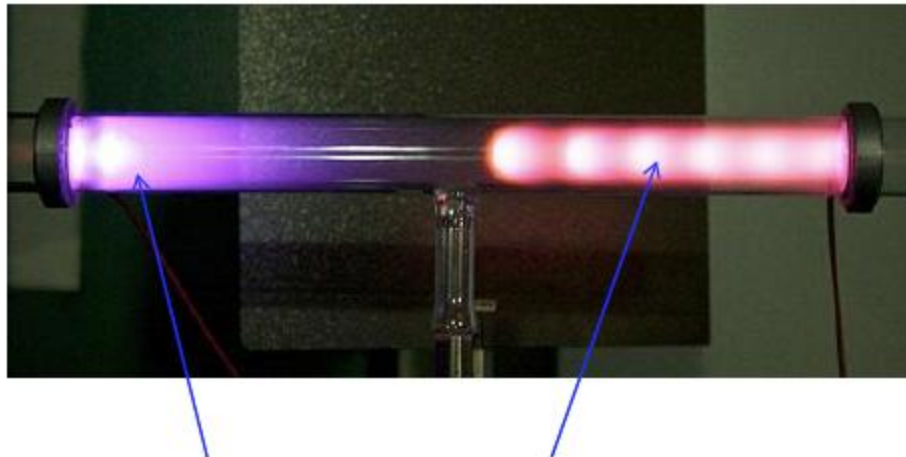


Doporučená literatura:

Reactive plasmas
Andre Ricard

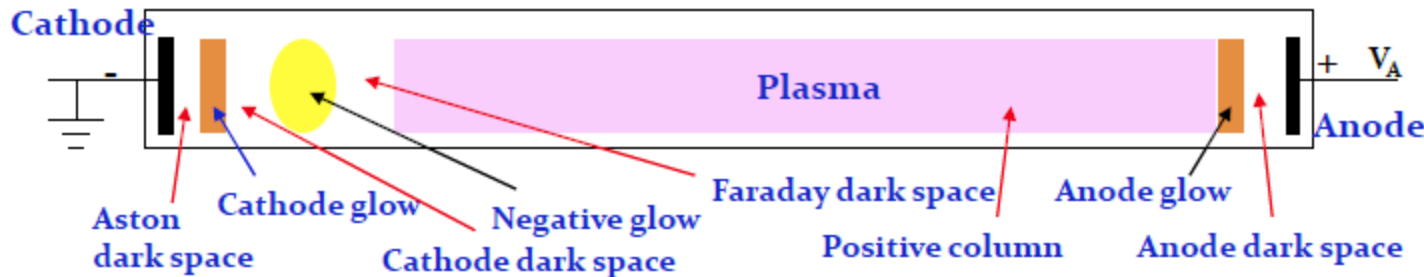
Glow discharge...

Structure of glow discharge



Glow discharge...

Structure of glow discharge

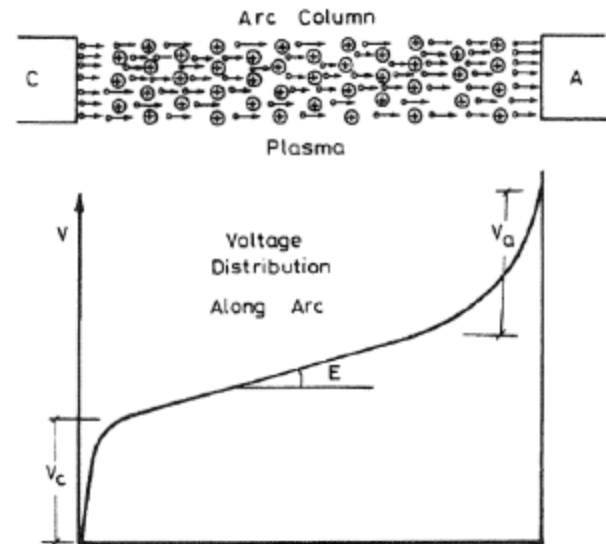
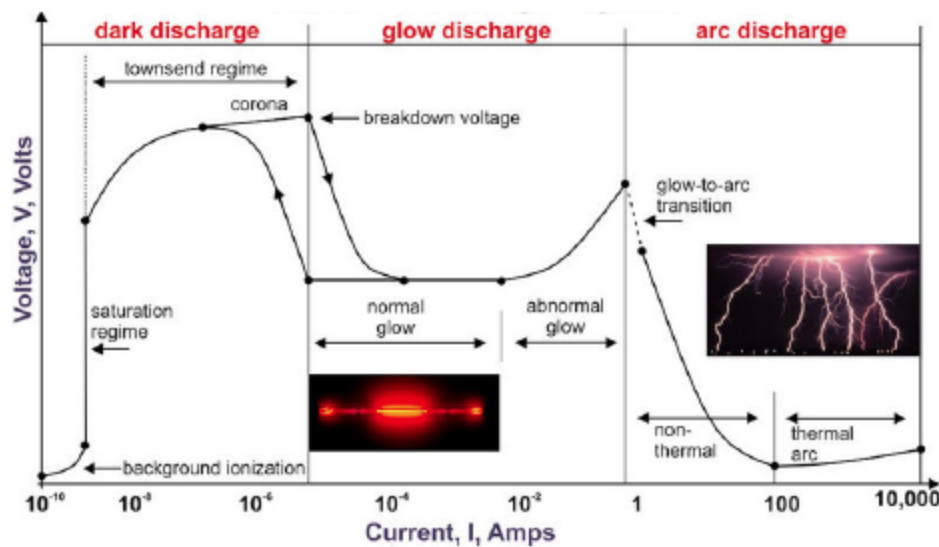


- **Cathode** : cathode material, secondary electron emission coefficients
- **Aston dark space** : a thin region with a strong electric field, and a negative space charge. Electrons are **too low density and/or energy** to excite the gas
- **Cathode glow** : reddish or orange color in air due to **emission by excited atoms sputtered off the cathode surface, or incoming positive ions**. High ion number density
- **Cathode (Crookes, Hittorf) dark space** : moderate electric field, a positive space charge and a relatively high ion density
- **Cathode region** : Most of the voltage drop, known as **cathode fall V_c** , most of the power dissipation, electrons are accelerated in this region, the axial length of the cathode region determined by **Paschen minimum**
- **Negative glow** : accelerated electrons produce **ionization and intense excitation**, hence **brightest light intensity**, relatively low electric field, longer than cathode glow, typical electron density of 10^{16} electrons/m³
- **Faraday dark space** : **low electron energy** due to ionization and excitation, electron number density decreased by recombination and radial diffusion
- **Positive column** : **quasi-neutral plasma**, small electric field of 1V/cm, electron number density of $10^{15}\text{--}10^{16}$ electrons/m³, temperature of 1-2 eV, **long uniform glow**
- **Anode glow** : bright region at the boundary of the anode sheath
- **Anode dark space** : **anode sheath**, negative space charge, higher electric field than positive column

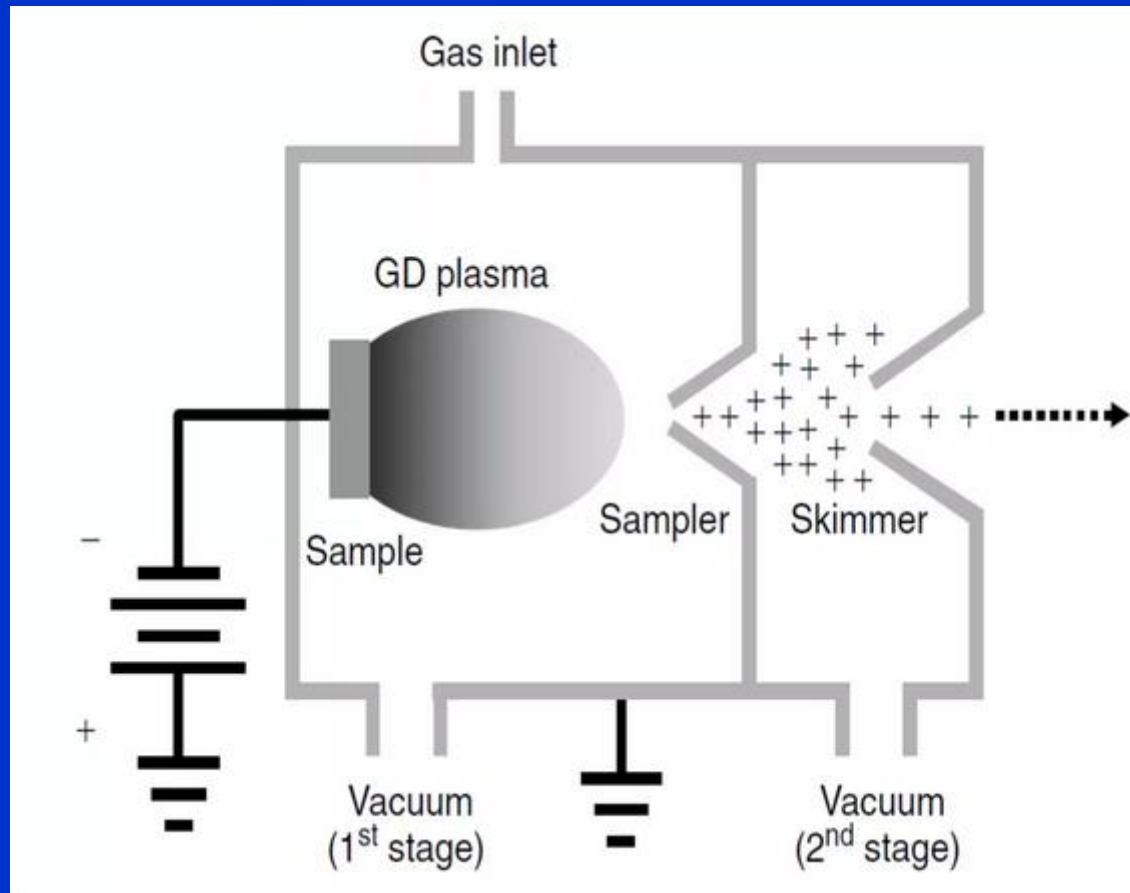
Arc discharge...

Arc discharge

- Electrons emitted from the cathode spot can be produced mainly by thermionic emission if the cathode is made of a high-melting-point metal (e.g., carbon, tungsten, or molybdenum). With cathodes of low melting point, electrons can be supplied by field emission from points of micro-roughness where the electric field is highly concentrated.
- An additional important source of electrons at the cathode is ionized metal vapor.

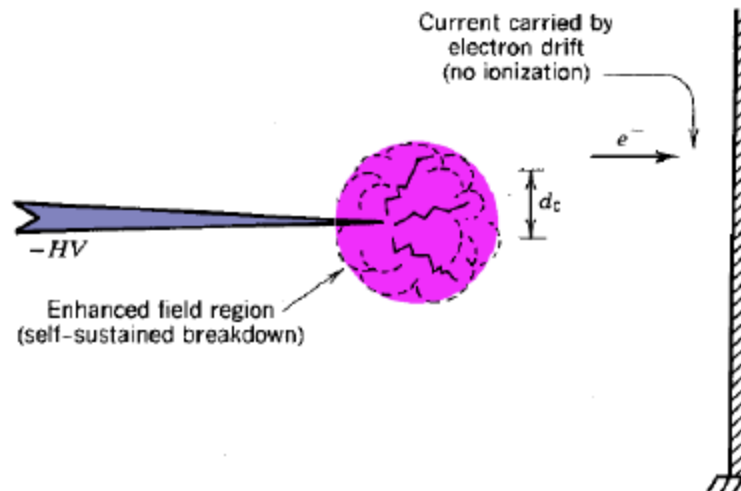


GLOW DISCHARGE MASS SPECTROMETRY



Corona discharges

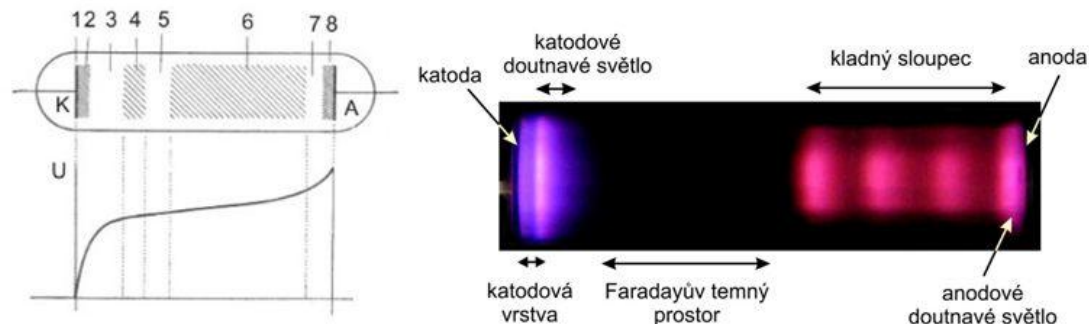
- Corona discharges appear in gases when electrodes have strong two-dimensional variations.
- Corona (crown in Latin) is a pattern of bright sparks near a pointed electrode. In such a region, the electric field is enhanced above the breakdown limit so that electron avalanches occur.



Glow discharges

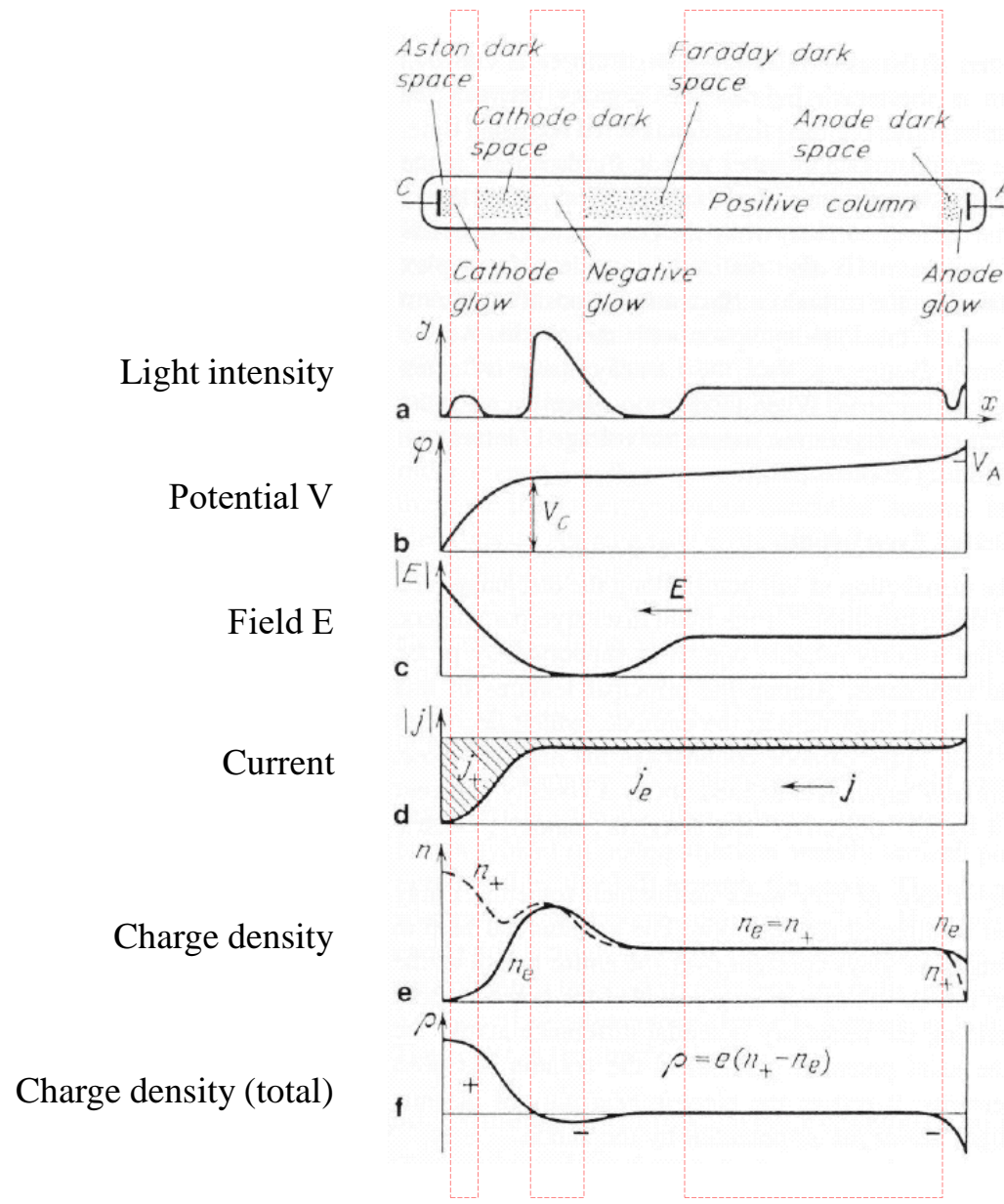
DOUTNAVÝ A TEMNÝ VÝBOJ

- TEMNÝ VÝBOJ: První samostatný výboj, bez světelných projevů.
- DOUTNAVÝ VÝBOJ: Katodový úbytek (stovky voltů), rozložení prostorových nábojů, nerovnováha: $T_e = 15-80$ tis. K, $T_{i/n} = 300$ K
- KATODOVÁ ČÁST VÝBOJE:
 - 1)Astonův prostor
 - 2)Katodová vrstva
 - 3)Crokesův temný prostor
 - 4)Doutnavé katodové světlo
 - 5)Faradayův temný prostor
- KLADNÝ SLOUPEC VÝBOJE:
 - 6)Kladný světelný sloupec
 - 7)Temný anodový prostor
 - 8>Anodové doutnavé světlo

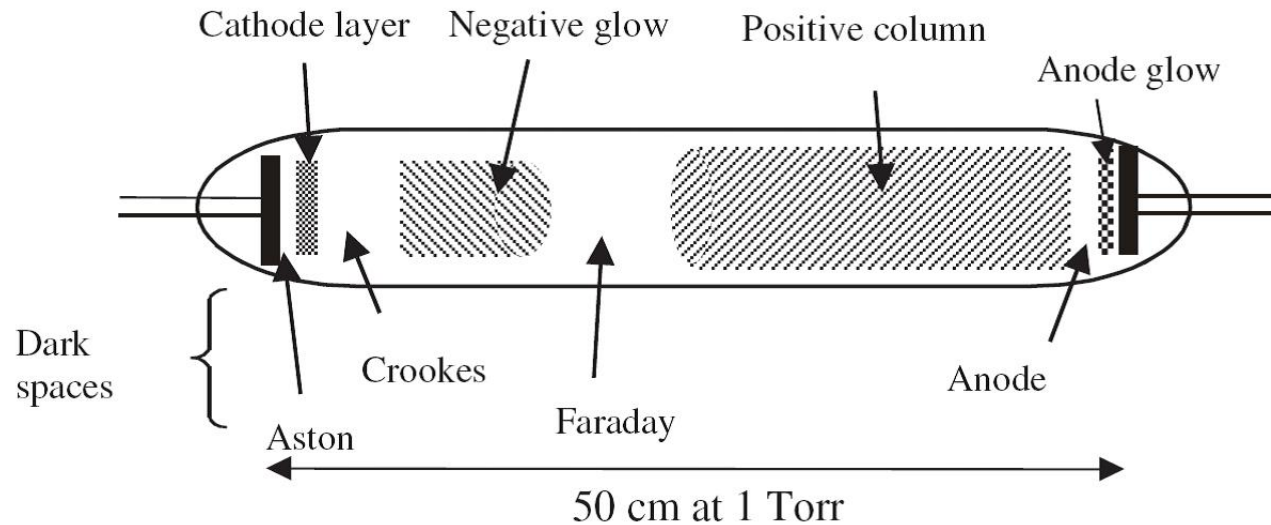


Obr.: 21. U-graf Doutnavý výboj,
popis

Potentials along the Tube



Regions in the Glow Discharge Tube II



Potentials along the Tube

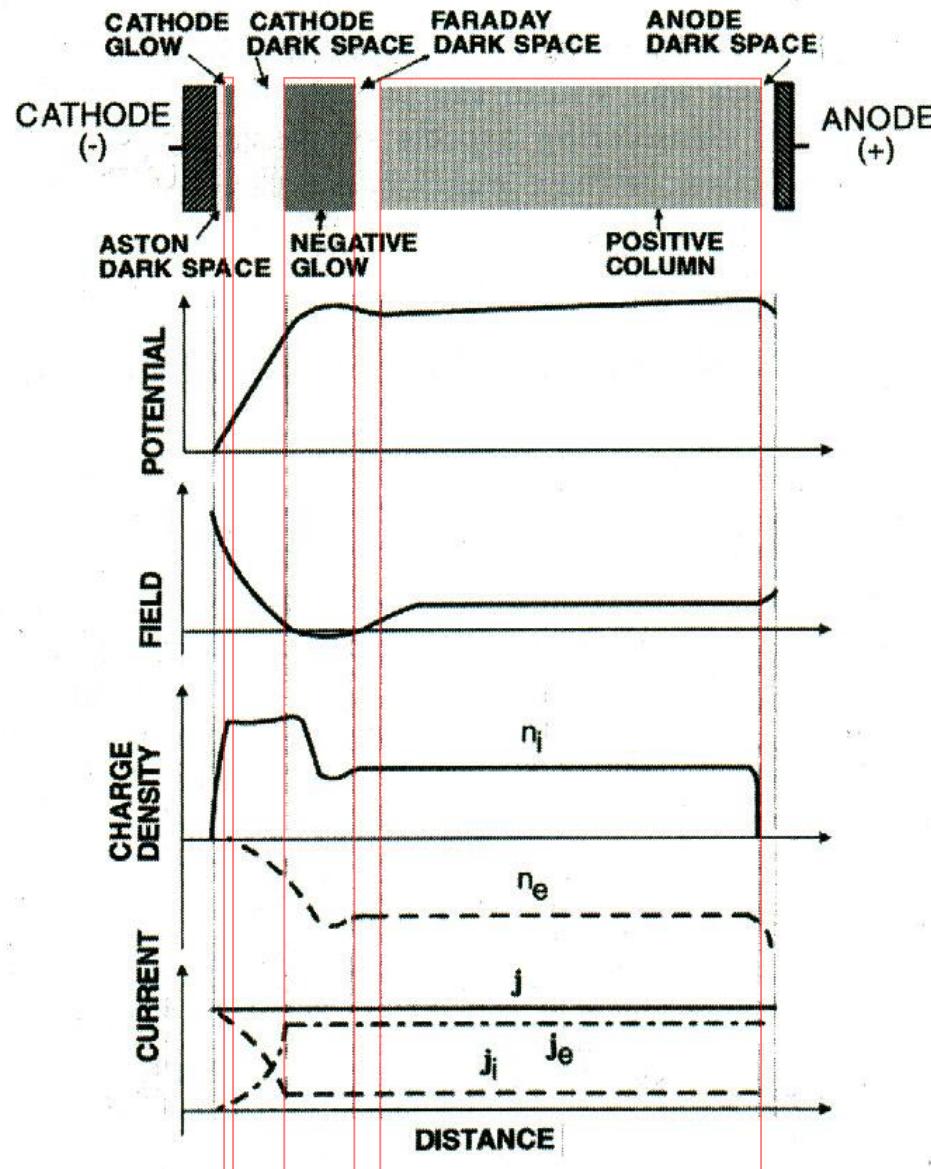


Figure 4-3 Structure of a DC glow discharge with corresponding potential, electric field, charge, and current distributions.

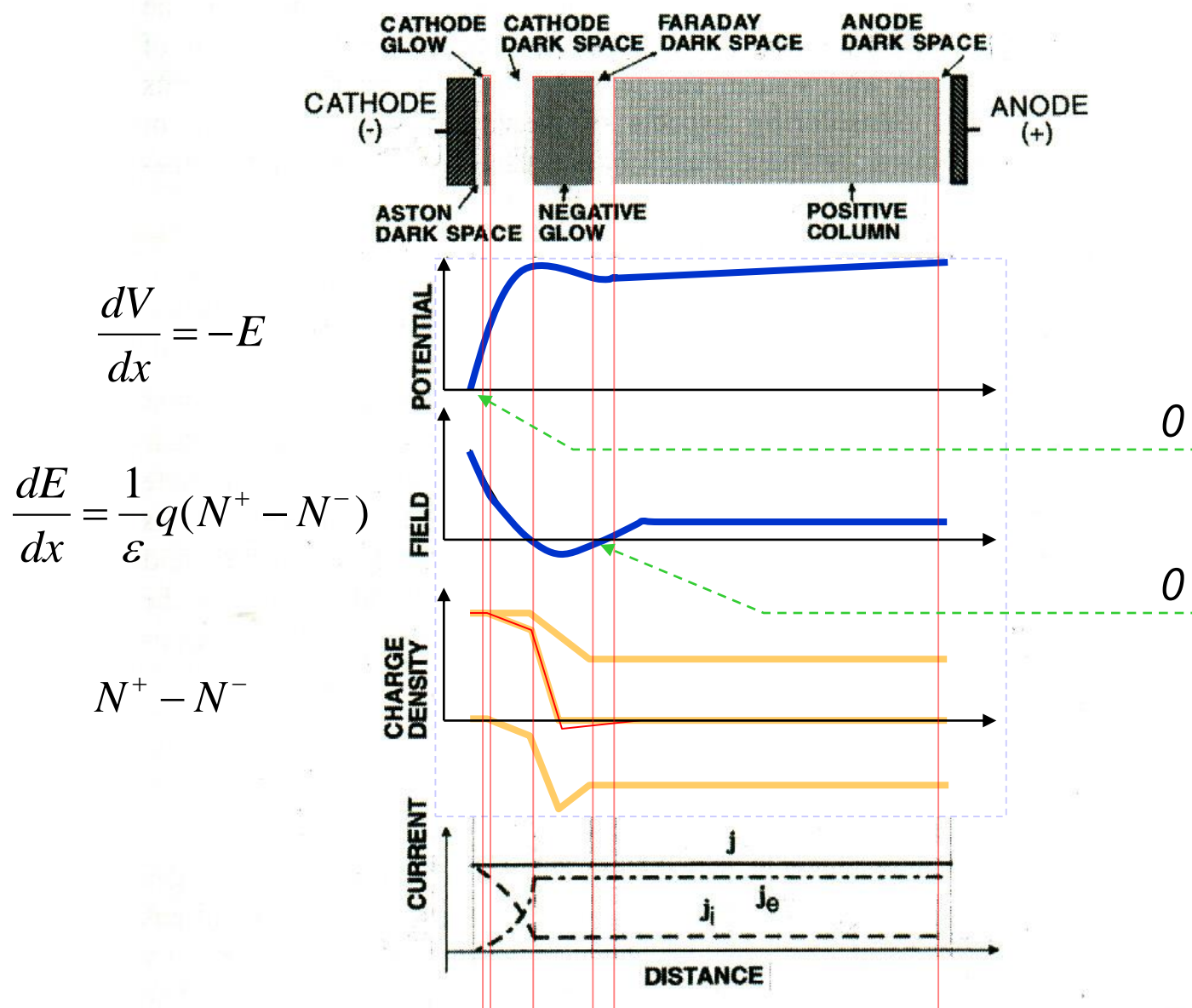


Figure 4-3 Structure of a DC glow discharge with corresponding potential, electric field, charge, and current distributions.

Calculation of avalanche...

Definition of breakdown voltage and time delay

Electrical breakdown in gases does not take place instantly upon applying a voltage U_b to the electrodes of gas-filled tube, but after a corresponding delay known as electrical breakdown time delay t_d that is mutually dependent on U_b . Due to the statistical nature of processes which initiate breakdown, U_b and t_d are mutually dependent stochastic variables with certain distributions. The distribution function of t_d defines the probability of electrical breakdown in any time interval.

U_b is the voltage when the gas transits from non-selfsustaining to self-sustaining discharge

Due to the fluctuation of the parameters α and γ with time, the electrical breakdown usually does not occur for the same voltage in a series of experiments. Also, the breakdown voltage depends on the time dependence of the applied voltage.

t_d is the time elapsed from the instant of time when applied voltage reaches the breakdown voltage to the moment when it starts to decrease due to the breakdown in gas-filled tube

The other definition states that t_d is the time interval between the moment of U_w ($U_w > U_s$) application on the tube and the moment when the tube current exhibits a detectable discharge.

The t_d consists of the statistical time delay (t_s) and formative time (t_f), i.e. $t_d = t_s + t_f$

Breakdown voltage as a function of rate

U_b is the measured breakdown voltage and k is the rate of the increase of the applied voltage

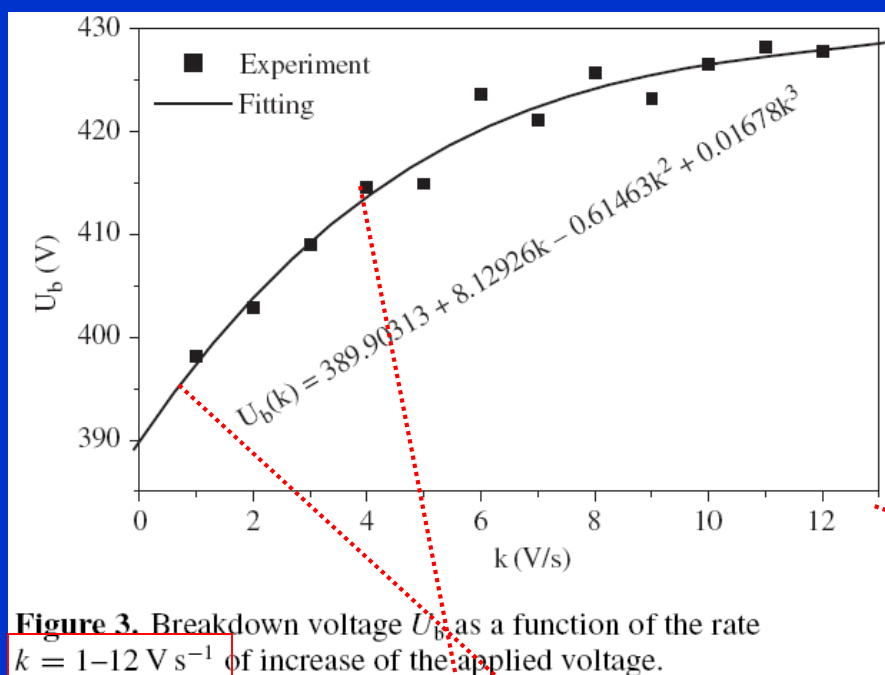


Figure 3. Breakdown voltage U_b as a function of the rate $k = 1\text{--}12 \text{ V s}^{-1}$ of increase of the applied voltage.

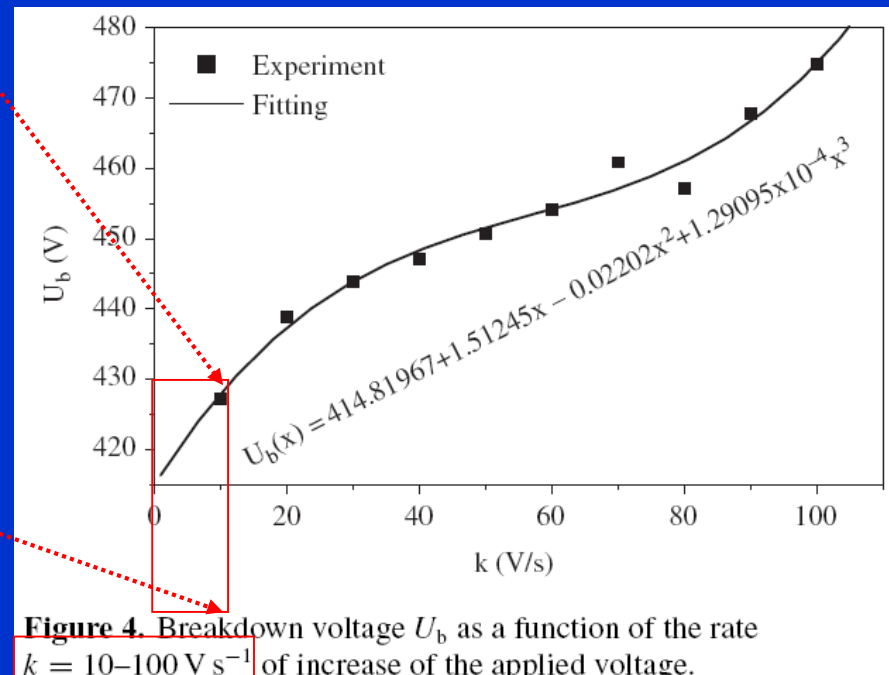
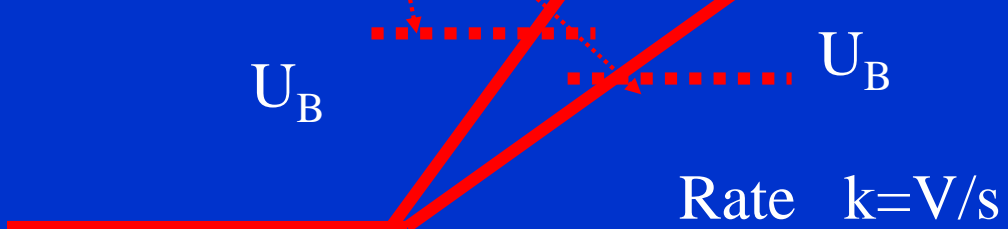


Figure 4. Breakdown voltage U_b as a function of the rate $k = 10\text{--}100 \text{ V s}^{-1}$ of increase of the applied voltage.



Breakdown voltage as a function of rate

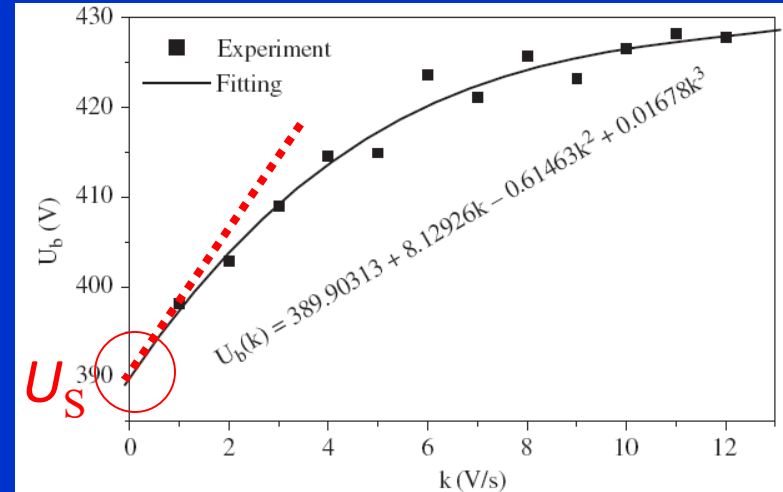
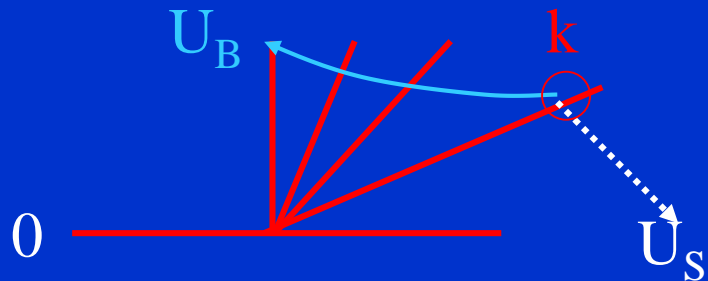


Figure 3. Breakdown voltage U_b as a function of the rate $k = 1-12 \text{ V s}^{-1}$ of increase of the applied voltage.

estimated U_S value was $\approx 390\text{V}$

Extrapolation of the $U_b = f(k)$ dependence to the intersect with U_b -axis (for $k = 0$) gives the estimation of U_s .

The t_d consists of the statistical time delay (t_s) and formative time (t_f), i.e. $t_d = t_s + t_f$

Breakdown voltage as a function of rate Statistical character of τ_d

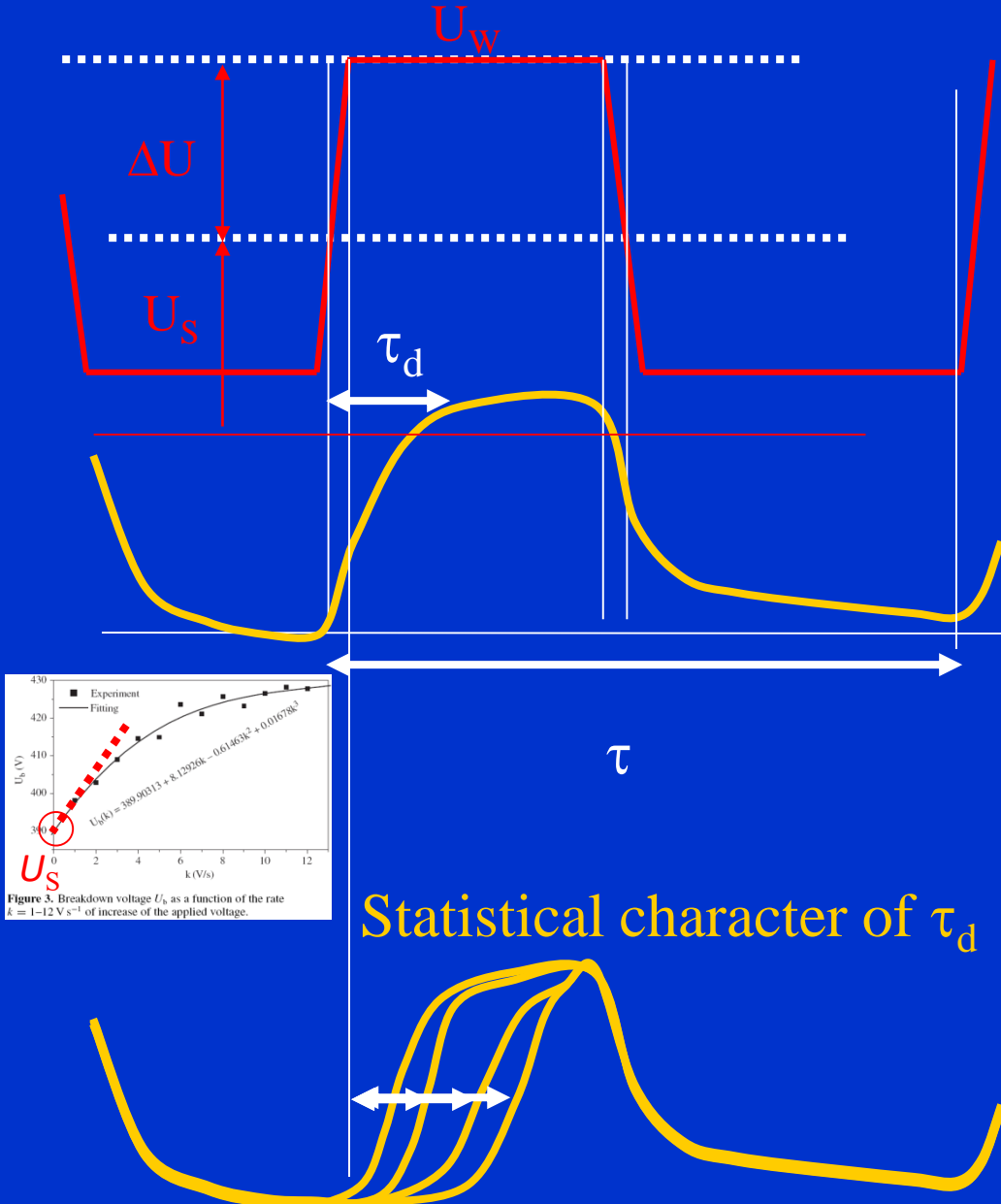


Figure 3. Breakdown voltage U_b as a function of the rate $k = 1-12 \text{ V s}^{-1}$ of increase of the applied voltage.

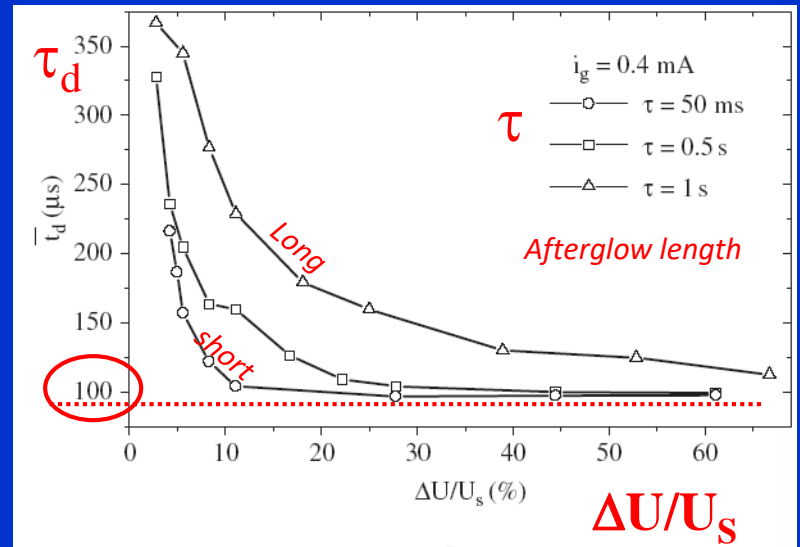


Figure 9. Mean value of time delay $\bar{\tau}_d$ as a function of overvoltage $\Delta U/U_s$ for three different values of afterglow period for nitrogen-filled tube at pressure 1.3 mbar [27] (©1998 IEEE).

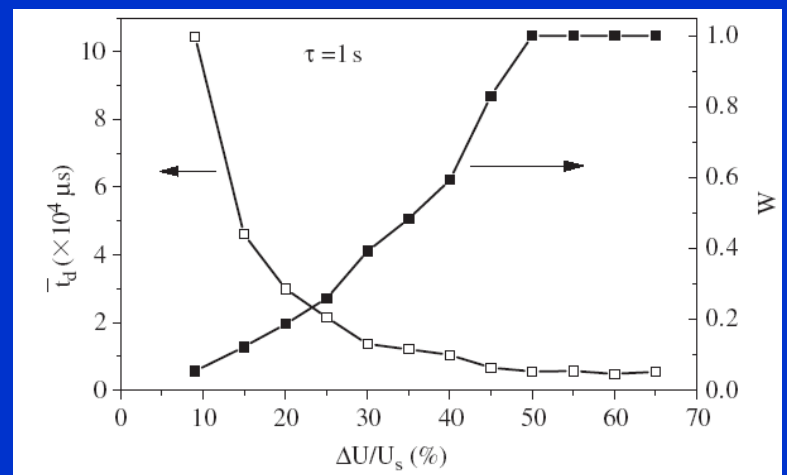
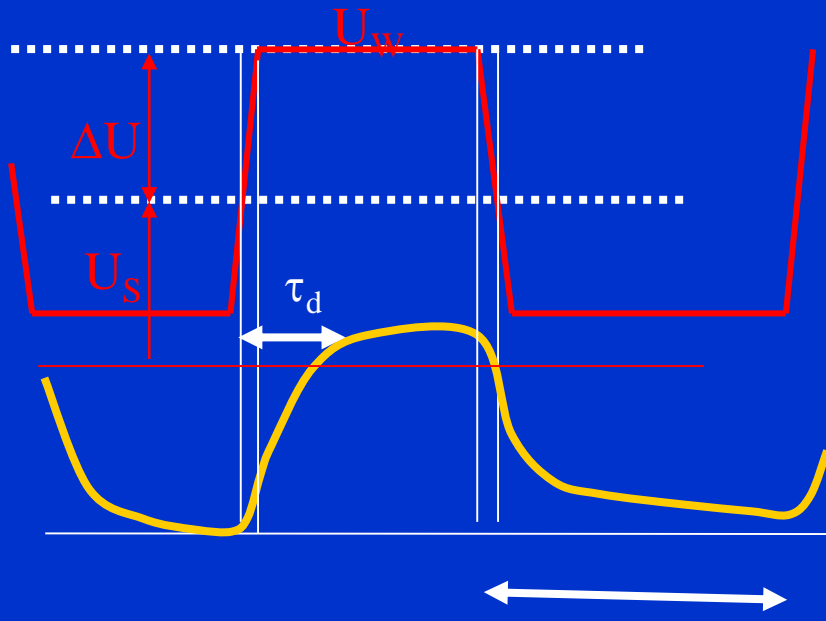
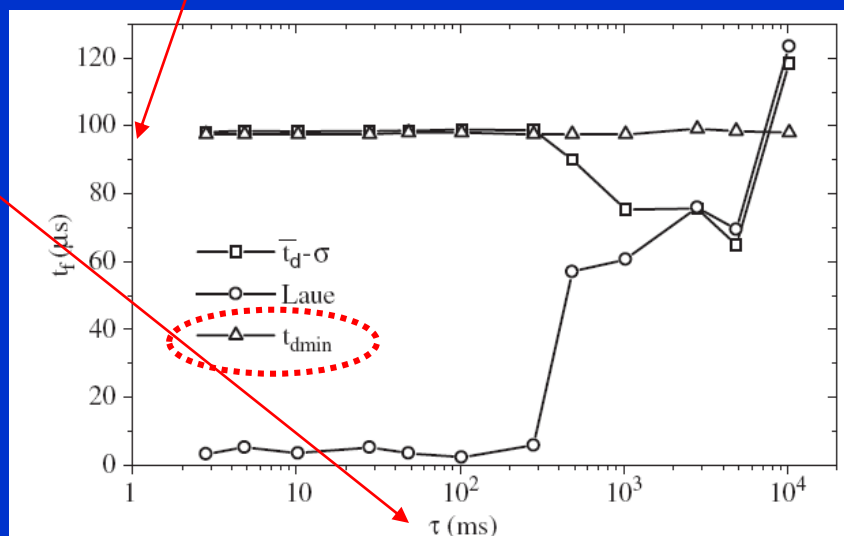
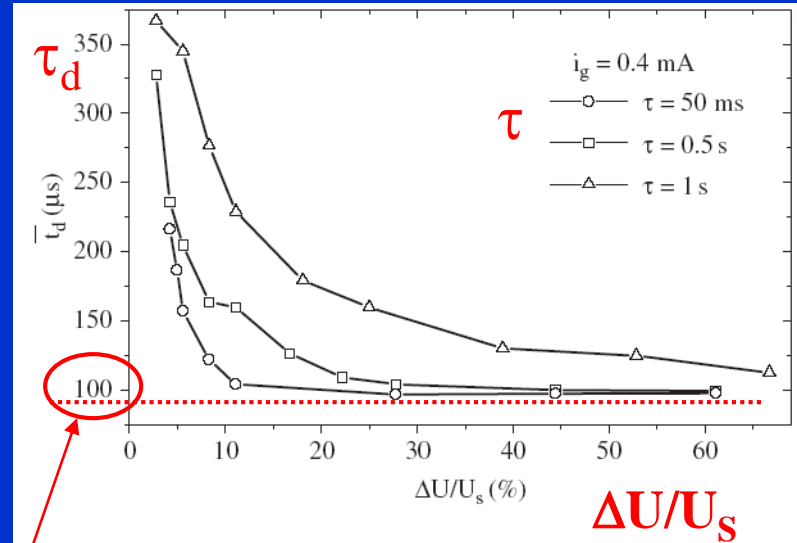


Figure 8. Mean value of time delay $\bar{\tau}_d$ and breakdown probability W as a function of overvoltage for kripton-filled tube at pressure 2.7 mbar [31].

Breakdown voltage as a function of rate



Statistical character of τ_d



Influence of different experimental parameters on time delay

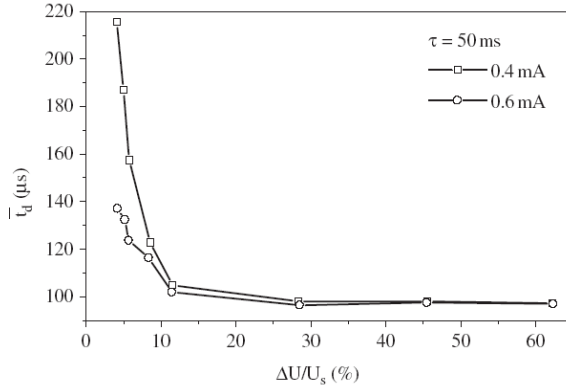


Figure 10. Mean value of time delay \bar{t}_d as a function of overvoltage $\Delta U/U_s$ for two different values of glow current for nitrogen-filled tube at pressure 1.3 mbar [27] (©1998 IEEE).

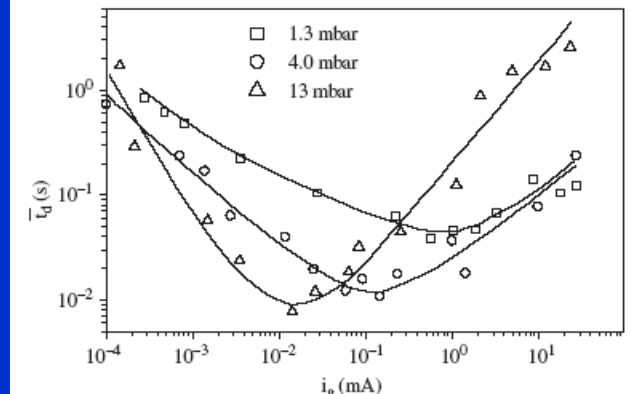


Figure 14. Mean value of time delay \bar{t}_d as a function of glow current i_g for three nitrogen-filled tubes with different pressures [40].

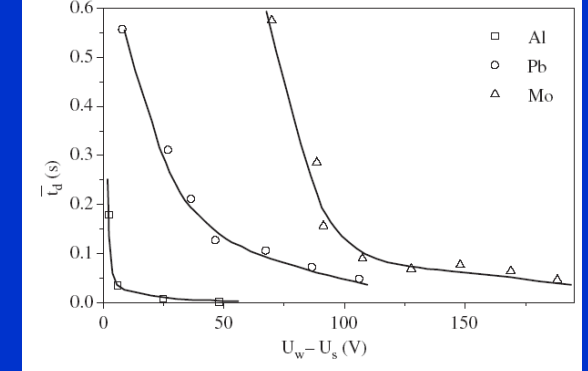


Figure 12. Mean value of time delay \bar{t}_d as a function of difference between the applied voltage and the static breakdown voltage $U_w - U_s$ for nitrogen-filled tube at pressure 7.0 mbar with three pairs of electrodes made of Al, Pb and Mo [35].

Discharge current

Pressure (diffusion...)

Electrode material

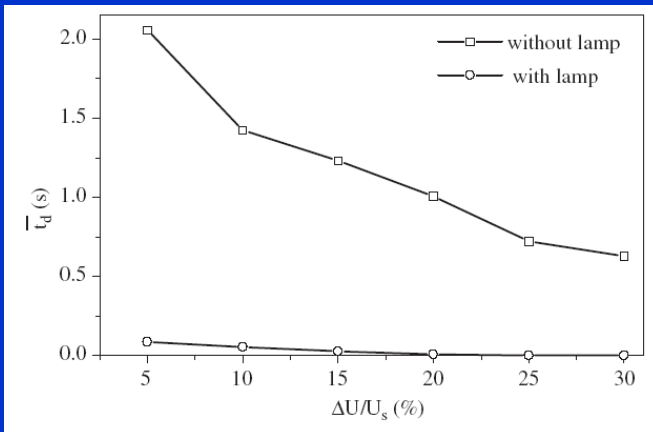


Figure 11. Mean value of time delay \bar{t}_d as a function of overvoltage $\Delta U/U_s$ for nitrogen-filled tube at pressure 1.3 mbar in the cases with/without illumination lamps [32].

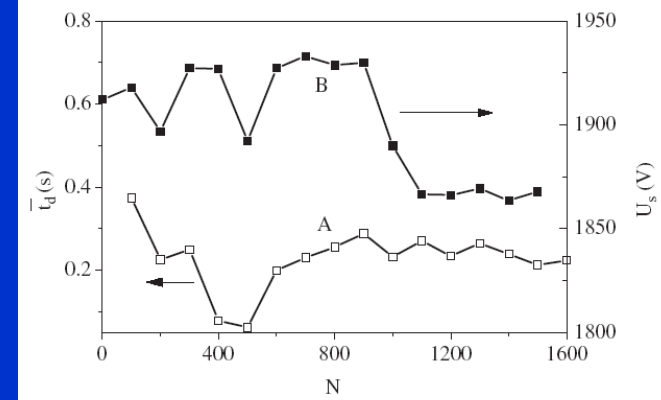


Figure 13. Mean value of time delay \bar{t}_d and static breakdown voltage U_s as a function of a number of breakdowns N for nitrogen-filled tube at pressure 97.5 mbar. (A) $\bar{t}_d = f(N)$, $\tau = 10\text{ s}$; (B) $U_s = \varphi(N)$ [39].

Illumination

Number of breakdowns

Breakdown dependence on history

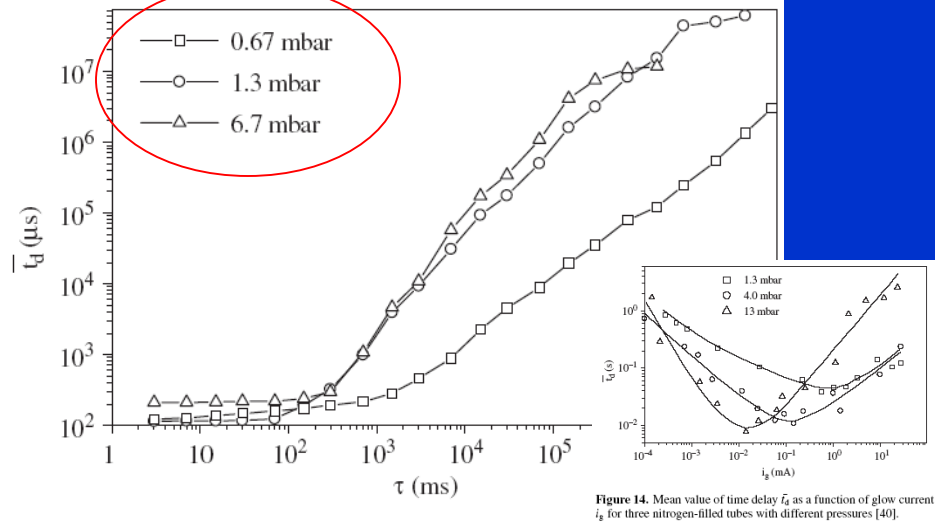
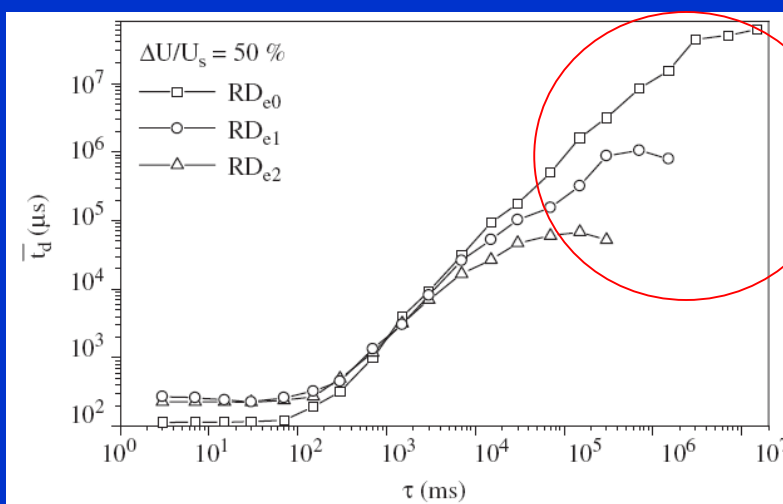
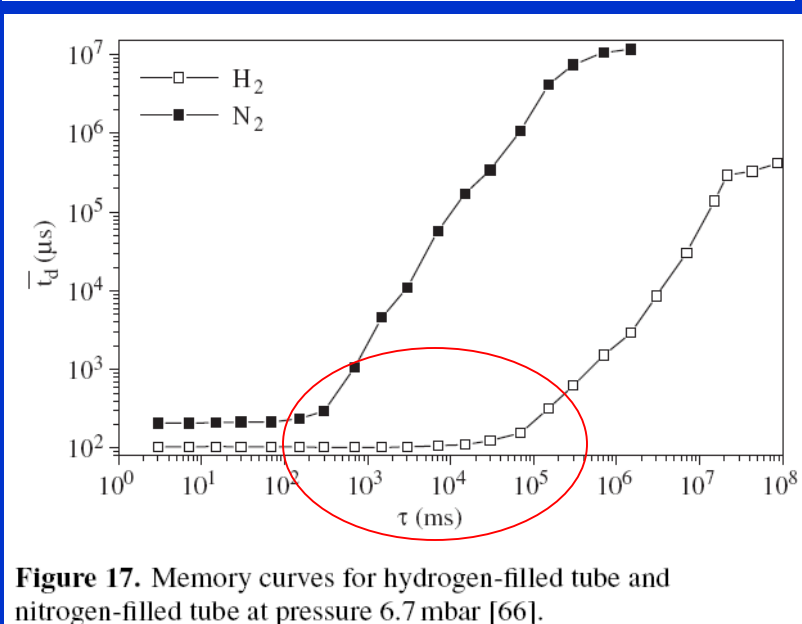
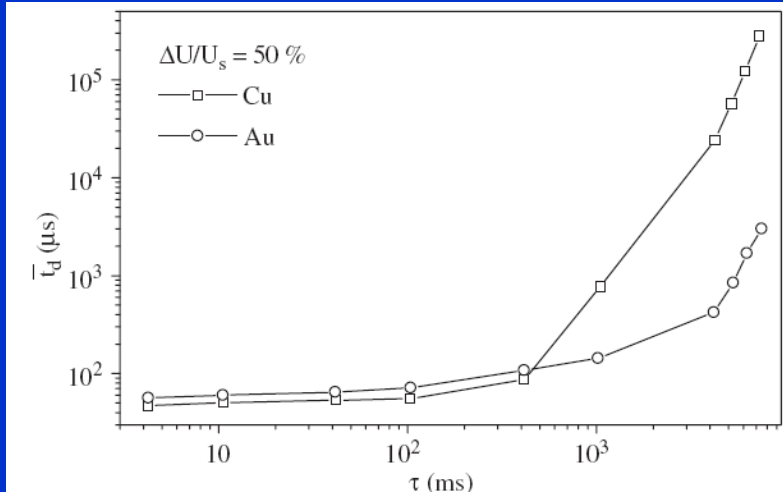


Figure 14. Mean value of time delay t_4 as a function of glow current i_g for three nitrogen-filled tubes with different pressures [40].



Townsend 1st ionization coefficient

- When an electron travels a distance equal to its free path λ_e in the direction of the field E , it gains an energy of $eE\lambda_e$. For the electron to ionize, its gain in energy should be at least equal to the ionization potential V_i of the gas:

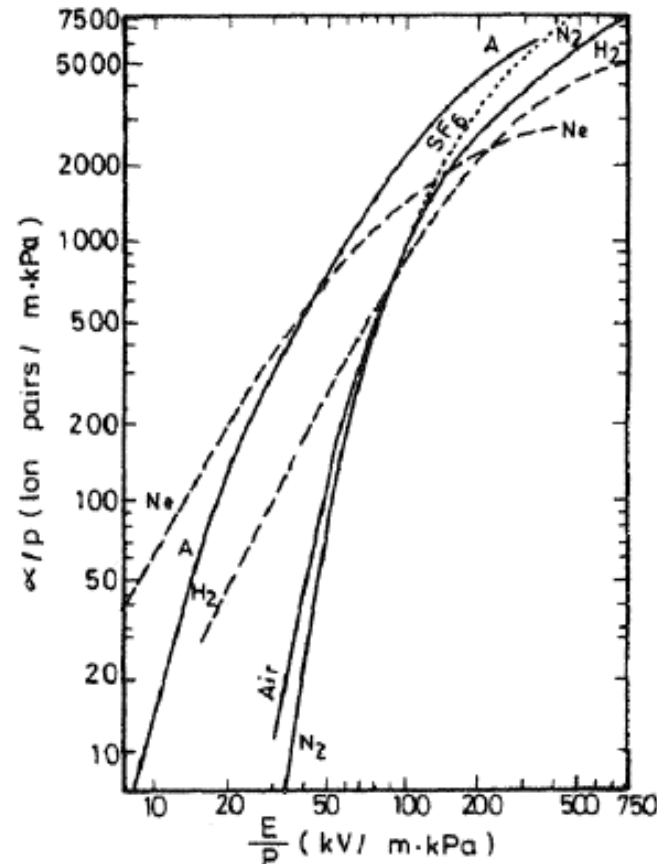
$$e\lambda_e E \geq eV_i \quad \lambda_e = \frac{1}{n\sigma} \propto \frac{1}{p}$$

- The Townsend 1st ionization coefficient is equal to the number of free paths ($= 1/\lambda_e$) times the probability of a free path being more than the ionizing length λ_{ie} ,

$$\alpha \propto \frac{1}{\lambda_e} \exp\left(-\frac{\lambda_{ie}}{\lambda_e}\right) \propto \frac{1}{\lambda_e} \exp\left(-\frac{V_i}{\lambda_e E}\right)$$

$$\alpha/p = A \exp\left(-\frac{B}{E/p}\right)$$

- A and B must be experimentally determined for different gases.



Calculation of avalanche...

Townsend's criterion for breakdown

- Secondary electron emission by ion impact: when heavy positive ions strike the cathode wall, secondary electrons are released from the cathode material.
- The self-sustaining condition is given by

$$M = \frac{e^{\alpha d}}{1 - \gamma(e^{\alpha d} - 1)} \rightarrow \infty$$

$$\alpha d = \ln\left(1 + \frac{1}{\gamma}\right)$$



- Paschen's law

Townsend 2nd ionization coefficient

$$\alpha/p = A \exp\left(-\frac{B}{E/p}\right) \quad \oplus$$

$$\alpha d = \ln\left(1 + \frac{1}{\gamma}\right)$$

$$\alpha d = A p d \exp\left(-\frac{B}{E/p}\right) = A p d \exp\left(-\frac{B p d}{V_B}\right) = \ln\left(1 + \frac{1}{\gamma}\right)$$

$$V_B = \frac{B p d}{\ln[A p d / \ln(1 + 1/\gamma)]} = f(p d)$$

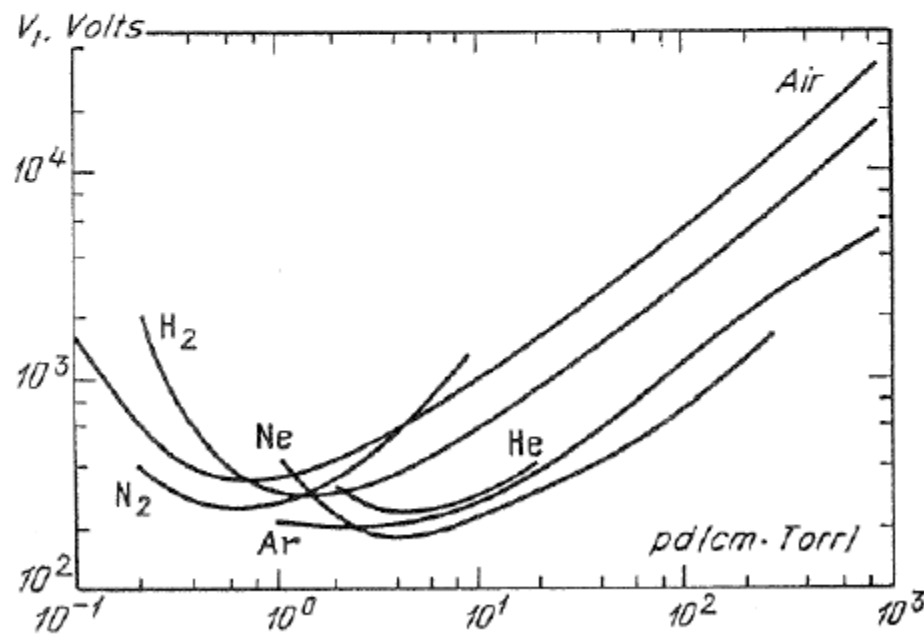
Calculation of avalanche...

Paschen curve

- Minimum breakdown voltage

$$V_{B,min} = \frac{eB}{A} \ln \left(1 + \frac{1}{\gamma} \right)$$

at $(pd)_{min} = \frac{e}{A} \ln \left(1 + \frac{1}{\gamma} \right)$

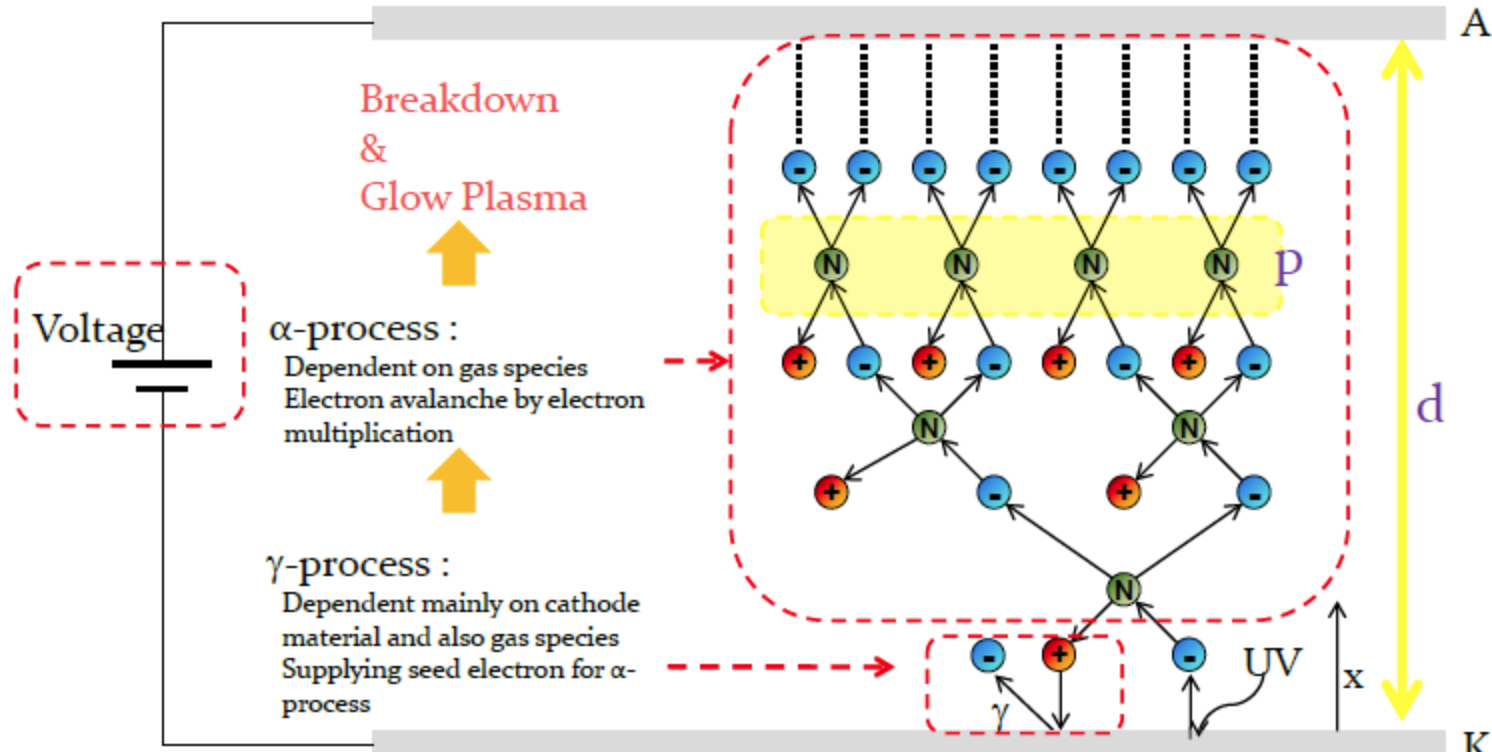


| Gas | $V_{B,min}$ (V) | $(pd)_{min}$ (torr-cm) |
|-----------|-----------------|------------------------|
| Air (dry) | 327 | 0.567 |
| A | 137 | 0.9 |
| H_2 | 273 | 1.15 |
| He | 156 | 4.0 |
| CO_2 | 420 | 0.51 |
| N_2 | 251 | 0.67 |
| O_2 | 450 | 0.7 |

- Main factors:
 - Pressure
 - Voltage
 - Electrode distance
 - Gas species
 - Electrode material (SEE)
- Small pd : too small collision
- Large pd : too often collision

Calculation of avalanche...

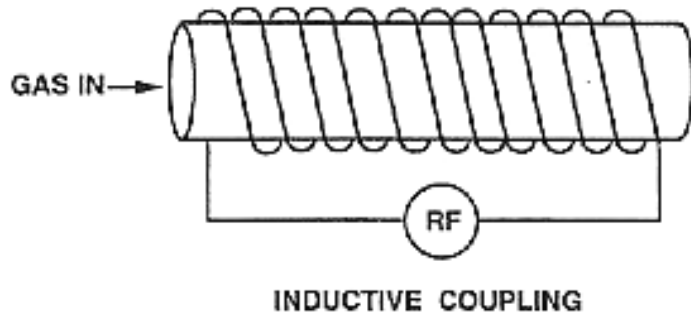
Summary of Townsend gas breakdown theory



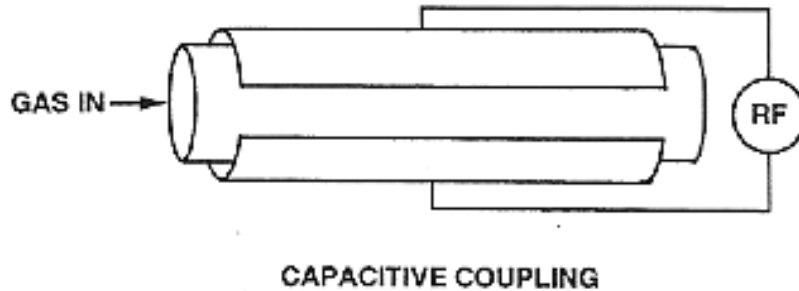
- Two processes (α and γ) are required to sustain the discharge.
- How about electronegative gases (e.g. SF₆) which are widely used for gas insulation?

Calculation of avalanche...

Electrodeless Reactors



Inductive coupling

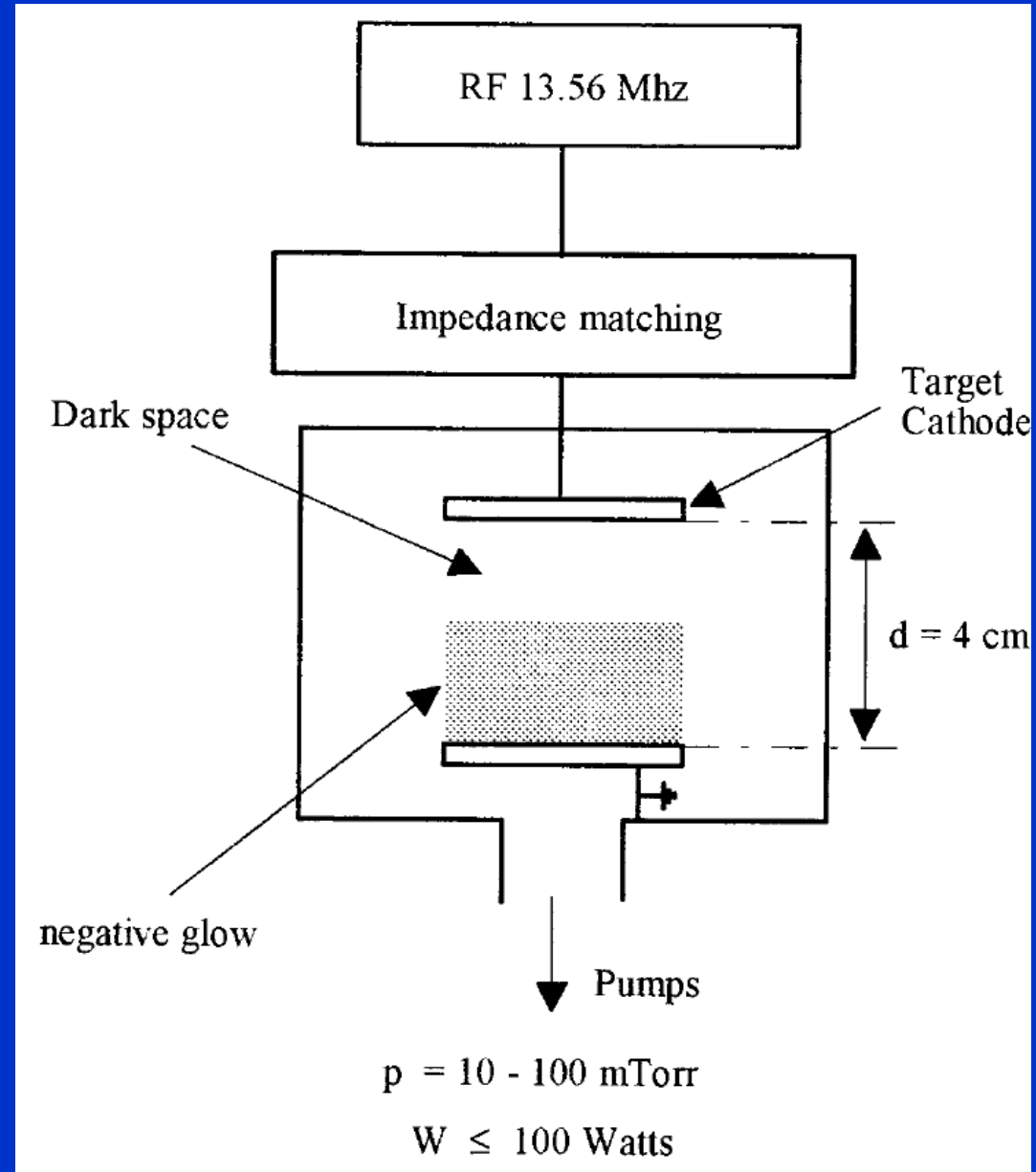


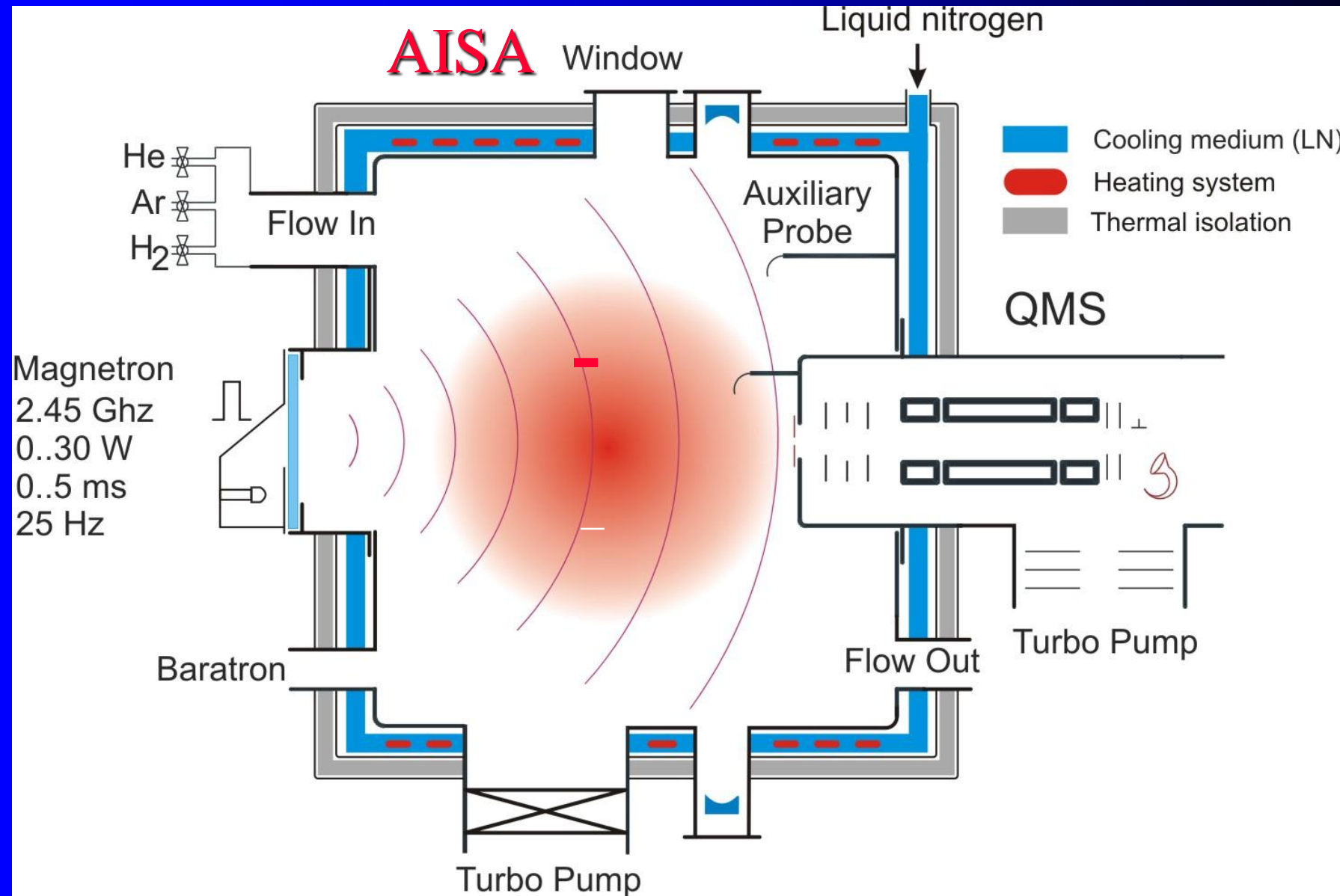
Capacitive coupling

However, for the deposition of films by RF sputtering, internal cathode targets are required.

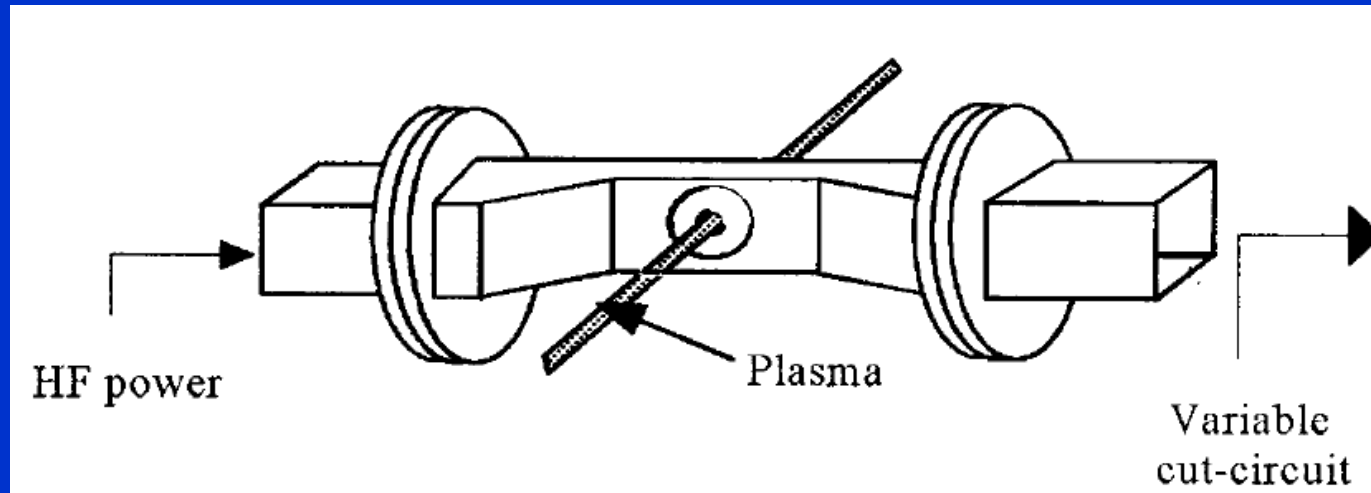
RF diode discharge

For technological applications –
surface treatments





Microwave discharge

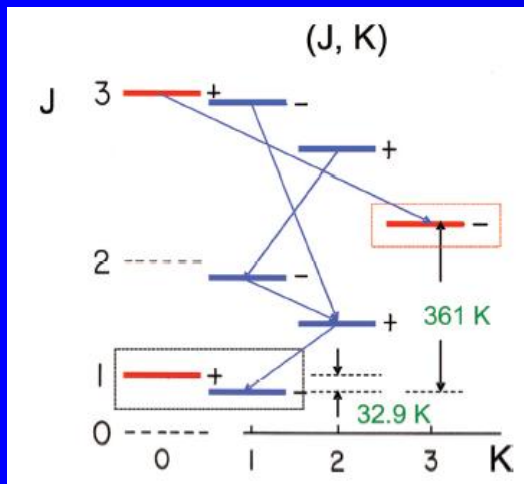


Microwave discharge → surfaguige discharge

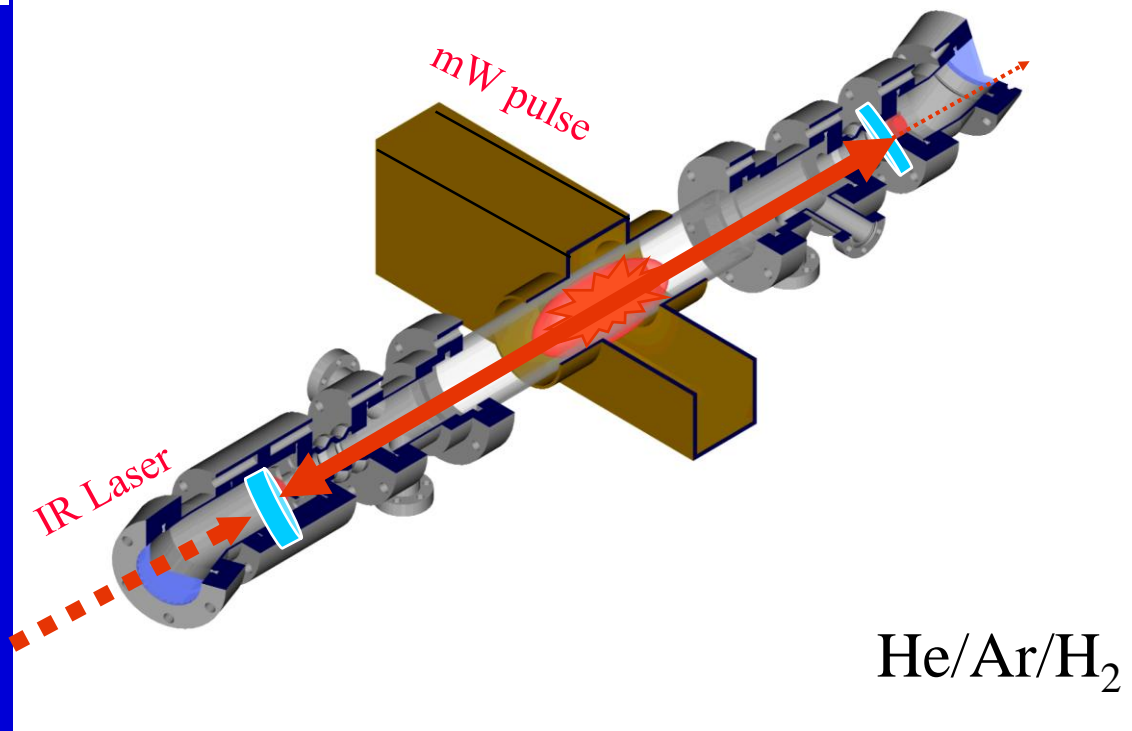
Stationary afterglow + Spectroscopic identification of recombining ions

$$\frac{d[H_3^+]}{dt} = -\alpha[H_3^+]n_e = -\alpha[H_3^+]^2$$

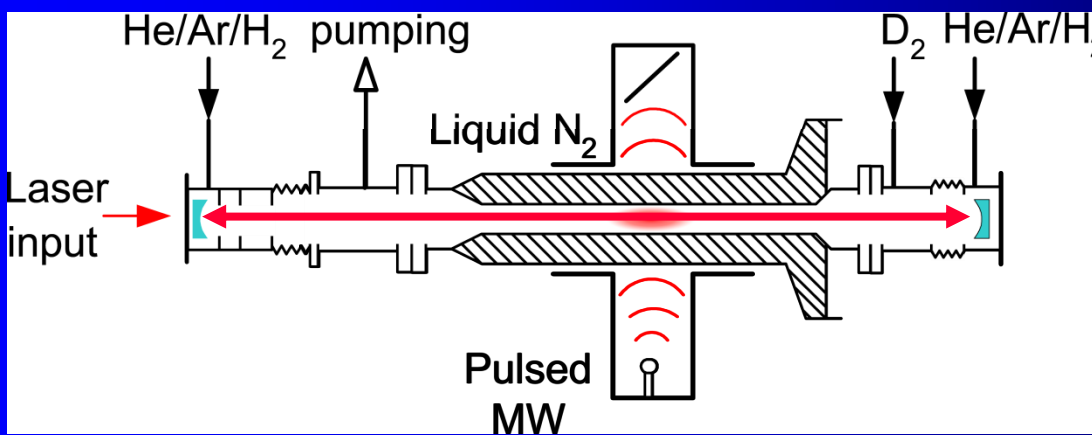
IR-CRDS
Laser absorption spectroscopy

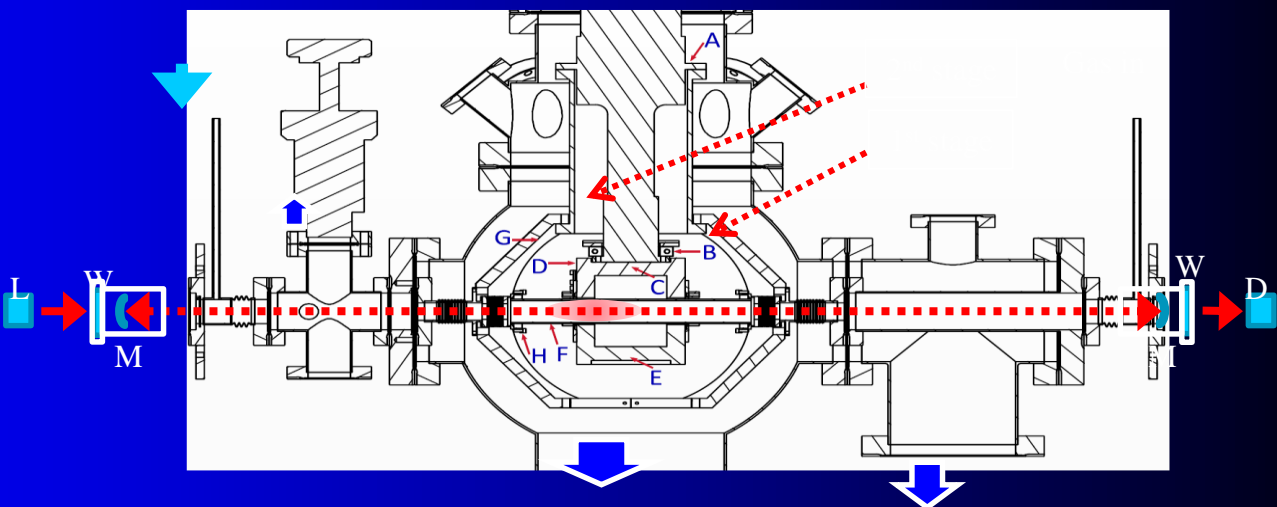
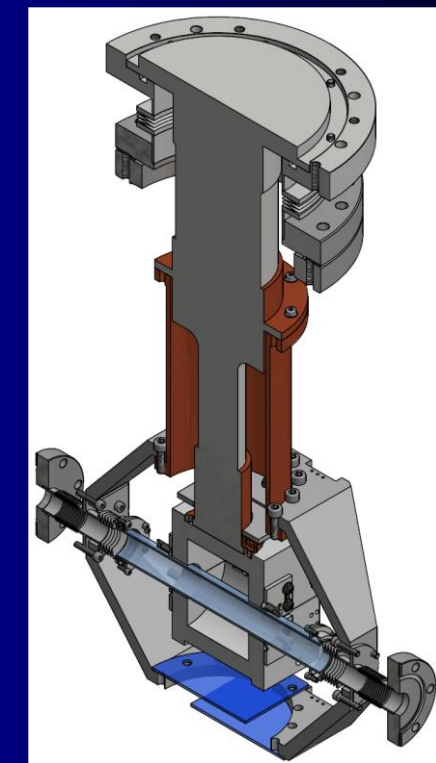
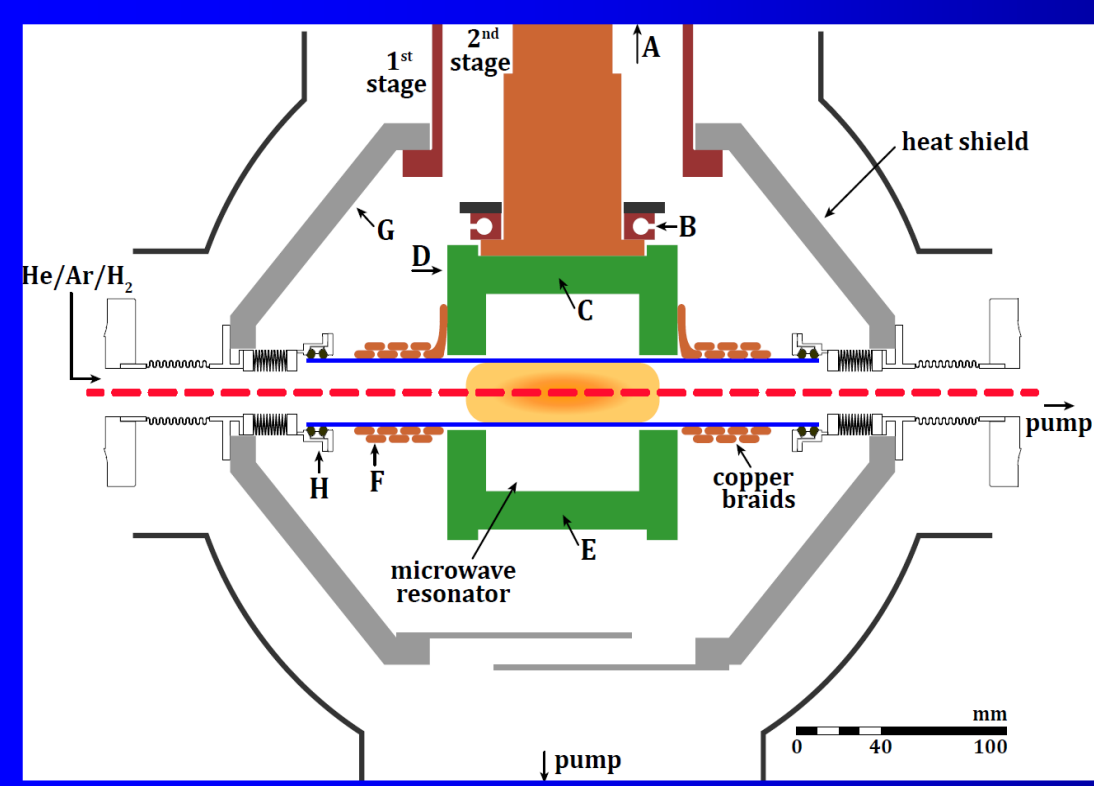


CRDS

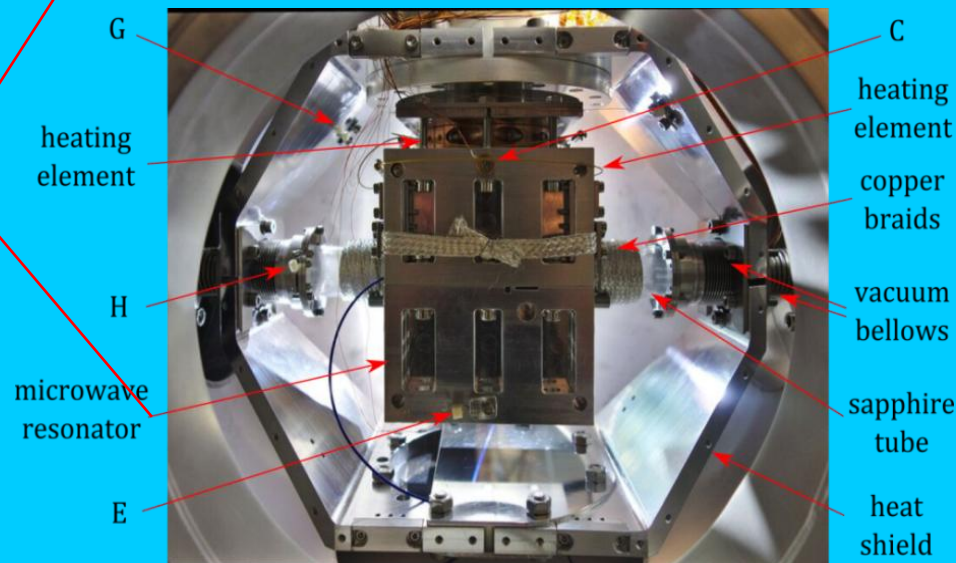
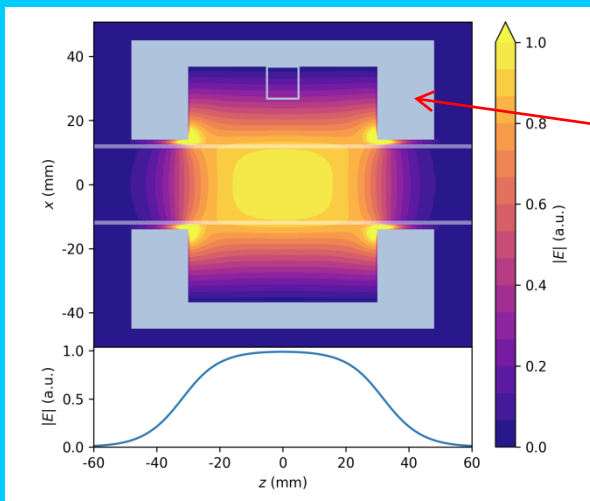
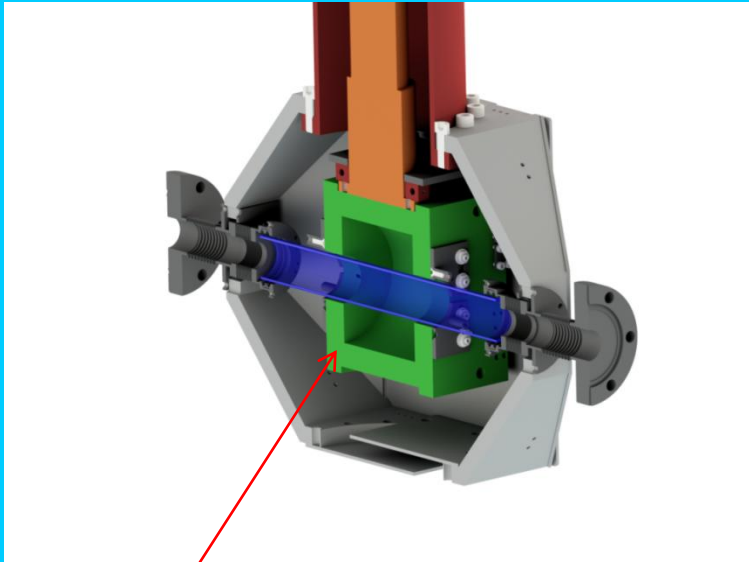
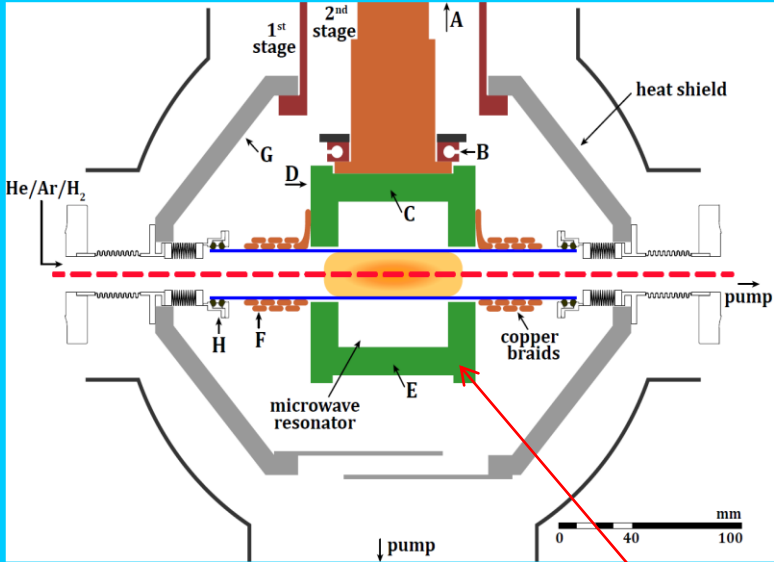


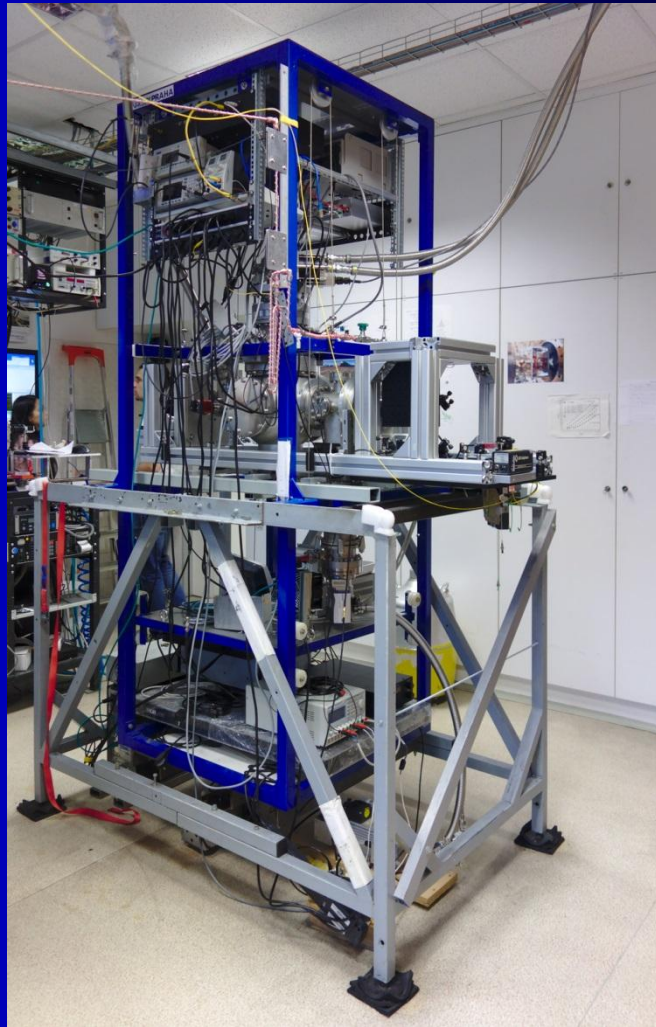
He/Ar/H₂



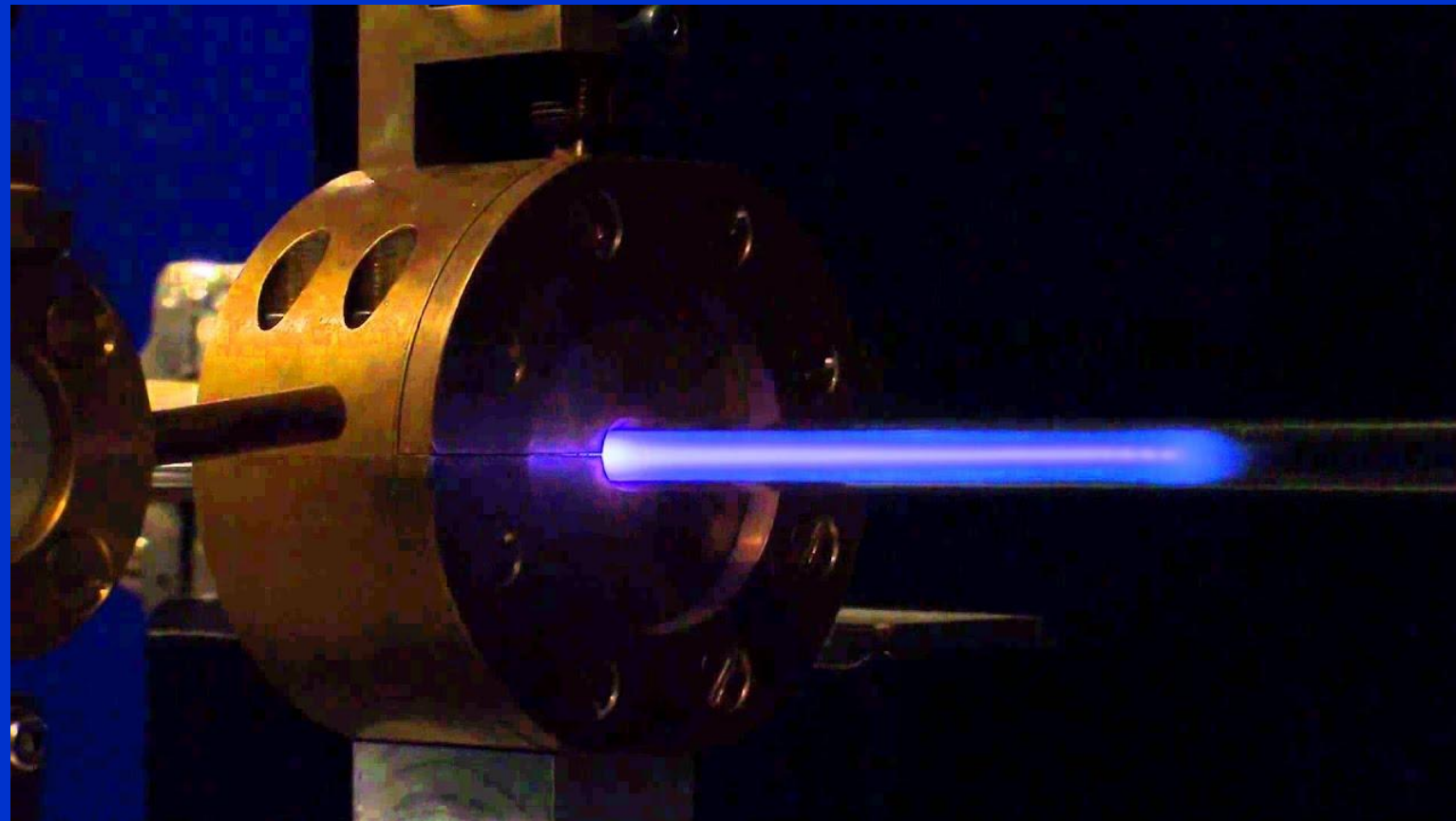


Recombination





surfatron

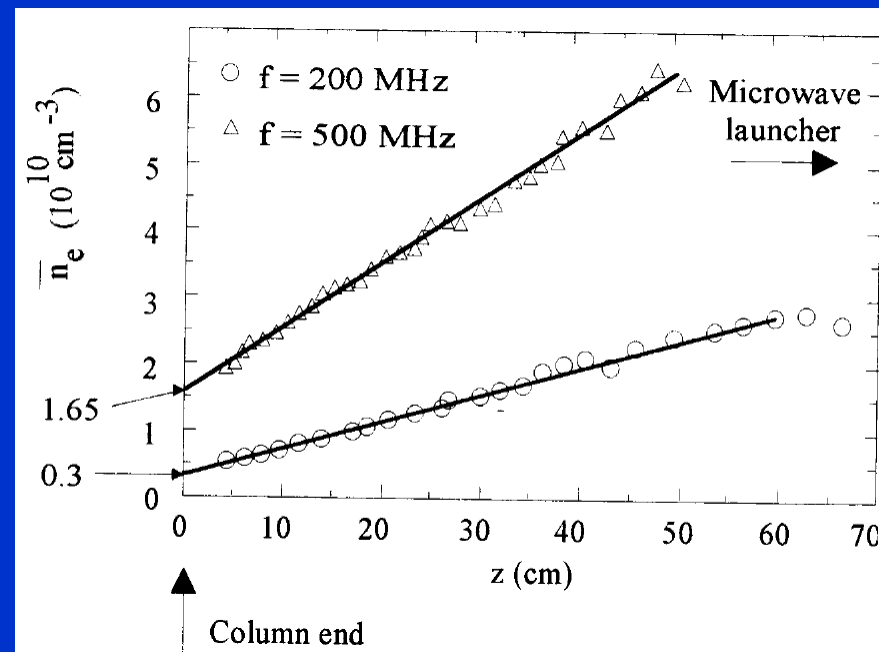
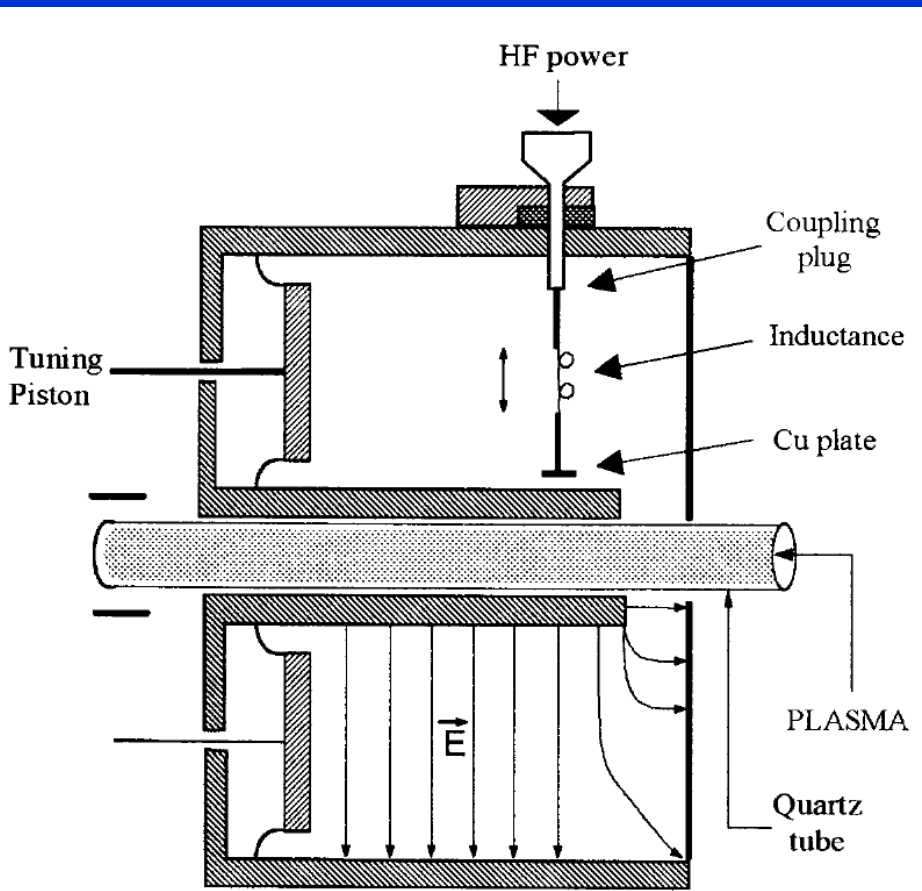


Surfatron discharge

A special characteristic of surface waves is to propagate along the discharge tube wall and to penetrate inside the tube to create the plasma. The radial distribution of electric field is given by the following equation (note 2 p. 11) :

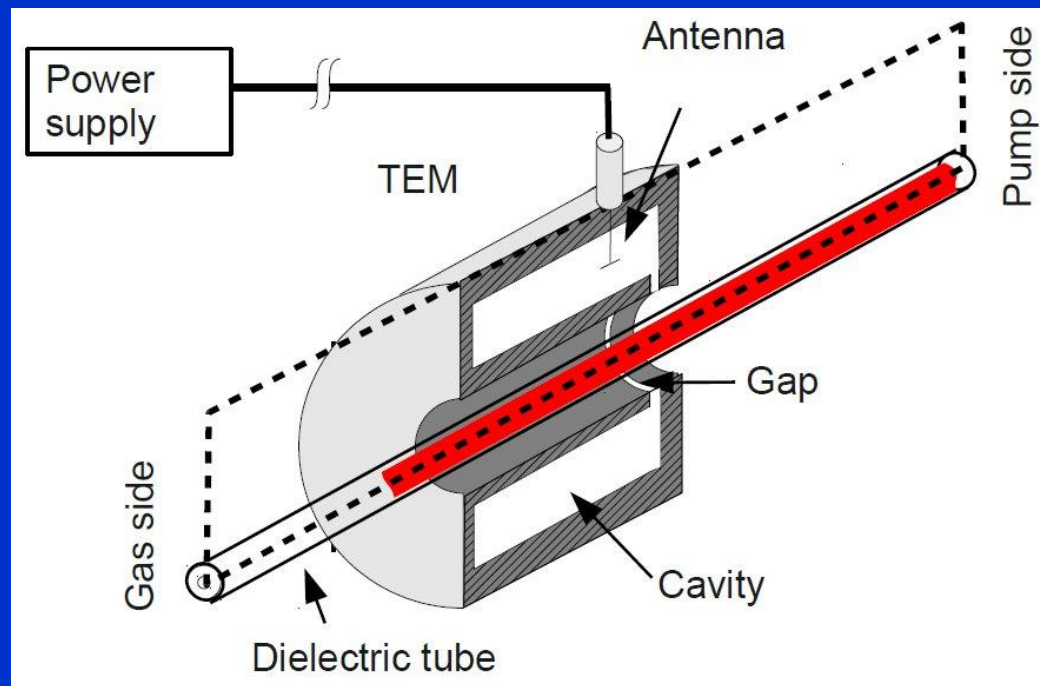
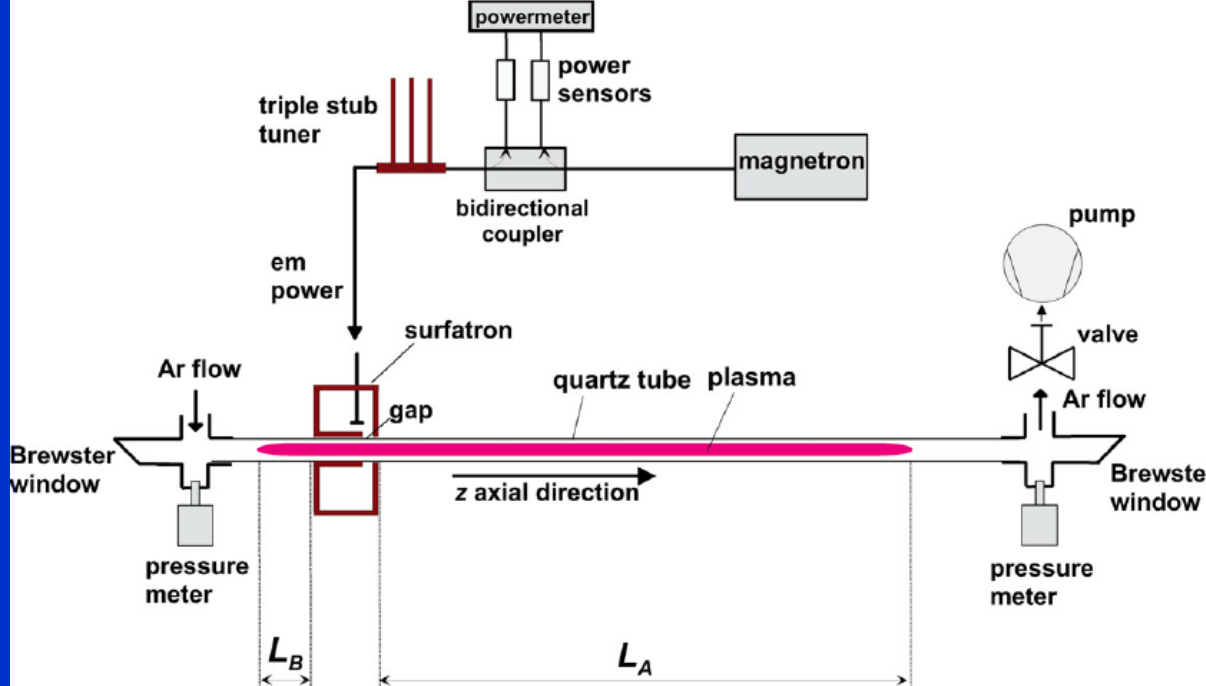
$$E(r) = A I_0 (B n_e^{1/2} r) \quad (1-34)$$

where A and B are constant values and I_0 is the modified Bessel function.



Axial distribution of electron density, measured in microwave plasma columns (Ar, 0.1 Torr, $R = 1.3 \text{ cm}$) at 200 and 500 MHz.

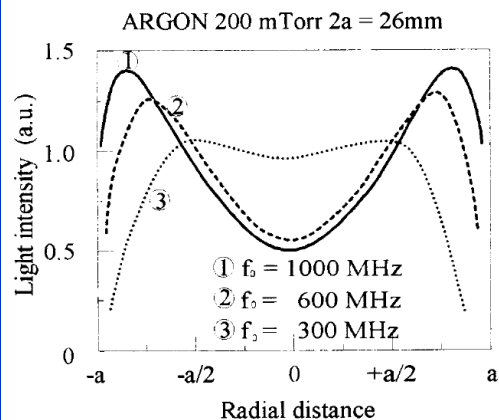
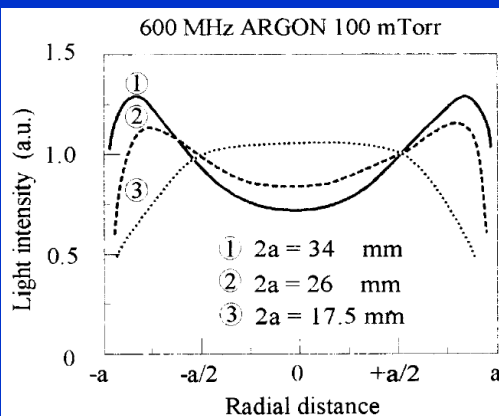
surfatron



surfatron



3.5 mbar



Thus, the $E(r)$ value is maximum for $r = R$ and it is minimum for $r = 0$. The local maximum of electric field at the tube wall is more pronounced as the electron density and the tube radius increase. This effect has been observed by analyzing the plasma light⁽⁹⁾

Radial distribution of the Ar I 549.6 nm line intensity in microwave discharge.

(a) 600 MHz, 0.1 Torr and several values of diameter (2a)

(b) diameter 2a = 26 mm and several values of microwave frequencies.

Surfatron plasma source working at frequency 2.45 GHz for technological applications

V. Stranak¹⁻², M. Tichy², J. Blazek¹, Z. Navratil³, P. Slavicek³, P. Adamek¹, P. Spatenka⁴

¹University of South Bohemia, Dept. of Physics, 371 15 Ceske Budejovice, Czech Republic

²Charles University in Prague, Fac. of Math. and Physics, 180 00 Praha 8, Czech Republic

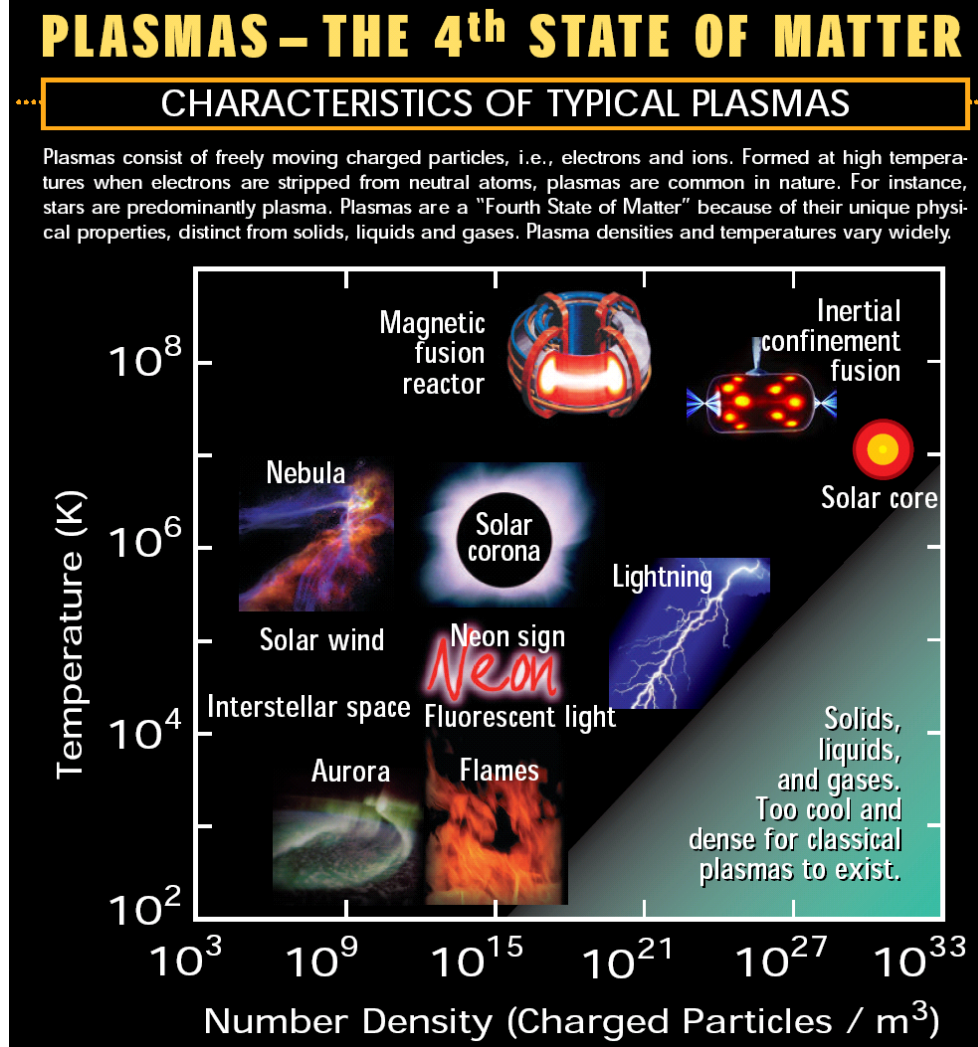
³Masaryk University Brno, Dept. of Physical Electronics, 611 37 Brno, Czech Republic

e-mail: milan.tichy@mff.cuni.cz

⁴Technical University of Liberec, Faculty of Mechanical Engineering, 461 17 Liberec, CR

Types of plasmas (electron density)

- Stars (density $n < 10^7 \text{ cm}^{-3}$)
- Solar winds (density $n < 10^7 \text{ cm}^{-3}$)
- Coronas (density $n < 10^7 \text{ cm}^{-3}$)
- Ionosphere (density $n < 10^7 \text{ cm}^{-3}$)
- Glow discharge (density $n = 10^8 \sim 10^{14} \text{ cm}^{-3}$)
- Arcs (density $n = 10^8 \sim 10^{14} \text{ cm}^{-3}$)
- High-pressure arc (density $n \sim 10^{20} \text{ cm}^{-3}$)
- Shock tubes (density $n \sim 10^{20} \text{ cm}^{-3}$)
- Fusion reactors (density $n \sim 10^{20} \text{ cm}^{-3}$)



Paschen law – data gama

$$i = \frac{i_0 \exp(\delta d)}{1 - \gamma \exp(\delta d) - 1}, \quad (5.5)$$

V důsledku emise opouští povrch katody elektrony s hustotou toku γj_{\perp}

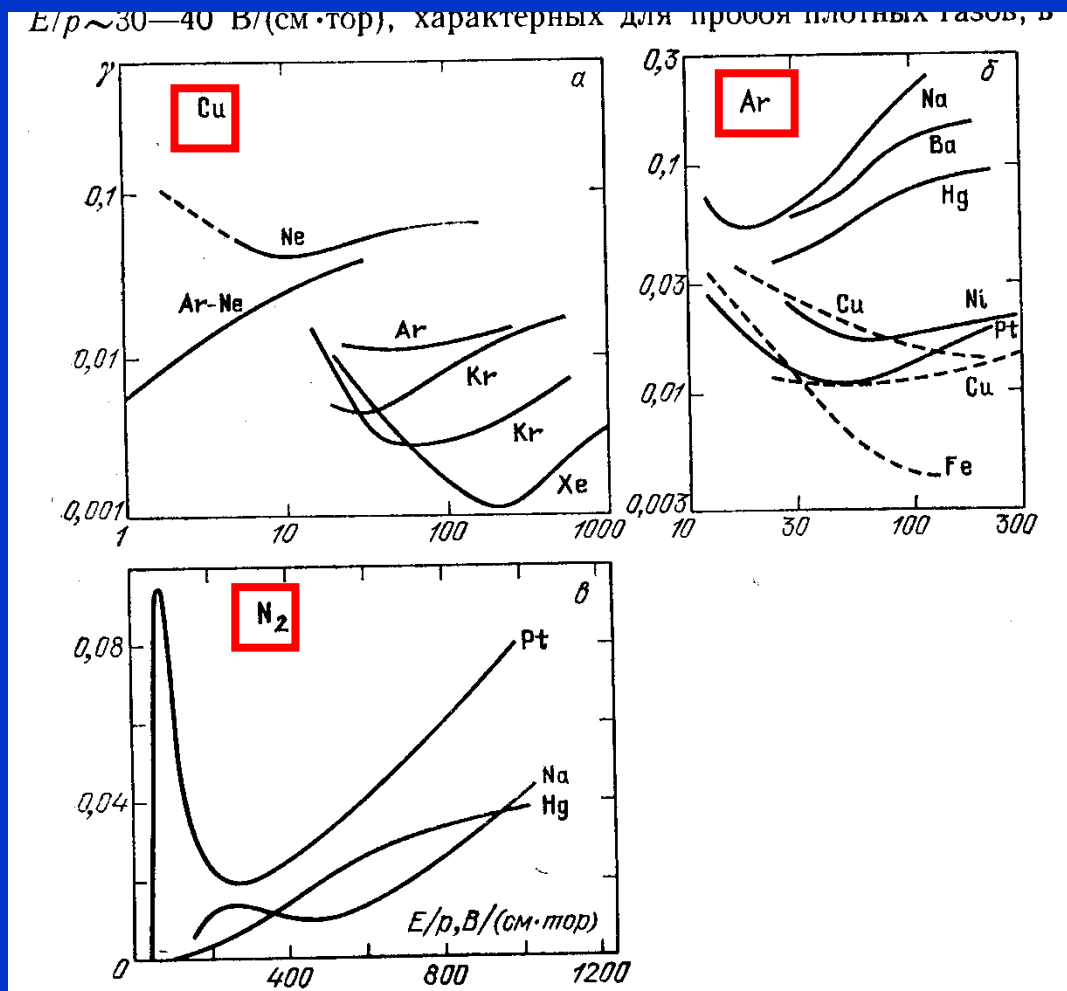
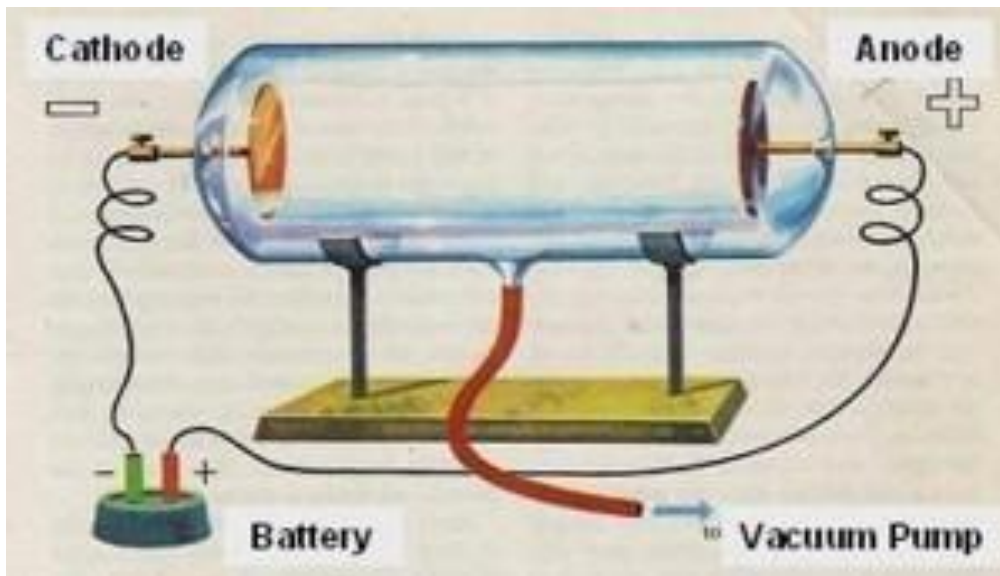


Рис. 6.13. Коеффициент ионно-электронной эмиссии, определенный из разрядного эксперимента (п. 4.1): *a* — медный катод в инертных газах; *б* — различные металлы в Ar; *в* — различные металлы в N₂ [6]

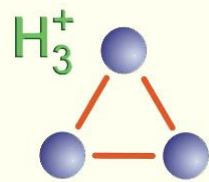
Calculation of avalanche...

Regions in the DC Glow Discharge Tube



A glass tube, about *16 inches long* and *1 1/2 inches in diameter*, is hermetically sealed at both ends. Two metal probes are fused into the tube at each end. The physicist applies a potential of a few thousand volts across both probes. With the aid of a vacuum pump he sucks the *air* out of the tube, thus lowering the pressure inside the glass tube.

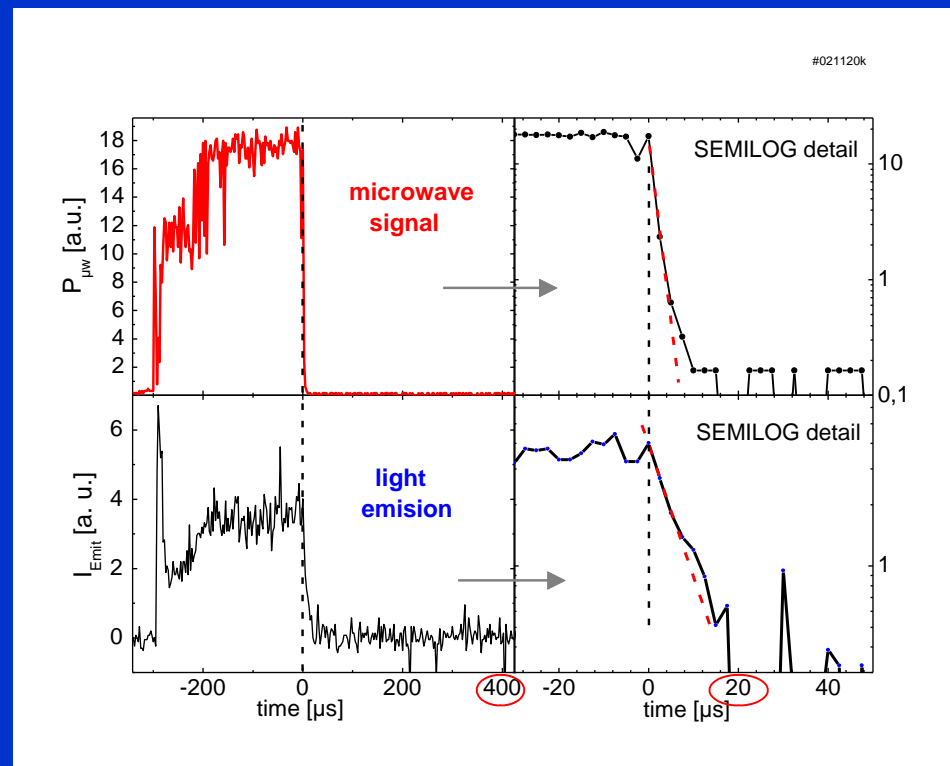
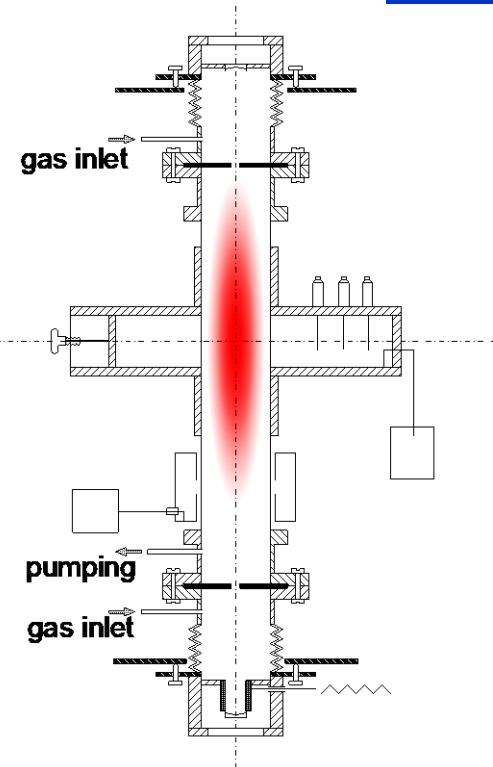
Formation and destruction of $\text{H}_3^+(v=0)$ in He/Ar/H₂ microwave discharge



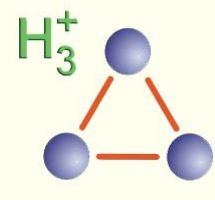
Laser – Single-mode tuneable diode laser,
 $\lambda = 1470 \pm 10\text{nm}$; $P \sim 3 \text{ mW}$
Mirrors – R = 99.994%,

PULSE REGIME

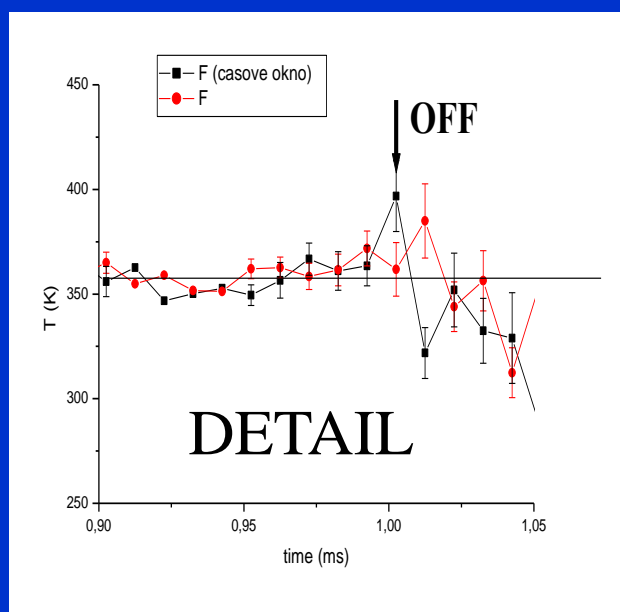
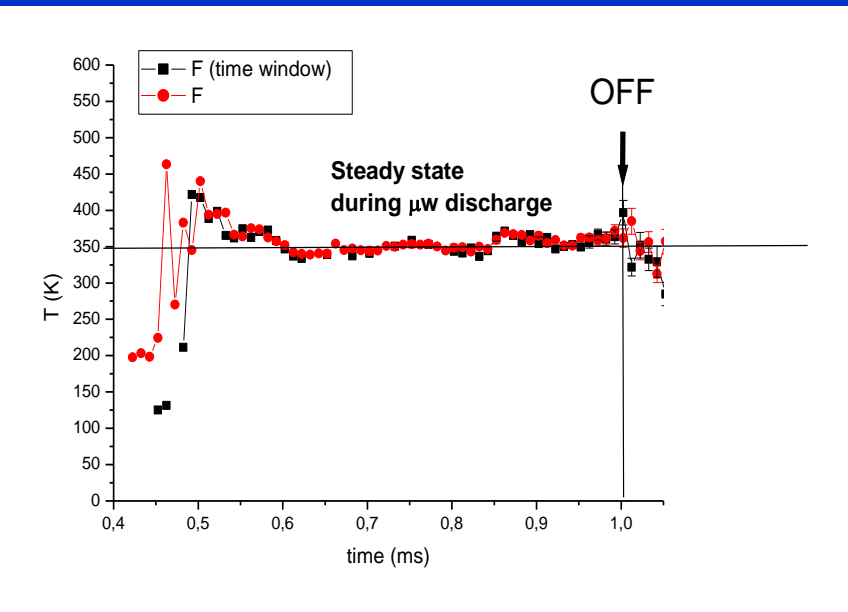
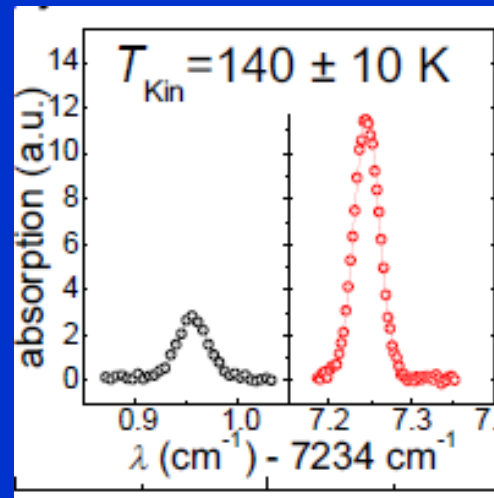
TEST TUBE



Kinetic temperature of $\text{H}_3^+ (\nu=0)$ measured from the Doppler broadening

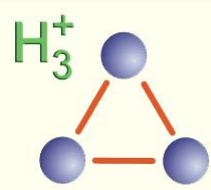


μw PULSES



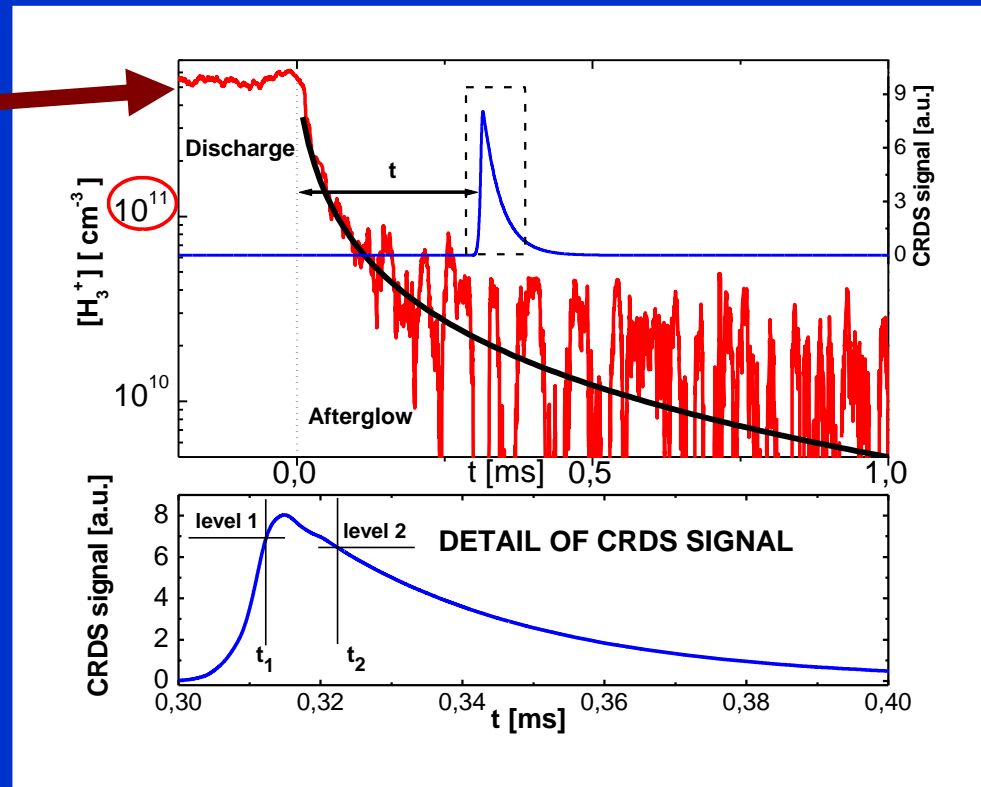
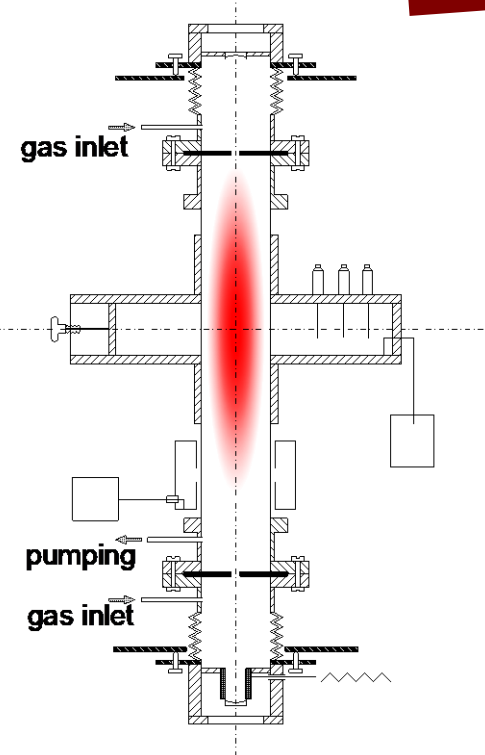
From the spectrum rotational temperature is determined

Recombination of H_3^+ (v=0) in He/Ar/ H_2 Stationary afterglow



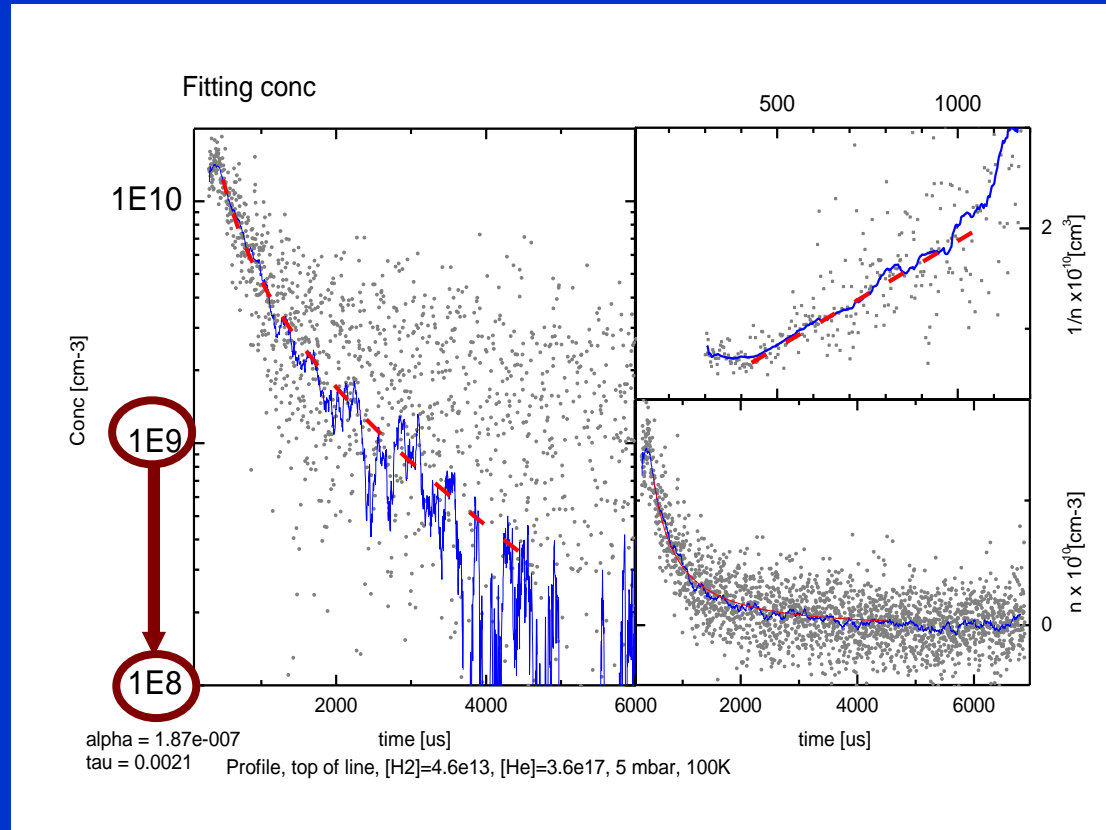
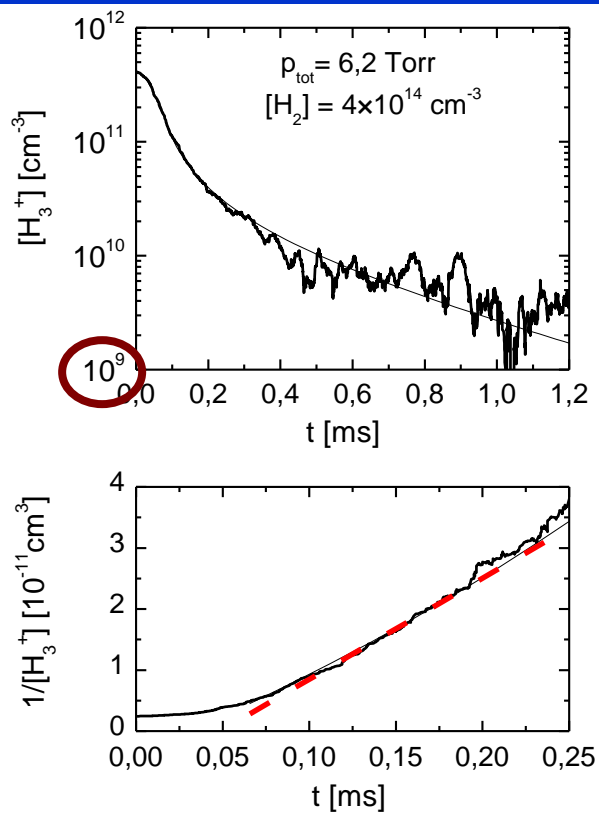
PULSE REGIME

TEST TUBE



CRDS 2003

Yesterday's results

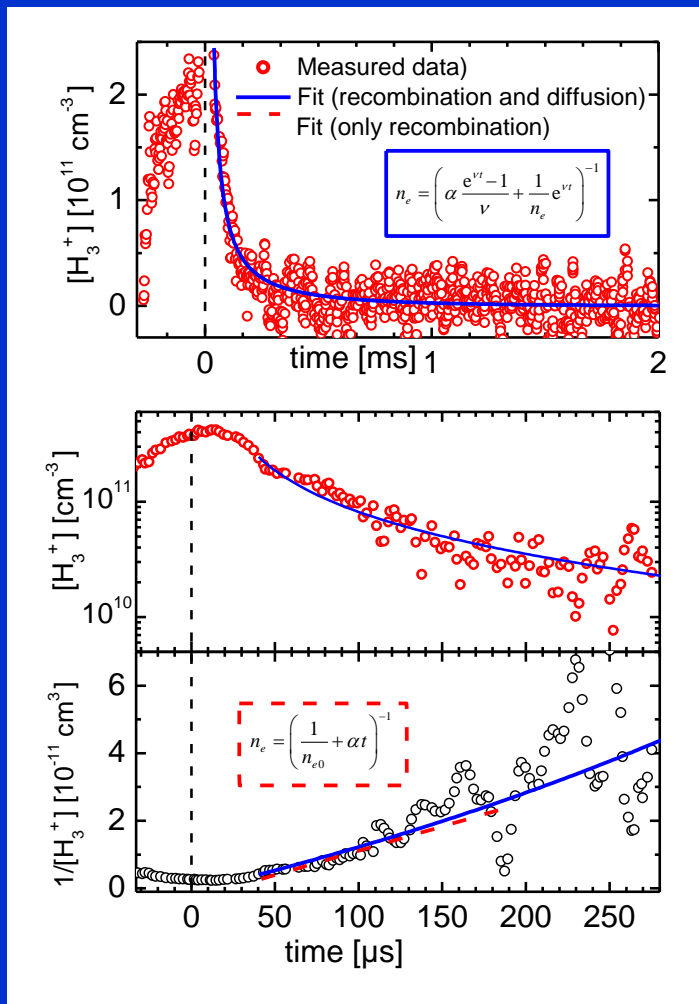


$100\mu\text{s}$

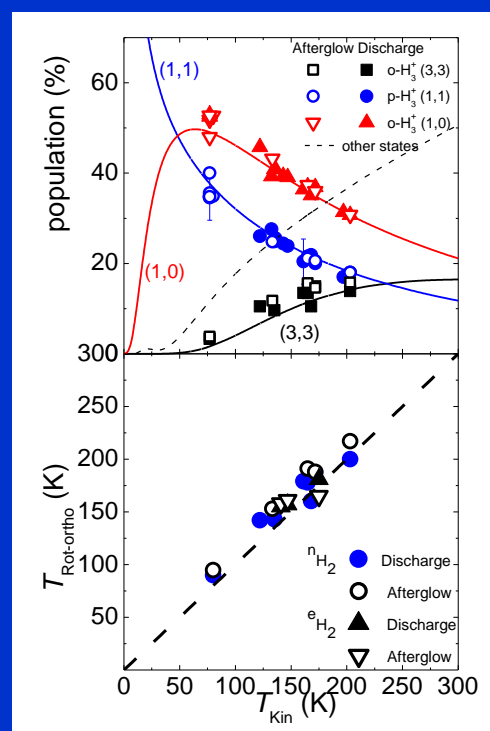
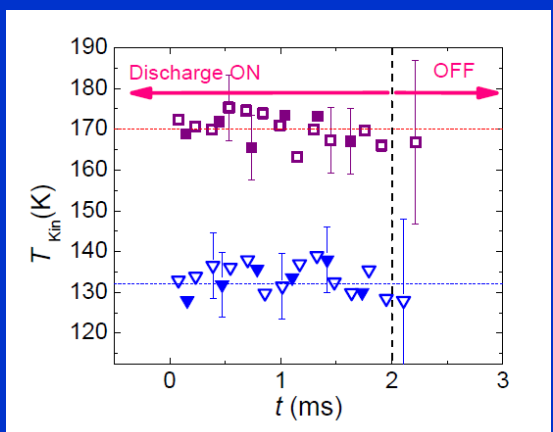
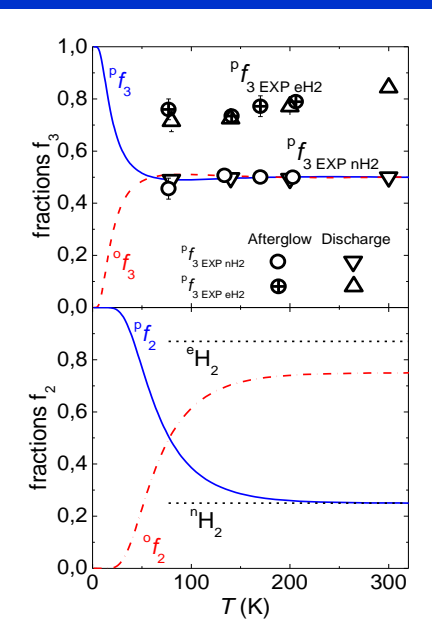
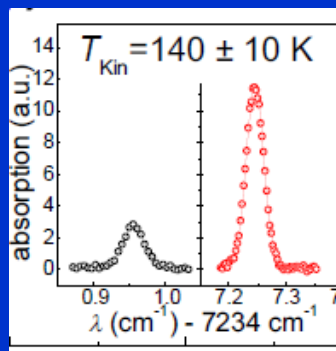
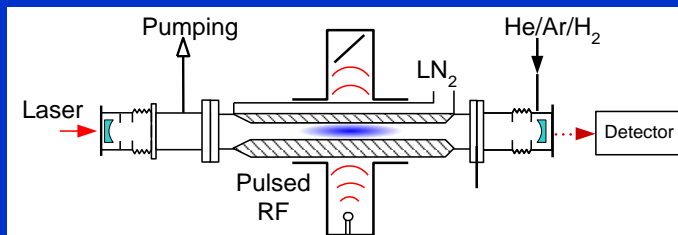
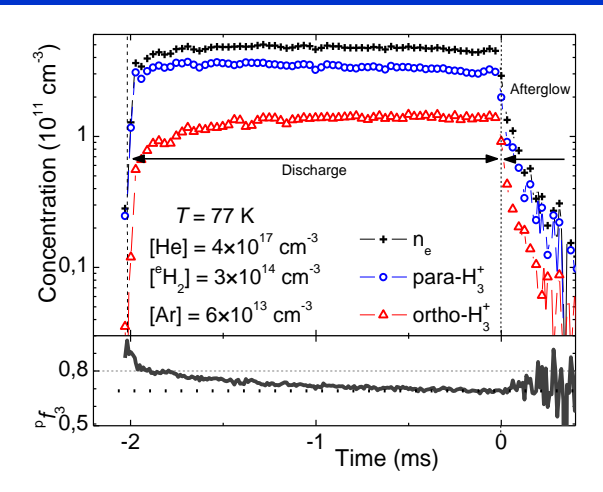
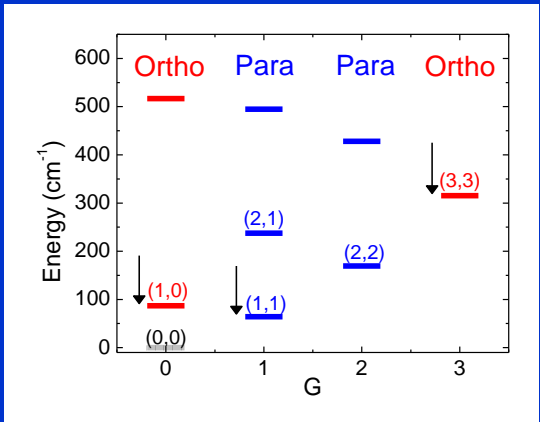


$1000\mu\text{s}$

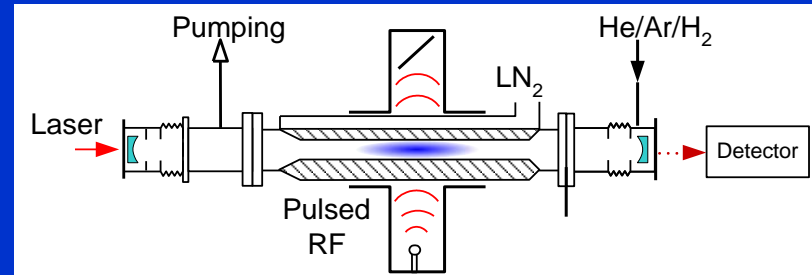
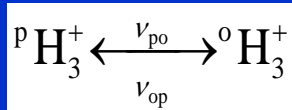
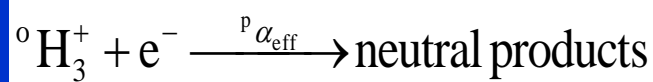
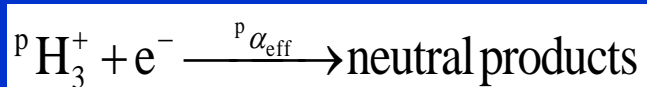
Decay of $\text{H}_3^+ (\nu=0)$ iteration



Spectroscopy of discharge in He/Ar/H₂



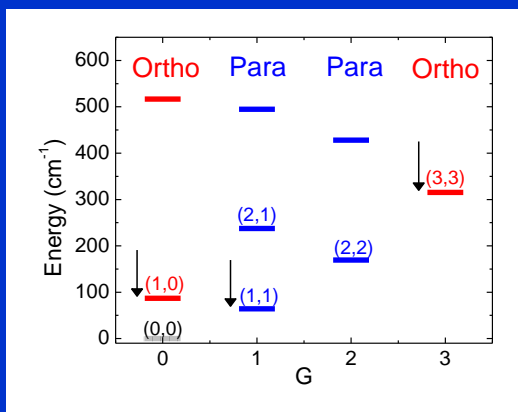
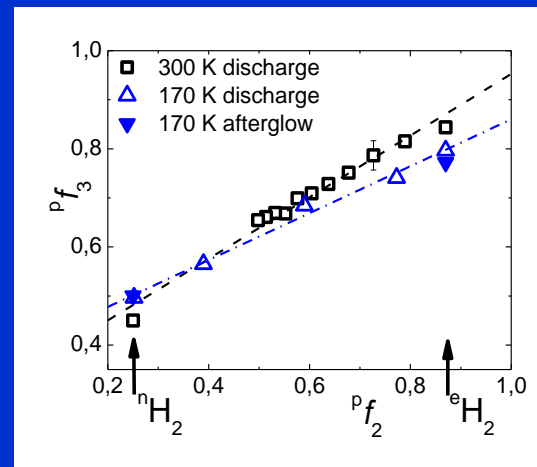
Formation of para-H₃⁺ and ortho-H₃⁺



$$\frac{d[{}^p\text{H}_3^+]}{dt} = -{}^p\alpha_{\text{eff}} [{}^p\text{H}_3^+] n_e - \frac{[{}^p\text{H}_3^+]}{\tau_D} - \nu_{po} [{}^p\text{H}_3^+] + \nu_{op} [{}^o\text{H}_3^+]$$

$$\frac{d[{}^o\text{H}_3^+]}{dt} = -{}^o\alpha_{\text{eff}} [{}^o\text{H}_3^+] n_e - \frac{[{}^o\text{H}_3^+]}{\tau_D} + \nu_{po} [{}^p\text{H}_3^+] - \nu_{op} [{}^o\text{H}_3^+]$$

$$\frac{dn_e}{dt} = -({}^p\alpha_{\text{eff}} {}^p f_3 + {}^o\alpha_{\text{eff}} {}^o f_3) n_e^2 - \frac{n_e}{\tau_D}$$



Calculation of avalanche...

Calculation of avalanche...

DC glow discharges

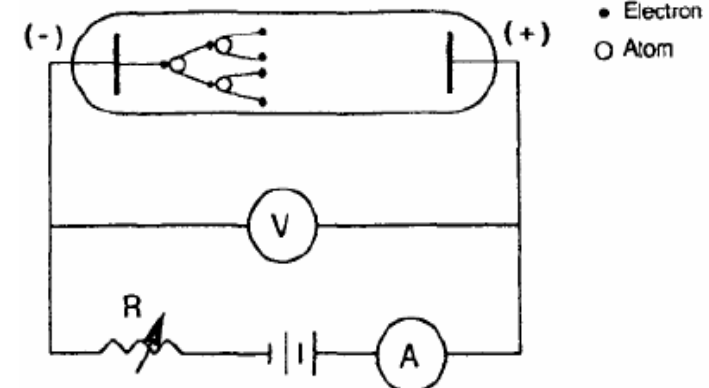
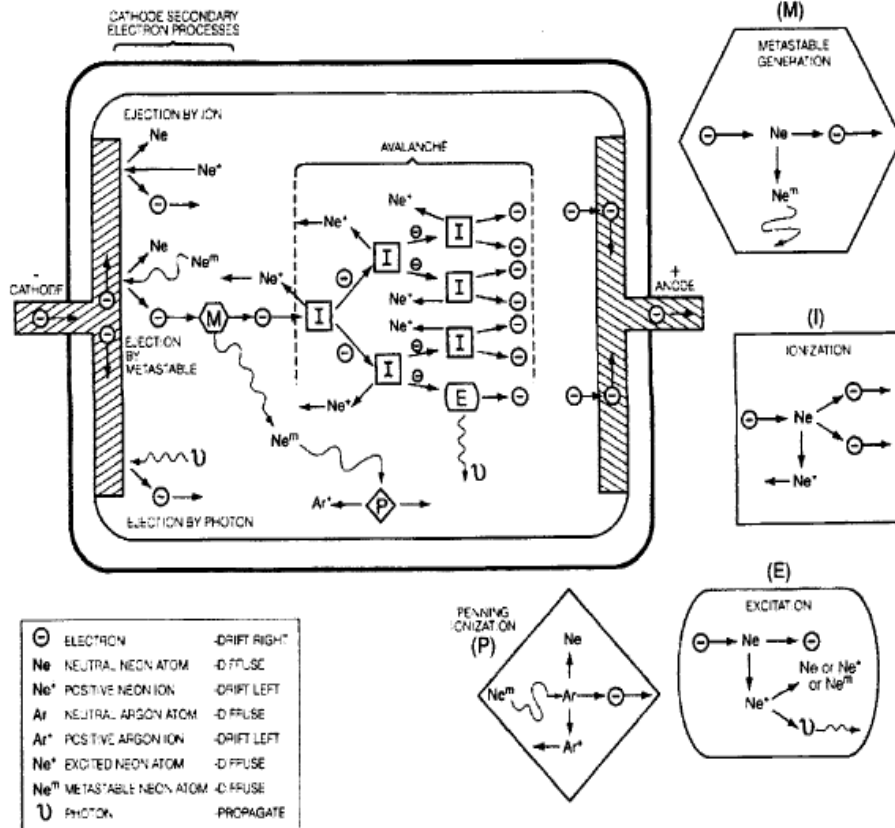


Fig. 2-1 DC glow-discharge setup.

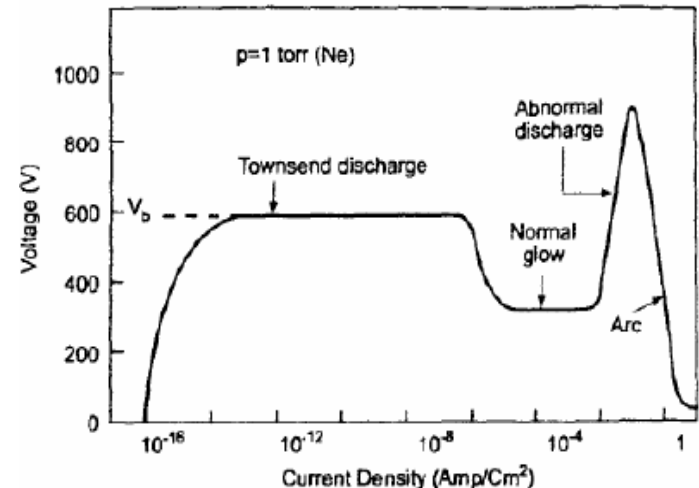


Fig. 2-2 The I-V characteristic of a DC glow discharge.

DC 글로우 방전의 모식도

- Electron multiplication
- Emission of secondary electron from a cathode

Paschen's law 1

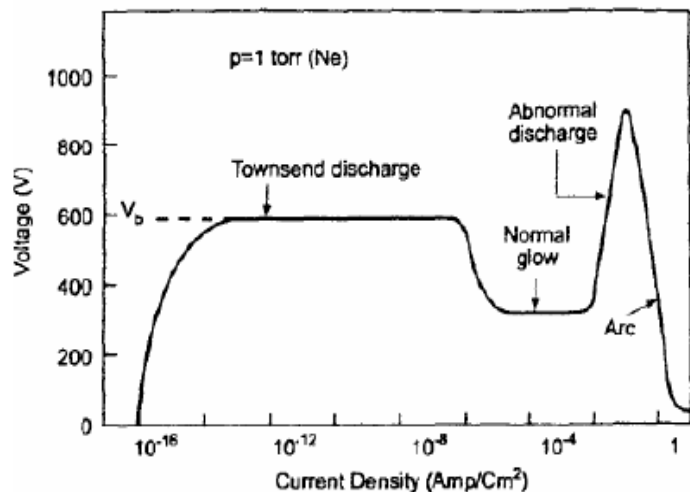


Fig. 2-2 The I-V characteristic of a DC glow discharge.

$$I = \frac{I_0 e^{\alpha d}}{1 - \gamma(e^{\alpha d} - 1)}$$

When $1 - \gamma(e^{\alpha d} - 1) = 0$,
the breakdown occurs.

$$\alpha = A \cdot p \exp\left(-\frac{B \cdot p}{E}\right)$$

and $V_b = Ed$,



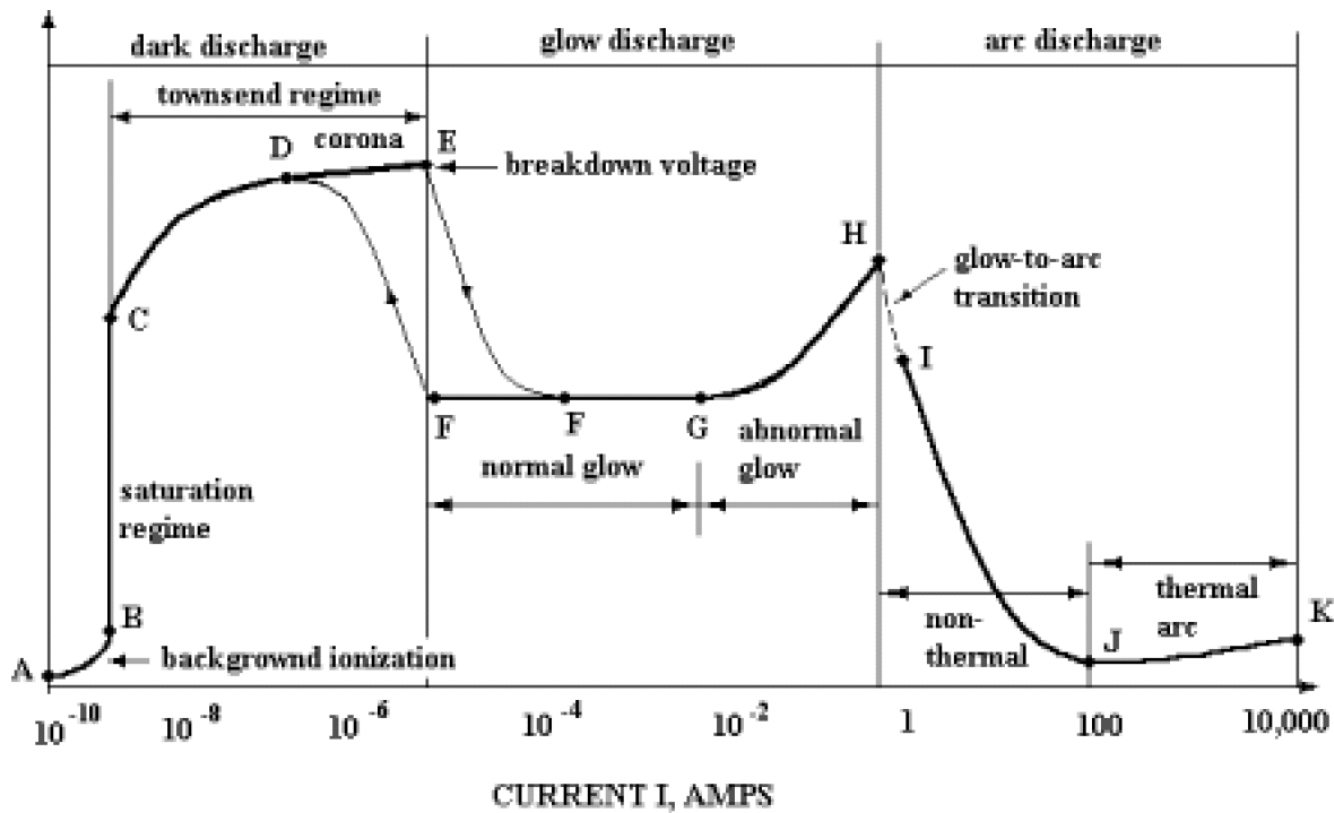
$$V_b = \frac{C_1(pd)}{C_2 + \ln(pd)}$$

where

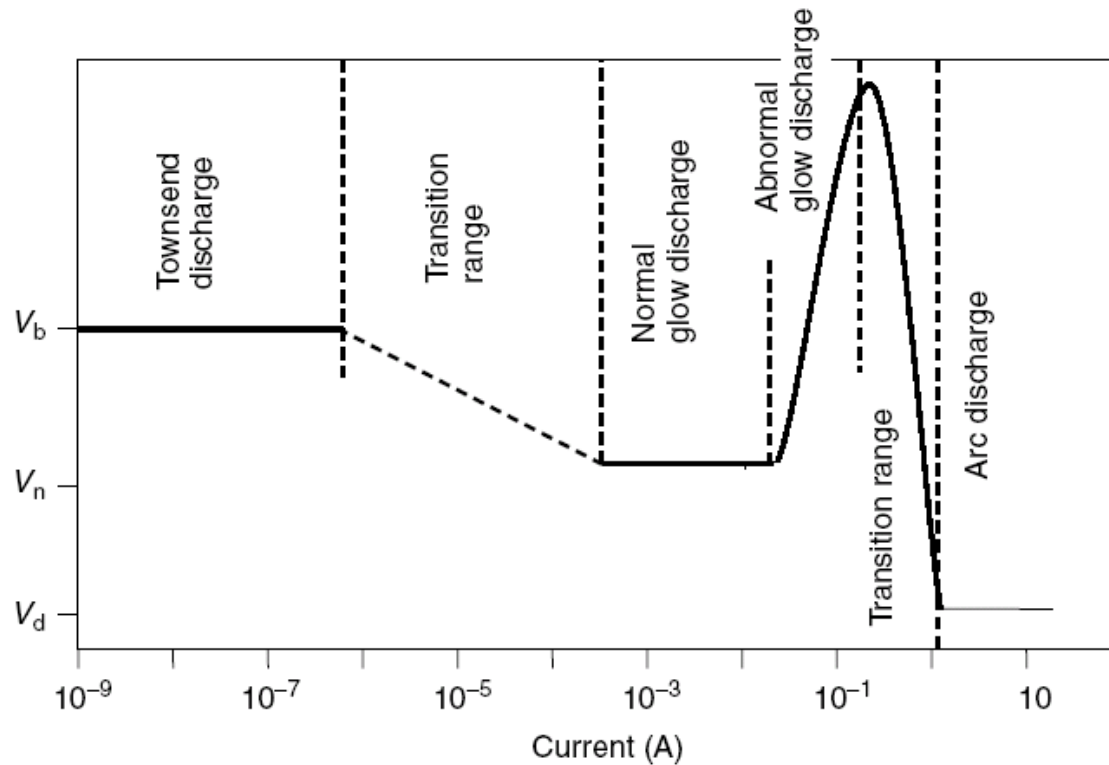
d = distance between electrodes

C_1 and C_2 = constants that change with the nature of the gas

VOLTAGE V, VOLTS



Current–voltage (i – V) characteristics of direct current (dc) electrical discharge



V_b is the breakdown voltage,

V_n is the normal operating voltage, and

V_d is the operating voltage of arc discharge.

Characteristics of DC glow discharge 1

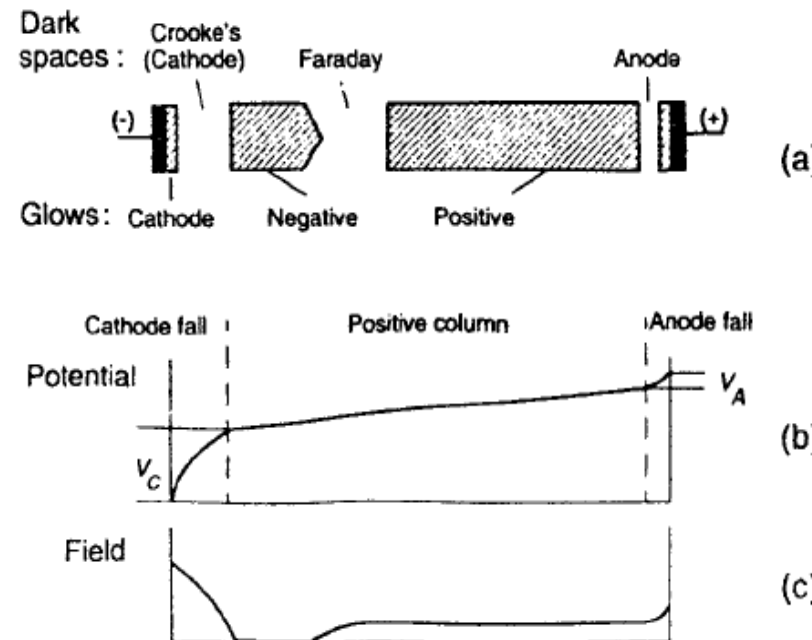
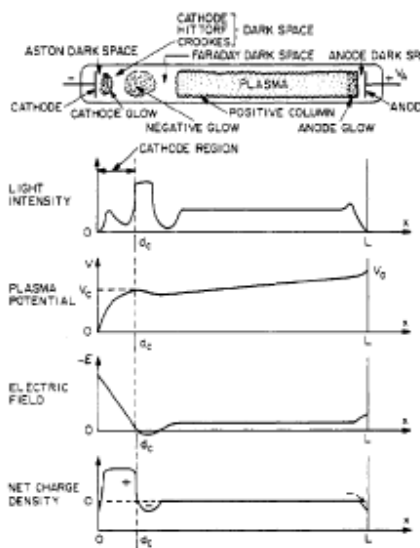


Fig. 2-4 Regions and characteristics of a DC glow discharge: (a) discharge regions; (b) potential distribution in discharge tube; (c) distribution of electric field in discharge tube.

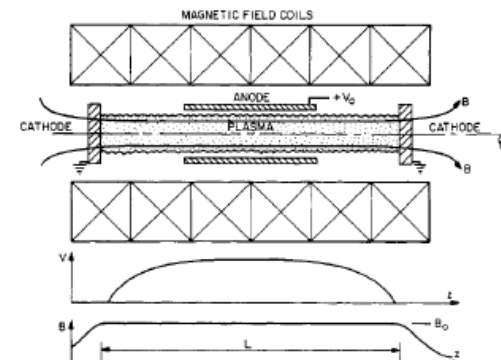
- The dark regions are called the cathode or Crooke's dark space, the Faraday dark space, and the anode dark space.
- The luminous regions are called the cathode glow, the negative glow, and the positive column.

Low pressure normal glow discharge



- **Cathode:** made of an electrically conducting metal, γ , of which has a significant effect on the operation of the discharge tube.
- **Aston dark space:** a thin region with a strong electric field and a negative space charge. The electrons are of too low a density and/or energy to excite the gas, so it appears dark.
- **Cathode glow:** has a relatively high ion number density. The length depends on the type of gas and the gas pressure.
- **Cathode (Crookes, Hittorf) dark space:** has a moderate electric field, a positive space charge, and a relatively high ion density.

Penning discharge plasma sources produce a dense plasma at pressures far below than most other glow discharges



- Strong axial magnetic fields: to prevent electrons from intercepting the anode.
- Axial electric fields: electrons are reflected by opposing cathodes.
- Multiple reflection of the electrons along axis.

Glow Discharge Tube

Electrified air
makes a
beautiful glow.

How does it work?

- An electric current passes through the tube.
- The air between the electrodes becomes ionized.
- The ions glow.
- The glow is called a "glow discharge".

What's glowing?

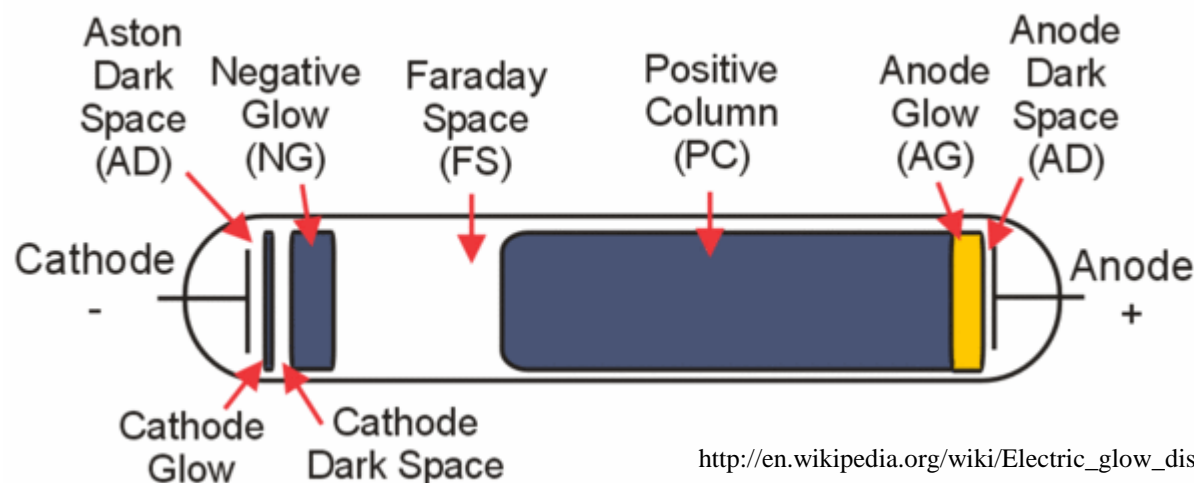
- The glow discharge tube contains gases.
- The gases are excited by the electric current.
- The excited gases give off light.



The glowing air is called a "glow discharge".
The glowing air is caused by the electric current passing through the tube.
The glowing air is caused by the electric current passing through the tube.

+

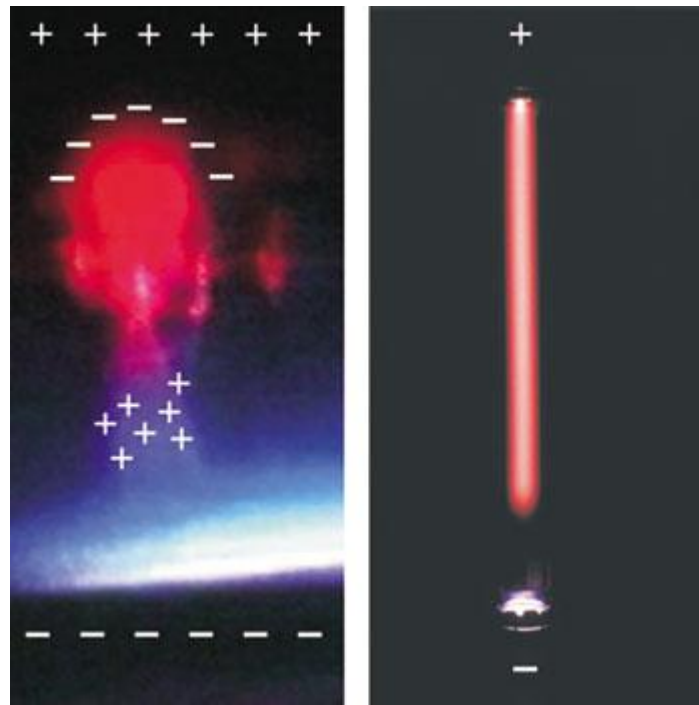
-



http://en.wikipedia.org/wiki/Electric_glow_discharge

<http://www.exo.net/~pauld/origins/glowdischarge.html>

Sprite and Glow Discharge Tube

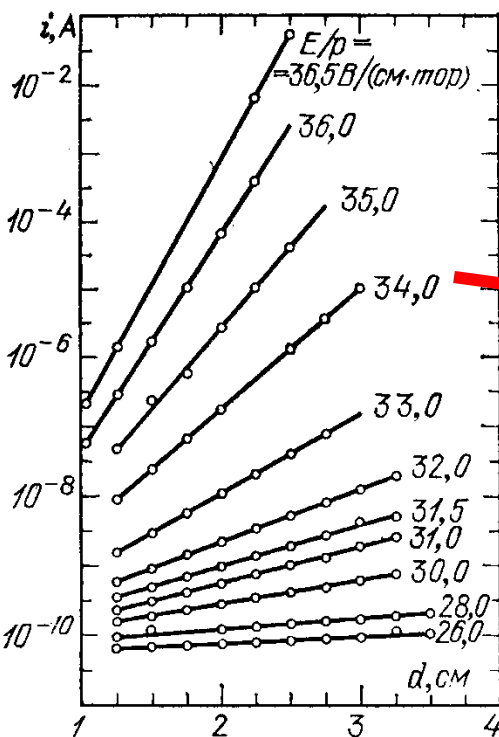


Sprite light in the atmosphere (**left**) and in a laboratory glow discharge tube (**right**). In both cases, the light near the positive (anode) end is red and arises from the collisional excitation of neutral nitrogen molecules by free electrons. Also in both cases, the light near the negative (cathode) end is blue and arises from the collisional excitation of N_2^+ ions by free electrons.

Calculation of avalanche...

Calculation of avalanche...

Electric discharges - data



$$\frac{dj_-}{dx} = \alpha n_- = \frac{\alpha}{V_-} n_- V_- = \delta j_-$$

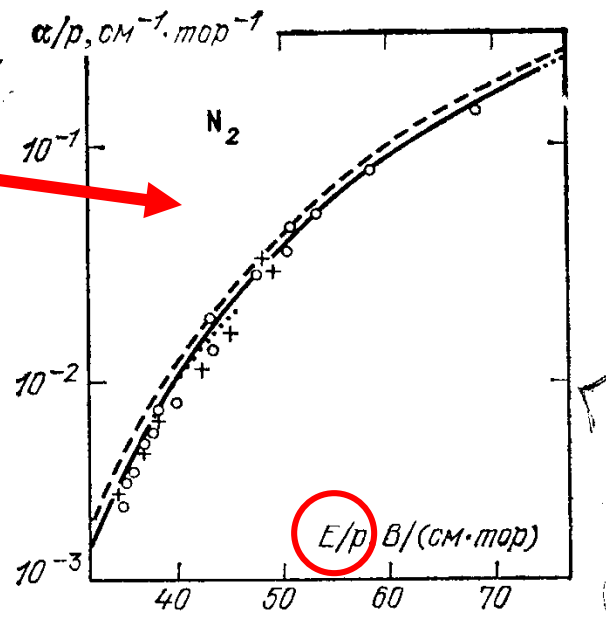


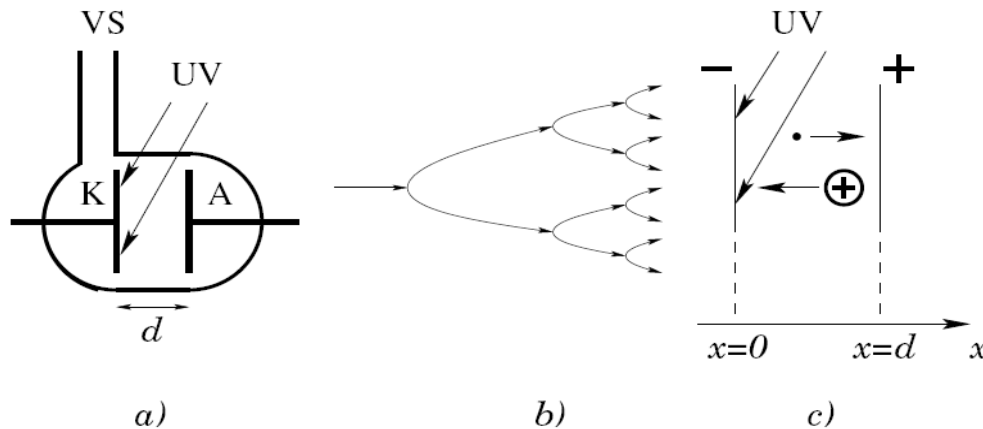
Рис. 5.3. Экспериментальный график, демонстрирующий постоянство α и экспоненциальный характер нарастания тока в разрядном промежутке; ионизационные коэффициенты определяются наклонами прямых [6]

Рис. 5.4. Ионизационный коэффициент Таунсенда α в N_2 по разным измерениям

$$E/N \dots \dots 1 \text{ Townsend} = 1 \text{ Td} = 10^{-17} \text{ V cm}^2 = 10^{-21} \text{ V m}^2$$

$$E/p \text{ at } 293 \text{ K (cca } 20 \text{ C)} \dots \dots 1 \text{ V/cmTorr} = 3.034 \text{ Td, resp.} \quad 1 \text{ Td} = 0.3296 \text{ V/cmTorr}$$

Electric discharges Townsend avalanche theory



Obr. 5.2: Zapaľovanie výboja: a) výbojka na meranie zapaľovacieho napäťa: K - katóda, A - anóda, UV - ultrafialové žiarenie zabezpečujúce emisiu primárnych elektrónov, VS - napojenie na vákuový systém; b) elektrónová lavína; c) označenie polohy elektród

medzi elektródami (obr. 5.2 c). Povrch katódy K sa nachádza v mieste $x = 0$ a povrch anódy A v mieste $x = d$. Elektróny sa pohybujú smerom k anóde a vytvorené kladné ióny ku katóde, kde zanikajú. Podobne ako v odseku 4.3.1, môžeme napísť rovnicu kontinuity pre elektróny v jednorozmernej geometrii a v ustálenom stave

$$\frac{dj_-}{dx} = \alpha n_- = \frac{\alpha}{V_-} n_- V_- = \delta j_-, \quad (5.2)$$

kde V_- je driftová rýchlosť elektrónov v elektrickom poli (v homogénnom poli je konštantná) a $\delta = \alpha/V_-$ je **prvý Townsendov koeficient**. Analogická rovnica platí aj pre kladné ióny

$$\frac{dj_+}{dx} = \alpha n_+ = \delta j_-. \quad (5.3)$$

$$\frac{dj_-}{dx} = \alpha n_- = \frac{\alpha}{V_-} n_- V_- = \delta j_-$$

Prvý Townsendov koeficient δ má rozmer m^{-1} a označuje počet ionizácií, ktoré vykoná jeden elektrón v smere elektrického poľa na jednotkovej dráhe (na rozdiel od ionizačnej frekvencie α udávajúcej počet ionizácií za jednotku času). Ak rovnice odčítame, dostaneme

$$\frac{d(j_+ - j_-)}{dx} = 0 \quad \Rightarrow \quad j_+ - j_- = K = \text{konšt.}$$

Potom hustota elektrického prúdu medzi elektródami $i = e(j_+ - j_-) = eK$ je taktiež konštantná, napriek tomu, že hustoty toku elektrónov a iónov sa menia s polohou x .

V homogénnom poli je Townsendov koeficient δ konštantný a preto môžeme rovnice kontinuity ľahko integrovať

$$j_- = C \exp(\delta x); \quad j_+ = C \exp(\delta x) + i/e,$$

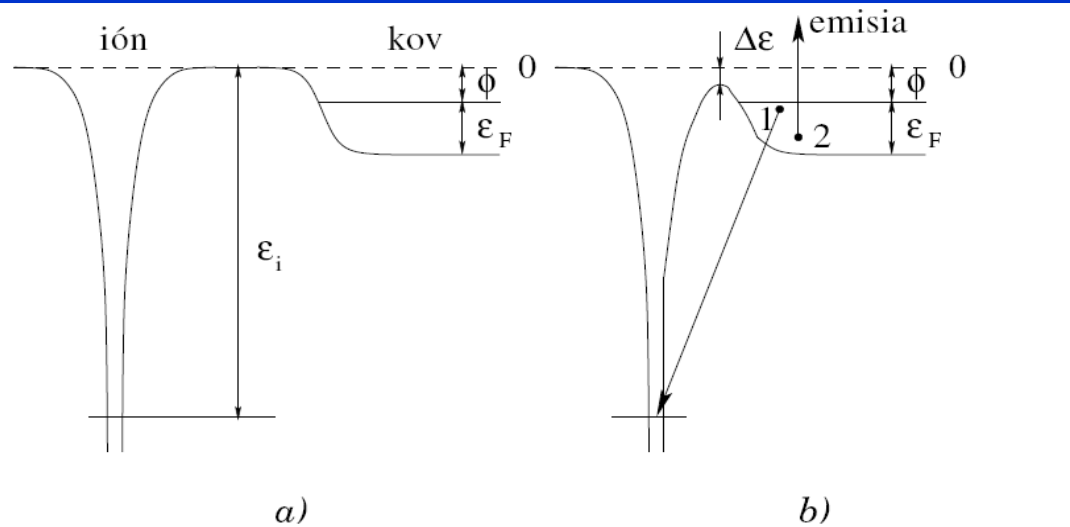
kde C je integračná konštanta. Hodnota tejto integračnej konštanty sa dá určiť z hustoty toku elektrónov na katóde: $C = j_-(0)$. Potom

$$j_- = j_-(0) \exp(\delta x); \quad j_+ = j_-(0) \exp(\delta x) + i/e. \quad (5.4)$$

Problém určenia hustoty toku $j_-(0)$ spočíva v tom, že okrem primárnych elektrónov emitovaných z katódy ultrafialovým žiarením (ich hustotu toku označíme j_0), elektróny emitujú aj dopadajúce kladné ióny. Tento typ emisie sa nazýva **potenciálková emisia**.

Electric discharges

Potenciálová emisia



Obr. 5.3: Emisia elektrónu pri dopade kladného iónu na povrch kovu: a) ión je ďaleko od povrchu: ϵ_i - ionizačná energia atómu, Φ - výstupná práca kovu a ϵ_F - Fermiho energia; b) kladný ión pri dopade na povrch kovu: 1 - elektrón prechádza na neobsadenú hladinu v ióne, 2 - emitovaný elektrón preberá prebytočnú energiu **Augerova emisia**

plynu. Ak však vypneme ultrafialové žiarenie, hustota primárnych elektrónov i_0 klesne na nulu a potom tiež $i = 0$. Lavínová ionizácia sa teda samostatne neudrží. Preto tento typ výboja nazývame **nesamostatný výboj** alebo tiež **Townsendov výboj**. Townsendov výboj je teda predprierazovým štádiom. Pri dostatočne silných poliach sa začne lovej emisie opúšťajú povrch elektróny s hustotou toku γj_+ . Koeficient γ reprezentuje výtažok elektrónov pri emisii, ktorý sa často (nelogicky) nazýva koeficient sekundárnej emisie. V teórii zapalňovania výboja sa zvykne nazývať **druhý Townsendov koeficient** (v staršej literatúre aj tretí Townsendov koeficient). Obvykle nadobúda hodnoty $0,1 - 10^{-3}$ (pre ióny veľkých organických molekúl až 10^{-10}).

Electric discharges

Teraz sa vrátime k rovniciam (5.4). Hustotu toku $j_-(0)$ možno totiž napísat ako súčet toku primárnych elektrónov a elektrónov od potenciálovej emisie

$$j_-(0) = j_0 - \gamma j_+(0).$$

Záporné znamienko pred hustotou toku kladných iónov súvisí s orientáciou súradníc, pretože $j_-(x) \geq 0$, $j_0 > 0$ a $j_+(x) \leq 0$. Z (5.4) vyplýva $j_+(0) = j_-(0) + i/e$, čo umožní napísat výslednú hustotu toku elektrónov na katóde

$$j_-(0) = \frac{j_0 - \gamma i/e}{1 + \gamma}.$$

Týmto vzťahom už máme určený súvis medzi hustotami toku nabitých častic a hodnotami j_0 a hustotou prúdu i . Pripomeňme, že z orientácie osi x vyplýva $i \leq 0$. Kladné ióny – na rozdiel od elektrónov – sa pohybujú smerom ku katóde. Smerom k anóde ich hustota toku by mala klesať. Vzhľadom na to, že anóda neemituje kladné ióny zo svojho povrchu, hustota toku kladných iónov na anóde je nulová: $j_+(d) = 0$. Potom postupne dostaneme nasledujúce vzťahy

$$j_+(d) = j_-(0) \exp(\delta d) + \frac{i}{e} = \frac{j_0 - \gamma i/e}{1 + \gamma} \exp(\delta d) + \frac{i}{e} = 0.$$

Z posledného vzťahu možno vypočítať hustotu elektrického prúdu

$$i = \frac{i_0 \exp(\delta d)}{1 - \gamma[\exp(\delta d) - 1]}, \quad (5.5)$$

Electric discharges

$$i = \frac{i_0 \exp(\delta d)}{1 - \gamma[\exp(\delta d) - 1]}, \quad (5.5)$$

V slabom elektrickom poli elektróny nezískavajú dostatočnú energiu na ionizáciu, preto $\delta = 0$. Vtedy $i = i_0$ – prúd medzi elektródami prenášajú len primárne elektróny od ultrafialového žiarenia. Ak elektrické pole zosilňujeme, zväčšuje sa aj prvý Townsendov koeficient δ a prúd i začne rýchlo narastať. Tento nárast súvisí s lavínovou ionizáciou plynu. Ak však vypneme ultrafialové žiarenie, hustota primárnych elektrónov i_0 klesne na nulu a potom tiež $i = 0$. Lavínová ionizácia sa teda samostatne neudrží. Preto tento typ výboja nazývame **nesamostatný výboj** alebo tiež **Townsendov výboj**. Townsendov výboj je teda predprierazovým štádiom. Pri dostatočne silných poliach sa začne

$$\gamma [\exp(\delta d) - 1] = 1, \quad (5.6)$$

hustota prúdu i diverguje a stáva sa nezávislá od hodnoty i_0 . Preto práve túto podmienku považujeme za kritérium zapálenia výboja. Hovoríme tiež, že nesamostatný výboj prechádza na **samostatný výboj**. Vtedy totiž kladné ióny dopadajúce na katódu emitujú dostatočný počet elektrónov, ktoré nahradia primárne elektróny od ultrafialového žiarenia. Preto výboj sa už udrží aj vtedy, keď katódu prestaneme ožarovať ultrafialovým žiareniom. V samostatnom výboji koncentrácia nabitých častic prudko narastie, takže priestorový náboj sa začne uplatňovať. Preto vzťah (5.5) už za týchto podmienok neplatí. V niektorých typoch výboja existujú oblasti, kde je aj nadalej prítomná lavínová ionizácia; treba ju už ale opísť rovnicami, ktoré zohľadňujú prítomnosť priestorového náboja.

Electric discharges

Paschenov zákon

E/p

$$\gamma [\exp(\delta d) - 1] = 1, \quad (5.6)$$

Podmienka (5.6) ešte nie je priamo použiteľná na určenie zápalného napäťa. Táto veličina je totiž schovaná v prvom Townsendovom koeficiente. Preto musíme sa teraz zaoberať problémom závislosti prvého Townsendovho koeficientu δ od intenzity elektrického poľa. Exaktné odvodenie je jedine možné pomocou kinetickej rovnice, k čomu treba ale poznať detailnú závislosť prierezov pre pružné zrážky a pre ionizáciu molekúl elektrónmi. Jednoduchší prístup využíva možnosť priameho merania δ od intenzity elektrického poľa s využitím rovnice (5.5). Prv než uvedieme poloempirické vzťahy, nájdeme zákony podobnosti pre prvy Townsendov koeficient.

Ak vyjadríme frekvenciu ionizácie α pomocou (4.16) a driftovú rýchlosť elektrónov pomocou pohyblivosti $V_- = \mu_- E$, prvy Townsendov koeficient sa dá napísat v tvare

$$\delta = \frac{\alpha}{|V_-|} = \frac{n_g \langle \sigma_i v_- \rangle}{|\mu_- E|}.$$

Formálne môžeme vykonať nasledujúce úpravy

$$V_- = \mu_- E = n_g \mu_- \frac{E}{n_g},$$

kde koeficient $n_g \mu_-$ nezávisí od koncentrácie molekúl plynu n_g

Paschen law

kde koeficient $n_g \mu_-$ nezávisí od koncentrácie molekúl plynu n_g (pozri odsek 3.4.3). Stredná hodnota $\langle \sigma_i v_- \rangle$, ktorá určuje schopnosť elektrónov ionizovať molekuly plynu, závisí od energie, ktorú elektrón nadobudne tesne pred zrážkou od elektrického poľa. Táto energia je úmerná práci $e|E|\langle \lambda_- \rangle$, ktorú vykoná elektrické pole na strednej voľnej dráhe elektrónu $\langle \lambda_- \rangle$, čo formálne môžeme zapísť (F_2 je zatiaľ neurčená funkcia)

$$\langle \sigma_i v_- \rangle = F_2(e|E|\langle \lambda_- \rangle) = F_2\left(en_g\langle \lambda_- \rangle \frac{|E|}{n_g}\right).$$

Výrazy $n_g \mu_-$ a $en_g\langle \lambda_- \rangle$ nezávisia od koncentrácie molekúl n_g a teda aj od tlaku plynu. Je zrejmé, že veličiny V_- a α/n_g závisia od E a n_g prostredníctvom pomery $|E|/n_g$, takže prvý Townsendov koeficient možno napísat

$$\frac{\delta}{n_g} = \Phi\left(\frac{|E|}{n_g}\right),$$

kde Φ je zatiaľ neurčená funkcia. Pomer $|E|/n_g$ je významnou veličinou vo fyzike elektrických výbojov, ktorej rozmer je Vm^2 . Na praktické meranie je to však príliš veľká jednotka. Preto sa zaviedla jednotka **Townsend**

$$1 \text{ Townsend} = 1 \text{ Td} = 10^{-17} \text{ Vcm}^2 = 10^{-21} \text{ Vm}^2.$$

Pomocou pomery $|E|/p_0$ možno vyjadriť δ v tvare

$$\frac{\delta}{p_0} = F\left(\frac{|E|}{p_0}\right), \quad (5.7)$$

Electric discharges

$$\frac{\delta}{p_0} = F\left(\frac{|E|}{p_0}\right) \quad \delta = \frac{\alpha}{|V_-|} = \frac{n_g \langle \sigma_i v_- \rangle}{|\mu_- E|}.$$

so zatiaľ neznámou funkciou F . Ak si označíme ako δ_z hodnotu prvého Townsendovho koefficientu, ktorý spĺňa podmienku (5.6) (platí $\delta_z d = \ln(1 + 1/\gamma)$), môžeme formálne vyjadriť intenzitu elektrického poľa $|E_z|$ potrebného na zapálenie výboja

$$\frac{|E_z|}{p_0} = F_{inv}\left(\frac{\delta_z}{p_0}\right) = F_{inv}\left[\frac{\ln\left(1 + \frac{1}{\gamma}\right)}{p_0 d}\right],$$

kde F_{inv} je inverzná funkcia k funkcií F . Z hodnoty elektrického poľa potrebného na zapálenie výboja už ľahko vypočítame aj zápalné napätie

$$U_z = d|E_z| = p_0 d F_{inv}\left[\frac{\ln\left(1 + \frac{1}{\gamma}\right)}{p_0 d}\right]. \quad (5.8)$$

Z tohto výsledku možno formulovať uzáver vo forme zákonitosti:

Paschenov zákon – Zápalné napätie U_z je pre daný plyn funkciou súčinu redukovaného tlaku p_0 a vzdialenosťi elektród d .

Electric discharges

Na aproximáciu experimentálnych hodnôt sa často používa poloempirický vzťah

$$\frac{\delta}{p_0} = A \exp\left(-\frac{Bp_0}{|E|}\right), \quad (5.9)$$

kde hodnoty konštánt možno nájsť v tabuľke 5.1 pre rôzne plyny. Tiež je uvedený rozsah hodnôt $|E|/p_0$ pre ktoré je aproximácia (5.9) použiteľná. Inverznou funkciou k funkcií

$$F(x) = A \exp\left(-\frac{B}{x}\right)$$

je funkcia

$$F_{inv}(x) = \frac{B}{\ln(A/x)}.$$

Electric discharges

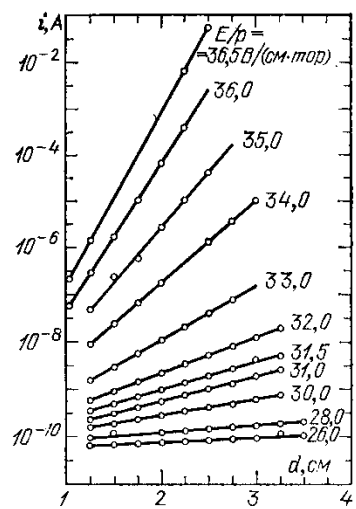


Рис. 5.3. Экспериментальный график, демонстрирующий постоянство α и экспоненциальный характер нарастания тока в разрядном промежутке; ионизационные коэффициенты определяются наклонами прямых [6]

Рис. 5.4. Ионизационный коэффициент Таунсена α в N_2 по разным измерениям

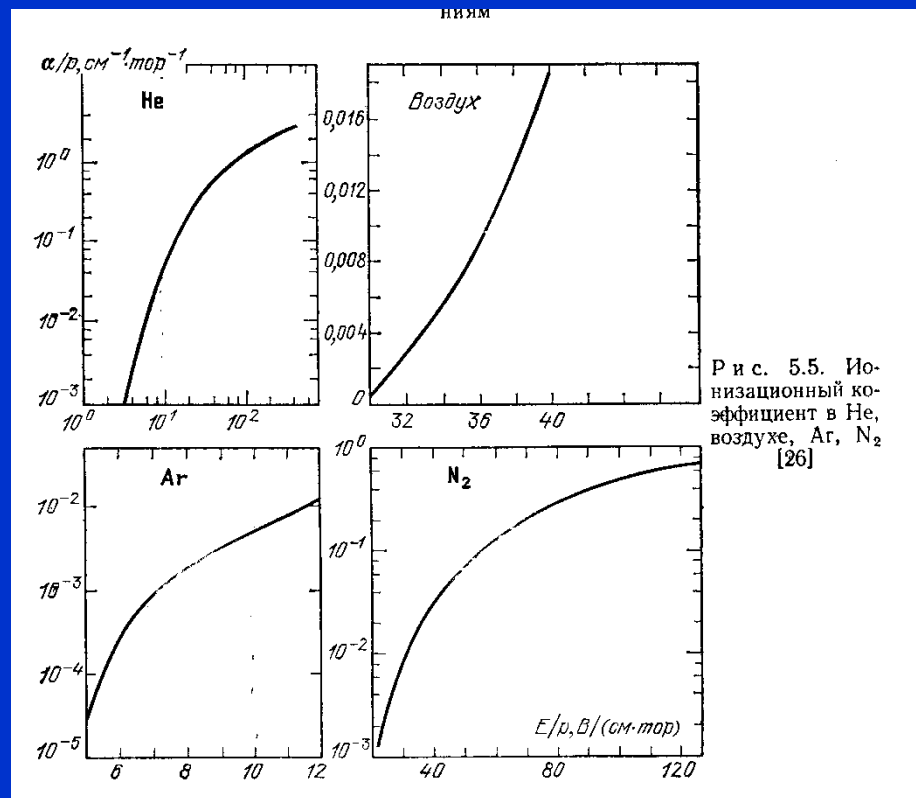
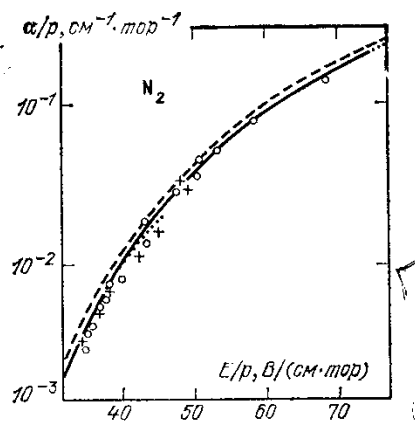


Рис. 5.5. Ионизационный коэффициент в He, воздухе, Ar, N_2 [26]

Data for Paschen law

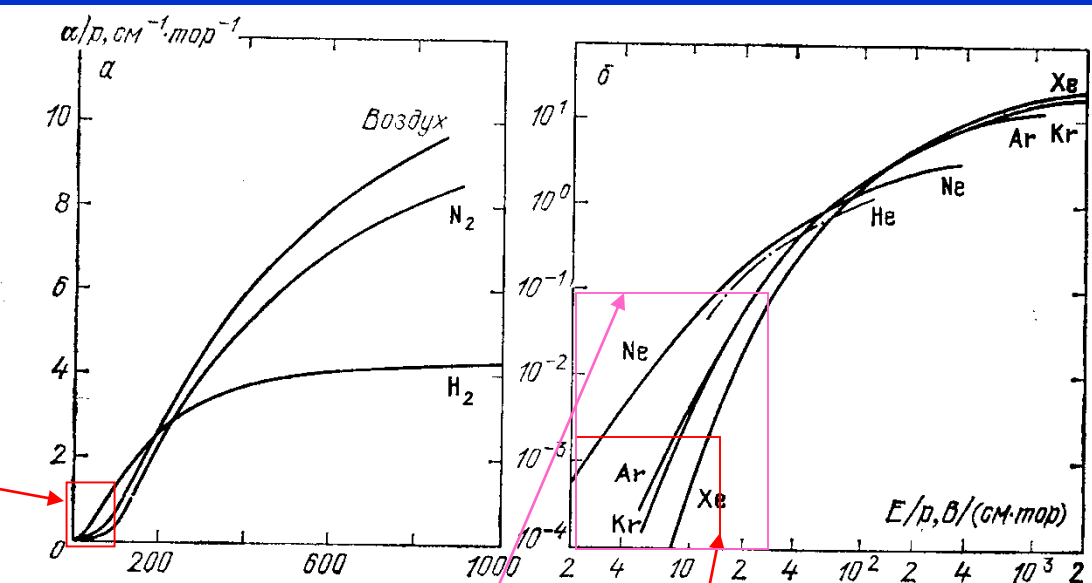
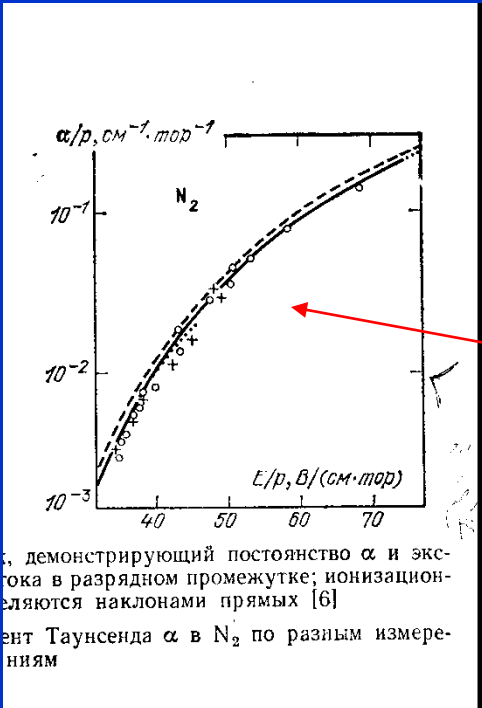


Рис. 5.6. Ионизационный коэффициент в широком диапазоне E/p : а — в H_2 , N_2 и в воздухе, б — в инертных газах [6]

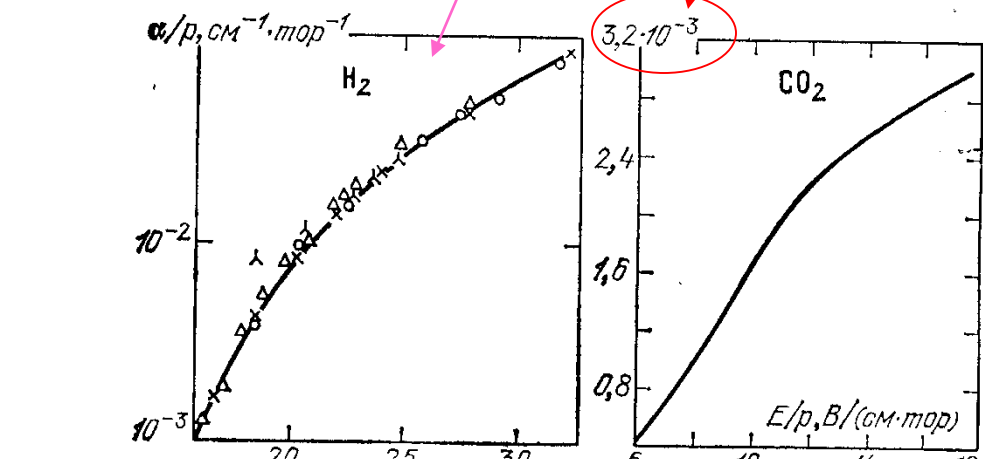


Рис. 5.7. Ионизационный коэффициент в H_2 [26] и CO_2 [6]

Paschen law – data gama

$$i = \frac{i_0 \exp(\delta d)}{1 - \gamma[\exp(\delta d) - 1]}, \quad (5.5)$$

V důsledku emise opouští povrch katody elektrony s hustotou toku γj_+

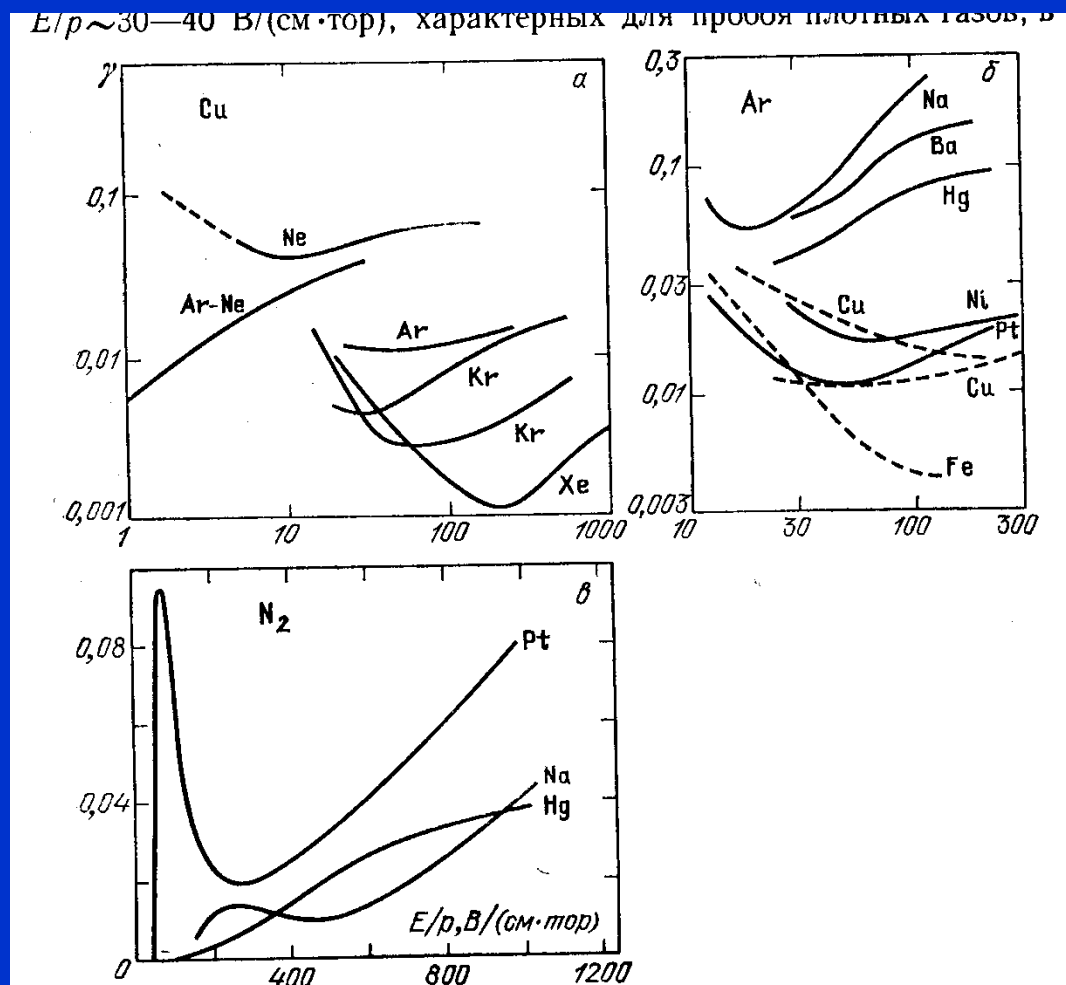


Рис. 6.13. Коэффициент ионно-электронной эмиссии, определенный из разрядного эксперимента (п. 4.1): а — медный катод в инертных газах; б — различные металлы в Ar; в — различные металлы в N₂ [6]

Electric discharges

Na aproximáciu experimentálnych hodnôt sa často používa poloempirický vzťah

$$\frac{\delta}{p_0} = A \exp\left(-\frac{Bp_0}{|E|}\right), \quad (5.9)$$

kde hodnoty konštánt možno nájsť v tabuľke 5.1 pre rôzne plyny. Tiež je uvedený rozsah hodnôt $|E|/p_0$ pre ktoré je aproximácia (5.9) použiteľná. Inverznou funkciou k funkcií

$$F(x) = A \exp\left(-\frac{B}{x}\right)$$

je funkcia

$$F_{inv}(x) = \frac{B}{\ln(A/x)}.$$

Electric discharges

Tabuľka 5.1: Koeficienty A a B pre poloempirický vzťah (5.9) podľa [19]. Posledný stĺpec označuje rozsah hodnôt $|E|/p_0$, v ktorom možno aproximáciu použiť

| Plyn | A [cm ⁻¹ Torr ⁻¹] | B [Vcm ⁻¹ Torr ⁻¹] | oblasť E /p ₀ [Vcm ⁻¹ Torr ⁻¹] |
|------------------|---|--|--|
| He | 3 | 34 | 20 – 150 |
| Ne | 4 | 100 | 100 – 400 |
| Ar | 14 | 180 | 100 – 600 |
| Kr | 17 | 240 | 100 – 1000 |
| Xe | 26 | 350 | 200 – 800 |
| vzduch | 15 | 365 | 100 – 800 |
| H ₂ | 5 | 130 | 150 – 600 |
| N ₂ | 12 | 342 | 100 – 600 |
| CO ₂ | 20 | 466 | 500 – 1000 |
| H ₂ O | 13 | 290 | 150 – 1000 |
| Hg | 20 | 370 | 200 – 600 |

Použitím tejto funkcie vo vzťahu (5.8) dostaneme

$$U_z = \frac{B p_0 d}{\ln(A p_0 d) - \ln[\ln(1 + 1/\gamma)]} \quad (5.10)$$

Electric discharges

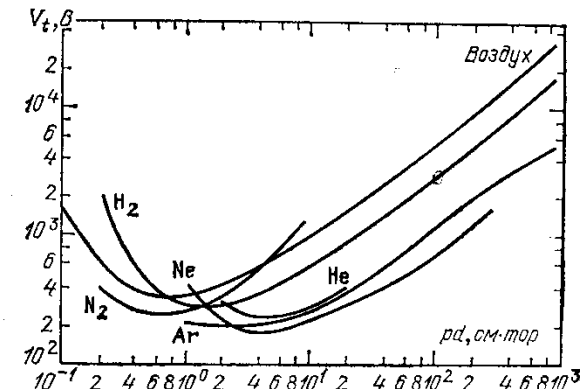
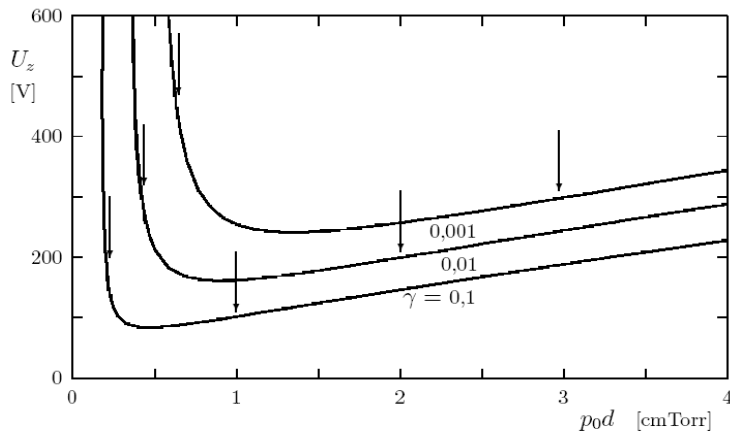
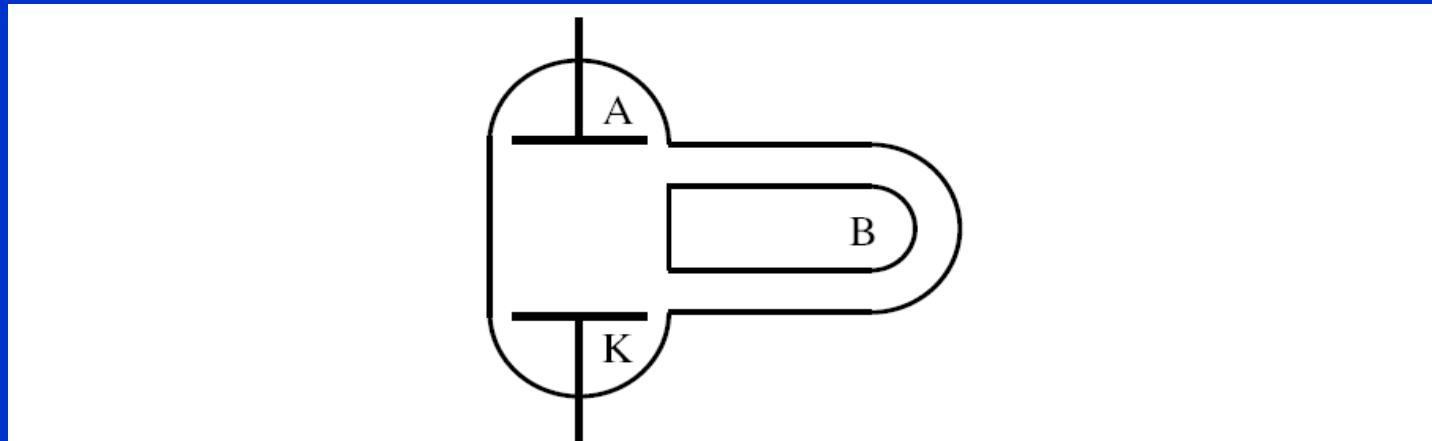


Рис. 13.2. Потенциал зажигания в различных газах в широком диапазоне pd (кривые Пашена)

Obr. 5.5: Zápalné napätie U_z výboja v argóne ako funkcia súčinu p_0d pre rôzne hodnoty druhého Townsendovho koeficientu γ . Medzi zvislými šípkami sa nachádza oblasť hodnôt E/p_0 z tab. 5.1, v ktorej platí vzťah (5.9)



Обр. 5.6: Вýbojka s bočnou dráhou B na demonštráciu nestability nízkotlakovej vetvy Paschenovej krvky

Paschen law curves

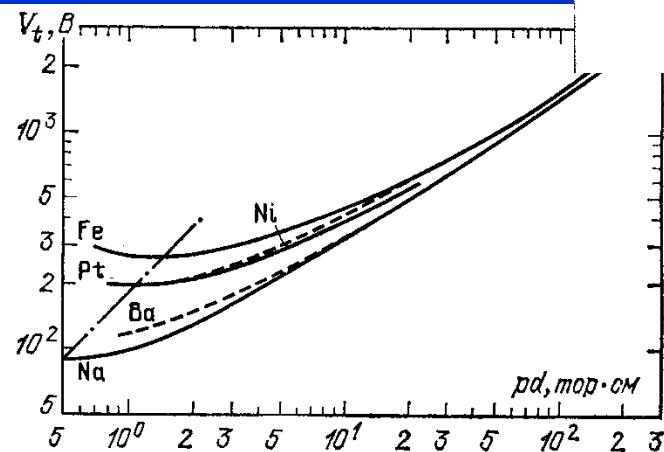


Рис. 13.3. Влияние материала катода на напряжение пробоя аргона. Штрих-пунктирная прямая соединяет точки минимума. Ее наклон 45° соответствует независимости $(E/p)_{\min}$ от материала катода [6]

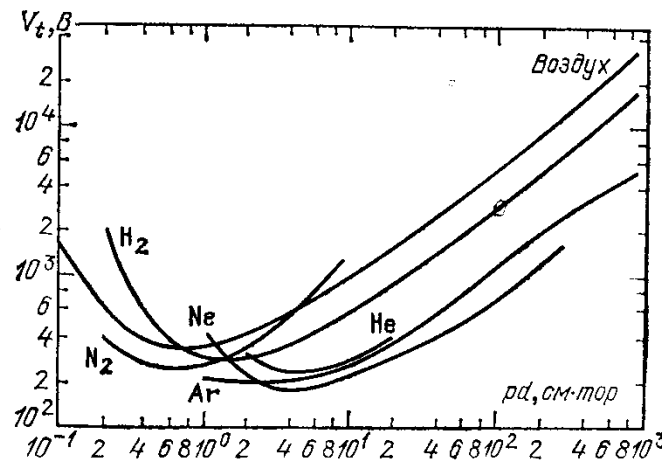


Рис. 13.2. Потенциал зажигания в различных газах в широком диапазоне pd (кривые Пащена)

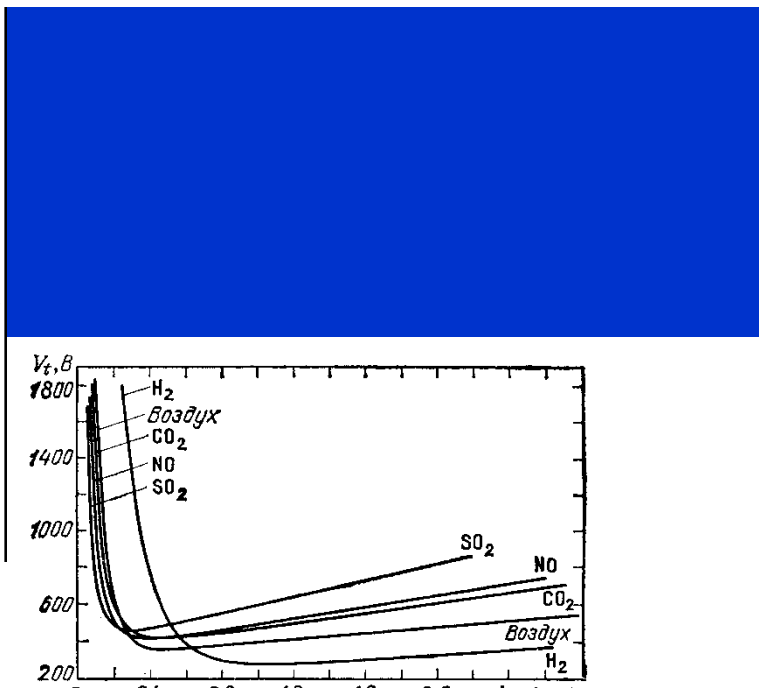


Рис. 13.4. Кривые Пащена в укрупненном масштабе [6]

Electric discharges – electron attachment versus ionization

$$dN_e/dx = (\alpha - a) N_e, \quad N_e \sim \exp [(\alpha - a) x],$$

указывают, что $\alpha_{\text{эф}} \rightarrow 0$ при $(E/p)_1 \approx 35 \text{ В/(см} \cdot \text{тор)}$, что как раз соответствует $(E/p)_{\text{предел}} \approx 26 \text{ кВ/(см} \cdot \text{атм)}$. При $E/p < (E/p)_1$ размножение

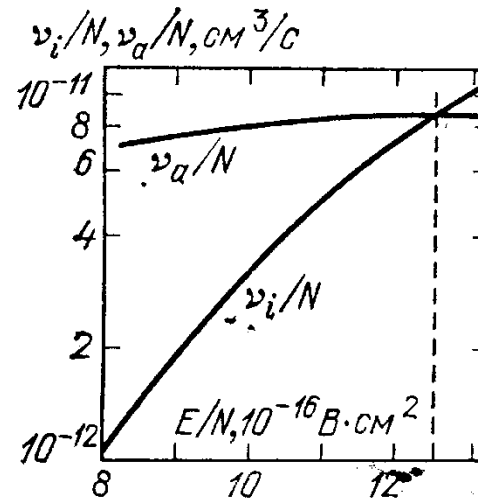
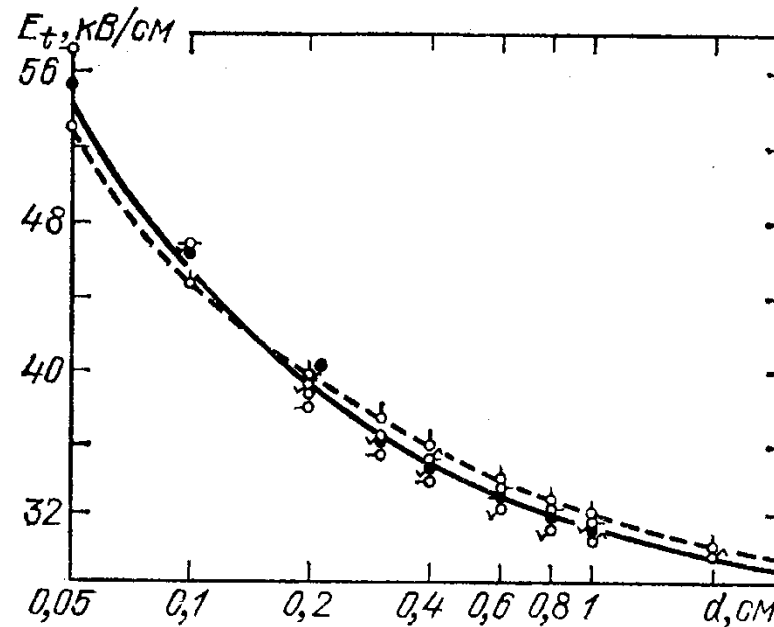


Рис. 13.5. Пробивающие поля в плоском воздушном промежутке длины d при $p=1 \text{ атм}$ по данным разных авторов [21]

Рис. 13.6. Частоты ионизации и прилипания в воздухе, рассчитанные на основе решения кинетического уравнения. Пересечение при $E/p=41 \text{ В/(см} \cdot \text{тор)}$ [10]

Paschen low curves

Таблица 13.1. Ориентировочные пороги пробоя газов при высоких давлениях

| Газ | Постоянное поле, недлинные промежутки, $p \sim 1$ атм | | СВЧ, $p \sim 100$ —300 тор |
|------------------------------------|---|----------------------|----------------------------|
| | E_t/p , кВ/(см·атм) | E_t/p , В/(см·тор) | |
| He | 10 | 13 | 3 |
| Ne | 1,4 | 1,9 | 3—5 |
| Ar | 2,7 | 3,6 | 5—10 |
| H ₂ | 20 | 26 | 10—15 |
| N ₂ | 35 | 46 | ~25 |
| O ₂ | 30 | 40 | 35 |
| Воздух | 32 | 42 | ~30 |
| Cl ₂ | 76 | 100 | |
| CCl ₂ F ₂ *) | 76 | 100 | |
| CSF ₈ | 150 | 200 | |
| CCl ₄ | 180 | 230 | |
| SF ₆ **) | 89 | 117 | |

*) Фреон
**) Элегаз

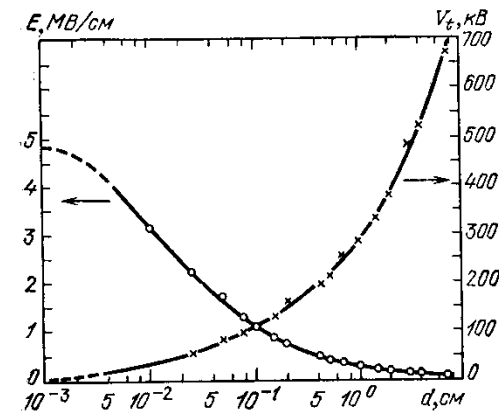


Рис. 13.7. Напряжение и поле пробоя вакуумного промежутка между шаром диаметром 2,5 см и диском диаметром 5 см из стали в зависимости от длины промежутка [3]

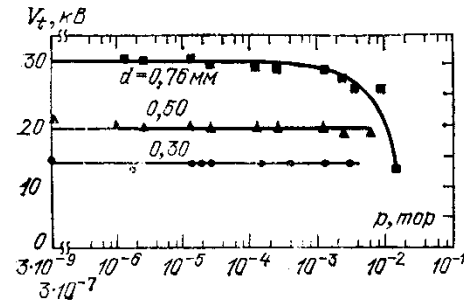


Рис. 13.8. Напряжения пробоя коротких промежутков d между стальными электродами в зависимости от давления заполняющего их водорода. Независимость от p свидетельствует о вакуумном характере пробоя. Загиб вниз верхней кривой соответствует переходу к левой ветви кривой Пашена [15.3]

RF discharges

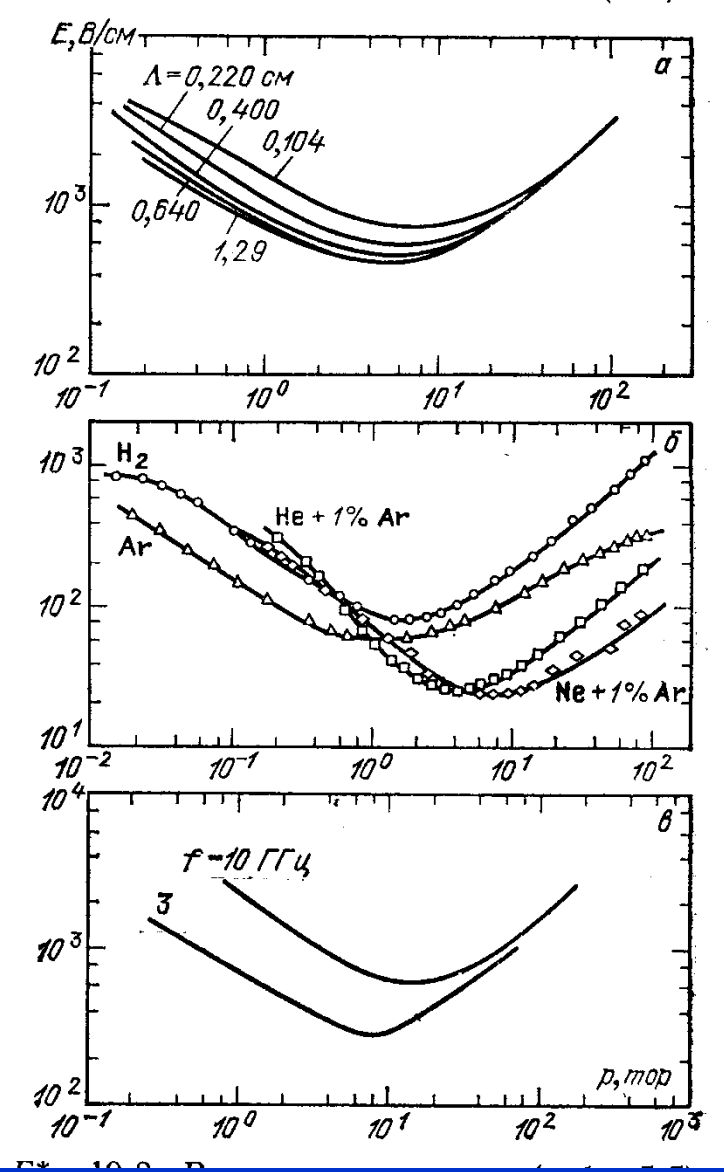


Рис. 13.10. Измеренные пороги СВЧ пробоя: *α* — воздух, частота $f=9,4 \text{ ГГц}$, около кривых указаны диффузионные длины Λ ; *β* — несколько газов, $f=0,99 \text{ ГГц}$, $\Lambda=0,63 \text{ см}$; *γ* — Нег-газ (гелий с добавкой паров ртути), $\Lambda=0,6 \text{ см}$ [24]

Electric discharges

Table 4.3. Cross sections of photoionization of atoms and molecules from the ground state close to the threshold

| Gas | $\hbar\omega = I, \text{ eV}$ | $\lambda, \text{\AA}$ | $\sigma_\nu, 10^{-18} \text{ cm}^2$ |
|----------------|-------------------------------|-----------------------|-------------------------------------|
| H | 13.6 | 912 | 6.3 |
| He | 24.6 | 504 | 7.4 |
| Ne | 21.6 | 575 | 4.0 |
| Ar | 15.8 | 787 | 35 |
| Na | 5.14 | 2412 | 0.12 |
| K | 4.34 | 2860 | 0.012 |
| Cs | 3.89 | 3185 | 0.22 |
| N | 14.6 | 852 | 9 |
| O | 13.6 | 910 | 2.6 |
| O ₂ | 12.2 | 1020 | ~ 1 |
| N ₂ | 15.58 | 798 | 26 |
| H ₂ | 15.4 | 805 | 7 |

Electric discharges

7.3.2 Ionization Kinetics Equation

When oscillation displacements are small, electron densities obey an equation of type (2.44):

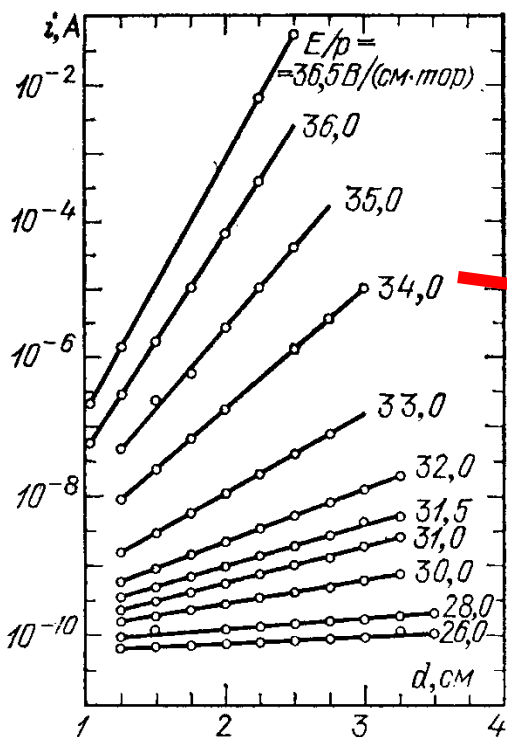
$$\partial n_e / \partial t = D_{\nabla}^2 n_e + (\nu_i - \nu_a) n_e , \quad D \equiv D_e \quad (7.6)$$

(electrons diffuse freely in breakdown). If the condition $\omega \gg \nu_m \delta$ (Sect. 5.5.2) holds (it is satisfied for microwave frequencies), the electron energy distribution is quasisteady and the ionization and attachment frequencies, ν_i and ν_a , are determined by the root-mean-square field E . The dependencies $\nu_i(E)$, $\nu_a(E)$ are much stronger than $D_e(E)$, so that $D_e(E) \approx \text{const}$. For simplification, assume that the field is spatially homogeneous, and hence, ν_i and ν_a are independent of coordinates. Averaging (7.6) over the volume, we obtain, in accord with the results of Sect. 4.5, an equation for the mean density, or (which is equivalent) for the total number of electrons, N_e , in the discharge volume:

$$dN_e / dt = (\nu_i - \nu_a - \nu_d) N_e , \quad \nu_d = D / A^2 , \quad (7.7)$$

where ν_d is the frequency of diffusion losses of electrons. This equation describes the ionization kinetics of the gas.

Electric discharges – data semi-empirical approach



$$\frac{dj_-}{dx} = \alpha n_- = \frac{\alpha}{V_-} n_- V_- = \delta j_-$$

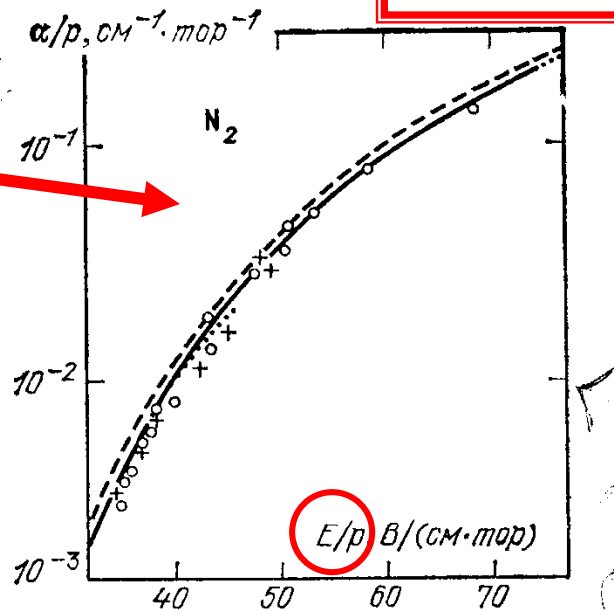


Рис. 5.3. Экспериментальный график, демонстрирующий постоянство α и экспоненциальный характер нарастания тока в разрядном промежутке; ионизационные коэффициенты определяются наклонами прямых [6]

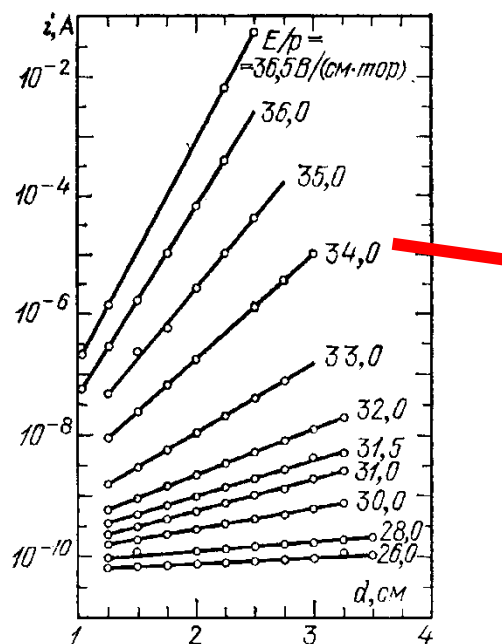
Рис. 5.4. Ионизационный коэффициент Таунсенда α в N_2 по разным измерениям

$$E/N \dots \dots 1 \text{ Townsend} = 1 \text{ Td} = 10^{-17} \text{ V cm}^2 = 10^{-21} \text{ V m}^2$$

$$E/p \text{ at } 293 \text{ K (cca } 20 \text{ C)} \dots \dots 1 \text{ V/cmTorr} = 3.034 \text{ Td, resp.} \quad 1 \text{ Td} = 0.3296 \text{ V/cmTorr}$$

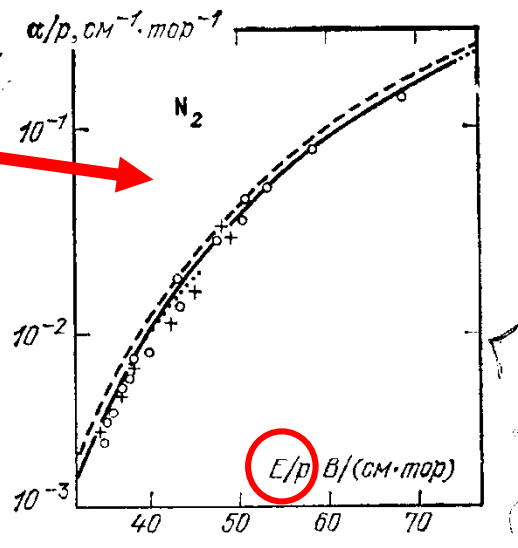
Breakdown cannot be simply explained by ionization

POZOR ROZDIEL



Р и с. 5.3. Экспериментальный график, демонстрирующий постоянство α и экспоненциальный характер нарастания тока в разрядном промежутке; ионизационные коэффициенты определяются наклонами прямых [6]

Р и с. 5.4. Ионизационный коэффициент Таунсенда α в N_2 по разным измерениям



$$\frac{dj_-}{dx} = \alpha n_- = \frac{\alpha}{V_-} n_- V_- = \delta j_-$$

i : charge current

α : Townsend ionization coefficient

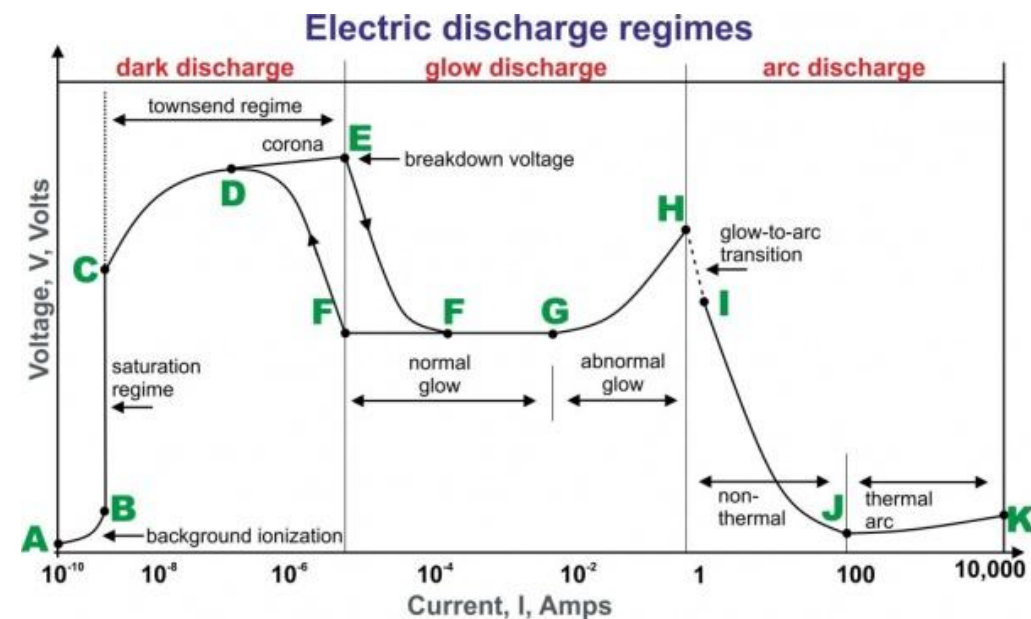
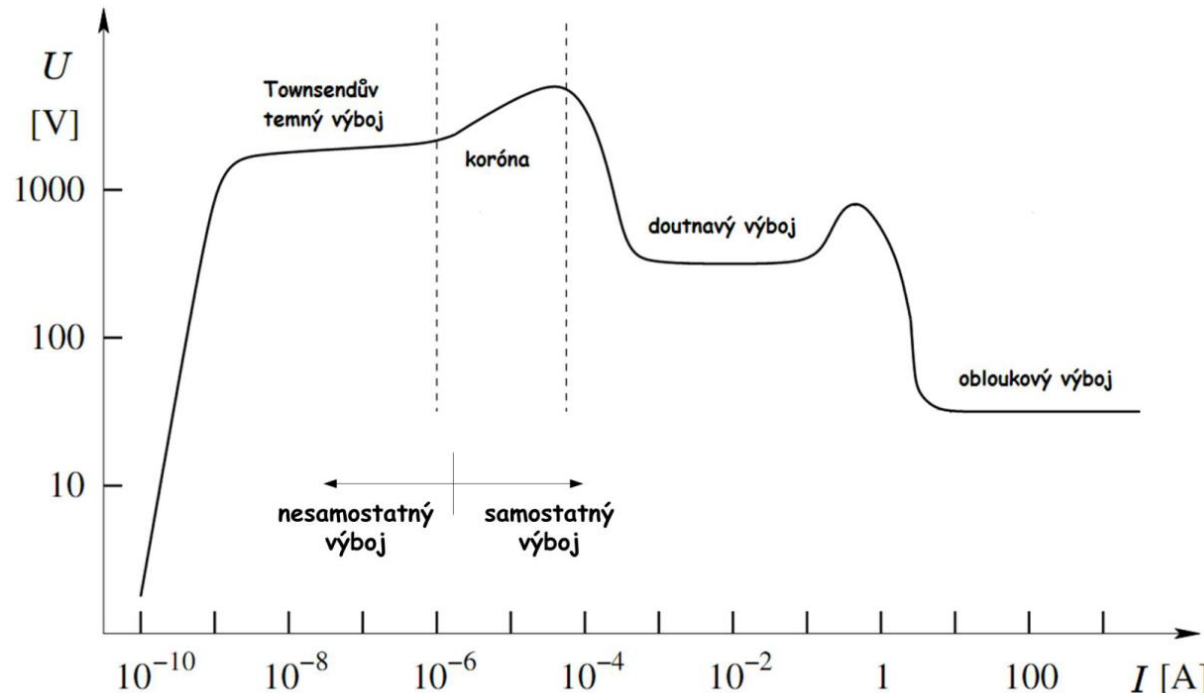
γ_e : Townsend secondary-electron emission coefficient

d : Distance between electrodes

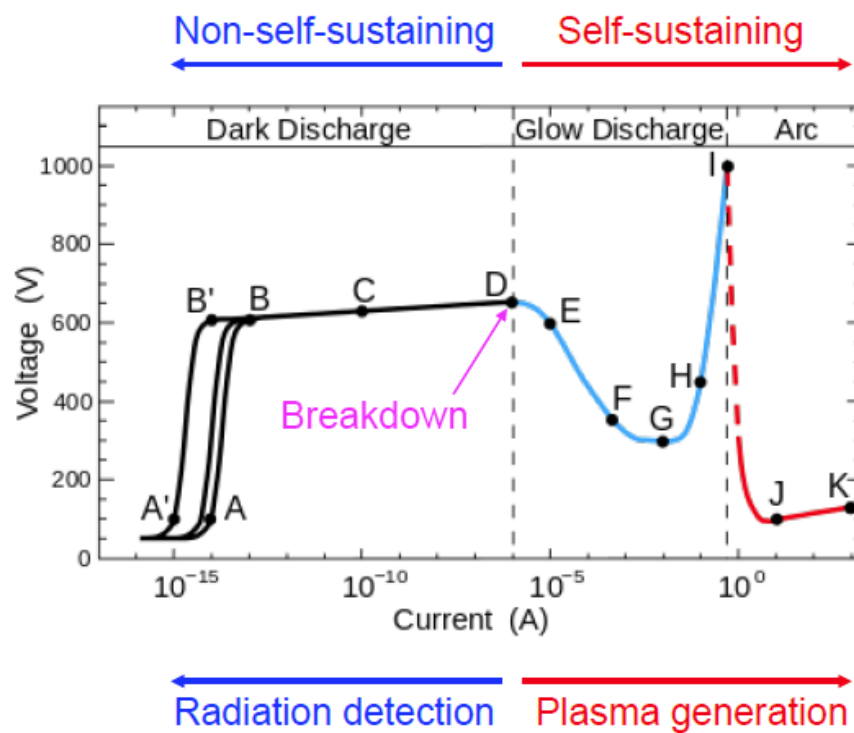
$$E/N \dots 1 \text{ Townsend} = 1 \text{ Td} = 10^{-17} \text{ Vcm}^2 = 10^{-21} \text{ Vm}^2$$

$$E/p \text{ at } 293 \text{ K (cca } 20 \text{ C)} \dots 1 \text{ V/cmTorr} = 3.034 \text{ Td, resp.} \quad 1 \text{ Td} = 0,3296 \text{ V/cmTorr}$$

Principal Glow Discharge Mechanism by Biased Parallelplate



Typical characteristic curve for gas discharges: self-sustaining or non-self-sustaining



Voltage-current characteristics of electrical discharge in neon at 1 torr, with two planar electrodes separated by 50 cm.

A: random pulses by cosmic radiation

B: saturation current

C: avalanche Townsend discharge

D: self-sustained Townsend discharge

E: unstable region: corona discharge

F: sub-normal glow discharge

G: normal glow discharge

H: abnormal glow discharge

I: unstable region: glow-arc transition

J: electric arc

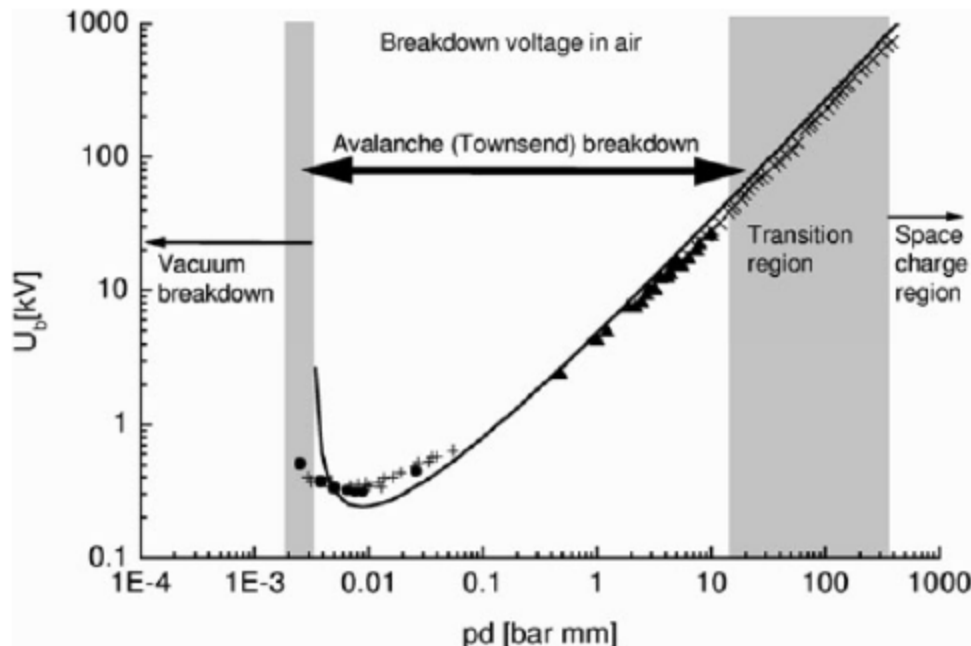
K: electric arc

A-D region: dark discharge; ionisation occurs, current below 10 microamps.

F-H region: glow discharge; the plasma emits a faint glow.

I-K region: arc discharge; large amounts of radiation produced.

Limitation of Townsend theory

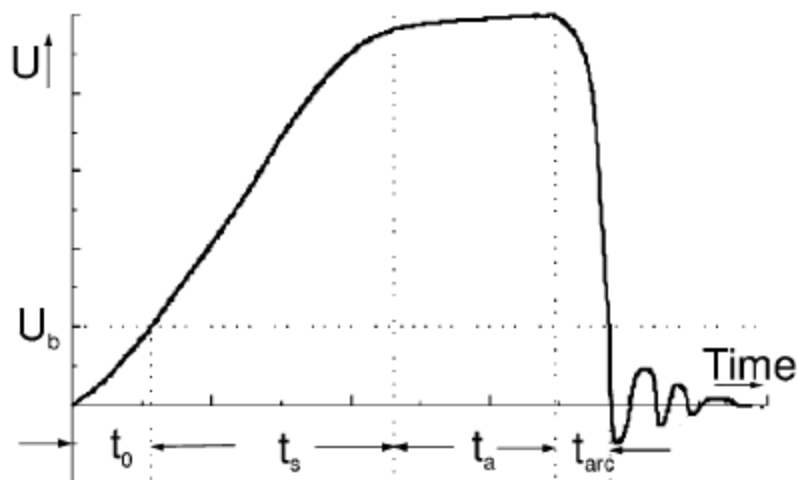


The Townsend quasi-homogeneous breakdown mechanism can be applied **only for relatively low pressures and short gaps** ($pd < 200 \text{ Torr} \cdot \text{cm}$).

1. The spark breakdown at high pd and considerable overvoltage develops **much faster than the time necessary for ions to cross the gap and provide the secondary emission**. $\rightarrow \gamma$ process fails.
2. The spark channel is observed to have a zig-zag shape at high pd regime.
3. The discharge at high pd is independent of electrode material.

Pulsed breakdown

- Static characteristics : slowly-varying voltage
→ Townsend mechanism
- Dynamic characteristics : fast rising pulse
→ Overvoltage breakdown & discharge time lag



- t_0 : the time until the static breakdown voltage is exceeded
- t_s : the **statistical delay time** until an electron able to create an avalanche occurs
- $t_a (t_f)$: the avalanche build-up time until the critical charge density is reached (**formative time**)
- t_{arc} : the time required to establish a low-resistance arc across the gap

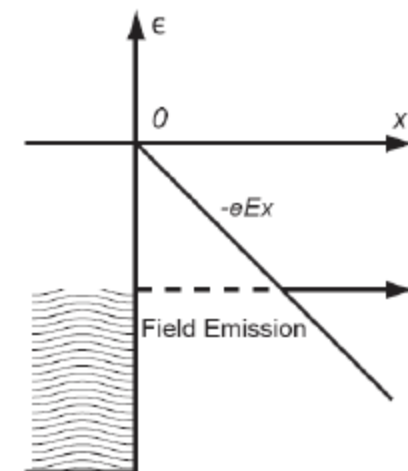
Breakdown delay time = statistical delay time + formative time

Statistical delay time

- The statistical delay time results from **the statistics of electron appearance** in the gap.
- The sources of electrons that initiate the self-breakdown of a gap
 - Natural radioactivity and cosmic radiation
 - ✓ They produce $0.1 \sim 10$ free electrons per cm^3 per second in a gas at atmospheric pressure
 - Field emission by tunneling
 - ✓ Fowler-Nordheim eq.
$$J = C \frac{E^2}{W} \exp\left(-D \frac{W^{3/2}}{E}\right)$$
 - Electron detachment from molecules
- Total number of electrons appearing in the gap

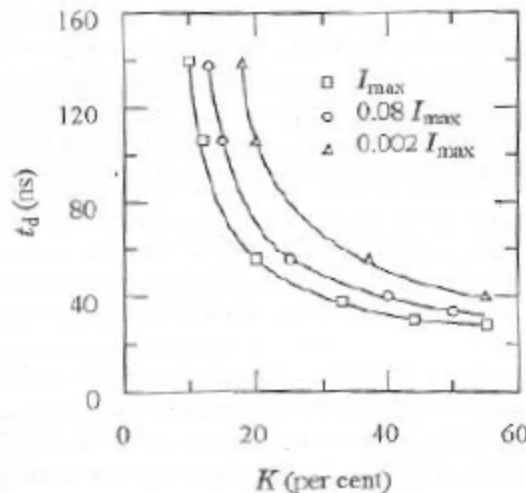
$$\dot{N}(t) = \dot{N}_{0n} + \dot{N}_F(t) + \dot{N}_\delta(t)$$

Natural occurrence Field emission Electron detachment



Formative time measurements

- The statistical delay time can be neglected if the gap is intensely irradiated with the light of an auxiliary spark. Then the measured delay time will be equal to the formative time.
- In an early experiment with 30% overvoltage for air gap, Rogowski found that the formative time was 10^{-8} sec, order of the drift time of the electrons in the gap.
- Many experiments confirmed that the formative time depends on the overvoltage and the intensity of irradiation.

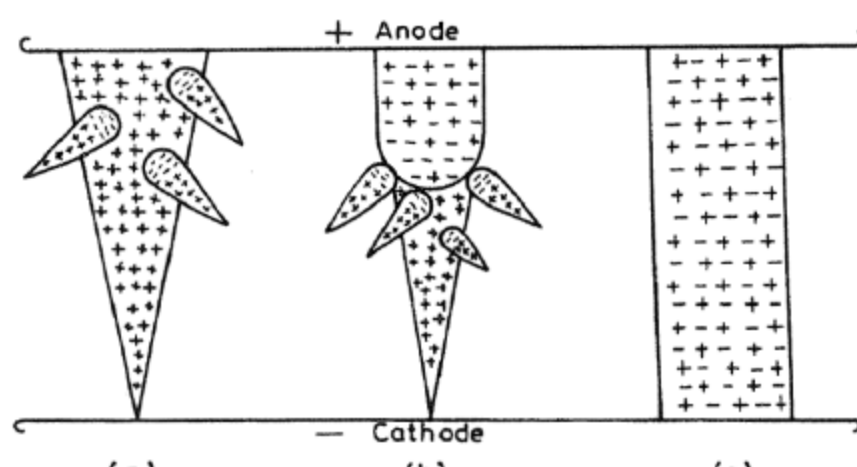


- Need for new theory → Streamer mechanism

Streamer mechanism

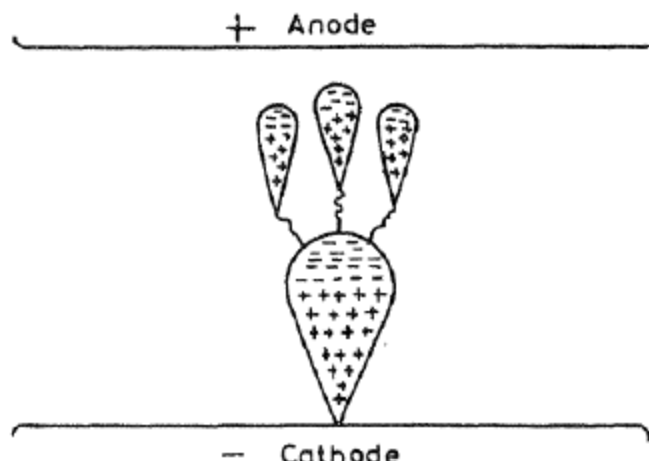
- The streamer concept was proposed by Loeb and Meek for the positive streamer and, independently by Raether for the negative streamer.
- Basic idea is that at a certain stage in the development of a single avalanche, **photoionization** of the gas in the inter-electrode space becomes the most important mechanism in determining the breakdown of the gap.

Meek & Loeb



Cathode-directed streamer

Raether

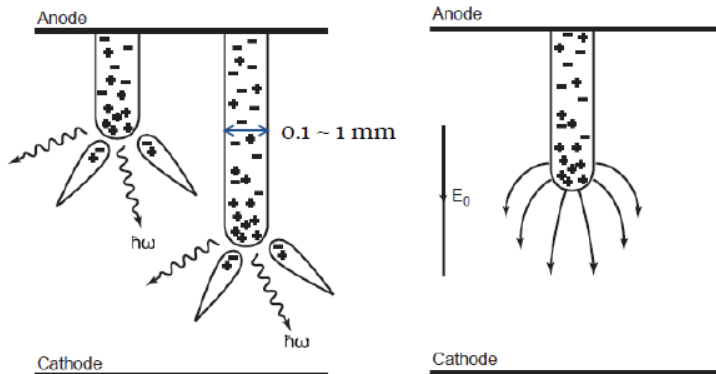


Anode-directed streamer

Calculation of avalanche...

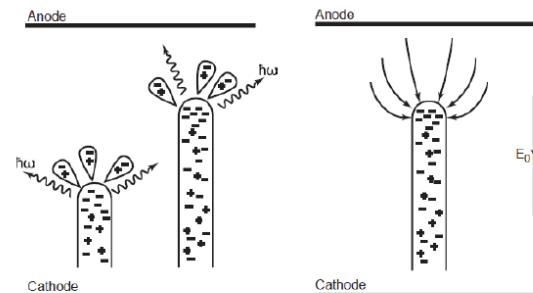
Positive streamer (cathode-directed streamer)

- If the gap is short, the transformation occurs only when the avalanche reaches the anode. Such a streamer that grows from anode to cathode and called the cathode-directed or positive streamer.



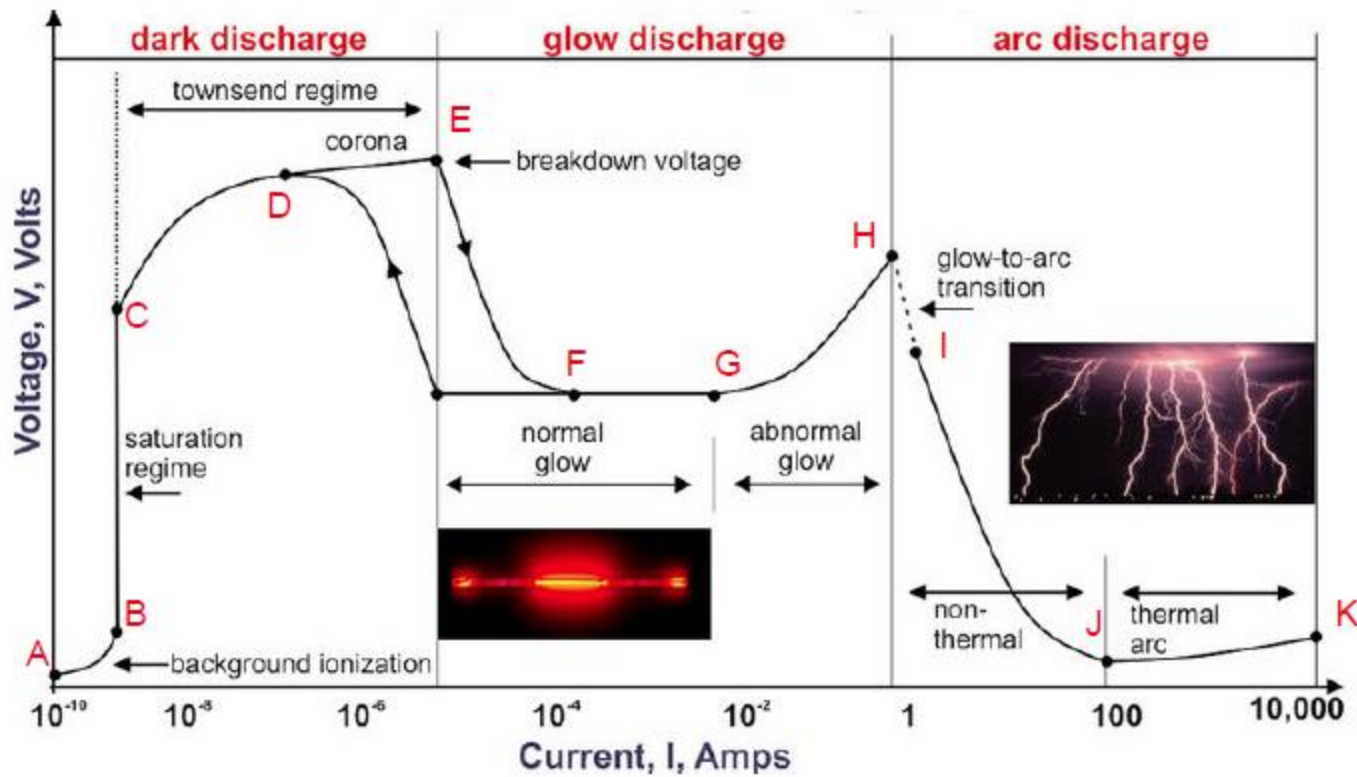
Negative streamer (anode-directed streamer)

- If the gap and overvoltage are large, the avalanche-to-streamer transformation can take place far from the anode, and the anode-directed or negative streamer grows toward both electrodes.



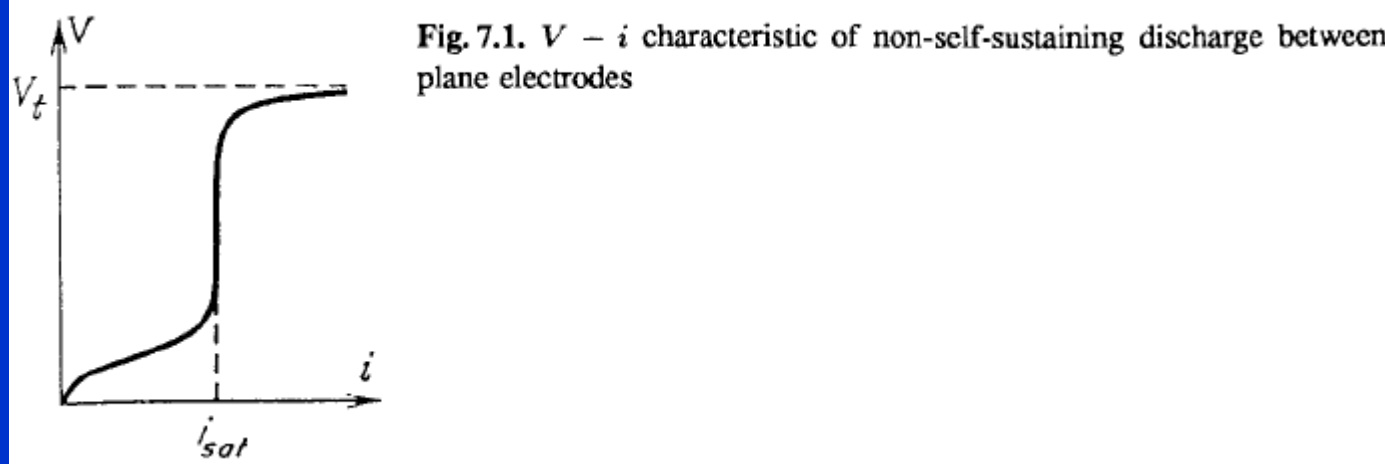
Calculation of avalanche...

Typical current-voltage characteristics for electrical discharge of gases

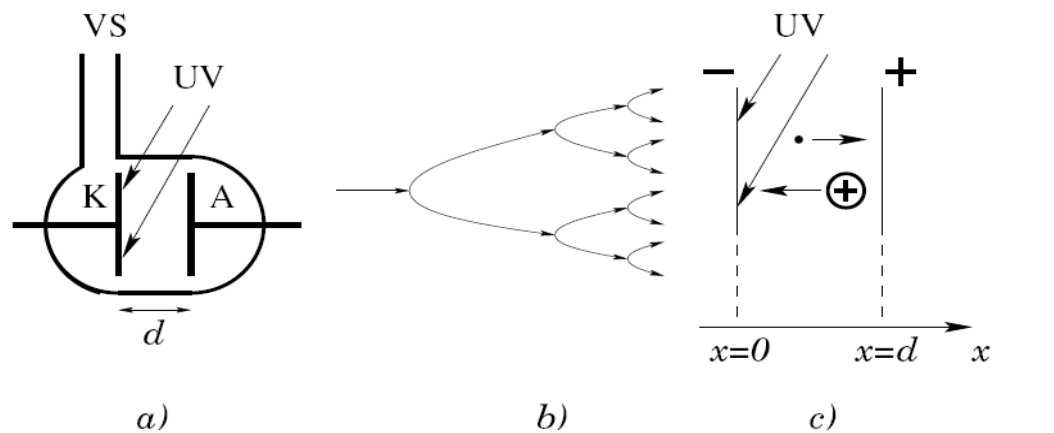


Electric discharges

7.2 Breakdown and Triggering of Self-Sustained Discharge in a Constant Homogeneous Field at Moderately Large Product of Pressure and Discharge Gap Width

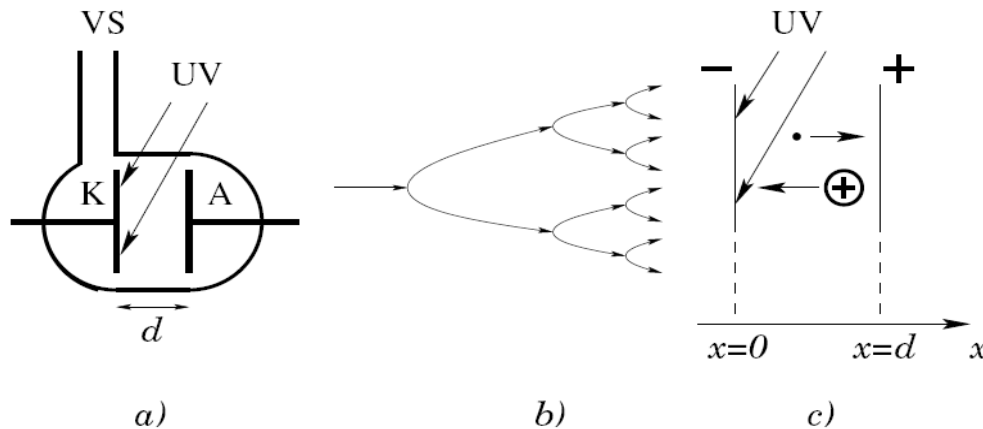


Electric discharges Townsend avalanche theory



Obr. 5.2: Zapaľovanie výboja: a) výbojka na meranie zapaľovacieho napäťia: K - katóda, A - anóda, UV - ultrafialové žiarenie zabezpečujúce emisiu primárnych elektrónov, VS - napojenie na vákuový systém; b) elektrónová lavína; c) označenie polohy elektród

Electric discharges Townsend avalanche theory



Obr. 5.2: Zapaľovanie výboja: a) výbojka na meranie zapaľovacieho napäťa: K - katóda, A - anóda, UV - ultrafialové žiarenie zabezpečujúce emisiu primárnych elektrónov, VS - napojenie na vákuový systém; b) elektrónová lavína; c) označenie polohy elektród

medzi elektródami (obr. 5.2 c). Povrch katódy K sa nachádza v mieste $x = 0$ a povrch anódy A v mieste $x = d$. Elektróny sa pohybujú smerom k anóde a vytvorené kladné ióny ku katóde, kde zanikajú. Podobne ako v odseku 4.3.1, môžeme napísť rovnicu kontinuity pre elektróny v jednorozmernej geometrii a v ustálenom stave

$$\frac{dj_-}{dx} = \alpha n_- = \frac{\alpha}{V_-} n_- V_- = \delta j_-, \quad (5.2)$$

kde V_- je driftová rýchlosť elektrónov v elektrickom poli (v homogénnom poli je konštantná) a $\delta = \alpha/V_-$ je **prvý Townsendov koeficient**. Analogická rovnica platí aj pre kladné ióny

$$\frac{dj_+}{dx} = \alpha n_+ = \delta j_-. \quad (5.3)$$

$$\frac{dj_-}{dx} = \alpha n_- = \frac{\alpha}{V_-} n_- V_- = \delta j_-$$

Prvý Townsendov koeficient δ má rozmer m^{-1} a označuje počet ionizácií, ktoré vykoná jeden elektrón v smere elektrického poľa na jednotkovej dráhe (na rozdiel od ionizačnej frekvencie α udávajúcej počet ionizácií za jednotku času). Ak rovnice odčítame, dostaneme

$$\frac{d(j_+ - j_-)}{dx} = 0 \quad \Rightarrow \quad j_+ - j_- = K = \text{konšt.}$$

Potom hustota elektrického prúdu medzi elektródami $i = e(j_+ - j_-) = eK$ je taktiež konštantná, napriek tomu, že hustoty toku elektrónov a iónov sa menia s polohou x .

V homogénnom poli je Townsendov koeficient δ konštantný a preto môžeme rovnice kontinuity ľahko integrovať

$$j_- = C \exp(\delta x); \quad j_+ = C \exp(\delta x) + i/e,$$

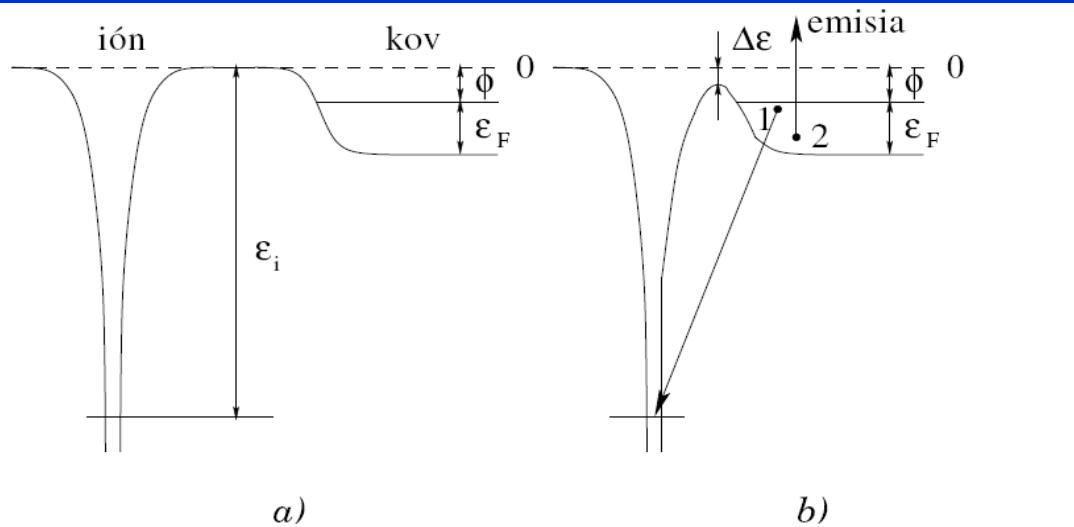
kde C je integračná konštanta. Hodnota tejto integračnej konštanty sa dá určiť z hustoty toku elektrónov na katóde: $C = j_-(0)$. Potom

$$j_- = j_-(0) \exp(\delta x); \quad j_+ = j_-(0) \exp(\delta x) + i/e. \quad (5.4)$$

Problém určenia hustoty toku $j_-(0)$ spočíva v tom, že okrem primárnych elektrónov emitovaných z katódy ultrafialovým žiarením (ich hustotu toku označíme j_0), elektróny emitujú aj dopadajúce kladné ióny. Tento typ emisie sa nazýva **potenciálková emisia**.

Electric discharges

Potenciálová emisia



Obr. 5.3: Emisia elektrónu pri dopade kladného iónu na povrch kovu: a) ión je ďaleko od povrchu: ϵ_i - ionizačná energia atómu, Φ - výstupná práca kovu a ϵ_F - Fermiho energia; b) kladný ión pri dopade na povrch kovu: 1 - elektrón prechádza na neobsadenú hladinu v ióne, 2 - emitovaný elektrón preberá prebytočnú energiu **Augerova emisia**

plynu. Ak však vypneme ultrafialové žiarenie, hustota primárnych elektrónov i_0 klesne na nulu a potom tiež $i = 0$. Lavínová ionizácia sa teda samostatne neudrží. Preto tento typ výboja nazývame **nesamostatný výboj** alebo tiež **Townsendov výboj**. Townsendov výboj je teda predprierazovým štádiom. Pri dostatočne silných poliach sa začne lovej emisie opúšťajú povrch elektróny s hustotou toku γj_+ . Koeficient γ reprezentuje výtažok elektrónov pri emisii, ktorý sa často (nelogicky) nazýva koeficient sekundárnej emisie. V teórii zapalňovania výboja sa zvykne nazývať **druhý Townsendov koeficient** (v staršej literatúre aj tretí Townsendov koeficient). Obvykle nadobúda hodnoty $0,1 - 10^{-3}$ (pre ióny veľkých organických molekúl až 10^{-10}).

Breakdown condition: Paschen's law

When the electric field in the interelectrode space **E is sufficiently high to create the multiplication** of the electrons and ions, **the avalanche appears**. If this multiplication creates a sufficient number of electrons and ions, it will lead to the electrical breakdown. However, if the processes of free charge species losses are emphasized, the avalanche multiplication can cease. Due to the **statistical nature** of both creation and loss of free species, breakdown may not occur even if applied voltage U_w is higher than the breakdown voltage U_b .

The breakdown condition for the gases at low pressures can be obtained using Townsend's theory, including the fact that influence of the space charge can be neglected in the early stage of the breakdown. Space charge is needed for the determination of the regime that will be established after the breakdown.

$$N_a = N_0 \frac{\exp(\alpha d)}{1 - \gamma[\exp(\alpha d) - 1]},$$

The breakdown condition

$$\gamma[\exp(\alpha d) - 1] = 1 \quad \alpha d = \ln\left(1 + \frac{1}{\gamma}\right)$$

$$\alpha = Ap \exp\left(-\frac{Bp}{E}\right)$$

It also means that the current can be sustained if the external source of radiation is absent ($N_0 = 0$), i.e. it is self-sustaining discharge. In other words, equation (5) represents a condition for breakdown initiation.

$$Apd \exp\left(-\frac{Bp}{E}\right) = \ln\left(1 + \frac{1}{\gamma}\right)$$

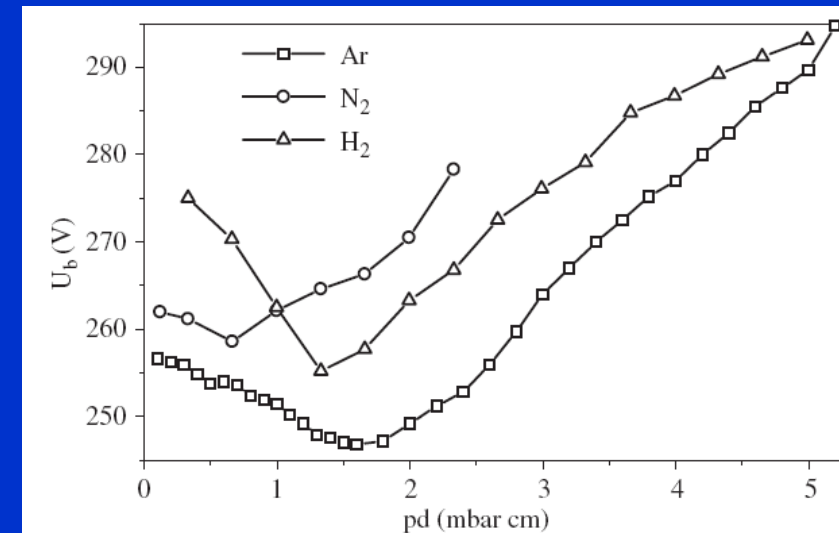
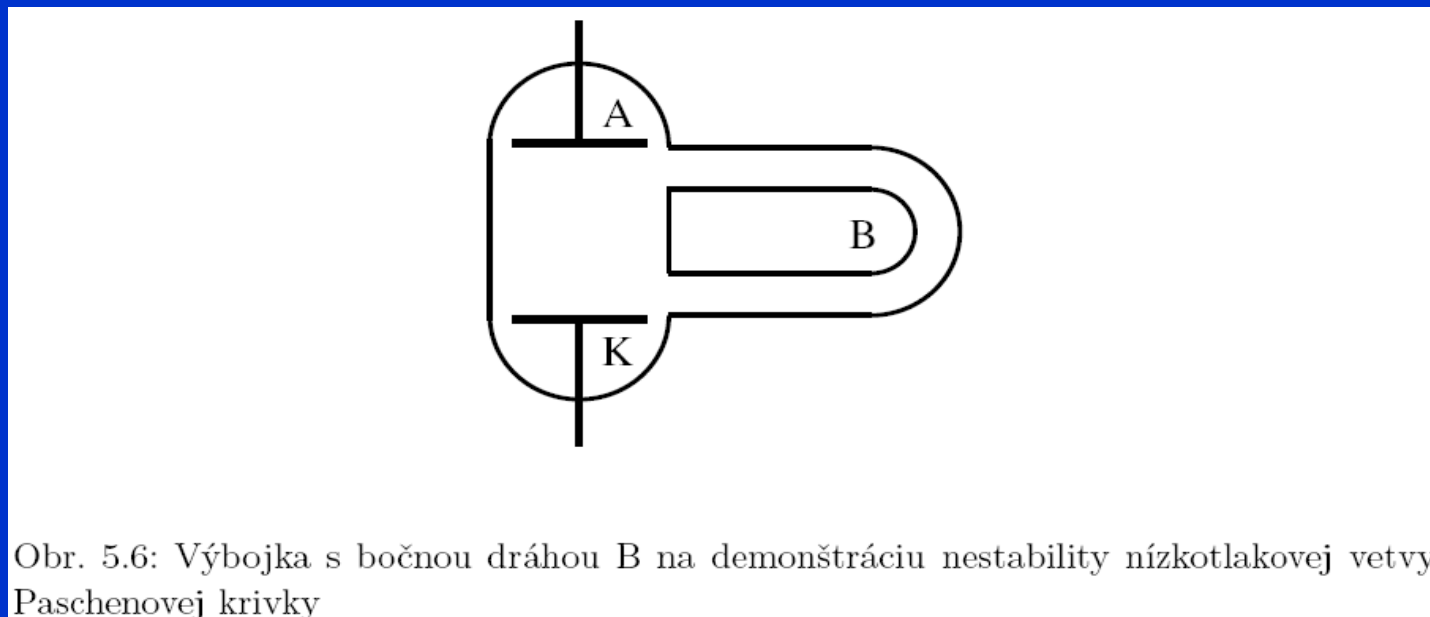
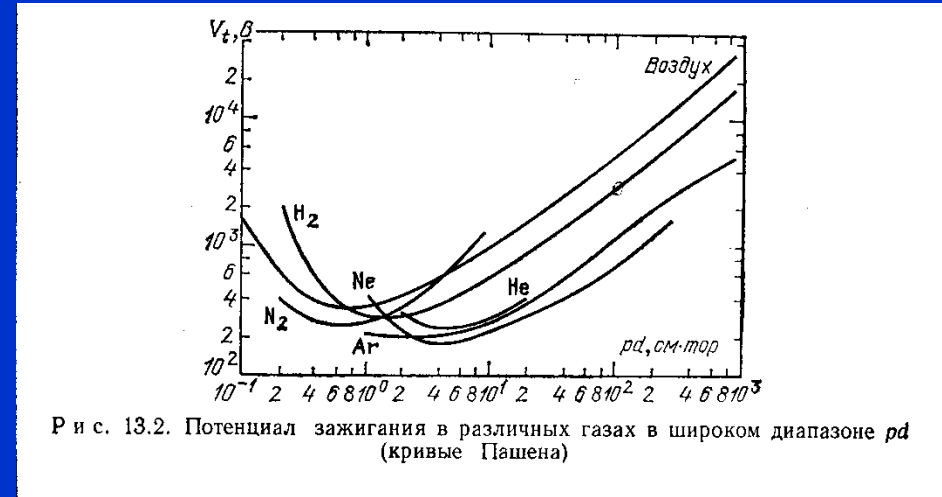


Figure 1. Breakdown voltage U_b in three gases as a function of pd values (Paschen curves).

$$U_b = \frac{Bpd}{\ln(Apd) - \ln[\ln(1 + 1/\gamma)]}$$

Electric discharges



Electric discharges

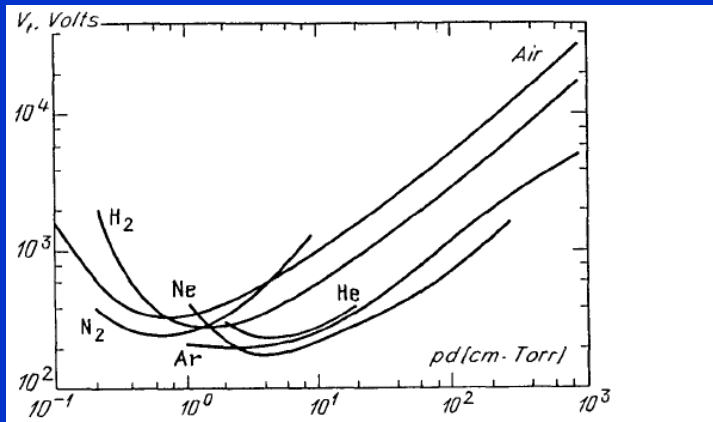


Fig. 7.2. Breakdown potentials in various gases over a wide range of pd values (Paschen curves) on the basis of data given in [7.1, 2]

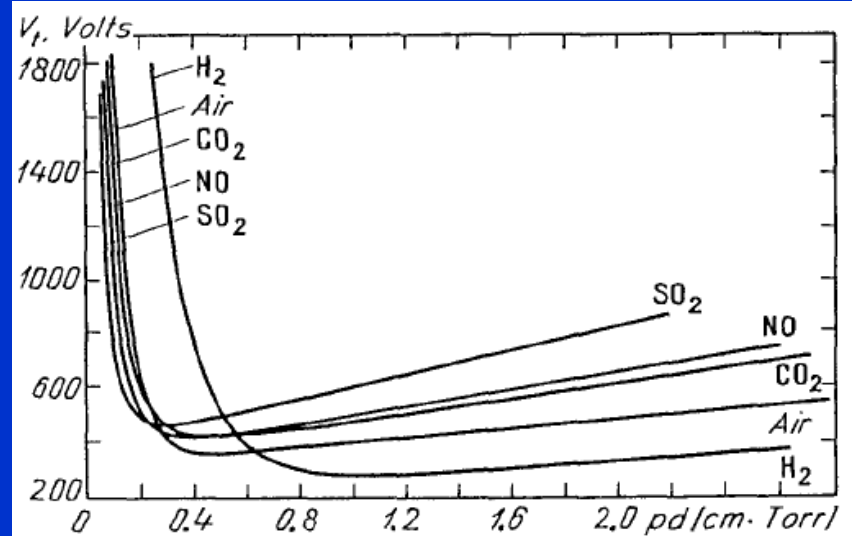


Fig. 7.3. Paschen curves on an enlarged scale [7.3]

$$U_b = \frac{Bpd}{\ln(Apd) - \ln[\ln(1 + 1/\gamma)]}$$

$$(pd)_{\min} = \frac{\bar{e}}{A} \ln \left(\frac{1}{\gamma} + 1 \right), \quad \left(\frac{E}{p} \right)_{\min} = B, \quad V_{\min} = \frac{\bar{e}B}{A} \ln \left(\frac{1}{\gamma} + 1 \right)$$

Paschen law curves

Ar

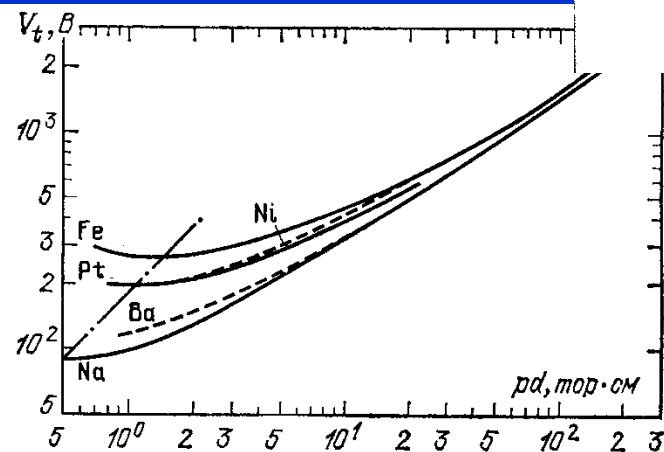


Рис. 13.3. Влияние материала катода на напряжение пробоя аргона. Штрих-пунктирная прямая соединяет точки минимума. Ее наклон 45° соответствует независимости $(E/p)_{\min}$ от материала катода [6]

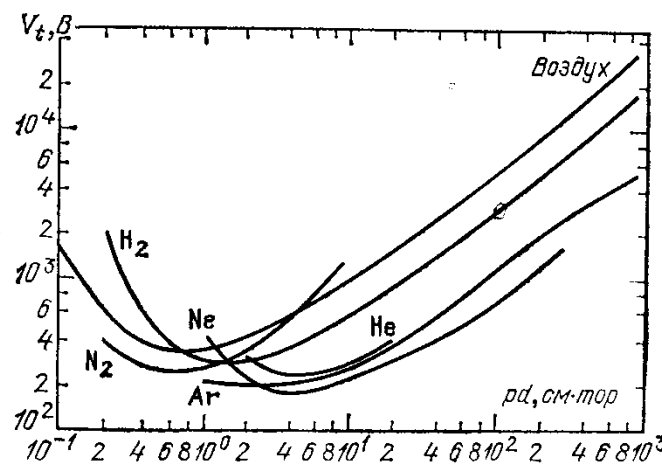


Рис. 13.2. Потенциал зажигания в различных газах в широком диапазоне pd (кривые Пащена)

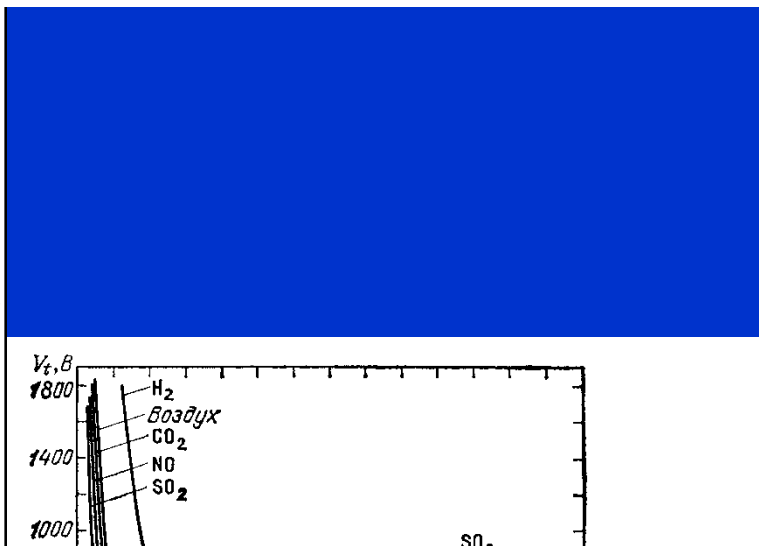


Рис. 13.4. Кривые Пащена в укрупненном масштабе [6]

Electric discharges

Breakdown Fields in Moderately Large Gaps in Air and Other Electronegative Gases at Atmospheric Pressure. Limiting Values of pd for the Townsend Breakdown Mechanism

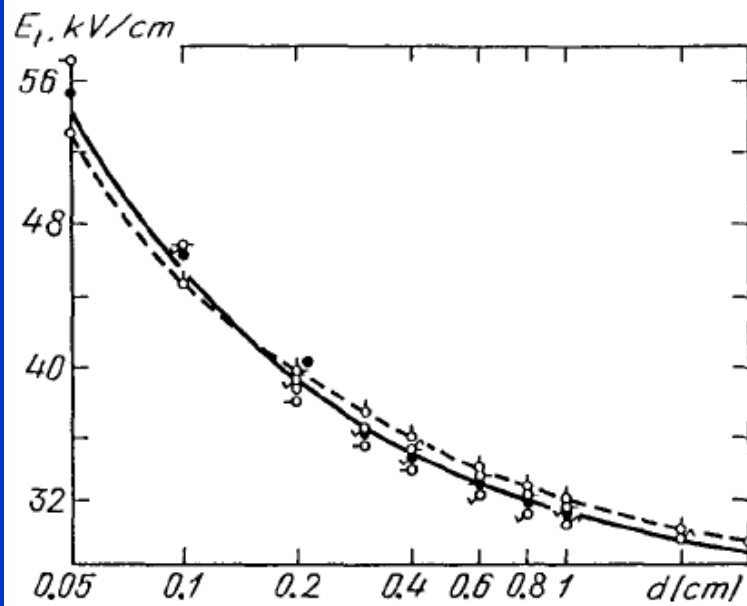
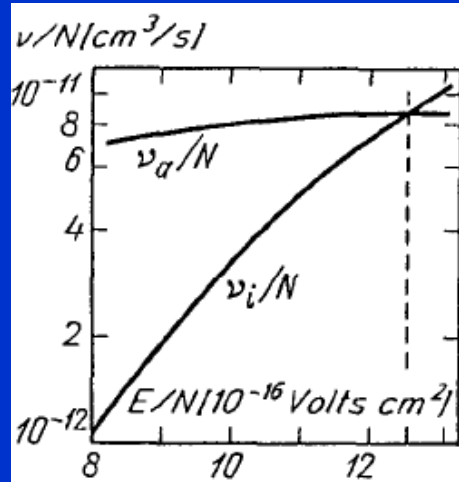


Fig. 7.4. Breakdown fields in a plane gap of length d in air at $p = 1$ atm.
From [7.1]



$$dN_e/dx = (\alpha - a)N_e, \quad N_e \propto \exp(\alpha - a)x;$$

Fig. 7.5. Ionization and attachment frequencies in air, calculated using the solution of the kinetic equation. Intersection at $E/p = 41$ V/cm-Torr

Electric discharges

Table 7.1. Approximate values of breakdown threshold at high pressure

| Gas | Constant field, gap width less than several cm, $p \sim 1$ atm | Microwaves, $p \sim 100\text{--}300$ Torr |
|-----------------------------------|--|---|
| | E/p kV/(cm·atm) | E/p V/(cm·Torr) |
| H ₂ | 10 | 13 |
| Ne | 1.4 | 1.9 |
| Ar | 2.7 | 3.6 |
| H ₂ | 20 | 26 |
| N ₂ | 35 | 46 |
| O ₂ | 30 | 40 |
| Air | 32 | 42 |
| Cl ₂ | 76 | 100 |
| CCl ₂ F ₂ * | 76 | 100 |
| CSF ₈ | 150 | 200 |
| CCl ₄ | 180 | 230 |
| SF ₆ | 89 | 117 |

* Freon

Paschen low curves

Таблица 13.1. Ориентировочные пороги пробоя газов при высоких давлениях

| Газ | Постоянное поле, недлинные промежутки, $p \sim 1$ атм | | СВЧ, $p \sim 100$ —300 тор |
|------------------------------------|---|----------------------|----------------------------|
| | E_t/p , кВ/(см·атм) | E_t/p , В/(см·тор) | |
| He | 10 | 13 | 3 |
| Ne | 1,4 | 1,9 | 3—5 |
| Ar | 2,7 | 3,6 | 5—10 |
| H ₂ | 20 | 26 | 10—15 |
| N ₂ | 35 | 46 | ~25 |
| O ₂ | 30 | 40 | 35 |
| Воздух | 32 | 42 | ~30 |
| Cl ₂ | 76 | 100 | |
| CCl ₂ F ₂ *) | 76 | 100 | |
| CSF ₈ | 150 | 200 | |
| CCl ₄ | 180 | 230 | |
| SF ₆ **) | 89 | 117 | |

*) Фреон
**) Элегаз

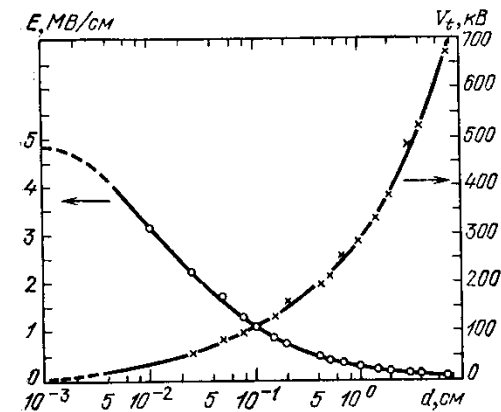


Рис. 13.7. Напряжение и поле пробоя вакуумного промежутка между шаром диаметром 2,5 см и диском диаметром 5 см из стали в зависимости от длины промежутка [3]

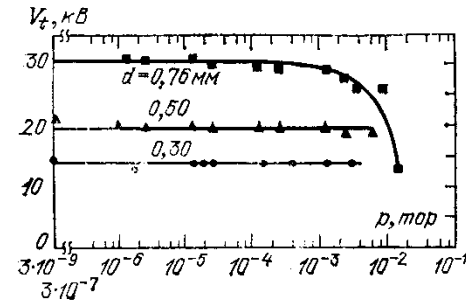


Рис. 13.8. Напряжения пробоя коротких промежутков d между стальными электродами в зависимости от давления заполняющего их водорода. Независимость от p свидетельствует о вакуумном характере пробоя. Загиб вниз верхней кривой соответствует переходу к левой ветви кривой Пашена [15.3]

Electric discharges

Breakdown in Microwave Fields and Interpretation of Experimental Data Using the Elementary Theory

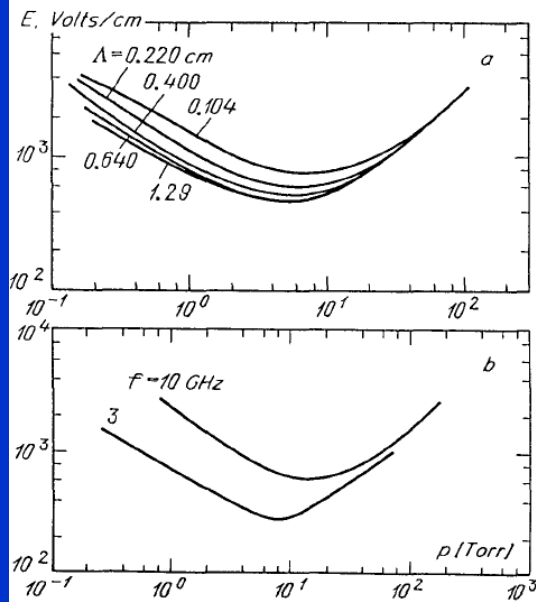


Fig. 7.8. Measured thresholds of microwave breakdown [7.6] (a) air, $f = 9.4$ GHz, diffusion length Λ is indicated for each curve; (b) He gas (He with an admixture of Hg vapor), $\Lambda = 0.6$ cm

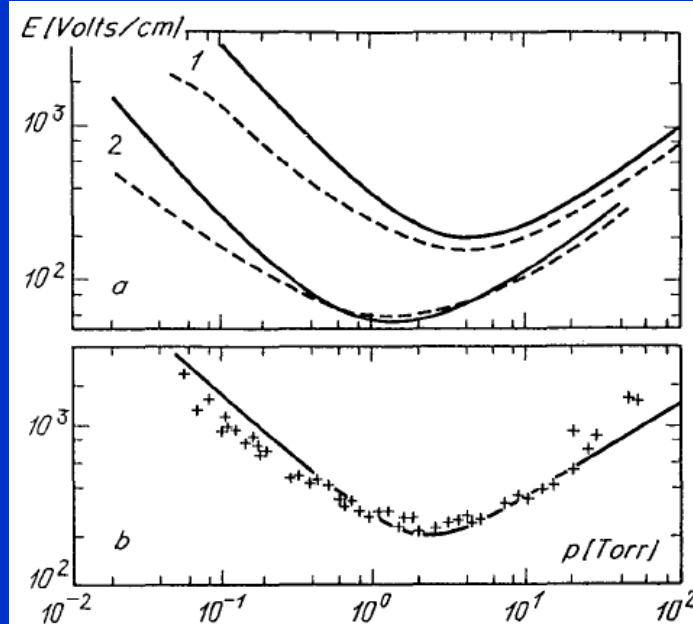


Fig. 7.10. Thresholds of microwave breakdown: (a) Ar, (1) $f = 2.8$ GHz, $\Lambda = 0.15$ cm; (2) $f = 0.99$ GHz, $\Lambda = 0.63$ cm; (b) Xe, $f = 2.8$ GHz, $\Lambda = 0.10$ cm. Solid curves, results of calculations [7.7]; dashed curves and crosses give experimental data [7.5]

for the total number of electrons, N_e , in the discharge volume:

$$dN_e/dt = (\nu_i - \nu_a - \nu_d)N_e, \quad \nu_d = D/\Lambda^2, \quad (7.7)$$

where ν_d is the frequency of diffusion losses of electrons. This equation describes the ionization kinetics of the gas.

Influence of diffusion length

RF discharges

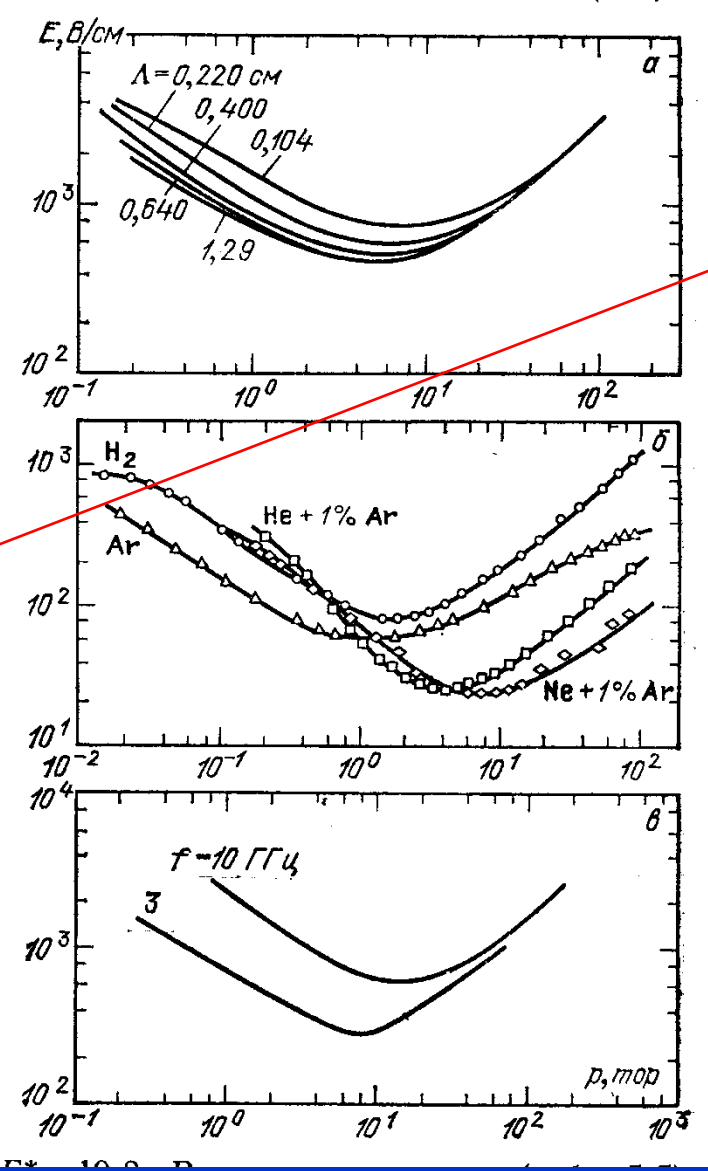


Рис. 13.10. Измеренные пороги СВЧ пробоя: *α* — воздух, частота $f=9,4 \text{ ГГц}$, около кривых указаны диффузионные длины Λ , *β* — несколько газов, $f=0,99 \text{ ГГц}$, $\Lambda=0,63 \text{ см}$; *γ* — Нег-газ (гелий с добавкой паров ртути), $\Lambda=0,6 \text{ см}$ [24]

Influence of diffusion length

Electric discharges

Influence of diffusion length

7.3.2 Ionization Kinetics Equation

When oscillation displacements are small, electron densities obey an equation of type (2.44):

$$\partial n_e / \partial t = D_{\nabla}^2 n_e + (\nu_i - \nu_a) n_e , \quad D \equiv D_e \quad (7.6)$$

(electrons diffuse freely in breakdown). If the condition $\omega \gg \nu_m \delta$ (Sect. 5.5.2) holds (it is satisfied for microwave frequencies), the electron energy distribution is quasisteady and the ionization and attachment frequencies, ν_i and ν_a , are determined by the root-mean-square field E . The dependencies $\nu_i(E)$, $\nu_a(E)$ are much stronger than $D_e(E)$, so that $D_e(E) \approx \text{const}$. For simplification, assume that the field is spatially homogeneous, and hence, ν_i and ν_a are independent of coordinates. Averaging (7.6) over the volume, we obtain, in accord with the results of Sect. 4.5, an equation for the mean density, or (which is equivalent) for the total number of electrons, N_e , in the discharge volume:

$$dN_e / dt = (\nu_i - \nu_a - \nu_d) N_e , \quad \nu_d = D / A^2 , \quad (7.7)$$

where ν_d is the frequency of diffusion losses of electrons. This equation describes the ionization kinetics of the gas.

Electric discharges

7.3.3 Steady-State Background Criterion

Assume that the external field is switched on in a time small in comparison with the characteristic time of multiplication and remains constant during the avalanche buildup. This constraint covers not only stationary, but also pulsed fields with not too short pulses and sufficiently small rise time. Under this assumption, $\nu_i(t), \nu_a(t) = \text{const}$ after the moment $t = 0$ at which the field is switched on, and (7.7) has an exponential solution typical of an avalanche process:

$$N_e = N_{e0} \exp [(\nu_i - \nu_a - \nu_d)] = N_{e0} \exp (t/\Theta), \quad (7.8)$$

where Θ is the *avalanche time constant*, and N_{e0} is the number of seed electrons that start the avalanche.¹ Breakdown is impeded in experiments with short pulses, since the probability of an electron appearing in the region of the field at the necessary moment is quite low and the avalanche has to be initiated by injecting a small number of electrons. For this purpose, a weak radioactive source is used.

According to (7.8), an avalanche develops if $\nu_i - \nu_a - \nu_d > 0$; this condition is met if the field exceeds a threshold E_t determined by the *steady-state breakdown criterion*:

$$\nu_i(E_t) = \nu_d + \nu_a(E_t). \quad (7.9)$$

As an example, consider breakdown in helium, for $p = 1 \text{ Torr}$, $\lambda = 3 \text{ cm}$, diffusion length $A = 1 \text{ cm}$, $D = 2 \cdot 10^6 \text{ cm}^2/\text{s}$, time of diffusion to the walls $\nu_d^{-1} \approx 5 \cdot 10^{-7} \text{ s}$, diffusion frequency $\nu_d \approx 2 \cdot 10^6 \text{ s}^{-1}$, and no attachment. The avalanche develops if $\nu_i > \nu_d \approx 2 \cdot 10^6 \text{ s}^{-1}$. We will show a little later that the ionization frequency $\nu_i \propto E^2$ under the most favorable conditions for multiplication (zero electron energy losses). If losses, especially inelastic, are nonzero, the ν_i vs. E curve is much steeper. Hence, if the field increases by 10 % in comparison with E_t , then $\Theta^{-1} = \nu_i - \nu_d \geq 0.2\nu_d \approx 4 \cdot 10^5 \text{ s}^{-1}$. The number of electrons is doubled every $\Theta / \ln 2 \leq 1.7 \mu\text{s}$, which is a very high rate. In many cases, it is sufficient for a reliable realization of breakdown. As a result, stationary criterion (7.9) determines with good accuracy [like criterion (7.1)] the breakdown threshold of gases for “not too short” pulses.

Electric discharges

7.5 Optical Breakdown

The discovery of the *optical breakdown* effect, in 1963 [7.8], became possible only after the development of *Q*-switched lasers that produce light pulses of tremendous power, called “giant pulses”. When the light of such a (ruby) laser was passed through a focusing lens, a spark flashed in the air, in the focal region, as in the electrical breakdown of a discharge gap. The discovery was a complete surprise for physicists and produced a sensation at the time, though the element of surprise has worn off by now. Gas breakdown at optical frequencies requires a tremendous field strength, 10^6 – 10^7 V/cm, in the light wave; this was unthinkable before the advent of the laser. Furthermore, the necessary light intensity, about 10^5 MW/cm², could only be reached by focusing the light of not just an ordinary laser, but one operating in the giant pulse regime. The new effect caused unparalleled interest among physicists. In a short time, it was experimentally and theoretically investigated to such a degree [7.7], that by now we know at least as much about it as about its closest analogue, the microwave field breakdown.

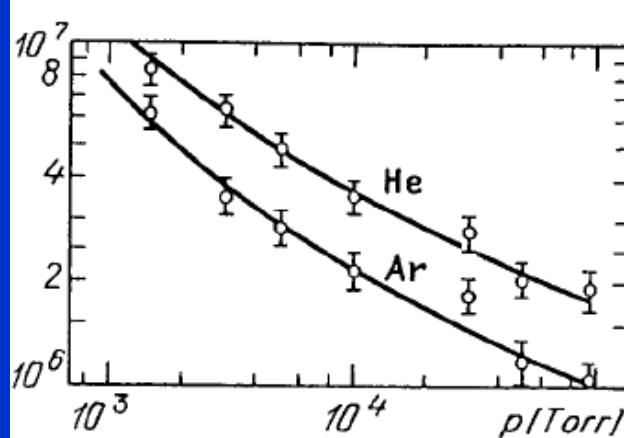


Fig. 7.11. Measured threshold fields for the breakdown of Ar and He by ruby laser radiation; pulse length 30 ns, diameter of focal spot $2 \cdot 10^{-2}$ cm [7.9]

Electric discharges

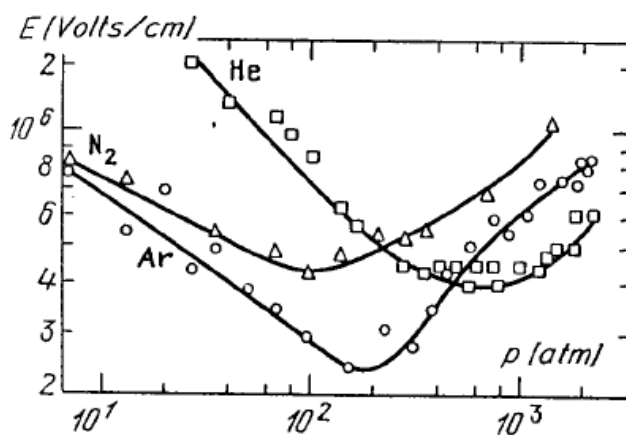


Fig. 7.12. Breakdown thresholds in Ar, He, N₂ for ruby laser radiation over a wide pressure range [7.10]. Pulse length 50 ns, focal spot diameter 10⁻² cm

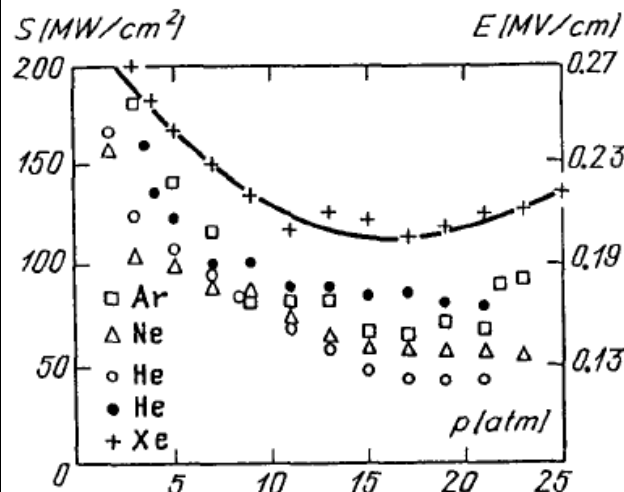


Fig. 7.13. Breakdown thresholds of inert gases in the radiation of a CO₂ laser [7.7]. The black dots represent data for helium of a higher purity

7.5.3 Breakdown Thresholds of Atmospheric Air

These data are very important. Quite a few physical experiments employ high-intensity laser beams. Electrical breakdown of air on the beam path to the target is an obstacle for light propagation because of absorption in the plasma. For example, in such experiments with high-power beams as target irradiation for fusion experiments one has to send the beam to the target through vacuum. The threshold intensity for the giant pulse of a ruby laser and an ordinary focal spot diameter of 10⁻² cm is $S_t \approx 10^{11} \text{ W/cm}^2$, and the field is $E_t \approx 6 \cdot 10^6 \text{ V/cm}$.

The breakdown threshold of nonfiltered air by focused CO₂ laser radiation is roughly $2 \cdot 10^9 \text{ W/cm}^2$, and that of dust-free air is not lower than 10^{10} W/cm^2 . The tiniest dust particles floating in the air greatly facilitate the breakdown by CO₂ laser radiation, while their effect is negligible for the neodymium and, in particular, ruby lasers. This difference appears because the short-wave radiation of solidstate lasers “supplies itself” with the seed electrons required for starting an avalanche. The long-wave radiation of CO₂ lasers cannot do this in a pure gas.

Electric discharges

7.7 Breakdown in RF and Low-Frequency Ranges

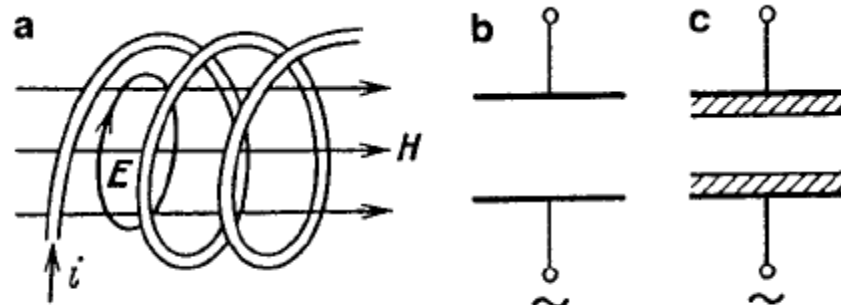


Fig. 7.18. Excitation of rf discharges: (a) inductively coupled through a solenoid coil; (b) voltage applied to electrodes in contact with plasma; (c) electrodes insulated from plasma (electrodeless, capacitively coupled rf discharge)

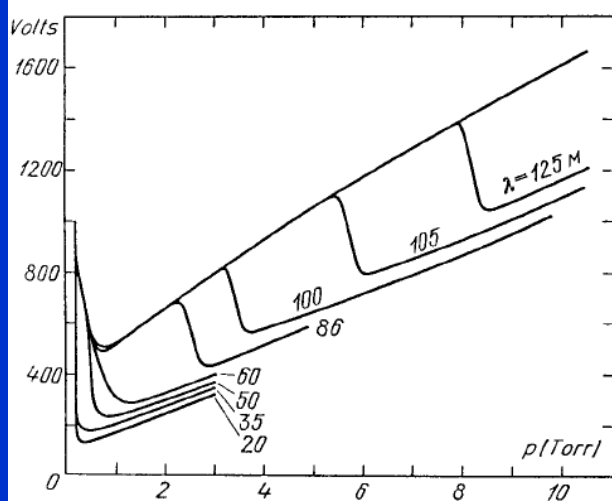


Fig. 7.20. Ignition potentials of ccrf discharge for various oscillation wavelengths [7.15]

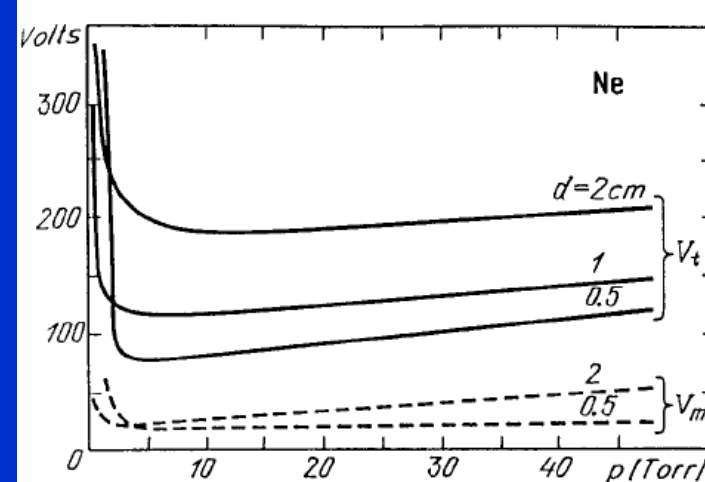
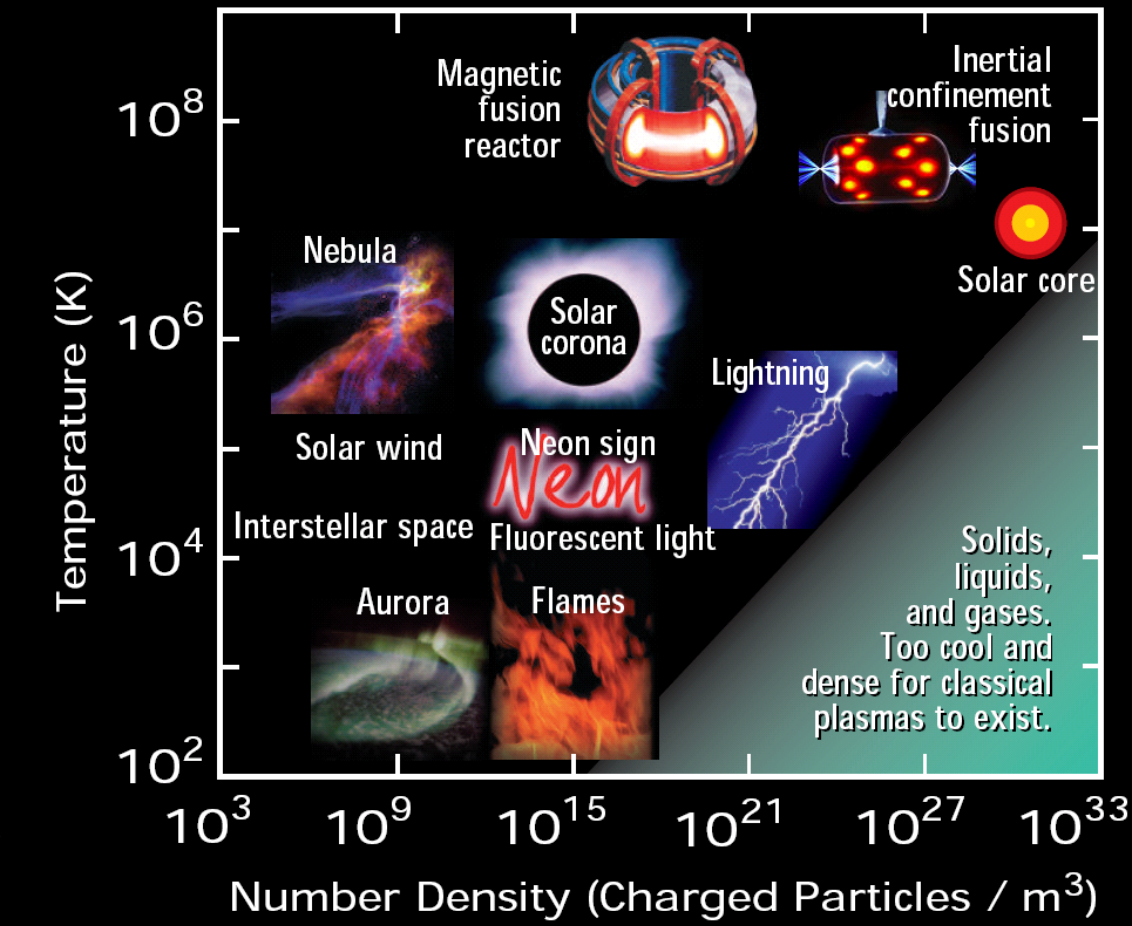


Fig. 7.19. Ignition potential of capacitively coupled rf discharge in neon (V_t), $f = 158$ MHz; d is the distance between the planar electrodes (which are covered by glass). Dashed curves show the burning voltage of a steady discharge, V_m [7.15]

PLASMAS – THE 4th STATE OF MATTER

CHARACTERISTICS OF TYPICAL PLASMAS

Plasmas consist of freely moving charged particles, i.e., electrons and ions. Formed at high temperatures when electrons are stripped from neutral atoms, plasmas are common in nature. For instance, stars are predominantly plasma. Plasmas are a "Fourth State of Matter" because of their unique physical properties, distinct from solids, liquids and gases. Plasma densities and temperatures vary widely.



Types of plasmas (electron density)

- Stars (density $n < 10^7 \text{ cm}^{-3}$)
- Solar winds (density $n < 10^7 \text{ cm}^{-3}$)
- Coronas (density $n < 10^7 \text{ cm}^{-3}$)
- Ionosphere (density $n < 10^7 \text{ cm}^{-3}$)
- Glow discharge (density $n = 10^8 \sim 10^{14} \text{ cm}^{-3}$)
- Arcs (density $n = 10^8 \sim 10^{14} \text{ cm}^{-3}$)
- High-pressure arc (density $n \sim 10^{20} \text{ cm}^{-3}$)
- Shock tubes (density $n \sim 10^{20} \text{ cm}^{-3}$)
- Fusion reactors (density $n \sim 10^{20} \text{ cm}^{-3}$)

$$1 \text{ Townsend} = 1 \text{ Td} = 10^{-17} \text{ Vcm}^2 = 10^{-21} \text{ Vm}^2.$$

$$1 \text{ V/cm Torr} = 3,034 \text{ Td}; \quad \text{resp.} \quad 1 \text{ Td} = 0,3296 \text{ V/cm Torr}.$$

Electrical discharge regime

● Dark discharge

- A – B During the background ionization stage of the process the electric field applied along the axis of the discharge tube sweeps out the ions and electrons created by ionization from background radiation. Background radiation from cosmic rays, radioactive minerals, or other sources, produces a constant and measurable degree of ionization in air at atmospheric pressure. The ions and electrons migrate to the electrodes in the applied electric field producing a weak electric current. Increasing voltage sweeps out an increasing fraction of these ions and electrons.
- B – C If the voltage between the electrodes is increased far enough, eventually all the available electrons and ions are swept away, and the current saturates. In the saturation region, the current remains constant while the voltage is increased. This current depends linearly on the radiation source strength, a regime useful in some radiation counters.
- C – D If the voltage across the low pressure discharge tube is increased beyond point C, the current will rise exponentially. The electric field is now high enough so the electrons initially present in the gas can acquire enough energy before reaching the anode to ionize a neutral atom. As the electric field becomes even stronger, the secondary electron may also ionize another neutral atom leading to an avalanche of electron and ion production. The region of exponentially increasing current is called the Townsend discharge.
- D – E Corona discharges occur in Townsend dark discharges in regions of high electric field near sharp points, edges, or wires in gases prior to electrical breakdown. If the coronal currents are high enough, corona discharges can be technically "glow discharges", visible to the eye. For low currents, the entire corona is dark, as appropriate for the dark discharges. Related phenomena include the silent electrical discharge, an inaudible form of filamentary discharge, and the brush discharge, a luminous discharge in a non-uniform electric field where many corona discharges are active at the same time and form streamers through the gas.

● Breakdown

- E Electrical breakdown occurs in Townsend regime with the addition of secondary electrons emitted from the cathode due to ion or photon impact. At the breakdown, or sparking potential V_B , the current might increase by a factor of 10^4 to 10^8 , and is usually limited only by the internal resistance of the power supply connected between the plates. If the internal resistance of the power supply is very high, the discharge tube cannot draw enough current to break down the gas, and the tube will remain in the corona regime with small corona points or brush discharges being evident on the electrodes. If the internal resistance of the power supply is relatively low, then the gas will break down at the voltage V_B , and move into the normal glow discharge regime. The breakdown voltage for a particular gas and electrode material depends on the product of the pressure and the distance between the electrodes, pd , as expressed in Paschen's law (1889).

● Glow discharge

- F – G After a discontinuous transition from E to F, the gas enters the normal glow region, in which the voltage is almost independent of the current over several orders of magnitude in the discharge current. The electrode current density is independent of the total current in this regime. This means that the plasma is in contact with only a small part of the cathode surface at low currents. As the current is increased from F to G, the fraction of the cathode occupied by the plasma increases, until plasma covers the entire cathode surface at point G.
- G – H In the abnormal glow regime above point G, the voltage increases significantly with the increasing total current in order to force the cathode current density above its natural value and provide the desired current. Starting at point G and moving to the left, a form of hysteresis is observed in the voltage-current characteristic. The discharge maintains itself at considerably lower currents and current densities than at point F and only then makes a transition back to Townsend regime.

● Arc discharge

- H – K At point H, the electrodes become sufficiently hot that the cathode emits electrons thermionically. If the DC power supply has a sufficiently low internal resistance, the discharge will undergo a glow-to-arc transition, H-I. The arc regime, from I through K is one where the discharge voltage decreases as the current increases, until large currents are achieved at point J, and after that the voltage increases slowly as the current increases.